Improvements in the accuracy and precision of isotope ratio measurements by double focussing inductively coupled plasma mass spectrometry

PLEASE CITE THE PUBLISHED VERSION

PUBLISHER

© Christopher Ingle

REPOSITORY RECORD

Ingle, Christopher P.. 2019. "Improvements in the Accuracy and Precision of Isotope Ratio Measurements by Double Focussing Inductively Coupled Plasma Mass Spectrometry". figshare. https://hdl.handle.net/2134/13820.

Improvements in the Accuracy and Precision of Isotope Ratio
Measurements by Double Focussing Inductively Coupled Plasma
Mass Spectrometry

by

Christopher Ingle

A Doctoral Thesis

Submitted in partial fulfilment of the requirements for the award of the degree of

Doctor of Philosophy of Loughborough University

May 2003

Abstract

Inductively coupled plasma mass spectrometry is a well-established technique for the measurement of isotope ratios. Double focussing mass analysers enable increased resolution to be applied to separate spectroscopic interferences, or the use of multi-collector detection techniques for high precision isotope ratio determinations.

For the Central Science Laboratory (CSL), trace elements team, methods were developed for Zn and Fe isotope ratio measurements in acid digested faecal samples from a human nutritional study. For Zn, a novel high resolution/multi-collector combination was employed; for Fe a single collector, high resolution method was used. In both cases, samples from the nutritional study known to contain the analytes in natural isotopic abundance were used to correct for the mass bias. Two independent methods for determining Zn and Fe isotope ratios were used to validate the measurement strategies. The team at CSL are also involved in the authentication of food products. Isotope ratio and elemental concentration data were used to determine the geographical origin of rice samples, and to distinguish between traditional and modern Basmati rice grown in India and Pakistan.

NERC Isotope Geosciences Laboratory are primarily concerned with the achievable accuracy and precision of an isotope ratio measurement. Use of a mass bias correction expression appropriate to the ICP-MS instrument is essential for high quality isotope ratio measurements. Cd and Sn were used to study the variation of the mass bias in a double focussing ICP-MS system with time, absolute mass and mass difference. It was proposed that mass bias should be considered as a result of the change in the instrument response with mass, and not a fundamental parameter in its own right. A method for determination of the best mass bias correction model for an individual instrument, through examination of the instrument response function was developed.

Keywords: ICP-MS, high resolution, multi-collector, isotope ratios, applications, mass bias correction.

Acknowledgements

Contents

Chapter 2 Isotope Ratio Measurements by Inductively Coupled Plasma Mass Spectrometry

Chapter 3   Combined High Resolution/Multi-Collector ICP-MS for Measurement of Total Zn and Zn Isotope Ratios in Faecal Samples from a Human Nutrition Study

Chapter 4   Development of a High Resolution ICP-MS Method for the Measurement of Fe and Fe Isotope Ratios in Acid Digests of Faecal Samples from a Human Nutrition Study

Chapter 5 Instrument Response Functions, Mass Bias & Matrix Effects in Isotope Ratio Measurements and Semi-Quantitative Analysis by Double Focussing ICP-MS

Chapter 6 The Authentication of Premium Rice Using Trace Element Concentrations and Isotope Ratios

Publications and Presentations

Publications

The use of background ions and a multivariate approach to characterise and optimise the dominant H_2-based chemistries in a hexapole collision cell used in ICP-MS

C. Ingle, P. Appelblad, M. Dexter, H. Reid and B. Sharp, *J. Anal. At. Spectrom.*, 2001, **16**, 1076

The effect of adventitious water in hexapole collision cell inductively coupled plasma mass spectrometry

M. Dexter, P. Appelblad, C. Ingle, J. Batey, H. Reid and B. Sharp, *J. Anal. At. Spectrom.*, 2002, **17**, 183

Development of a high-resolution ICP-MS method, suitable for the measurement of iron and iron isotope ratios in acid digests of faecal samples from a human nutrition study

C. Ingle, N. Langford, L. Harvey, J. Dainty, S. Fairweather-Tait, B. Sharp, M. Rose, H. Crews, and J. Lewis, *J. Anal. At. Spectrom.*, 2002, **17**, 1498.

An ICP-MS methodology using a combined high-resolution/multi-collector detector system for the measurement of total zinc and zinc isotope ratios in faecal samples from a human nutrition study

C. Ingle, N. Langford, L. Harvey, J. Dainty, S. Fairweather-Tait, B. Sharp, M. Rose, H. Crews, and J. Lewis, *J. Anal. At. Spectrom.*, 2002, **17**, 1502.

Instrument response functions, mass bias and matrix effects in isotope ratio measurements and semi-quantitative analysis by single and multi-collector ICP-MS

C. Ingle, M. Horstwood, R. Parrish, J. Lewis and B. Sharp, *J. Anal. At. Spectrom.*, 2003, **18**, 219.

Conference Papers and Posters

Development of a combined multi-collector/high resolution inductively coupled plasma mass spectrometry technique for the measurement of Zn in faeces
<u>C. Ingle</u>, B. Sharp, J. Lewis, poster presentation, RSC Analytical Research Forum, Norwich, UK, July 2001

Investigation and modelling of mass bias in a double focussing ICP-MS system in single and multi-collector modes
<u>C. Ingle</u> and B. Sharp, oral presentation, 11th Biennial National Atomic Spectroscopy Symposium, Loughborough, UK, July 2002

Investigation of the noise characteristics of a collision/reaction cell ICP-MS system
<u>C. Ingle</u>, N. Marlin, E. Silva and B. Sharp, poster presentation, RSC Analytical Research Forum, Kingston-upon-Thames, UK, July 2002

Instrument response functions and mass bias in sector field ICP-MS
<u>C. Ingle</u>, M. Horstwood, R. Parrish and B. Sharp, oral presentation, 8th International Conference on Plasma Source Mass Spectrometry, Durham, UK, September 2002

Training Record

6/10/99	Faculty of Science Postgraduate training – C. Hinde 'What is a PhD?'
7/10/99	Pilkington Library 'Finding books using the library OPAC'
13/10/99	Department of Chemistry Safety Lecture – B. Sharp
15/10/99	Department of Chemistry Fire Safety Lecture – D. Wilson
20/10/99	Faculty of Science Postgraduate training – M. Lansdale 'What a student can expect from a supervisor/ director of research'
27/10/99	Faculty of Science Postgraduate training – R. Kirkwood, R. Rhodes 'Getting the most out of the library, computing services and the internet'
3/11/99	Faculty of Science Postgraduate training – M. Turpin 'Time and project management'
23/11/99	Project meeting – NIGL
12/4/00	Project meeting – CSL
8/5/00	UKAS Training – CSL Sample handling, balance and pipette calibration
17/7/00	10th Biennial National Atomic Spectroscopy Symposium Workshop 'New mass spectrometries for elemental analysis'
13/10/00	Project meeting – CSL
4-8/2/01	European Winter Conference on Plasma Spectrochemistry Hafjell, Norway
16/2/01	Project meeting – NIGL
27/2, 6/3, 13/3/01	Loughborough University Staff Development 'Teaching skills for research assistants and postgraduates'
18/7/01	Meeting with J. Dainty, Institute of Food Research, Norwich Kinetic modelling techniques and elemental absorption calculations
18/9/01	Project meeting – CSL Summary of work presented
1/5/02	Project meeting – CSL
8/7/02	11th Biennial National Atomic Spectroscopy Symposium Workshop 'Quality assurance and accreditation'
18/9/02	Project meeting – NIGL Summary of work presented

Chapter 1

Inductively Coupled Plasma Mass Spectrometry (ICP-MS)

1.1 Introduction

Since the first coupling of an inductively coupled plasma (ICP) to a mass
spectrometer over twenty years ago,[1] ICP-MS has become a widely used method
of elemental analysis. Over this time, continuous instrumental and procedural
developments have meant that the technique is now capable of accurate and
precise measurement of elements across the periodic table, in a wide range of
sample types. Along with the broad range of analytes and samples that can be
measured, the principal advantages of analysis by ICP-MS are its relative speed
and simplicity, high sensitivity across the mass spectrum and wide dynamic range.
Additionally, ICP-MS is capable of both quantitative measurements and isotopic
determinations, unlike many other forms of atomic spectrometry.

This chapter provides an overview of the instrumentation and analytical processes
involved in ICP-MS. The background to the work presented in this thesis is also
discussed.

1.2 Instrumentation for Analysis by ICP-MS

1.2.1 The plasma

The basic apparatus required to form an ICP consists of two or three turns of
copper tubing coiled around a glass torch, through which Ar gas is streamed. A
Tesla coil is used to produce a spark that seeds the Ar with high energy electrons,
which are accelerated by the magnetic and induced electric fields surrounding the
coil. These electrons collide with Ar atoms, ionising them and thereby releasing
further electrons resulting in a chain reaction that sustains the ICP. Continuous,
symmetrical gas flows and a magnetic field of sufficient strength are required to
maintain a stable plasma. Typical r.f. power levels are 1-1.5 kW, resulting in a

plasma temperature of around 10,000 K. The temperature in the central channel is 6500 – 7000 K, which combined with the significant residence time of the sample in the plasma (several milliseconds), is sufficient to cause vaporisation, atomisation and ionisation of the analyte.

1.2.2 Sample introduction

There are many ways of introducing a sample to the ICP, however the most common remains nebulisation of a liquid sample using a low flow rate of Ar gas (typically 0.5-1 L min^{-1}). Samples are either propelled to the nebuliser using a peristaltic pump or drawn by the gas flow through the nebuliser (natural aspiration). A plethora of nebuliser designs exist,[2] one of the most widely used is the concentric nebuliser, typically made of glass. In this type of nebuliser, the sample travels along the inside tube and is nebulised at the tip by gas flowing through the outer tube. The sample aerosol is then swept into a spray chamber, wherein larger droplets are removed by impact with the spray chamber walls or with a glass bead placed there for the purpose. The aerosol (now with droplet diameters less than 10 μm) is carried through to the ICP *via* an injector, typically 1.5 mm internal diameter. The injector is usually made of glass and manufactured as part of the ICP torch, however demountable alumina and platinum injectors have been employed to reduce background levels for certain elements (*e.g.* Si).[2]

1.2.3 The interface

The basic layout of the interface region of an ICP-MS system is shown in Fig. 1.1.
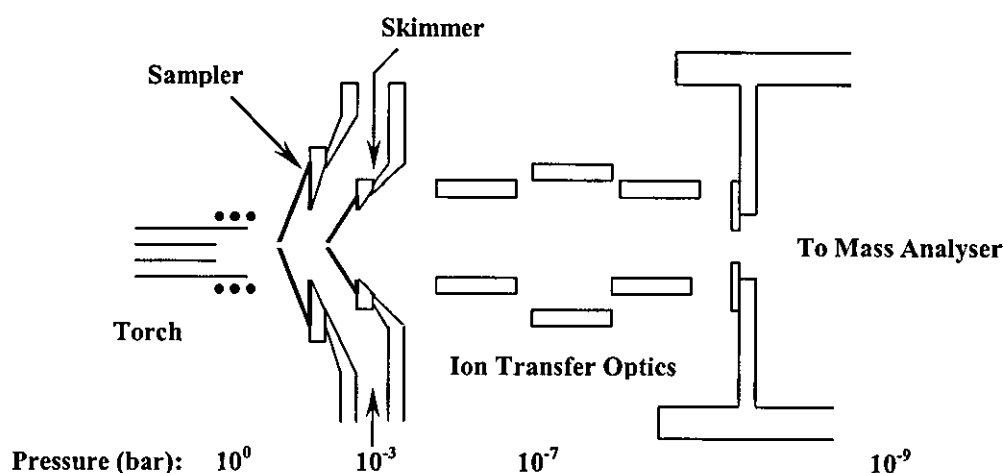
Fig. 1.1 Interface region of an ICP-MS system

2

The sampler cone extracts a jet from the plasma, which forms a shock wave structure enclosing the so-called zone of silence. The skimmer cone extracts ions from within the zone of silence, forming a gas jet of ions and neutrals that is guided to the mass analyser by the ion optics. Various vacuum pumping stages are used to transfer from the atmospheric pressure plasma to the low vacuum required in the mass analyser.[3]

1.2.4 Mass analysers

1.2.4.1 Quadrupole mass analysers

Quadrupole ICP-MS instruments are by far the most widely used systems. The quadrupole mass filter consists of four rods, each with a rounded side, which produce an approximately hyperbolic field when r.f. and dc voltages are applied across opposite pairs of rods. At a certain applied voltage, an ion entering the field will either pass along the full length of the filter, or hit one of the rods and be lost from the system depending on its trajectory. In the presence of the field, ion trajectory is dependent on the mass of the ion, since the field affects heavier ions to a lesser extent than lighter ions. Ramping the voltages applied to the rods scans the range of ion masses that will pass along the full length of the analyser. Quadrupole analysers are easy to operate, mechanically simple, capable of high speed electronic scanning, have a linear mass scale and are cheap compared to other types of ICP-MS instrumentation.[4, 5]

1.2.4.2 Double focussing mass analysers

The double focussing mass spectrometer is based upon the combination of a magnetic sector and an electrostatic analyser. A magnetic analyser is simply a curved flight tube between the poles of an electromagnet. If ions of mass m are accelerated by an electric potential, U_a and pass through a magnetic sector field, B, the ions will move in a circular path of radius r_m. The mass to charge ratio (m/z) of the ions transmitted by the analyser is given by:[6]

$$m/z = \frac{B^2 r_m^2}{2U_a}$$
1.1

The radius r_m is dependent on the momentum, and therefore on both the mass and energy of the ions. Ions from an ICP have a wide spread of energies (~ 6 eV), meaning that species of the same mass may not all be focussed to the same point by the magnetic sector. Therefore, energy focussing of the ion beam is required for a magnetic sector analyser to be coupled to an ICP ion source. This is generally achieved through the use of an electrostatic analyser (ESA), made up of two curved plates with a voltage applied between them. The path of an ion between the plates is determined by its kinetic energy. At a particular voltage, ions of the same energy are focused to the exit slit of the ESA.

The combination of magnetic sector (mass and energy focussing) and ESA (energy focussing only) results in the double focussing arrangement shown in Fig. 1.2 that is mass selective only. The layout shown in Fig. 1.2, with the magnetic sector before the ESA, is known as reverse Nier-Johnson geometry and has been shown to provide better performance for ICP-MS than having the ESA as the first sector.[3]
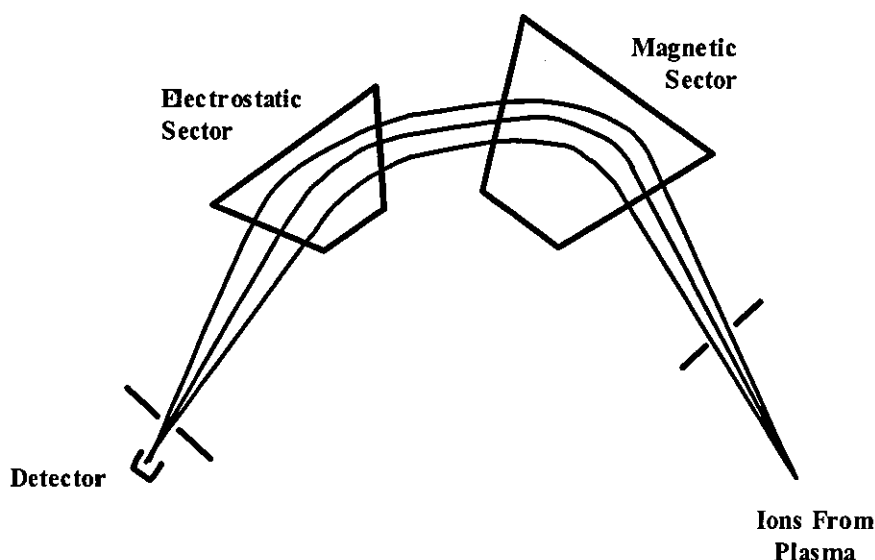
Fig. 1.2 The double focussing mass spectrometer

The resolution of a double focussing ICP-MS system can be increased by narrowing the slits at the entrance and exit of the mass analyser. This enables peaks that occur at the same nominal mass (*e.g.* $^{56}Fe^+$ and $^{40}Ar^{16}O^+$) to be separated, increasing the range of elements to which this technique may be

4

applied. At comparable resolution, double focussing ICP-MS instruments are generally more sensitive than quadrupole based spectrometers; the higher extraction potentials required in double focussing systems for proper formation of the ion beam have the added effect of increasing ion transmission.[6] The backgrounds are also lower for double focussing ICP-MS as the ion beam is bent through such an angle that no photons or neutral species can reach the detector,[7] although developments in the design of quadrupole instruments to include off-axis filter rods have recently reduced the background observed in these systems.

A double focussing mass analyser can also be coupled to an array of detectors to allow simultaneous detection of a number of ion signals. A schematic of a multi-collector ICP-MS instrument is given in Fig 1.3. The geometries of the system demand that the magnet is placed after the ESA to achieve the desired splitting of ions of different mass.[8-10]
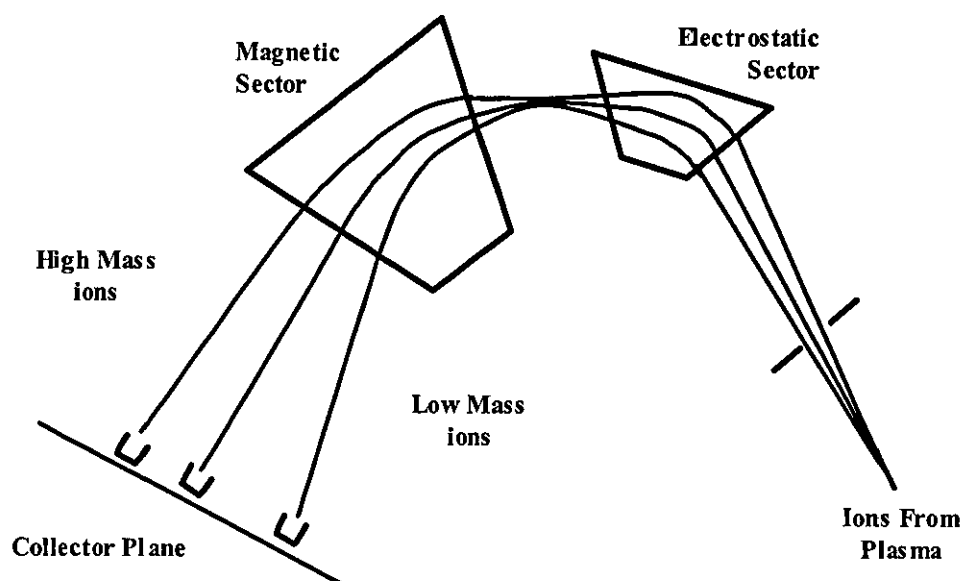
Fig. 1.3 Schematic of a multi-collector ICP-MS instrument

Simultaneous ion detection allows extremely precise isotope ratio measurements to be performed. As ions that are detected at the same time will also have left the plasma at the same time, the noise associated with them will be highly correlated, and will cancel when the ion signals are ratioed. Most multi-collector ICP-MS measurements are limited to low resolution, and therefore restricted to isotopes

free from spectral interference. Additionally, the extra hardware used in these systems renders them extremely expensive, at least five times the cost of a quadrupole based instrument.

The principal systems used in this work were Axiom double focussing ICP-MS instruments manufactured by Thermo (formerly VG) Elemental, based at the Natural Environment Research Council (NERC) Isotope Geosciences Laboratory (NIGL) in Keyworth, Nottingham and the Central Science Laboratory (CSL) in Sand Hutton, York. These instruments are both equipped with a single electron multiplier detector and an array of Faraday collectors, and can be operated in single or multi-collector modes. In single collector mode, the width of the source and collector slits can be changed allowing continuous variation of resolution from 400 to approximately 12,000 (see section 2.2.1). A potential of 6000 V is applied to the interface to extract ions from the plasma, with the remainder of the analyser grounded.

Other commercial double focussing ICP-MS systems include the Element and Element 2 single collector instruments from Thermo Finnigan, with three fixed resolution settings of 300, 4000 and 10,000. The ions are accelerated using 6000 V applied to the whole analyser behind the interface, allowing the ICP and the interface to be operated at ground potential, thereby reducing the high voltage hazard to the user. Thermo Finnigan also manufacture the Neptune multi-collector ICP-MS system with 9 Faraday collectors and the capability of increased resolution for two collector channels.

Nu Instruments also produce multi-collector ICP-MS systems. The Nu Plasma is available with up to 15 detectors in the array and the Nu Plasma 1700 allows multiple channels to be simultaneously monitored at increased resolution. Both these instruments have fixed collector arrays, the mass of the isotope measured in each position is set by a 'zoom lens' positioned after the double focussing analyser.

The Isoprobe from Micromass uses a different approach to solve the problem of the energy dispersion of the magnetic sector. A hexapole collision cell filled with

an inert gas such as helium provides the energy focussing in this system. Similar to the Thermo Finnigan instruments, the plasma and interface are grounded. Ion acceleration is achieved by the application of an 6000 V potential to the entire instrument behind the interface. The system has an array of Faraday collectors and is capable of resolutions up to approximately 3000.

1.2.4.3 Time-of-flight-mass analysers (TOFMS)[11]

ICP-TOFMS instruments have only recently become commercially available. As in other TOF systems, ions of different mass are separated according to the time taken to pass through the field free region inside the spectrometer. Two different ion extraction configurations exist, longitudinal, in which the flight tube is in-line with the plasma, and orthogonal, in which the flight tube and the plasma are perpendicular to one another. ICP-TOFMS instruments are very fast scanning; around 10,000 spectra can be acquired per second. The principal advantage of TOF systems is therefore in the measurement of transient signals, *e.g.* those arising from separation techniques such as gas chromatography and capillary electrophoresis, and sample introduction techniques such as laser ablation, electrothermal vaporisation or hydride generation. The sensitivity of ICP-TOFMS instruments is typically an order of magnitude worse than modern quadrupole instruments, however the number of publications in this area is increasing and TOF performance is improving.[12]

1.2.5 Detection of ions

The most widely used ion detector in ICP-MS is the electron multiplier. This device consists of a surface with a resistive coating that emits a burst of electrons when struck by an ion. These electrons then strike the surface causing further emission, and the number of electrons is multiplied along the length of the detector to produce a measurable current pulse. Although a single continuous surface is traditionally used, more modern designs consist of 12 to 24 discrete dynodes with a larger total surface area than a continuous electron multiplier. Discrete dynode detectors generally have better longevity and stability than the continuous design, as the workload of the device is spread over a wider area.

Electron multipliers can be used in two modes. In pulse counting mode, the current pulses produced are converted to logic pulses by digital circuitry, which are recorded by a counter. This digital mode prevents multiplier noise from influencing the measurement, but is prone to counting fatigue at count rates approaching 10^6 counts s^{-1}, limiting the linear dynamic range of the system. Analogue mode may be used to extend the linear range. An amplifier is used to measure the mean current produced in the detector, which is then converted to a counts s^{-1} reading. Detection limits in this acquisition mode are approximately 50 times higher than in pulse counting mode.[3]

The Faraday collector (essentially a metal cup) is an alternative ion detection system in which the voltage produced by ions arriving at the collector is converted to an equivalent counts s^{-1} reading. Faraday collectors are used in multi-collector systems as they are relatively easy to calibrate, provide a uniform response across the array, and generally have very good linearity.[3] The disadvantage of using Faraday collectors is that they are significantly less sensitive than the standard electron multiplier detectors; detection limits are typically a factor of 1000 higher for Faradays.[3]

1.3 Analytical Characteristics of Double Focussing ICP-MS

1.3.1 Data acquisition modes

Using quadrupole ICP-MS systems, the only method of altering the m/z of the ions that pass through the mass analyser is to vary the potentials applied to the pairs of rods, as described above. With double focussing mass analysers, there is a choice of acquisition modes. Firstly, data may be acquired statically. From equation 1.1, at a given magnetic field setting, ions of different mass pass through the analyser on paths of different radii. Several ions can be detected simultaneously if collectors are placed at these different radii (see above). The maximum number of isotopes it is possible to detect in this manner is limited by the number of collectors available.

It is generally more practical to use a fixed single collector, and vary the *m/z* of the ions transmitted by the mass analyser. This can be achieved by changing the parameters of either the magnetic or electrostatic sectors. Magnetic sector scanning allows data acquisition across the mass spectrum from *m/z* 2 to 250, however the speed with which the magnetic field can be changed is limited. Even with modern laminated magnets, the scan speed is significantly slower than a quadrupole mass analyser. Electrostatic scanning is achieved by varying the acceleration voltage while maintaining a constant magnetic field. Although a faster scan mode, due to loss of sensitivity the mass range covered by electrostatic scanning is limited to approximately 15 % of the mass at the centre of the scan. That is, if the centre mass was 100, the total range that could be measured would be *m/z* 92.5 to 107.5.

1.3.2 Peak shape

The double focussing mass analyser produces flat-topped peaks in low resolution mode, compared with the round topped-peaks of a quadrupole instrument. This is an advantage when the peak-jumping mode of data acquisition is used. Instrumental or mass calibration drift may cause the exact mass at which the measurement is taken to vary. On a rounded peak, this means the intensity recorded in replicate sweeps can change. With a flat-topped peak, the result will be the same even if some drift does occur, allowing extremely high precision measurements to be made.[13] Flat-topped peaks also provide the signal stability essential to high precision measurement by multi-collector ICP-MS techniques. In high resolution mode, double focussing mass analysers produce rounded peaks. In order to maximise ion transmission in this mode, it is an advantage to have tall, thin peaks that enable the maximum resolution to be achieved for a given slit width.

1.3.3 Figures of merit

As mentioned above, with the same detector system, double focussing ICP-MS systems are more sensitive than quadrupole based instruments. Combined with background levels in double focussing ICP-MS of less than 0.1 counts s^{-1}, these instruments can achieve detection limits below 0.5 pg ml^{-1} for many elements.[6] The electron multiplier detectors used in these systems have a linear range up to

nine orders of magnitude, if the response of the pulse counting and analogue modes is properly calibrated. Faraday collectors used in multi-collector ICP-MS systems are significantly less sensitive than electron multipliers, and have a linear range of 4 orders of magnitude, however this is only a limitation if extreme isotope ratios are to be measured.

The capability of double focussing mass analysers to operate at increased resolution widens the range of elements that can be accurately determined by ICP-MS. The precision of measurements can also be improved in comparison to quadrupole ICP-MS, a detailed discussion is presented in the following chapter.

1.4 Objectives

The work covered in this thesis reflects the different requirements of the project sponsors.

The Central Science Laboratory, trace elements team has a requirement for high sample throughput and reliable methods for isotope ratio analysis in a variety of food and clinical samples. The absolute achievable precision is not necessarily of interest, the determinations must simply be good enough to meet the requirements of the customer. In keeping with this philosophy, the methods described in Chapters 3 and 4 were developed for the measurement of Zn and Fe in acid digested faecal samples from a nutritional study. The required precision levels were determined by nutritionists using kinetic modelling techniques. Two independent methods for determining Zn and Fe isotope ratios were used to validate the measurement strategies.

NERC Isotope Geosciences Laboratory are primarily concerned with the achievable accuracy and precision of an isotope ratio measurement. One of the primary applications of isotope ratio analysis in the geological sciences is the determination of the age of samples. The natural abundance of certain isotopes is variable due to the decay of radioactive isotopes. The ratio of these radiogenic isotopes to isotopes whose abundance is naturally invariant can be used, together

with the decay constants of the radioactive parent isotopes, to calculate the amount of radioactive decay that has occurred, and thence determine the time since formation of the sample.[14] The better the quality of the isotope ratio measurement, the lower the error in the age determination. Use of a mass bias correction expression appropriate to the ICP-MS instrument is essential for high quality isotope ratio measurements. The mass bias correction has been shown to be the largest contributing factor to isotope ratio uncertainty for several isotope systems.[15] Insight into the relationship between the change in instrument response with analyte mass and the mass bias of the system, and the method for determination of the best mass bias correction model for an individual instrument (Chapter 5) are therefore of great value.

Chapter 6 describes the investigation of trace element concentrations and isotope ratios measured by double focussing ICP-MS for the authentication of premium rice. The issue of food authenticity is a major concern for regulatory authorities and consumers alike. As the amount of legislation regarding the traceability of produce increases, it is essential that methods to enforce the laws be in place. It is hoped that the use of trace element data as a means of determining the geographical origin of foods can be expanded to a broader range of food products.

References

1   R. S. Houk, V. A. Fassel, G. D. Flesch, H. J. Svec, A. L. Gray and C. E. Taylor, *Anal. Chem.*, 1980, **52**, 2283.

2   A. Montaser, M. G. Minnich, J. A. McLean, H. Liu, J. A. Caruso and C. W. Mcleod, 'Sample introduction in ICP-MS' in *Inductively Coupled Plasma Mass Spectrometry*, ed. A. Montaser, Wiley-VCH, New York, 1998.

3   P. J. Turner, D. J. Mills, E. Schröder, G. Lapitajs, G. Jung, L. A. Iacone, D. A. Haydar and A. Montaser, 'Instrumentation for Low- and High-Resolution ICP-MS' in *Inductively Coupled Plasma Mass Spectrometry*, ed. A. Montaser, Wiley-VCH, New York, 1998.

4   F. Vanhaeke, L. Moens and R. Dams, *J. Anal. At. Spectrom.*, 1998, **13**, 1189.

5   J.-F. Ying and D. J. Douglas, *Rapid Commun. Mass Spectrom.*, 1996, **10**, 649.

6   N. Jakubowski, L. Moens and F. Vanhaecke, *Spectrochim. Acta Part B*, 1998, **53**, 1739.

7   J. S. Becker and H.-J. Dietze, *J. Anal. At. Spectrom.*, 1997, **12**, 881.

8   A. J. Walder and P. A. Freedman, *J. Anal. At. Spectrom.*, 1992, **7**, 571.

9   A. J. Walder, I. D. Abell, I. Platzner and P. A. Freedman, *Spectrochim. Acta Part B*, 1993, **48**, 397.

10 A. J. Walder, I. Platzner and P. A. Freedman, *J. Anal. At. Spectrom.*, 1993, **8**, 19.

11 S. J. Ray and G. M. Hieftje, *J. Anal. At. Spectrom.*, 2001, **16**, 1206.

12 H. Emteborg, X. Tian, M. Ostermann, M. Berglund and F. C. Adams, *J. Anal. At. Spectrom.*, 2000, **15**, 239.

13 F. Vanhaecke, L. Moens, R. Dams and P. Taylor, *Anal. Chem.*, 1996, **68**, 567.

14 M. A. Geyh and H. Schleicher, *'Absolute age determination: Physical and chemical dating methods and their application'*, Springer-Verlag, Heidelberg, 1990.

15 P. K. Appelblad, I. Rodushkin and D. C. Baxter, *Anal. Chem.*, 2001, **73**, 2911.

Chapter 2

Isotope Ratio Measurements by Inductively Coupled Plasma Mass Spectrometry

2.1 Introduction

The isotopic composition of most elements is constant in nature, however in some cases variation has arisen due to radioactive decay, mass dependent natural processes (such as evaporation) and/or anthropogenic causes such as nuclear activity. The measurement of variable isotope ratios can be used to determine the age of geological samples, to identify pollution sources, to assess the authenticity of food and other products and to monitor radioactive contamination. Additionally, enriched isotope spikes are used to alter otherwise invariant isotope ratios in tracer studies to investigate the transport of elements through biological and environmental systems. Isotope ratios have also found wide application in the measurement of elemental concentrations, using the isotope dilution technique. This method may be applied to any element with at least two isotopes and involves determination of the change in an isotope ratio in a sample upon addition of a spike enriched in one of the isotopes that make up the ratio. Although labour intensive, isotope dilution can provide elemental concentration data of greater accuracy and precision than alternative methods of calibration.[1]

Thermal ionisation mass spectrometry (TIMS) is the established technique for isotope ratio measurements, providing excellent levels of precision (0.005-0.01 % relative standard deviation (RSD)[2]), and extremely reliable results. However, samples for TIMS require extensive clean up before they can be analysed, making analysis using this technique extremely time consuming. TIMS is also limited by the ionisation potential of the analyte element. Elements such as boron and osmium (ionisation potentials 8.3 and 8.7 eV respectively) cannot be determined directly.[3]

ICP-MS is an attractive alternative to TIMS; the ionising power of the ICP enables the technique to be applied to the determination of elements across the periodic table in a wide range of sample matrices. The potential of ICP-MS for isotope ratio measurements was recognised early in the history of the method.[4] This chapter reviews the use of ICP-MS for isotope ratio measurements, with the emphasis on the application of double focussing instrumentation.

2.2 Factors Affecting the Accuracy and Precision of Isotope Ratio Determinations by ICP-MS

2.2.1 Spectral interference

Spectral interferences are single atom or molecular species with the same nominal mass-to-charge ratio as the analyte. They originate in the sample matrix or atmospheric and plasma gases and can be separated into three distinct groups.[5] Firstly, isobaric interferences occur where isotopes of different elements coincide at the same nominal mass *e.g.* ^{64}Ni and ^{64}Zn. Where alternative isotopes are not available, or a specific analyte isotope is required, isobaric interferences must be corrected for mathematically. This is done by monitoring another isotope of the interfering element, and calculating the contribution of the interference to the analyte signal.

Molecular ions, also called polyatomic ions, make up the second group of spectral interferences. These species arise from combinations of species present in the solvent, sample matrix, and atmospheric and plasma gases, *e.g.* ^{40}Ar^{35}Cl$^+$ overlaps ^{75}As$^+$, ^{14}N$_2$$^+$ on ^{28}Si. The mechanism by which these ions are formed is by no means certain. Some of the possible sources are: secondary discharges in the interface region, matrix species that survive the passage through the plasma and major plasma species forming cluster ions in the plasma boundaries and sampling and expansion regions.[5]

The third type of spectral interferences is multiply charged ions. These interferences are a particular problem when elements with relatively low second ionisation potential, such as Ba, Sr and the rare earth elements, are present in the

sample matrix. The doubly charged ions appear in the spectrum at half the isotope mass, for example the interference from $^{138}Ba^{2+}$ occurs at a mass-to-charge ratio (m/z) of 69.

Whether or not an interfering signal can be separated from the analyte depends on the resolution of the system, defined as:

$$Resolution = \frac{m}{\Delta m}$$
2.1

Where Δm is the peak width, in mass units, of an interference free peak at 5 % of the peak height. Alternatively, if two neighbouring peaks have equal intensity, h, Δm is defined as the mass difference necessary to achieve a valley height between the peaks of $0.1h$. This is known as the 10 % valley definition. Although these two definitions are equivalent, the first is more useful since in practise it is rare to find peaks of equal intensity next to each other.

Some common interferences, together with the analyte species with which they interfere and the resolution required to separate them, are given in Table 2.1.[5,6] There are many other interferences, including isobars, that require a much greater resolution to be separated from the analyte signal than the examples listed, e.g. a resolution of around 4×10^6 is needed to separate $^{90}Zr^{18}O^+$ and ^{108}Pd.

Table 2.1 Theoretical mass resolution required to separate some typical interferences

Nuclide	Molecular ion	Mass difference	Resolution
$^{39}K^+$	$^{38}Ar^1H^+$	0.007	5700
$^{40}Ca^+$	$^{40}Ar^+$	0.0002	193 000
$^{51}V^+$	$^{35}Cl^{16}O^+$	0.020	2600
$^{55}Mn^+$	$^{40}Ar^{15}N^+$	0.024	2300
$^{56}Fe^+$	$^{40}Ar^{16}O^+$	0.022	2500
^{75}As	$^{40}Ar^{35}Cl^+$	0.010	7800
$^{80}Se^+$	$^{40}Ar_2^+$	0.008	9700

The resolution of quadrupole based ICP-MS systems is typically around 400, sufficient to separate the signals of ions one mass unit apart, but not enough to separate any spectral interferences. An ICP coupled to a double focussing mass analyser is the most widely used instrumentation capable of measuring at high resolution (see Fig. 1.2). Altering the widths of the entrance and exit slits sets the resolution of the system; the more narrow the slits, the higher resolution. Most modern double focussing single collector ICP-MS instruments are capable of a maximum resolution of between 10 000 and 12 000. Loss of sensitivity at increased resolution is unavoidable as the slits are closed, and is a price that must be paid for interference-free analysis. Transmission of ions at a resolution setting of 10 000 is typically less than 3 % of the transmission at a resolution of 300.[7] Although higher resolution sector based instruments have been developed,[8] the low ion transmission, and therefore low sensitivity, associated with increasing resolution means that these systems are not currently applicable to general use.

Douglas and co-workers[9, 10] have investigated the possibilities of altering the operating parameters of the quadrupole mass analyser to enable high resolution analytical measurements. Although not widely used, this system has the inherent quadrupole advantages of mechanical simplicity, light weight and high speed electronic scanning, combined with resolving power comparable to a double focussing instrument. The quadrupole can also be operated in a normal mode to give higher sensitivity for uninterfered isotopes, with electronic switching to high resolution when required, even while peak hopping to the isotope of interest.

ICP-MS systems with time-of-flight (TOF) mass analysers are capable of operating at resolution settings up to approximately 2000, sufficient to separate some polyatomic interferences.[11] Thus far however, there have been few publications that have exploited this capability.

If an instrument capable of high resolution analysis is not available, or an interference requires more than the maximum resolution to be separated from the analyte signal, other ways of surmounting the problem of spectral interference must be used, as discussed in the following sections.

2.2.1.1 Sample preparation procedures

Wherever possible, nitric acid should be the only acid used in sample preparation. As H, N and O species are present in the plasma and entrained atmospheric gases, no further interferences are introduced by nitric acid. The use of hydrochloric, phosphoric and sulfuric acids can lead to many and varied interfering species, and a significantly more complicated mass spectrum.

Co-precipitation of either the interfering species or the analyte element is a viable method of eliminating a matrix-based spectroscopic interference, as is the separation of the matrix using chelating or ion exchange resins. The eluent from the column can be directly aspirated into the ICP-MS instrument, reducing the sample handling and time required. The partition of isotopes between the resin and solution phases has been found to be mass dependent for several elements,[12] resulting in variations in isotope ratios across a chromatographic peak. Care must therefore be taken monitor and correct for this fractionation if separation procedures are carried out on-line. It must also be ensured that no contamination is introduced during the process, and that good recovery of the analyte species is achieved.

2.2.1.2 Sample introduction methods

Desolvation, either through cooling the spray chamber or the use of a membrane, is an effective technique for reducing the polyatomic interferences due to water and other solvent molecules.[13] Oxides, hydroxides and nitrides can all be reduced while increasing the analyte signal. Ultrasonic nebulisation can be combined with desolvation to improve sensitivity without significantly affecting the background.[14] This technique is particularly useful in cases where only small amounts of sample are available.

Electrothermal vaporisation (ETV) is another method for reducing the amount of solvent that reaches the ICP. Bjorn *et al.*[15] found that ETV significantly reduced most spectral interferences in comparison with pneumatic nebulisation. Since this method increases the transport efficiency, however, it is reasonable to assume that some matrix-based interferences will be enhanced.[16]

Hydride generation not only improves the transport efficiency but also separates the analyte element from the matrix, alleviating non-spectroscopic interferences due to complex matrices such as seawater.[17] Although the technique is limited to those elements that are hydride forming, this includes some elements that are difficult to analyse using standard ICP-MS such as As and Se. Vapour generation can be used in a similar way for a different range of elements.[18]

Sample introduction techniques such as slurry nebulisation,[19] powder dispersion and laser ablation avoid the use of any acid digestion, allowing fast, simple sample preparation that introduces no interferences in addition to those present in the sample matrix.[16] Additionally, the dry plasma conditions resulting from these methods have been shown to reduce the levels of some spectral intereferences.[20]

2.2.1.3 Plasma alterations[16]

Mixed gas plasmas, involving the addition of a second gas such as N_2 to the main Ar stream, have been found to reduce the signal due to $ArCl^+$, Cl_2^+, Ar_2^+ and other polyatomic ions, although the interferences at some masses were seen to increase. Besides N_2, H_2, He and Xe have also been used to form mixed gas plasmas with Ar. The use of a mixed gas plasma depends on the application involved, *e.g.* an Ar-N_2 ICP is not suitable for Si determinations, due to the $^{14}N_2^+$ interference at m/z 28, the major isotope of Si.

The microwave induced plasma (MIP) enables other gases, in particular helium, to be used to form a plasma ion source. Since argon is the source of many important interferences, the use of a He MIP gives rise to a substantially cleaner spectrum above m/z 40. The higher ionisation potential of He compared to Ar leads to a plasma with increased ionising power. This facilitates the analysis of elements that are harder to ionise (*e.g.* Br, Cl, P), but also results in more N, O and H based interferences. The levels of these species are further enhanced as the lower power and gas flows used in an MIP, compared to an ICP, leads to greater entrainment of atmospheric gases.

2.2.1.4 Cold plasma techniques

The operation of a plasma at lower than normal power, resulting in a lower temperature in the plasma, has been used to reduce the influence of argon based molecular ions.[21] The background can be significantly reduced or even eliminated at m/z 40($^{40}Ar^+$), 41 ($^{40}Ar^1H^+$), 56 ($^{40}Ar^{16}O^+$) etc. enabling measurement of isotopes that are impossible with conventional quadrupole ICP-MS. Typically, 600 W forward power is used for cold plasma conditions, compared to 1300 W for normal operation. In combination with cold plasma, a grounded metal screen or shield is positioned between the torch and the RF coil after plasma ignition. This eliminates the secondary discharge and therefore reduces the formation of molecular ions.[22]

Cold plasma techniques have been applied for the determination of K,[21] Ca,[23] Fe, Na and Li,[24] however the technique has been shown to be prone to non-spectroscopic interferences, even at moderate matrix element concentrations.[25] Although these effects may be overcome through the use of an internal standard, cold plasma is most useful for the analysis of high purity acids and other samples of low salt concentration.[26]

2.2.1.5 Multivariate correction methods

The measurement of polyatomic interferences and multiply charged ions at alternative isotopes can be used to correct the analyte signal in a similar way to isobaric interferences. Methods such as multiple linear regression and principal component analysis can be used to great effect, as long as the interferences arising from a particular matrix are known in detail.

de Boer has used a spreadsheet based calculation method to estimate the contributions of interferences to the mass spectrum in the range 51-88.[27] It was concluded that spectral fitting was applicable to the mass range in question, but was limited by instabilities in the molecular ion interference level. This model has recently been taken further to include real time adjustment of the equations used to calculate the contributions of interferences to analyte signals, involving the measurement of an 'interference check solution.[28] Another technique using the 'Massive Inference' algorithm[29] has been used to calculate the contributions of

molecular ions to analyte signals. Once the molecular ions expected from the sample matrices were entered into the software, the mass spectrum of a number of different certified reference materials could be accurately reproduced.[30]

A method based on empirical modelling and experimental design has also been developed, specifically for the interferences from a sodium, calcium, chlorine and sulfur matrix.[31] It was found that the dependence of the magnitude of the interference on matrix composition is a complex expression including quadratic terms and interactions between matrix elements.

2.2.1.6 Collision/reaction cells

Collision cells provide chemical resolution, using ion-molecule chemistry to remove (or at least reduce the number of) polyatomic ions. They also have the effect of thermalising the ions, reducing the energy spread, thereby enhancing transmission through the mass analyser. Collision cells have the inherent disadvantages of severe loss of low mass analyte signal, and the introduction of new interferences to the mass spectrum from reactions occurring in the cell. These effects are minor, however, compared to the advantages that can be seen.[32-35]

As well as reducing polyatomic ions, collision cells have also been used to overcome isobaric interferences, either by selectively reacting the interfering element to move it away from the isotope of interest,[34] or selectively reacting the analyte element, and moving it to a clear part of the mass spectrum. This approach has been exploited for the determination of the ^{87}Sr / ^{86}Sr isotope ratio in the presence of Rb.[36] CH_3F was used as a reactive cell gas to convert Sr^+ to SrF^+, the $^{87}SrF^+$ / $^{86}SrF^+$ ratio measured in geological samples was in good agreement with the ^{87}Sr / ^{86}Sr isotope ratio determined by TIMS. The bias correction factor for the SrF^+ ratio was more significant than that required for the standard Sr ratio, possibly due to mass dependence of the rate constant for the reaction involved.

2.2.2 Noise in ICP-MS analysis

The ICP is a reasonably stable source, however any ions measured sequentially will have uncorrelated noise associated with them due to the different plasma conditions they have experienced.[37] This noise is minimised through isotope ratio

measurements.[38] Noise spectral analysis reveals the relationship between the intensity and frequency of noise. The level of noise decreases with increasing frequency between 0 and 5 Hz with a $1/f$ relationship, thereafter the overall noise remains fairly constant. The spectrum is punctuated by spikes corresponding to noise associated with the sample introduction system (peristaltic pump and nebuliser), pick up from ac power lines and an audio frequency noise component due to processes occurring in the plasma. If the isotopes of interest are rapidly scanned such that the time separating the measurement of the isotopes is less than the period of low frequency noise, then the ratio of two isotopes will effectively be free from this noise. Through this and optimisation of other measurement parameters, isotope ratio measurements on ^{107}Ag / ^{109}Ag to a precision of 0.05 % RSD have been achieved using a quadrupole ICP-MS system.[38] The remaining noise was due to a combination of counting statistics and instability in mass bias and mass calibration.

Bandura et al.[39] have demonstrated the potential of a collision/reaction cell for improving the precision of isotope ratio measurements in quadrupole ICP-MS; precision levels of 0.1 %RSD have been reported for such systems.[40, 41] The theory behind this observation is as follows. Two ions of different mass are sampled simultaneously from the plasma at time T. In a standard quadrupole ICP-MS system, both ions will arrive at the detector at time T + t, and only one or the other can be detected. When a pressurised collision cell is in the path of the ions, it is conceivable that ion A will undergo a greater number of collisions with cell gas atoms/molecules than ion B, meaning that ion A will take longer to reach the detector. If the ions arrive at the detector at sufficiently different times, they can both be detected. As the ions left the plasma at the same time, the noise associated with each ion is highly correlated and cancels more effectively when the ratio A / B is calculated, resulting in improved isotope ratio precision.

Double focussing systems cannot scan as quickly as quadrupole mass analysers, therefore the time between measurement of two isotopes comprising a ratio is longer in double focussing ICP-MS. This means that the noise associated with each isotope is less correlated and cancels less efficiently when the isotope ratio is calculated, leading to worse measurement precision. In low resolution mode, this

loss of precision is countered by the reproducibility of the measurement of the flat topped peaks produced by double focussing mass analysers, as discussed in Chapter 1. An isotope ratio precision of 0.1 %RSD is routinely achievable by double focussing ICP-MS.[2]

Isotope ratio precision can only be further improved by detecting ions simultaneously. As the ions will have left the plasma at the same time, the noise associated with them will be the same, and will cancel when the ion signals are ratioed. Houk and co-workers[42] designed an instrument that splits the ion beam into two after extraction, with each beam having its own quadrupole channel and detector. A high degree of correlation between the two signals resulted in good isotope ratio precisions (< 0.5 % RSD), however sensitivity was around 100 times lower than for conventional quadrupole ICP-MS systems.

Double focussing ICP-MS systems, coupled to multiple Faraday collector arrays, are capable of measuring isotope ratios to precisions of less than 0.01 % RSD, comparable to that achievable by TIMS.[43] Multi-collector ICP-MS has been applied to isotopic determinations for elements across the mass range, a detailed discussion is presented below. Most multi-collector ICP-MS systems can only be used at low resolution, and so are limited to measurement of uninterfered isotopes. Specialised sample preparation and/or sample introduction techniques are required to extend the use of multi-collector ICP-MS to a wider range of elements.[44]

2.2.3 Non-spectral interferences
Also known as matrix effects, non-spectral interferences are common to all types of ICP-MS instrument. They are caused by concomitant species in the sample matrix and by the ICP-MS instrumentation itself. Processes such as sample transport, ionisation in the plasma, ion extraction and the behaviour of ions once in the ion beam are influenced, leading to a reduction or enhancement in the analyte signal.[16] The types of species present and their concentration in the matrix is directly linked to the effects that are seen. By convention, this work uses the full names of elements considered to be part of the sample matrix, and chemical symbols for all analyte elements.

The make up of the sample matrix can have an effect on the temperature in the plasma, which in turn affects the atomisation, vaporisation and ionisation processes that occur therein. In particular, the introduction of organic solvents, for example due to coupling of liquid chromatography to ICP-MS, has been seen to cause a reduction in temperature and electron density in the plasma due to the energy required to dissociate the stable molecular species that are present.[45] Matrix matching of standards or dilution with a common solvent is required to ensure accurate calibrations.

An excess of easily ionisable elements in the sample matrix also affects the plasma conditions. These kinds of levels are found in many human samples (*e.g.* serum, urine), and in environmental samples such as seawater. These effects have been found to depend on the properties of the analyte species as well as the matrix.[46] In general, as the ionisation potential of the analyte increases, the recovery of the analyte in the presence of a certain matrix decreases. Non-analyte signals, such as Ar based polyatomic species, are also affected by the presence of the matrix. It has been suggested that these signals could be used to predict the extent of the matrix effect in a given sample.[47]

High salt matrices can also lead to solids building up on the sampler and skimmer cones, leading to suppression of the analyte signal. The salt build up has a major effect on the sampling process, as well as simply blocking the path into the spectrometer. It has been shown that it is preferable to allow some deposition in order to condition the cones to the sample matrix prior to analysis. This allows a steady state situation to be reached where the rate of solid build up is equivalent to the rate of dissociation.[16]

The extent of non-spectral interference observed as a result of a particular matrix is strongly dependent on instrumental parameters (*e.g.* nebuliser flow rate, torch injector diameter, RF power), as well as the actual instrument being used. Different levels of interference have been observed from 60 % suppression to 100 % enhancement of the same analytes in the presence of the same matrix concentration.[46]

Matrix effects can be avoided by separating out the analyte species prior to analysis using selective precipitation, chelating resins or ion exchange columns. However, these processes are time consuming, it is difficult to be sure of 100 % analyte recovery and additional bias or contamination could easily be introduced, affecting the accuracy of the overall analytical process. The amount of matrix introduced to the ICP can also be reduced by the use of alternative sample introduction techniques. Desolvating membranes used in conjunction with micro-concentric or ultrasonic nebulisers greatly reduce the number of solvent molecules that reach the plasma, allowing more efficient processing of the analyte species. Methods such as flow injection, where the sample is injected into an aqueous carrier stream, significantly reduce the quantity of the matrix while also allowing high sample throughput.[16] Flow injection is less likely to clog the cone orifices than continuous nebulisation, and reduces sample consumption. Since a transient signal is produced, however, there is less time for analytical measurements, limiting both the number of elements it is possible to determine and the achievable isotope ratio precision.

The design of the nebuliser and spray chamber, physical properties of the solvent such as viscosity and surface tension, and the nebuliser gas flow all have an influence on the size distribution of the particles that reach the plasma, which in turn affects the ionisation characteristics of the ICP. Differences in plasma conditions experienced by samples and standards must be prevented by matching them in terms of solvent, ensuring similar nebulisation and transport characteristics. It has been suggested that a spray chamber operated at a lowered temperature has a beneficial effect on the degree of matrix effects observed due to a reduced solvent load on the ICP.[13] Individual droplets can cause severe signal fluctuations due to their behaviour in the plasma, even down to the level of the vaporisation of droplets causing local temperature variations, affecting the ionisation of analyte species.[48]

2.2.4 Mass bias

The transmission of ICP-MS instruments is mass dependent, therefore all isotope ratios measured by ICP-MS deviate from the true value. This error is known as the mass bias. Study of the sources of uncertainty in isotope ratio measurement by

ICP-MS has shown that for several isotope systems, mass bias correction is the most significant contributing factor to the total uncertainty.[49]

It was put forward some time ago that the majority of mass bias observed in ICP-MS is due to space charge effects occurring in the skimmer region.[50] Various methods have been applied for the reduction of the space charge effect including the use of non-optimal ion lens settings (tuning the instrument to reduce the space charge at the expense of some sensitivity), alterations to the ion lens and vacuum interface design,[51] the use of mixed gas plasmas[52] and the addition of electrons to the ion beam behind the skimmer.[53]

Although high accelerating voltages do reduce the space charge (and so should reduce the mass bias),[54] a quadrupole mass analyser requires low ion kinetic energies and a narrow energy distribution for effective mass resolution. This means that after a greater accelerating potential on extraction, the ions must be slowed again before entering the quadrupole. In this deceleration, it is expected that space charge effects will occur, and mass dependent effects will be seen.[55]

Since double focussing ICP-MS generally utilises an accelerating potential of the order of 8000 V, the space charge effect is expected to be less than in a quadrupole ICP-MS system.[56, 57] A higher accelerating voltage results in a less divergent ion beam so that high ion transmission is maintained even when the source slit is narrowed for high resolution work.[6] Several groups have found that the mass bias is in fact similar for double focussing and quadrupole instrumentation.[2, 5] This suggests that the majority of mass bias effects take place in the field free region between the cones, or immediately behind the skimmer where there is no penetration from the extraction field.

A mathematical correction must be applied to take the mass bias into account. This requires the measurement of a known isotope ratio to calculate the bias, which is then applied to the analyte ratio. The reference ratio is either determined in reference solutions analysed periodically through the sample run (external standardisation or standard bracketing) or in the sample solutions themselves (internal standardisation). The advantage of external correction is that the mass

25

bias is measured at the same mass and relative abundance as the analyte, however the magnitude of the mass bias may change in the time lapse between measurement of the standard and the sample. Internal standardisation allows near continuous monitoring of the mass bias and can also be used to correct for matrix effects. This method may be inaccurate, however, as the isotopes used to calculate the mass bias are different from the analyte isotopes.

The calculated mass bias is applied to the analyte ratio using standard mathematical models,[57, 58] which are discussed in detail in Chapter 5.

2.2.5 Detector dead time (pulse counting detectors)

When an ion strikes the detector, there is a finite period of time while the detector processes that signal, known as the dead time (typically 10-30 ns). Any ion arriving at the detector during this time will not be counted, and so the observed count rate is lower than the actual count rate.[59] The dead time typically starts to play a role when count rates are around 10^6 counts per second or higher, and can be important when measuring extreme isotope ratios. Detector dead time must be monitored regularly as it is prone to changes with the age of the detector.[60] The expression generally used for correcting for detector dead time is as follows:

$$I_{true} = \frac{I_{obs}}{1 - \tau I_{obs}} \qquad\qquad 2.2$$

I_{true} and I_{obs} are the true and observed count rates respectively, τ is the dead time in seconds. It should be noted that this equation is a simplification of the true expression for dead time correction given by Russ and Bazan[61] as:

$$I_{true} = \frac{I_{obs}}{1 - \tau I_{true}} \qquad\qquad 2.3$$

This equation was derived by setting the true counts equal to the observed counts plus the counts missed due to the dead time.

The detector dead time is traditionally determined according to the method proposed by Russ.[62] An isotope ratio differing from unity is measured in standard solutions of different concentration levels with any automatic dead time in the instrument set to zero. For each concentration level, the isotope ratio corrected for dead time and divided by the true ratio is plotted against the dead time used in the correction. The intersection of the curves for different elemental concentrations corresponds to the correct detector dead time for the instrument.

Held and Taylor[60] recently proposed a linear method for dead time calculation, however this model requires prior knowledge of the mass bias to solve the relevant equation. They proposed simultaneous evaluation of the mass bias by measuring an isotopic ratio with a value close to unity, so that the measured data should be unaffected by dead time.

Appelblad and Baxter[63] have outlined an extension of the Held and Taylor model. This method requires measurement of an element with two isotopes that are of significantly differing abundance. By plotting the count rate of the major isotope divided by the count rate of the minor isotope against the major isotope count rate, a linear plot is obtained. The intercept is R_{true}/κ, where R_{true} is the true isotope ratio and κ represents a mass bias correction equation, and the gradient is $\tau(1 - R_{true}/\kappa)$ where τ is the detector dead time. In this way, both the mass bias and the detector dead time can be determined experimentally as part of instrument calibration. The model can also be used to correct data post acquisition.

Pulse-to-pulse timing measurements using an oscilloscope have been used to directly evaluate the detector dead time.[64] This method may be used as a validation of the isotope ratios method described above, which can be influenced by elemental contamination and non-linear detector behaviour.

2.3 Application of Quadrupole ICP-MS to Isotope Ratio Measurements

One of the key advantages of quadrupole mass analysers is their ability to scan quickly across a broad mass range. For isotope ratio determinations, individual masses are monitored. When operating in this mode, the quadrupole is inherently unstable, and therefore not suited to highly accurate and precise ratio measurements.[58] Typical isotope ratio precision for quadrupole ICP-MS is 0.1 to 0.5 %RSD,[2] although as discussed above, optimisation of acquisition parameters has enabled a precision of 0.05 %RSD to be recorded for ^{107}Ag / ^{109}Ag.[38]

The basic advantages of quadrupole ICP-MS, including ease of operation, widespread availability and mechanical simplicity,[9, 59] have meant that the technique has been used in isotopic determinations for a wide range of geological,[65, 66] biological[23, 67-69] and environmental applications.[70-73]

2.4 Isotope Ratio Determinations Using Double Focussing ICP-MS

Double focussing ICP-MS instrumentation has been widely applied to the measurement of isotope ratios. Single collector double focussing ICP-MS (SC-ICP-MS) has two principal advantages over quadrupole systems in these determinations. Firstly, the flat topped peaks produced by the double focussing mass analyser in low resolution mode provide improved isotope ratio precision, and secondly the range of elements to which isotopic analysis can be applied is broadened through the use of increased resolution to separate spectral interferences. Multi-collector double focussing ICP-MS (MC-ICP-MS) enables isotope ratios to be measured to a precision comparable to that achievable by TIMS.[2] The reported uses of double focussing ICP-MS in both single and multi-collector modes are reviewed in the following section, elements are considered in mass order.

2.4.1 Lithium

Li is the lightest metallic element and has two stable isotopes, ^{6}Li (7.5 % natural abundance) and ^{7}Li (92.5 %). Commercial Li reagents are depleted in ^{6}Li, which

is used in nuclear weapon manufacture; the abundance for this isotope may be as low as 2 %.[74] Due to the high relative mass difference between the Li isotopes they are severely affected by mass bias in ICP-MS measurements. An error of around 10 % is expected, reference materials with certified isotopic composition must be used to monitor and correct for this bias. The high relative mass difference also means that mass dependent natural processes, such as evaporation and adsorption, can significantly alter the Li isotopic abundance. This propensity for the isotopes to fractionate in nature allows variation in the Li isotope ratio to be used as a geochemical tracer.[75] Due to the high level of precision required for geological investigations, MC-ICP-MS techniques have been most widely applied. MC-ICP-MS Li isotope ratio data was first reported in 1999,[76] a precision of 0.11 %RSD was achieved. Subsequently, MC-ICP-MS has been used for the measurement of Li isotope ratios to illustrate a lack of Li isotope fractionation during volcanic rock formation, [77] for the investigation of geological processes in the Earth's history,[78, 79] and has recently been applied to a wider variety of rock types.[80]

2.4.2 Boron

Similar to Li, B has two stable isotopes, ^{10}B (20 %) and ^{11}B (80 %). The large relative mass difference between the isotopes has lead to significant fractionation in nature, in particular in the marine environment where the absorption of B into sediments from seawater favours the ^{10}B isotope. B isotope ratios have traditionally been determined using TIMS, however the high ionisation potential of this element means that the ratios must be measured indirectly *via* the $CsBO_2^+$ species. As previously mentioned, the ionising power of the ICP is much greater than that of a thermal source, allowing direct B measurements to be made. SC-ICP-MS instrumentation has been used to determine the sources of anthropogenic B input into surface and ground water.[81] The characteristic ^{10}B / ^{11}B ratio in detergents was measured to a precision of 0.1 to 0.2 %RSD, sufficient to discriminate between different B sources. The application of MC-ICP-MS to the measurement of the B isotope ratio has recently been reported.[82] The technique was applied to derive a mathematical relationship describing the effect of pH on the fractionation of the B isotopes between seawater and calcite rock.

2.4.3 Magnesium

Mg has 3 stable isotopes: ^{24}Mg (79 %), ^{25}Mg (10 %) and ^{26}Mg (11 %). Analysis of Mg by ICP-MS may be affected by spectral interference from species such as C_2^+, C_2H^+, CN^+, NaH^+, $^{48}Ca^{2+}$ and tailing from $^{23}Na^+$. These interferences pose no problem to the analysis of clean standard solutions, as illustrated by Vanhaecke *et al.*[83] in one of the first independent reports of isotope ratio measurement using a commercial SC-ICP-MS system. In low resolution mode, Mg isotope ratios were measured to a precision of 0.033 %RSD.

As Mg has many physiological functions, including muscle operation, protein synthesis and energy supply, the uptake and transport of Mg within organisms are of great interest. Stable isotopes can be used to investigate the Mg distribution in biological systems, however spectral interferences are problematic due to the significant levels of carbon, calcium and sodium in samples from such systems. Although cool plasma techniques have been found to alleviate some interferences, they were not removed completely.[84] At a resolution setting of 3000, all the above interferences are separated from the Mg isotopes. This approach has been used to measure accurate isotope ratios to a precision of 0.2 %RSD, and applied to the investigation of Mg transport in fish.[84]

Mg isotope ratios have also been measured by MC-ICP-MS, a precision level of 0.01 %RSD has been reported.[85] Spectral interferences were reduced using sample desolvation. Such highly precise determinations have been used to show the geological variations in the isotopic composition of Mg, and that the variation in carbonates is influenced more by mineralogical than by temperature effects.[86]

2.4.4 Silicon

Si is a difficult element to determine using quadrupole ICP-MS due to spectral interferences affecting all three isotopes, ^{28}Si (92.2 %), ^{29}Si (4.7 %) and ^{30}Si (3.1 %). The majority of these interferences are based on combinations of nitrogen, oxygen and hydrogen, and are therefore extremely abundant in the most common solutions used in ICP-MS, which are based on nitric acid. Additionally, the Si background in ICP-MS can be significant as the standard nebuliser, spray chamber, injector and torch are manufactured from silica. The interferences can be

separated from the Si isotopes using a resolution of 3000, well within the capabilities of commercial SC-ICP-MS instruments. Wildner[87] illustrated the capabilities such a system, an isotope ratio precision of 0.5 %RSD was achieved. It was suggested that the application of increased resolution would allow the highly accurate quantification of Si using isotope dilution techniques, and these methods have been applied for the determination of Si in a variety of certified reference materials, biological and clinical samples using a ^{30}Si isotopic spike.[88] PFA sample introduction apparatus and a sapphire injector were used to reduce the background level of Si.

Si isotope ratios have also been measured using MC-ICP-MS, allowing Si to be used as a geochemical tracer. ^{30}Si could not be measured directly due to the $^{14}N^{16}O^+$ interference, accurate results were obtained by extrapolation of ^{29}Si data.[89] Although not ideal, this approach may be preferred to the traditional method for Si isotope ratio measurements that involves the use of a hazardous fluorinating gas.

2.4.5 Sulfur
The four stable isotopes of sulfur (^{32}S 94.93 %, ^{33}S 0.76 %, ^{34}S 4.29 % and ^{36}S 0.02 %) are all overlapped by spectral interferences, the most severe being $^{16}O_2^+$ on the major isotope ^{32}S. SC-ICP-MS operated at a resolution of 4000 has been used for the determination of S isotope ratios to a precision of 0.1 %RSD.[90] Sample desolvation was used to reduce the intensity of the interferences, lowering the resolution required to achieve complete separation of the analyte and interfering peaks. Isotope dilution techniques using SC-ICP-MS operated at increased resolution have been used for the quantification of S in geological materials[91] and in diesel fuel,[92] an application with growing importance due to planned legislation limiting the amount of S permitted in fuels. This method has also been used in combination with capillary electrophoresis for the investigation of metallothionein distribution in brain tissue and other biological samples.[93, 94]

2.4.6 Potassium and calcium
Both K and Ca are essential elements in the human diet, and both are severely effected by argon based spectral interferences in ICP-MS. K has three stable

isotopes ^{39}K (93.26 %), ^{40}K (0.012 %) and ^{41}K (6.73 %). SC-ICP-MS has been used at a resolution setting of 9000 to separate ^{38}ArH$^+$ and ^{40}ArH$^+$ from the major K isotopes, allowing the measurement of the ^{41}K / ^{39}K ratio in biological samples.[43] The accuracy of the determination was confirmed by analysis of a certified isotopic reference material, an isotope ratio precision of 0.7 %RSD was achieved.

Ca has six stable isotopes: ^{40}Ca (96.94 %), ^{42}Ca (0.65 %), ^{43}Ca (0.14 %), ^{44}Ca (2.09 %), ^{46}Ca (0.004 %) and ^{48}Ca (0.19 %). Unfortunately, the major Ca isotope coincides with the major argon isotope at m/z 40, the mass difference between the two species is so small that the resolution required to separate them is in excess of 190 000, well beyond the capabilities of commercial double focussing ICP-MS systems. ^{42}Ca, ^{43}Ca and ^{44}Ca suffer from spectral interferences in the form of argon hydrides, CO_2^+, SiO^+ and Sr^{2+}, while the minor isotopes ^{46}Ca and ^{48}Ca are also affected by isobaric overlap from titanium isotopes. ^{42}Ca$^+$ / ^{43}Ca$^+$ and ^{44}Ca$^+$ / ^{43}Ca$^+$ have been measured in urine, using SC-ICP-MS at a resolution setting of 4000.[95] At this resolution, the polyatomic species were separated from the Ca isotopes, however a mathematical correction had to be applied for the doubly charged strontium interference. The isotope ratio precision of 0.4 %RSD was sufficient for the investigation of Ca absorption using stable isotope techniques. Subsequently, the same method has been used to investigate Ca absorption from foods.[96] Precisions of 0.23 %, 0.25 % and 0.05 %RSD were achieved for ^{42}Ca$^+$ / ^{43}Ca$^+$, ^{44}Ca$^+$ / ^{43}Ca$^+$ and ^{44}Ca$^+$ / ^{42}Ca$^+$ respectively.

Improved precision for Ca isotope ratios has been reported using MC-ICP-MS.[44] The polyatomic interfering species were reduced to an acceptable level through the use of sample desolvation to limit the amount of hydrogen, nitrogen and oxygen introduced to the plasma. The doubly charged Sr interference was again corrected for mathematically. The ^{44}Ca$^+$ / ^{42}Ca$^+$ was determined in an isotopic calcium carbonate reference material to a precision level of 0.01 %RSD. The variation of Ca isotope abundances found in natural samples was in agreement with previous studies by TIMS.

2.4.7 Titanium

Ti has five stable isotopes: ^{46}Ti (8.25 %), ^{47}Ti (7.44 %), ^{48}Ti (73.72 %), ^{49}Ti (5.41 %) and ^{50}Ti (5.18 %). Spectral interferences limit Ti determinations by quadrupole ICP-MS. These species are mostly based upon combinations of nitrogen, oxygen, hydrogen, silicon, phosphorous and sulfur, and can be separated from the Ti isotopes using a resolution of 3000. Makishima and Nakamura[97] have used SC-ICP-MS operated at increased resolution to determine Ti isotope ratios for use in isotope dilution calculation of the Ti concentration in silicate materials. Good reproducibility was achieved for Ti levels in a variety of geological reference materials.

Natural fractionation of Ti isotopes has been investigated using MC-ICP-MS.[98, 99] Sample desolvation was employed to reduce the levels of interfering species. Ti isotope ratios in natural samples relative to the same ratios in a reference material were determined to a precision of 0.02 %RSD.

2.4.8 Chromium, iron and nickel

Cr, Fe and Ni are all multi-isotopic elements that are difficult to determine by ICP-MS due to spectral interferences from ArC^+, ArN^+, ArO^+, $ArOH^+$ and related species. Although these polyatomic ions can be separated from the analyte isotopes using a resolution of 3000 to 4000, the isobaric overlaps of Cr and Fe at m/z 54, and Fe and Ni at m/z 58 pose a significant analytical challenge.

Cr has four stable isotopes: ^{50}Cr (4.35 %), ^{52}Cr (83.79 %), ^{53}Cr (9.50 %) and ^{54}Cr (2.36 %). Cr isotope ratios have been measured using SC-ICP-MS at increased resolution for the determination of Cr concentrations by isotope dilution methods. This technique has been applied to both geological[100] and environmental[101] reference materials. In both cases the isotopes used were selected to avoid the spectral overlap of ^{54}Fe.

The stable Fe isotopes are ^{54}Fe (5.85 %), ^{56}Fe (91.75 %), ^{57}Fe (2.12 %) and ^{58}Fe (0.28 %). Similar to Cr, Fe concentrations have also been determined by isotope dilution using high resolution SC-ICP-MS to measure the isotope ratios. Wu and Boyle[102] have quantified Fe in seawater in this manner, using co-precipitation to

concentrate the Fe prior to analysis. The determination of Fe in biological samples is of particular importance due to the key role of the element in the transport of oxygen in the body. The applicability of SC-ICP-MS to the isotope dilution determination of Fe in such samples has been illustrated,[103] an isotope ratio precision of 0.7 %RSD was achieved for $^{57}Fe^+$ / $^{56}Fe^+$, at a resolution setting of 3000. Vanhaeke et al.[104] investigated several methods for the elimination of spectral interferences. Using SC-ICP-MS, application of a resolution of 3000 was preferred to the use of cool plasma techniques. $^{54}Fe^+$ / $^{56}Fe^+$ and $^{57}Fe^+$ / $^{56}Fe^+$ were measured to a precision of 0.2 – 0.4 %RSD and $^{58}Fe^+$ / $^{56}Fe^+$ to around 1 %RSD in standard solutions containing no Cr or Ni.

Using sample desolvation and tuning of instrument parameters, the level of ArN^+ and ArO^+ have been reduced sufficiently to allow the determination of the ^{57}Fe / ^{54}Fe isotope ratio by MC-ICP-MS.[105] Precision better than 0.01 %RSD (95 % confidence level) was achieved for an Fe isotopic reference material and the method was successfully applied to isotopic measurements of geological samples, following a sample preparation procedure to eliminate Cr. A sample preparation procedure allowing the determination of Fe isotope ratios in whole blood by MC-ICP-MS has also been reported.[106] The ^{58}Fe isotope was not measured, allowing the use of Ni isotopes to correct for mass bias. Accurate measurement of Fe isotopic fractionation in a whole blood reference material was performed with a precision of 0.02 %RSD.

Fe isotope ratios have also been determined in solid samples using laser ablation MC-ICP-MS.[20] Argon based species were significantly reduced by the dry plasma conditions resulting from the laser ablation sample introduction; on peak background subtraction was used to account for the residual levels of interference. Sample-standard bracketing was used, resulting in precision of less than 0.1 %RSD for Fe isotope ratios in minerals and meteorites.

Ni has five stable isotopes: ^{58}Ni (68.08 %), ^{60}Ni (26.22 %), ^{61}Ni (1.14 %), ^{62}Ni (3.63 %) and ^{64}Ni (0.93 %). Like Cr, Ni isotope ratio measurements by double focussing ICP-MS have been limited to the isotope dilution determination of Ni concentrations in reference materials. SC-ICP-MS operated at increased resolution

has allowed accurate measurement of the Ni content of rocks[100] and natural waters.[107]

2.4.9 Copper

Cu has two stable isotopes ^{63}Cu (69.17 %) and ^{65}Cu (30.83 %). The determination of Cu isotope ratios in untreated samples is hindered by spectral interference from ^{40}Ar^{23}Na$^+$ and various sulfur, phosphorous and silicon containing species. In these cases, the time consuming separation of Cu from the sample matrix can be avoided through the application of increased resolution. SC-ICP-MS has been used at a resolution setting of 3000 for the determination of the Cu isotope ratio to a precision of 0.3 %RSD in a human serum reference material and 0.6 %RSD in an Antarctic sediment digest.[108] The level of Cu in the latter sample limited the achievable isotope ratio precision. Measurement of the Cu isotope ratio at increased resolution has been used in isotope dilution analysis for the determination of Cu concentrations in a variety of environmental, [101, 107, 109] geological[100] and biological samples.[93, 94, 103, 110]

With appropriate sample preparation procedures and sample desolvation, the levels of spectral interference for the Cu isotopes can be reduced sufficiently to allow determination of the ^{65}Cu / ^{63}Cu ratio using MC-ICP-MS.[111] The precision of these analyses (as good as 0.002 %RSD) was sufficient to measure variations in the Cu isotopic composition of natural materials.[111-113] MC-ICP-MS has also been used to investigate Cu isotopic fractionation during ion exchange processes[114] and increased ^{63}Cu has been found to correlated with increased ^{16}O abundance in chondrite rock samples.[115]

2.4.10 Zinc

Zn has five stable isotopes: ^{64}Zn (48.63 %), ^{66}Zn (27.90 %), ^{67}Zn (4.10 %), ^{68}Zn (18.75 %) and ^{70}Zn (0.62 %). Unfortunately, the major Zn isotope is overlapped by ^{64}Ni – a particular problem in ICP-MS analysis, as the sample and skimmer cones are most often made from nickel. All the Zn isotopes are affected by spectral interferences such as ArMg$^+$, ArCO$^+$, ArNO$^+$, SO$_2^+$, Cl$_2^+$ and Ba^{2+}. SC-ICP-MS has been applied to the determination of Zn isotope ratios in human faeces, urine and serum, using a resolution of 6000.[116] Isotope ratio precision of

0.7 %RSD was achieved for $^{67}Zn^+$ / $^{66}Zn^+$, $^{68}Zn^+$ / $^{66}Zn^+$ and $^{70}Zn^+$ / $^{66}Zn^+$, while the mathematical correction required to account for the Ni overlap degraded the precision of $^{64}Zn^+$ / $^{66}Zn^+$ to 1.2 %RSD. Similar to Cu, Zn isotope ratios have also been used in isotope dilution analysis for the determination of Zn concentrations in biological,[93, 94, 103, 110] geological[100] and environmental[107] samples.

Again like Cu, by use of sample preparation and desolvation techniques, the spectral interferences affecting the Zn isotopes can be reduced allowing isotope ratio determinations by MC-ICP-MS to a precision of 0.002 %RSD. Natural variations in Zn isotopic ratios have been found,[111] however the fractionation of Zn isotopes in ion exchange chromatography was smaller than that observed for Cu.[114]

2.4.11 Germanium and selenium

The stable isotopes of Ge are ^{70}Ge (20.8 %), ^{72}Ge (27.7 %), ^{73}Ge (7.7 %), ^{74}Ge (36.3 %) and ^{76}Ge (7.6 %). The Ge isotopic composition of terrestrial and extraterrestrial material has been determined by MC-ICP-MS by Hirata.[117] Using Ga to correct for mass bias, it was found that meteorites had significantly heavier Ge isotopic compositions than terrestrial samples, possibly due to Ge evaporation losses in meteoritic material. During such processes, lighter isotopes are lost more quickly, resulting in alteration of the isotopic composition. More recently, Ge isotope ratios have been measured in a standard solution to 0.01 %RSD using MC-ICP-MS.[118] It was noted that for natural samples, separation of Ge from the sample matrix is required for accurate isotope ratio determinations.

Se has six stable isotopes: ^{74}Se (0.9 %), ^{76}Se (9.4 %), ^{77}Se (7.6 %), ^{77}Se (23.8 %), ^{80}Se (49.6 %) and ^{82}Se (8.7 %). Se is badly affected by spectral interference from Ar_2^+ and related species. A resolution of over 10 000 is required to separate the ^{40}Ar dimer from the major Se isotope, ^{80}Se, approaching the maximum resolution achievable using commercial double focussing ICP-MS instrumentation. The potential of high resolution SC-ICP-MS for the isotope dilution determination of Se concentrations has been illustrated,[87] the Se isotope ratio precision was around 1 %RSD. Se determination by quadrupole ICP-MS is often carried out using hydride generation sample introduction to provide enhanced sensitivity,[119] and this

technique has been applied for the isotopic measurement of Se in geological materials using MC-ICP-MS.[120] Following separation of Se from the samples, the ^{82}Se / ^{78}Se ratio was measured to a precision of 0.013 %RSD, allowing variation in the Se isotopic composition of natural samples to be measured.

2.4.12 Rubidium and strontium

Rb has two stable isotopes, ^{85}Rb (72.17 %) and ^{87}Rb (27.83 %), the isotope ratio has been measured with a precision of 0.025 %RSD by MC-ICP-MS using Zr isotopes to correct for mass bias.[121] This resulted in improved reproducibility of Rb concentration measurements by isotope dilution.

Sr has four stable isotopes, ^{84}Sr (0.5 %), ^{86}Sr (9.9 %), ^{87}Sr (7.0 %) and ^{88}Sr (82.6 %). The exact abundance of the isotopes is variable in nature due to the β-decay of ^{87}Rb to ^{87}Sr. This variation forms the basis of the key Rb/Sr geochronology system and has found other applications in archaeology and food authenticity studies (see below). Due to the isobaric overlap of ^{87}Rb and ^{87}Sr, accurate Sr isotope ratios involving ^{87}Sr can only be achieved if any Rb present in the samples is removed prior to analysis. This is usually performed using an ion exchange resin, and is a time consuming and costly process.

Latkoczy et al.[122] have reported the determination of Sr isotope ratios by SC-ICP-MS in low resolution mode, a precision of 0.03 %RSD was achieved for measurement of the ^{87}Sr^{+} / ^{86}Sr^{+} ratio and accuracy was verified using an isotopic reference material. The method was applied to prehistoric bone samples containing negligible Rb levels, the quality of the Sr isotope ratios allowed anthropological conclusions to be drawn. Subsequently, laser ablation sample introduction has been used, allowing in situ measurement of Sr isotope ratios in bone samples[123] and fish otoliths[124] with a precision of 0.1 to 0.2 %RSD. Sr isotope ratio measurements by SC-ICP-MS following a cation exchange sample preparation procedure have been used for Rb/Sr geochronology.[125] An isotope ratio precision of 0.04 %RSD was recorded. The age of geological samples analysed by this method were in good agreement with the Rb-Sr ages of the same samples determined by TIMS. For samples containing significant levels of Rb, an on-line sample clean up procedure has been developed, involving the hyphenation

of ion chromatography to a SC-ICP-MS system.[126] This greatly simplified the sample preparation procedure required for the analysis of soil and bone samples, and provided accurate determination of the $^{87}Sr^+$ / $^{86}Sr^+$ ratio to a precision of 0.07 %RSD.

Sr isotope ratio measurements were among the first applications of MC-ICP-MS techniques.[127] Mass bias correction using the constant $^{88}Sr^+$ / $^{86}Sr^+$ ratio allowed accurate determination of $^{87}Sr^+$ / $^{86}Sr^+$ in an isotopic reference material to a precision of 0.008 %RSD. In recent years, the same approach has been applied by Ehrlich et al.[128] for Sr isotope ratios in natural water and rock samples to a precision level of 0.002 %RSD, and has been used for the investigation of a range of geological systems around the globe.[129-132] The precision of Sr isotope ratio measurements in these studies was consistently less than 0.005 %RSD, comparable to that achievable by TIMS. Laser ablation has also been used in combination with MC-ICP-MS for the accurate and precise determination of Sr isotope ratios.[133] Precision at the 0.01 %RSD level for $^{87}Sr^+$ / $^{86}Sr^+$ was sufficient for one study to draw conclusions on igneous rock formation processes,[134] and for another to make inferences on fish migration based on the Sr ratio measured in otoliths.[135]

2.4.13 Zirconium

Zr has five stable isotopes: ^{90}Zr (51.5 %), ^{91}Zr (11.2 %), ^{92}Zr (17.1 %), ^{94}Zr (17.4 %) and ^{96}Zr (2.8 %). Zr is an important element in geochronology (^{92}Zr-^{92}Nb chronometer). Zr isotopic composition yields information on previous ^{92}Nb content, which is an indicator of the formation sequence of the early solar system. Isobaric overlap from molybdenum isotopes may be problematic in Zr isotope ratio determinations, ion exchange chromatography is commonly used to separate Zr from the sample matrix. David et al.[136] have described the use of MC-ICP-MS for the determination of Zr concentration in terrestrial and extraterrestrial rocks using isotope dilution techniques. The resulting Zr/Hf ratios calculated were in good agreement with those calculated from isotope dilution TIMS data. This technique, combined with refined sample preparation procedures, has been used by other workers for the determination of Zr/Hf and Zr/Nb ratios in a range of geological materials.[137-139]

Laser ablation sample introduction for the determination of Zr isotope ratios by MC-ICP-MS has been described by Hirata and Yamaguchi.[140] Good agreement was found between ratios determined by laser ablation and solution nebulisation, although the precision of measurements by laser ablation (0.005 – 0.02 %RSD) was a factor of 2 worse than by solution nebulisation. This method has since been applied to a variety of rocks and meteorites, which, in combination with U-Pb age determination, has allowed accurate calculation of the value of the ^{92}Nb / ^{93}Nb ratio when the solar system was formed.[141]

2.4.14 Molybdenum

The seven stable isotopes of Mo are ^{92}Mo (14.8 %), ^{94}Mo (9.3 %), ^{95}Mo (15.9 %), ^{96}Mo (16.7 %), ^{97}Mo (9.6 %), ^{98}Mo (24.1 %) and ^{100}Mo (9.6 %). The applicability of SC-ICP-MS for the measurement of Mo stable isotope tracers has been assessed.[142] Although significant data in terms of the biokinetics of Mo in humans could be obtained, it was concluded that TIMS remained the method of choice for such determinations.

MC-ICP-MS has been used to determine the natural isotopic composition and atomic weight of Mo.[143] The results were in good agreement with TIMS data, and of a higher quality. In recent years, variation in the isotopic composition of Mo in seawater sediments has been reported, *via* measurement of the ^{97}Mo^{+} / ^{95}Mo^{+} ratio to a precision of 0.01 %RSD.[144] It was proposed that the fractionation was due to the differing efficiency of Mo scavenging from seawater, dependent upon the redox conditions. Measurement of the same ratio, to the same precision level, has been used to show fractionation of Mo isotopes during ion exchange processes and differences in the Mo isotopic composition between laboratory reagents and natural samples.[145] In this case, Zr or Ru was added to the samples and used to correct the mass bias. A Mo double isotope spike has also been used to measure the fractionation of the isotopes in geological samples.[146] Addition of the spike prior to any sample pre-treatment enabled natural variation in the samples to be separated from any fractionation induced by the preparation procedure, and allowed determination of the ^{98}Mo^{+} / ^{95}Mo^{+} ratio to a precision of 0.003 %RSD. Isobaric overlaps generally limit the number of Mo isotopes it is possible to

determine, however the abundance of all seven Mo isotopes has been measured in natural samples by MC-ICP-MS following solvent extraction for the separation of the sample matrix, and ion chromatography for the removal of elements with overlapping isotopes.[147] This also allowed calculation of the relative atomic mass of Mo.

2.4.15 Ruthenium and palladium and silver

Ru has seven stable isotopes: ^{96}Ru (5.5 %), ^{98}Ru (1.9 %), ^{99}Ru (12.8 %), ^{100}Ru (12.6 %), ^{101}Ru (17.1 %), ^{102}Ru (31.6 %) and ^{104}Ru (18.6 %). Pd has six stable isotopes ^{102}Pd (1.0 %), ^{104}Pd (11.1 %), ^{105}Pd (22.3 %), ^{106}Pd (27.3 %), ^{108}Pd (26.5 %) and ^{110}Pd (11.7 %). Despite the number of isotopes, there have been relatively few reports of Ru and Pd isotopic determinations. MC-ICP-MS has been used for the isotope dilution determination of both Ru and Pd concentrations in mantle rocks for the investigation of the behaviour of these elements during formation and differentiation of the mantle.[148, 149] Pd concentrations have also been determined in environmental and geological reference materials by isotope dilution using SC-ICP-MS.[150, 151] The Ru isotopic composition of pure chemicals measured by MC-ICP-MS has been shown to be in good agreement with that measured by TIMS.[152] It was noted however, that in the presence of Mo concentrations greater than 10^{-4} times the Ru concentration, the precision of the isotope ratio determinations was severely affected by the correction required to accurately account for the isobaric overlap.

Ag has two stable isotopes ^{107}Ag (51.84 %) and ^{109}Ag (48.16 %). Similar to Zr, Ag isotopic composition can be used as an indicator for an extinct radioactive nuclide. MC-ICP-MS has been used for the highly precise determination of ^{107}Ag^{+} / ^{109}Ag^{+}, which in combination with the Pd content of samples was used to infer the abundance of ^{107}Pd.[153] With reference to the initial ^{107}Pd / ^{108}Pd ratio in the solar system, this provided information on the age of a variety of meteoritic material.

2.4.16 Cadmium, indium, tin and tellurium

Cd has eight stable isotopes, ^{106}Cd (1.3 %), ^{108}Cd (0.9 %), ^{110}Cd (12.5 %), ^{111}Cd (12.8 %), ^{112}Cd (24.1 %), ^{113}Cd (12.2 %), ^{114}Cd (28.7 %) and ^{116}Cd (7.5 %). In has

two stable isotopes, ^{113}In (4.3 %) and ^{115}In (95.7 %); Sn has ten: ^{112}Sn (1.0 %), ^{114}Sn (0.7 %), ^{115}Sn (0.3 %), ^{116}Sn (14.5 %), ^{117}Sn (7.7 %), ^{118}Sn (24.2 %), ^{119}Sn (8.6 %), ^{120}Sn (32.6 %), ^{122}Sn (4.6 %) and ^{124}Sn (5.8 %). Te has eight stable isotopes, ^{120}Te (0.1 %), ^{122}Te (2.6 %), ^{123}Te (0.9 %), ^{124}Te (4.7 %), ^{125}Te (7.1 %), ^{126}Te (18.8 %), ^{128}Te (31.7 %) and ^{130}Te (34.1 %). Isotopic determination of more than one of these elements has often been reported, however isobaric overlap between them restricts the isotopes than can be reliably measured without isolation of the analytes.

Cd concentration has been measured using isotope dilution and ICP-MS in a variety of samples.[93, 101, 107] The performance of a SC-ICP-MS system for the isotope dilution determination of Cd in environmental and biological reference materials has been compared to that of a quadrupole based instrument.[154] The precision of isotope ratio measurements by SC-ICP-MS was two to three times better than that achieved using the quadrupole system. Park et al.[155] have used mathematical correction for the Sn overlap to allow isotope dilution determination of Cd in sediment reference materials by SC-ICP-MS. Accurate results were only obtained when the mass bias between the monitor and interfering Sn isotopes was taken into account.

MC-ICP-MS has been used for isotope dilution measurement of Cd, In and Te in geological samples.[156] Good agreement with previously published reference material data was achieved. Isotope dilution MC-ICP-MS has also been shown to provide Cd concentration data with smaller uncertainty than both quadrupole ICP-MS and TIMS isotope dilution analyses.[157]

Yi et al.[158] determined In and Sn concentrations in geological materials using isotope dilution MC-ICP-MS. Palladium was used to correct for mass bias for In analysis, antinomy was added prior to Sn measurements for the same purpose. It was proposed that in suitable samples, MC-ICP-MS could be suitable for measurement of the ^{115}In-^{115}Sn geochronometer.

The isotopic composition and atomic weight of both Sn and Te were determined by MC-ICP-MS more than 7 years ago.[143] These measurements were in good

agreement with TIMS determinations, with a factor of 2 improvement in precision. More recently, MC-ICP-MS has been used to illustrate the identical Sn isotopic composition of different laboratory reagents.[159] The $^{122}Sn^+$ / $^{116}Sn^+$ ratio was measured with a precision of 0.005 %RSD. Fractionation of Sn isotopes in a geological sample relative to standard materials was confirmed.

2.4.17 Neodymium, samarium and other lanthanides

Nd and Sm have seven stable isotopes each. For Nd: ^{142}Nd (27.2 %), ^{143}Nd (12.2 %), ^{144}Nd (23.8 %), ^{145}Nd (8.3 %), ^{146}Nd (17.2 %), ^{148}Nd (5.7 %) and ^{150}Nd (5.6 %); for Sm: ^{144}Sm (3.1 %), ^{147}Sm (15.0 %), ^{148}Sm (11.2 %), ^{149}Sm (13.8 %), ^{150}Sm (7.4 %), ^{152}Sm (26.8 %) and ^{154}Sm (22.8 %). ^{143}Nd and ^{144}Nd are the stable decay products of ^{147}Sm and ^{148}Sm respectively, however only the decay of ^{147}Sm occurs on a timescale that is useful for geochronology. Accurate and precise measurements of the ^{143}Nd / ^{144}Nd ratio, and the Nd and Sm concentrations are required to determine the formation age of geological samples; isobaric overlap of Nd and Sm isotopes at m/z 144 requires sample purification or mathematical correction to achieve accurate data. Due to their importance in geology, Nd isotope ratios were among the first to be determined by MC-ICP-MS.[160] In a pure Nd solution, $^{143}Nd^+$ / $^{144}Nd^+$ was measured with a precision of 0.004 %RSD, using $^{146}Nd^+$ / $^{145}Nd^+$ to correct for mass bias. Following correction for the $^{144}Sm^+$ overlap, no significant difference was found between $^{143}Nd^+$ / $^{144}Nd^+$ determined in the Nd standard and that measured in a Nd-Sm mixture.

Nd isotope ratios have since been measured by MC-ICP-MS in many geological investigations, with precision down to 0.001 %RSD.[129-131, 161, 162] Vance and Thirlwall[163] have used Nd isotopic measurements to emphasise the importance of accurate mass bias correction in MC-ICP-MS. Imperfections in mass bias correction were exposed, accurate isotope ratio data (compared to TIMS) was only obtained after implementing a secondary correction procedure.

The Nd-Sm chronometer system has been compared to the alternative Lu-Hf system in several studies using MC-ICP-MS.[164-167] In some cases results have been complimentary,[165, 166] however other studies have shown different behaviour

of the two systems depending on the geological conditions experienced by the samples.[164]

Isotopic analysis of the remaining lanthanides has been relatively limited, however Baker et al.[168] utilised the multi-element capabilities of ICP-MS to determine the concentration of elements from La to Lu by isotope dilution MC-ICP-MS. Data was acquired in three separate blocks (La to Eu, Eu to Gd and Er to Lu); replicate analysis of rock standards showed that the reproducibility of the elemental concentrations was within 1 %, inter-element ratios were reproduced to within 0.2 %.

Dy has seven stable isotopes: ^{156}Dy (0.1 %), ^{158}Dy (0.1 %), ^{160}Dy (2.3 %), ^{161}Dy (18.9 %), ^{162}Dy (25.5 %), ^{163}Dy (24.9 %) and ^{164}Dy (28.2 %). Dy isotopic composition has been determined using MC-ICP-MS.[169] Using ^{161}Dy$^+$ / ^{163}Dy$^+$ to correct other ratios for mass bias, mean isotope ratios and the calculated atomic weight of Dy were in good agreement with previous TIMS measurements. Isotope ratio precision of less than 0.001 %RSD was recorded for the MC-ICP-MS method.

2.4.18 Lutetium and hafnium

Lu has two stable isotopes, ^{175}Lu (97.4 %) and ^{176}Lu (2.6 %); Hf has six, ^{174}Hf (0.2 %), ^{176}Hf (5.3 %), ^{177}Hf (18.6 %), ^{178}Hf (27.3 %), ^{179}Hf (13.6 %) and ^{180}Hf (35.1 %). Although a lanthanide, Lu has been grouped with Hf as the decay of ^{176}Lu to ^{176}Hf forms the basis of a radiometric dating system for geological materials. Similar to the Nd-Sm system, good measurements of ^{176}Hf / ^{177}Hf and of Lu and Hf concentrations are required for the determination of sample formation age. Isobaric overlap between the elements and from ytterbium requires sample preparation or mathematical correction procedures to be applied. The more precise the isotope ratio, the lower the uncertainty of the calculated sample age, therefore multi-collector techniques are of great importance. Additionally, the ionisation potential of Hf is relatively high (6.65 eV) making it a difficult element to determine using a thermal ion source.[170] Walder et al.[160, 171] first reported the use of MC-ICP-MS for the determination of Hf isotope ratios. Isotope ratio precision for ^{176}Hf$^+$ / ^{177}Hf$^+$ following normalisation to the ^{179}Hf$^+$ / ^{177}Hf$^+$ ratio

was approximately 0.004 %RSD in both pure Hf solutions and Hf-Lu mixtures requiring correction for the isobaric overlap of [176]Lu.

Hf isotope ratios determined by MC-ICP-MS have since been used in a variety of geochemical and geochronological applications. In particular, the evolution and composition of the Earth's mantle and crust has been investigated[130, 131, 162, 165, 172-174] and the Hf isotopic composition in seawater and ocean ridges has been determined.[175, 176] Additionally the Lu-Hf systematics of a number of other systems have been analysed.[164, 177-179] MC-ICP-MS techniques have also been applied to the isotope dilution analysis of Hf in terrestrial and extraterrestrial rock samples.[136, 138]

In situ determination of Hf isotopic composition using laser ablation coupled to MC-ICP-MS has been reported.[180] Although interference from [176]Yb and [176]Lu was significant in the solid rock samples, the precision of Hf isotope ratio measurements on ten separate areas of a single zircon crystal was around 0.01 %RSD.

2.4.19 Tantalum and tungsten

Ta has only two isotopes, [180]Ta (0.01 %) and [181]Ta (99.99 %). Due to its extreme value, the Ta isotope ratio has been little studied. Münker *et al.*[137] have described the quantification of Ta in rock samples by isotope dilution analysis with MC-ICP-MS for detection, using a spike enriched in [180]Ta. An ion exchange resin was used to concentrate Ta and reduce the level of sample matrix. The same group found that the uncertainty of such determinations was limited by sample heterogeneity and blank levels, and not by the precision of the measurement.[138]

W has five stable isotopes [180]W (0.1 %), [182]W (26.5 %), [183]W (14.3 %), [184]W (30.6 %) and [186]W (28.4 %). The abundance of [182]W varies in nature due to decay from the now extinct radioisotope [182]Hf, forming the basis of a geochronometer. It is only with the advent of MC-ICP-MS that this system has come into greater use as W has a high first ionisation potential (7.98 eV) and is therefore difficult to measure by conventional TIMS techniques.[170] The greater ionising power of the ICP allows the routine isotopic analysis of W.

The isotopic composition and molecular weight of W measured by MC-ICP-MS was reported in 1995, the accuracy of the determinations was comparable to TIMS but with two orders of magnitude improvement in precision.[143] MC-ICP-MS has since been used to investigate the ^{182}Hf-^{182}W system for probing the timescale of formation of terrestrial rock samples,[181] and the timing of accretion and differentiation in the early history of the solar system.[182] Laser ablation sample introduction has been applied for the measurement of W isotope ratios in solid samples by MC-ICP-MS.[183] Although the precision of around 0.02 %RSD was three times worse than that achievable using standard techniques, it was sufficient to measure natural variation in W isotopic composition due to the decay of ^{182}Hf. The amount of W used in the laser ablation analysis was less than 10 % of that required for solution nebulisation.

2.4.20 Rhenium, osmium, iridium and platinum

Re has two stable isotopes ^{185}Re (37.4 %) and ^{187}Re (62.6 %). The seven stable isotopes of Os are ^{184}Os (0.02 %), ^{186}Os (1.59 %), ^{187}Os (1.96 %), ^{188}Os (13.24 %), ^{189}Os (16.15 %), ^{190}Os (26.26 %) and ^{192}Os (40.78 %). Re and Os form another radiometric dating system. ^{187}Os is the stable decay product of ^{187}Re, allowing the relative ^{187}Os abundance to be used as a basis for the age determination of minerals. This method generally involves the measurement of either the ^{187}Os / ^{186}Os or ^{187}Os / ^{188}Os ratio and Re and Os concentrations. It is necessary to separate the two elements prior to analysis in order to avoid the isobaric overlap of ^{187}Re and ^{187}Os. This is most often achieved through *in situ* generation of the volatile OsO_4 species,[184] a method that also provides enhanced sensitivity by increasing the transmission of Os to the ICP.

SC-ICP-MS has been applied to Re and Os determinations in several studies. Hassler *et al.*[185] described measurement of the ^{187}Os / ^{188}Os ratio to a precision of 0.78 %RSD, sample throughput was more than ten times that of TIMS. With the appropriate sample preparation procedure, the concentration of the platinum group elements could be determined on the material that remained following OsO_4 distillation. Use of a grounded Pt shield (see section 2.2.1.4) has been found to improve the sensitivity of Os determinations by SC-ICP-MS.[186] Accurate isotope

ratios were measured with a precision of 0.2 to 0.8 %RSD in samples with Os concentrations of 1 ng ml^{-1}. At higher Os levels, isotope ratio precision down to 0.15 %RSD was achieved, however it was found that use of the Pt shield did not improve on this value. Re and Os isotope ratios have been measured in geological samples using SC-ICP-MS with precision as good as 0.02 %RSD.[187] Anion exchange chromatography and OsO$_4$ distillation were used to separate Re and Os respectively from the matrix, allowing accurate determination of the Re-Os age of samples.

The performance of SC and MC-ICP-MS for the determination of Os isotope ratios has been compared to quadrupole ICP-MS by Boulyga *et al.*[188] Good agreement was found between the three instruments and the precision of the SC and quadrupole ICP-MS measurements was similar, at around 0.1 %RSD. Using MC-ICP-MS, isotope ratio precision of 0.001 %RSD was achieved. This technique was then applied to standard solutions with natural Os isotopic composition and to geological materials, wherein significant variation of ^{187}Os abundance was observed.

Re and Os isotopic measurements by MC-ICP-MS have been reported by several groups. Schoenberg *et al.*[189] described Os isotopic measurements that were within the analytical uncertainty of TIMS determinations, with a precision lower than 0.01 %RSD for 50 ng of an Os standard. Accurate isotope ratios were determined using lower amounts of Os through the use of several electron multiplier detectors. The precision for these measurements ranged from 0.6 %RSD (25 pg Os) to 0.07 %RSD (250 pg Os). In a separate acquisition, Ir was used to correct for mass bias in Re isotopic determinations. Using Faraday collectors to measure Ir and electron multiplier detectors for Re, accurate isotope ratios could be determined on as little as 0.2 pg of Re, with precision better than 1 %RSD. Norman *et al.*[190] have also used MC-ICP-MS for the determination of Os isotope ratios. The mass bias on ^{188}Os / ^{192}Os was corrected using ^{189}Os / ^{192}Os as an internal standard, yielding a precision of 0.08 %RSD for samples containing 10 ng Os. MC-ICP-MS has been used as the detection technique for isotope dilution analysis of Os in various geological samples including iron meteorites[191] and mantle periodites.[149]

Os isotope ratios have also been measured in solid samples using laser ablation sample introduction to MC-ICP-MS. Hirata et al.[192] reported an isotope ratio precision better than 0.05 %RSD for the ^{187}Os / ^{188}Os ratio, and found that the Re-Os ages determined for minerals was comparable to that calculated from other chronometry systems. More recently, laser ablation coupled to MC-ICP-MS has been used to investigate the Os composition in mantle sulfides.[193, 194] It should be noted that the analysis of unseparated samples requires a mathematical correction for the Re isobaric interference, which may degrade the achievable precision.

Ir has two stable isotopes, ^{191}Ir (37.3 %) and ^{193}Ir (62.7 %); Pt has six ^{190}Pt (0.01 %), ^{192}Pt (0.78 %), ^{194}Pt (32.97 %), ^{195}Pt (33.83 %), ^{196}Pt (25.24 %) and ^{198}Pt (7.16 %). The isotopic determination of Ir and Pt has been limited to isotope dilution analysis. The capability of SC-ICP-MS for the measurement of Pt in environmental samples without matrix separation has been illustrated;[150] a desolvating nebuliser was used to reduce the interference from HfO$^+$. MC-ICP-MS has been used for the isotope dilution analysis of both Ir and Pt in geological samples, specifically for investigation of the behaviour of these elements during mantle formation.[148, 149]

2.4.21 Mercury and thallium

Hg has seven stable isotopes ^{196}Hg (0.2 %), ^{198}Hg (10.0 %), ^{199}Hg (16.9 %), ^{200}Hg (23.1 %), ^{201}Hg (13.2 %), ^{202}Hg (29.9 %) and ^{204}Hg (6.9 %). Due to the highly toxic nature of this heavy element, the presence of Hg in the environment and the mechanisms by which it enters biological systems are of great concern. Stable isotope tracer studies can be used to investigate the mechanisms of Hg transport and uptake, as recently reviewed by Hintelmann and Ogrinc.[195] Due to the low levels of Hg in many samples, pre-concentration using a gold trap is often performed. The trap is heated to desorb the Hg, which can then be swept into the ICP using argon as a carrier gas. This sample introduction approach produces transient signals meaning that the time available for measurement, and therefore the achievable isotope ratio precision, is limited.

A comparison of different instrumentation for the measurement of Hg isotope ratios in coal samples has been presented by Evans et al.[196] Four different MC-ICP-MS instruments were used, along with quadrupole and time-of-flight based systems. Tl was used to correct for the mass bias. It was found that the isotope ratios varied during the thermalisation of the samples requiring integration of the entire transient peaks for each isotope prior to calculation of the ratio. This approach led to a sample-to-sample precision of around 0.025 %RSD for the multi-collector instruments, a factor of 10 to 20 better than that achievable using the quadrupole and time-of-flight ICP-MS systems. Hg isotopic abundances have also been determined in meteorites using MC-ICP-MS.[197] No difference was found between the Hg isotopic composition of the meteorites and that of terrestrial samples, in contrast to previous studies using neutron activation analysis.

Tl has two stable isotopes, ^{203}Tl (29.52 %) and ^{205}Tl (70.48 %). Tl has often been used to correct for mass bias in Pb isotopic determinations (see below), however the ^{205}Tl / ^{203}Tl ratio has also been determined in its own right by MC-ICP-MS. Rehkämper and Halliday[198] added a spike with known Pb isotopic composition to correct for the Tl mass bias, and measured ^{205}Tl / ^{203}Tl to a precision of 0.02 %RSD. This was a significant improvement on the precision achievable by TIMS. The same workers went on to show fractionation of the Tl isotopes in natural samples, related to precipitation and scavenging of Tl from seawater by ferromanganese particles.[199] Isotope dilution analysis of Tl has been carried out using MC-ICP-MS. This technique was shown to provide Tl concentration data with smaller uncertainty than both quadrupole ICP-MS and TIMS isotope dilution analyses.[157]

2.4.22 Lead
Pb has four stable isotopes, ^{204}Pb (1.4 %), ^{206}Pb (24.1 %), ^{207}Pb (22.1 %) and ^{208}Pb (52.4 %). The exact isotopic composition of natural Pb is variable since with the exception of ^{204}Pb, all of the isotopes are the product of the decay of radioactive isotopes. ^{206}Pb is the end product of ^{238}U decay, ^{207}Pb is generated by the decay of ^{235}U and ^{208}Pb is the stable isotope resulting from ^{232}Th decay. As the amount of ^{204}Pb remains unchanged over time, the ratio of the radiogenic Pb isotopes to ^{204}Pb is a function of the time since mineral formation and of the original quantities of

Pb, U and Th present in the mineral. These processes form the basis of several methods for the determination of the age and/or genesis of geological materials.[200] The U-Pb and Th-Pb systems are primarily used for radiometric dating and require measurement of the concentration of all the relevant isotopes. Analysis of the ratio of the radiogenic Pb isotopes to ^{204}Pb and of the ^{207}Pb / ^{206}Pb ratio provides information on the genesis of materials and can be used to identify Pb sources in biological and environmental systems. Due to the importance of the Pb isotope system, there have been many publications on this subject.

Pb isotope ratios determined by SC-ICP-MS has been reported by Vanhaecke et al.[83] Optimisation of scanning parameters and signal intensities provided a precision of 0.04 %RSD for the ^{207}Pb / ^{206}Pb ratio. Pb isotopic determinations using SC-ICP-MS have since been reported in a number of studies. The technique has been shown to provide comparable data to TIMS in terms of accuracy for determinations in complex matrices, with the improvement in sample throughput compensating for the worse isotope ratio precision.[201-203] Applications have included the assessment of anthropogenic Pb input into soils[204] and alpine snows,[205] the measurement of Pb isotope ratios in natural waters at the pg ml^{-1} level[14] and the tracing of Pb pollution in Antarctic marine sediments.[206] SC-ICP-MS has also been used for Pb isotopic measurements to determine the origin of Pb in archaeological samples,[207] for the investigation of Pb transport in biological tracer studies[208] and to probe the link between Pb isotope ratio variation and earthquake events.[209] Additionally, isotope dilution analysis using SC-ICP-MS has been used for the quantification of Pb in geological and environmental reference materials.[101]

Isotope ratios of Pb were among the first to be measured using MC-ICP-MS.[127] Even in early studies, precision of 0.02 %RSD and better was reported,[210] using Tl to correct for mass bias. The accuracy and precision of Pb isotope ratio measurements by MC-ICP-MS has since been evaluated in several publications.[211-218] Isotope ratio precision down to 0.002 %RSD has been reported,[213, 216] with accuracy comparing well with TIMS determinations. The Tl mass bias correction has been reported as being the most significant factor in the uncertainty of Pb isotope ratio measurements by MC-ICP-MS,[219] and the

correction has come under close examination from several authors. Hirata[211] showed that the mass bias varied with analyte mass, therefore requiring the Tl bias to be adjusted before being used to correct Pb isotope ratio data. This was also reported by White et al.[215] More recently, double Pb isotope spiking has been applied to expose systematic errors in the Tl normalisation.[220] The errors were thought to be related to the differing behaviour of Tl and Pb in the sample introduction system.

Several groups have reported the use of MC-ICP-MS for the measurement of Pb isotope ratios in complex sample matrices.[221-223] Precision matching that for standard solutions was achieved, even in the presence of large amounts of dissolved solids. Pb isotopic determinations have been carried out on solid samples using laser ablation,[37, 224, 225] and on volatile Pb species using gas chromatography prior to ICP-MS analysis.[226, 227] The isotope ratio precision of these analyses was five to ten times worse than continuous solution nebulisation.

Pb isotope ratios measured by MC-ICP-MS have been applied for the source determination of Pb in aerosols.[228, 229] Air from continental Europe was found to have higher levels of the radiogenic Pb isotopes than air in the UK. The potential of MC-ICP-MS for the assessment of the geographical origin of wine using Pb isotope ratios has also been illustrated.[230] Age determinations using the Pb-Pb and U-Th-Pb systems have been performed for both metamorphic and sedimentary rock systems using MC-ICP-MS.[231-233] Other geological applications have included the investigation of ferromanganese crusts,[234] and the study of magma and mantle formation and dynamics.[130, 131]

2.4.23 Thorium and uranium

Th has only one natural isotope, ^{232}Th; U has three: ^{234}U (~0.006 %), ^{235}U (~0.720 %) and ^{238}U (~99.274 %). Th and U are valuable in providing geochronological information as discussed above, however both elements have a number of radioisotopes that are also of interest, as their presence may be indicative of radioactive contamination. SC-ICP-MS has been applied to the determination of U isotope ratios in radioactive waste to a precision of 0.07 %RSD[235] and the accuracy of U determinations using this technique has been confirmed through the

analysis of certified reference materials.[236] SC-ICP-MS has since been applied to environmental samples for the monitoring of radioactive contamination[237-240] and to biological samples to assess the exposure of humans to depleted uranium.[241,242] McLean et al.[243] used a direct injection high efficiency nebuliser to improve sensitivity for the measurement of ratios of low level radioisotopes; the potential of SC-ICP-MS for the determination of Th and U isotope ratios in geological samples has also been illustrated.[244] Isotope dilution measurement of the concentration of Th and U isotopes using single collector systems has been reported in several studies, including determinations in complex matrices such as seawater[245] and urine.[246] In one case, ^{230}Th / ^{232}Th ratios as low as 10^{-6} were measured.[247] An increased resolution setting was used to improve the abundance sensitivity, allowing determination of the low level ^{230}Th radioisotope without any contribution from the tail of the much larger ^{232}Th peak.

U isotope ratio measurements were among the first performed using MC-ICP-MS.[171] Th and U isotope ratios using this technique have been shown to be in good agreement with TIMS,[248] with a factor of three to five improvement in precision.[249] More recently, U and Th isotopic measurements by MC-ICP-MS have been applied to age determinations of a variety of geological samples including monazites,[232,233] calcites,[250] sediments[251] and volcanic rocks,[252,253] and for the investigation of erosion timescales in river systems.[254] The technique has also been applied to the monitoring of radioactive U in soils,[239] seawater,[255,256] glacial ice and plant material.[257] Turner et al.[258] used a combination of Faraday and electron multiplier detectors for the precise measurement of extreme Th and U isotope ratios. The precision of these determinations was equivalent to that of TIMS determinations, however the ICP-MS technique used 10 to 100 times lower levels of the analyte elements.

A comparison of the performance of different ICP-MS systems in U isotopic determinations has been presented by Quétel et al.[259] The total uncertainty in U isotope measurements by MC-ICP-MS was five times lower than SC-ICP-MS and twenty-five times lower than quadrupole ICP-MS.

Laser ablation sample introduction to MC-ICP-MS has been used for Th and U isotopic determinations in solid samples.[260] The isotope ratio precision was a factor of ten worse than solution nebulisation, however the mean ratio values were in good agreement.

2.4.24 Plutonium

Pu has a number of radioisotopes, the most abundant being ^{239}Pu and ^{240}Pu. The principle sources of Pu in the environment are nuclear weapon detonations and releases form nuclear installations. The relative abundance of ^{239}Pu and ^{240}Pu can provide information regarding the source of Pu pollution, potentially providing evidence of unauthorised discharges and weapons tests.

^{239}Pu / ^{240}Pu isotope ratios measured by SC-ICP-MS have been found to be in good agreement with α-spectrometry and accelerator mass spectrometry,[261, 262] an isotope ratio precision of 2 %RSD has been reported for Pu concentrations in the fg ml^{-1} range.[263, 264] This technique has been used to determine Pu isotope ratios in environmental samples including seawater[265] and soils from around the Chernobyl nuclear power plant.[240]

The ^{238}UH$^+$ interference can have a considerable effect on Pu isotopic determinations by ICP-MS. Methods that have been used to overcome this problem include sample desolvation techniques to reduce the level of hydrogen introduced to the ICP[237, 266] and sample preparation procedures to remove U.[267] The resolution required to separate ^{238}UH$^+$ from ^{239}Pu is beyond the capabilities of current commercial double focussing ICP-MS instrumentation, however Wyse et al.[268] have shown the value of increased mass resolution for the identification of other polyatomic species affecting Pu analysis (e.g. PbO$_2$$^+$).

Improved Pu isotope ratio precision using MC-ICP-MS enables more detailed conclusions to be drawn regarding the source of Pu in the environment. This technique has been used to achieve Pu isotope ratio precision down to 0.1 %RSD, comparable to TIMS determinations.[269] A uranium double isotope spike was added to the samples and used to correct for mass bias, mathematical corrections were applied for the contribution of UH$^+$ and the tail of the ^{238}U$^+$ peak to the Pu

signal intensity. This method was subsequently applied to the investigation of atmospheric Pu deposition in glacial ice and plant material.[257]

2.4.25 Other radionuclides

SC-ICP-MS has been used for the determination of the concentration of several radioisotopes using isotope dilution techniques. The increased sensitivity of these systems compared to quadrupole based spectrometers provides a considerable advantage when determining the low levels of these isotopes present in natural samples. Becker and co-workers have demonstrated the capability of SC-ICP-MS for the measurement of ultra-trace concentrations of radionuclides with both solution[243, 270] and laser[271] sample introduction.

Using single collector instrumentation ^{99}Tc has been determined in soils using flow injection sample introduction[272] and a modified sample introduction system has been used for the determination of ^{129}I in biological reference materials.[273] Both SC and MC-ICP-MS has been applied for the determination of ^{231}Pa in seawater,[245, 256] allowing the isotope to be used as a tracer for particle scavenging and ocean water circulation. The ^{237}Np fallout from nuclear weapons tests and the resulting mobility of Np in soil has been investigated using SC-ICP-MS.[274] Results suggested Np was more mobile in the environment than Pu radioisotopes. Trace levels of ^{241}Am in soils[237] and sediments[275] have also been measured using SC-ICP-MS. Good agreement with α-spectrometry was achieved.

References

1   T. Catterick, B. Fairman and C. Harrington, *J. Anal. At. Spectrom.*, 1998, **13**, 1009.

2   K. G. Heumann, S. M. Gallus, G. Rädlinger and J. Vogl, *J. Anal. At. Spectrom.*, 1998, **13**, 1001.

3   I. S. Begley, '*A study of isotope ratio measurement by ICP-MS*', Ph., D., Loughborough University, 1996.

4   R. S. Houk, V. A. Fassel, G. D. Flesch, H. J. Svec, A. L. Gray and C. E. Taylor, *Anal. Chem.*, 1980, **52**, 2283.

5   N. Jakubowski, L. Moens and F. Vanhaecke, *Spectrochim. Acta Part B*, 1998, **53**, 1739.

6   P. J. Turner, D. J. Mills, E. Schröder, G. Lapitajs, G. Jung, L. A. Iacone, D. A. Haydar and A. Montaser, 'Instrumentation for Low- and High-Resolution ICP-MS' in *Inductively Coupled Plasma Mass Spectrometry*, ed. A. Montaser, Wiley-VCH, New York, 1998.

7   P. Marriott, R. Fletcher, A. Cole, I. Beaumont, J. Lofthouse, S. Bloomfield and P. Miller, *J. Anal. At. Spectrom.*, 1998, **13**, 1021.

8   M. Morita, H. Ito, M. Linscheid and K. Otsuka, *Anal. Chem.*, 1994, **66**, 1588.

9   J.-F. Ying and D. J. Douglas, *Rapid Commun. Mass Spectrom.*, 1996, **10**, 649.

10   W. Chen, B. A. Collings and D. J. Douglas, *Anal. Chem.*, 2000, **72**, 540.

11   S. J. Ray and G. M. Hieftje, *J. Anal. At. Spectrom.*, 2001, **16**, 1206.

12   T. Oi, H. Ogino, M. Hosoe and H. Kakihana, *Sep. Sci. Technol.*, 1992, **27**, 631.

13   C. S. Muñiz, J. M. Marchante-Gayón, J. I. G. Alonso and A. Sanz-Medel, *J. Anal. At. Spectrom.*, 1998, **13**, 283.

14   F. Poitrasson and S. H. Dundas, *J. Anal. At. Spectrom.*, 1999, **14**, 1573.

15   E. e. a. Bjorn, *Spectrochim. Acta Part B*, 1998, **53**, 1765.

16   E. H. Evans and J. J. Giglio, *J. Anal. At. Spectrom.*, 1993, **8**, 1.

17   M.-T. Wei and S.-J. Jiang, *J. Anal. At. Spectrom.*, 1999, **14**, 1177.

18   Hwang and Jiang, *J. Anal. At. Spectrom.*, 1997, **12**, 579.

19   L. Ebdon, M. E. Foulkes, H. G. M. Parry and C. T. Tye, *J. Anal. At. Spectrom.*, 1988, **3**, 753.

20   T. Hirata and T. Ohno, *J. Anal. At. Spectrom.*, 2001, **16**, 487.

21   S.-J. Jiang, R. S. Houk and M. A. Stevens, *Anal. Chem.*, 1988, **60**, 1217.

22   N. S. Nonose, N. Matsuda, N. Fudagawa and M. Kubota, *Spectrochim. Acta Part B*, 1994, **49**, 955.

23   K. Y. Patterson, C. Veillon, A. D. Hill, P. B. Moser-Veillon and T. C. O'Haver, *J. Anal. At. Spectrom.*, 1999, **14**, 1673.

24   S. D. Tanner, M. Paul, S. A. Beres and E. R. Denoyer, *At. Spectrosc.*, 1995, 16.

25   S. D. Tanner, *J. Anal. At. Spectrom.*, 1995, **10**, 905.

26   D. J. Douglas and S. D. Tanner, 'Fundamental considerations in ICP-MS' in *Inductively Coupled Plasma Mass Specrometry*, ed. A. Montaser, Wiley-VCH, New York, 1998.

27   J. L. M. de Boer, *Spectrochim. Acta Part B*, 1997, **52**, 389.

28   J. L. M. de Boer, *J. Anal. At. Spectrom.*, 2000, **15**, 1157.

29   S. Sibisi and J. Skilling, *J. R. Statist. Soc. B*, 1997, **59**, 217.

30   B. L. Sharp, A. S. Bashammakh, C. M. Thong, J. Skilling and M. Baxter, *J. Anal. At. Spectrom.*, 2002, **17**, 459.

31   M. Grotti, C. Gnecco and F. Bonfiglioli, *J. Anal. At. Spectrom.*, 1999, **14**, 1171.

32   Z. Du and R. S. Houk, *J. Anal. At. Spectrom.*, 2000, **15**, 383.

33   I. Feldmann, N. Jakubowski and D. Stuewer, *Fres. J. Anal. Chem.*, 1999, **365**, 415.

34   V. I. Baranov and S. D. Tanner, *J. Anal. At. Spectrom.*, 1999, **14**, 1133.

35   C. Ingle, P. Appelblad, M. Dexter, H. Reid and B. Sharp, *J. Anal. At. Spectrom.*, 2001, **16**, 1076.

36   L. Moens, F. Vanhaecke, D. R. Bandura, V. I. Baranov and S. D. Tanner, *J. Anal. At. Spectrom.*, 2001, **16**, 991.

37   A. J. Walder, I. D. Abell, I. Platzner and P. A. Freedman, *Spectrochim. Acta Part B*, 1993, **48**, 397.

38   I. S. Begley and B. L. Sharp, *J. Anal. At. Spectrom.*, 1994, **9**, 171.

39   D. R. Bandura, V. I. Baranov and S. D. Tanner, *J. Anal. At. Spectrom.*, 2000, **15**, 921.

40   S. F. Boulyga and J. S. Becker, *Fres. J. Anal. Chem.*, 2001, **370**, 618.

41   Q. Xie and R. Kerrich, *J. Anal. At. Spectrom.*, 2002, **17**, 69.

42   A. R. Warren, L. A. Allen, H.-M. Pang, R. S. Houk and M. Janghorbani, *Appl. Spectrosc.*, 1994, **48**, 1360.

43   J. S. Becker and H.-J. Dietze, *J. Anal. At. Spectrom.*, 1998, **13**, 1057.

44   L. Halicz, A. Galy, N. S. Belshaw and R. K. O'Nions, *J. Anal. At. Spectrom.*, 1999, **14**, 1835.

45   A. W. Boom and R. F. Browner, *Anal. Chem.*, 1982, **54**, 1402.

46   I. Rodushkin, T. Ruth and D. Klockare, *J. Anal. At. Spectrom.*, 1998, **13**, 159.

47   H. Ying, M. Antler, J. W. Tromp and E. D. Salin, *Spectrochim. Acta Part B*, 2002, **57**, 277.

48   S. E. Hobbs and J. W. Olesik, *Anal. Chem.*, 1992, **64**, 274.

49   P. K. Appelblad, I. Rodushkin and D. C. Baxter, *Anal. Chem.*, 2001, **73**, 2911.

50   G. R. Gillson, D. J. Douglas, J. E. Fulford, K. W. Halligan and S. D. Tanner, *Anal. Chem.*, 1988, **60**, 1472.

51   S. D. Tanner, L. M. Cousins and D. J. Douglas, *Appl. Spectrosc.*, 1994, **48**, 1367.

52   G. Xiao and D. Beauchemin, *J. Anal. At. Spectrom.*, 1994, **9**, 509.

53   N. Praphairaksit and R. S. Houk, *Anal. Chem.*, 2000, **72**, 4435.

54   T. W. Burgoyne, G. M. Hieftje and R. A. Hites, *Anal. Chem.*, 1997, **69**, 485.

55   S. D. Tanner, *Spectrochim. Acta Part B*, 1992, **47**, 809.

56   I. Feldmann, W. Tittes, N. Jakubowski, D. Stuewer and U. Giessmann, *J. Anal. At. Spectrom.*, 1994, **9**, 1007.

57   P. D. P. Taylor, P. De Bièvre, A. J. Walder and A. Entwistle, *J. Anal. At. Spectrom.*, 1995, **10**, 395.

58   I. S. Begley and B. L. Sharp, *J. Anal. At. Spectrom.*, 1997, **12**, 395.

59   F. Vanhaecke, G. de Wannemacker, L. Moens, R. Dams, C. Latkoczy, T. Prohaska and G. Stingeder, *J. Anal. At. Spectrom.*, 1998, **13**, 567.

60   A. Held and P. D. P. Taylor, *J. Anal. At. Spectrom.*, 1999, **14**, 1075.

61   G. P. I. Russ and J. M. Bazan, *Spectrochim. Acta Part B*, 1987, **42**, 49.

62 G. P. Russ in *Applications of Inductively Coupled Plasma Mass Spectrometry*, ed. A. R. Date and A. L. Gray, Blackie, Glasgow, 1989.

63 P. K. Appelblad and D. C. Baxter, *J. Anal. At. Spectrom.*, 2000, **15**, 557.

64 H. Ramebäck, M. Berglund, D. Vendelbo, R. Wellum and P. D. P. Taylor, *J. Anal. At. Spectrom.*, 2001, **16**, 1271.

65 F. Vanhaeke, G. De Wannemacker, L. Moens and J. Hertogen, *J. Anal. At. Spectrom.*, 1999, **14**, 1691.

66 T. Hirata and A. Masuda, *Meteoritics*, 1992, **27**, 568.

67 J. R. Encinar, J. I. G. Alonso, A. Sanz-Medel, S. Main and P. J. Turner, *J. Anal. At. Spectrom.*, 2001, **16**, 322.

68 D. C. Grégoire and J. Lee, *J. Anal. At. Spectrom.*, 1994, **9**, 393.

69 A. A. Menegário, M. F. Giné, J. A. Bendassolli, A. C. S. Bellato and C. O. Trivelin, *J. Anal. At. Spectrom.*, 1998, **13**, 1065.

70 J. S. Becker, H.-J. Dietze, J. A. McLean and A. Montaser, *Anal. Chem.*, 1999, **71**, 3077.

71 J. S. Becker and H. J. Dietze, *Fres. J. Anal. Chem.*, 1999, **364**, 482.

72 L. Halicz, J. W. H. Lam, M. J. Peters and P. J. Tisdale, *Spectrochim. Acta Part B*, 1994, **47**, 637.

73 J. P. V. Mota, M. R. F. de la Campa, J. I. G. Alonso and A. Sanz-Medel, *J. Anal. At. Spectrom.*, 1999, **14**, 113.

74 K. J. R. Rosman and P. D. P. Taylor, *J. Anal. At. Spectrom.*, 1999, **14**, 5N.

75 H. E. Gabler, *J. Geochem. Explor.*, 2002, **75**, 1.

76 P. B. Tomascak, R. W. Carlson and S. B. Shirey, *Chem. Geol.*, 1999, **158**, 145.

77 P. B. Tomascak, F. Tera, R. T. Helz and R. J. Walker, *Geochim. Cosmochim. Acta*, 1999, **63**, 907.

78 P. B. Tomascak, J. G. Ryan and M. J. Defant, *Geology*, 2000, **28**, 507.

79 P. B. Tomascak, E. Widom, L. D. Benton, S. L. Goldstein and J. G. Ryan, *Earth Planet. Sci. Lett.*, 2002, **196**, 227.

80 Y. Nishio and S. Nakai, *Anal. Chim. Acta*, 2002, **456**, 271.

81 H. E. Gabler and A. Bahr, *Chem. Geol.*, 1999, **156**, 323.

82 C. Lecuyer, P. Grandjean, B. Reynard, F. Albarède and P. Telouk, *Chem. Geol.*, 2002, **186**, 45.

83   F. Vanhaecke, L. Moens, R. Dams and P. Taylor, *Anal. Chem.*, 1996, **68**, 567.

84   G. De Wannemacker, A. Ronderos, L. Moens, F. Vanhaecke, M. J. C. Bijvelds and Z. I. Kolar, *J. Anal. At. Spectrom.*, 2001, **16**, 581.

85   A. Galy, N. S. Belshaw, L. Halicz and R. K. O'Nions, *Int. J. Mass Spectrom.*, 2001, **208**, 89.

86   A. Galy, M. Bar-Matthews, L. Halicz and R. K. O'Nions, *Earth Planet. Sci. Lett.*, 2002, **201**, 105.

87   H. Wildner, *J. Anal. At. Spectrom.*, 1998, **13**, 573.

88   P. Klemens and K. G. Heumann, *Fres. J. Anal. Chem.*, 2001, **371**, 758.

89   C. L. De la Rocha, *Geochem. Geophys. Geosys.*, 2002, **3**, 1037.

90   T. Prohaska, C. Latkoczy and G. Stingeder, *J. Anal. At. Spectrom.*, 1999, **14**, 1501.

91   A. Makishima and E. Nakamura, *Anal. Chem.*, 2001, **73**, 2547.

92   P. Evans, C. Wolff-Briche and B. Fairman, *J. Anal. At. Spectrom.*, 2001, **16**, 964.

93   A. Prange, D. Schaumloffel, P. Bratter, A. N. Richarz and C. Wolf, *Fres. J. Anal. Chem.*, 2001, **371**, 764.

94   D. Schaumloffel, A. Prange, G. Marx, K. G. Heumann and P. Bratter, *Anal. Bioanal. Chem.*, 2002, **372**, 155.

95   S. Stürup, M. Hansen and C. Mølgaard, *J. Anal. At. Spectrom.*, 1997, **12**, 919.

96   S. Stürup, *J. Anal. At. Spectrom.*, 2002, **17**, 1.

97   A. Makishima and E. Nakamura, *J. Anal. At. Spectrom.*, 2000, **15**, 263.

98   X. K. Zhu, A. Makishima, Y. Guo, N. S. Belshaw and R. K. O'Nions, *Int. J. Mass Spectrom.*, 2002, **220**, 21.

99   A. Makishima, X. K. Zhu, N. S. Belshaw and R. K. O'Nions, *J. Anal. At. Spectrom.*, 2002, **17**, 1290.

100   A. Makishima, K. Kobayashi and E. Nakamura, *Geostand. Newsl.*, 2002, **26**, 41.

101   T. Prohaska, C. R. Quétel, C. Hennessy, D. Liesegang, I. Papadakis, P. D. P. Taylor, C. Latkoczy, S. Hann and G. Stingeder, *J. Environ. Monit.*, 2000, **2**, 613.

102   J. F. Wu and E. A. Boyle, *Anal. Chim. Acta*, 1998, **367**, 183.

103 C. S. Muñiz, J. M. M. Gayon, J. I. G. Alonso and A. Sanz-Medel, *J. Anal. At. Spectrom.*, 1999, **14**, 1505.

104 F. Vanhaecke, L. Balcaen, G. De Wannemacker and L. Moens, *J. Anal. At. Spectrom.*, 2002, **17**, 933.

105 N. S. Belshaw, X. K. Zhu, Y. Guo and R. K. O'Nions, *Int. J. Mass Spectrom.*, 2000, **197**, 191.

106 A. Stenberg, D. Malinovsky, I. Rodushkin, H. Andren, C. Ponter, B. Ohlander and D. C. Baxter, *J. Anal. At. Spectrom.*, 2003, **18**, 23.

107 P. Evans and B. Fairman, *J. Environ. Monit.*, 2001, **3**, 469.

108 F. Vanhaecke, L. Moens, R. Dams, I. Papadakis and P. Taylor, *Anal. Chem.*, 1997, **69**, 268.

109 F. Vanhaeke, L. Moens and R. Dams, *J. Anal. At. Spectrom.*, 1998, **13**, 1189.

110 K. Polec-Pawlak, D. Schaumloffel, J. Szpunar, A. Prange and R. Lobinski, *J. Anal. At. Spectrom.*, 2002, **17**, 908.

111 C. N. Maréchal, P. Télouk and F. Albarède, *Chem. Geol.*, 1999, **156**, 251.

112 N. H. Gale, A. P. Woodhead, Z. A. Stos-Gale, A. J. Walder and I. Bowen, *Int. J. Mass Spectrom.*, 1999, **184**, 1.

113 X. K. Zhu, R. K. O'Nions and Y. Guo, *Chem. Geol.*, 2000, **163**, 139.

114 C. N. Maréchal and F. Albarède, *Geochim. Cosmochim. Acta*, 2002, **66**, 1499.

115 J. M. Luck, D. Ben Othman, J. A. Barrat and F. Albarède, *Geochim. Cosmochim. Acta*, 2003, **67**, 143.

116 S. Stürup, *J. Anal. At. Spectrom.*, 2000, **15**, 315.

117 T. Hirata, *Geochim. Cosmochim. Acta*, 1997, **61**, 4439.

118 A. Galy, C. Pomies, J. A. Day, O. S. Pokrovsky and J. Schott, *J. Anal. At. Spectrom.*, 2003, **18**, 115.

119 H. E. Taylor, R. A. Huff and A. Montaser, 'Novel applications of ICP-MS' in *Inductively Coupled Plasma Mass Spectrometry*, ed. A. Montaser, Wiley-VCH, New York, 1998.

120 O. Rouxel, J. Ludden, J. Carignan, L. Marin and Y. Fouquet, *Geochim. Cosmochim. Acta*, 2002, **66**, 3191.

121 T. Waight, J. Baker and B. Willigers, *Chem. Geol.*, 2002, **186**, 99.

122   C. Latkoczy, T. Prohaska, G. Stingeder and M. Teschler-Nicola, *J. Anal. At. Spectrom.*, 1998, **13**, 561.

123   T. Prohaska, C. Latkoczy, G. Schultheis, M. Teschler-Nicola and G. Stingeder, *J. Anal. At. Spectrom.*, 2002, **17**, 887.

124   S. R. Thorrold and S. Shuttleworth, *Can. J. Fish. Aquat. Sci.*, 2000, **57**, 1232.

125   F. Vanhaecke, G. De Wannemacker, L. Moens and P. Van den Haute, *Fres. J. Anal. Chem.*, 2001, **371**, 915.

126   C. Latkoczy, T. Prohaska, M. Watkins, M. Teschler-Nicola and G. Stingeder, *J. Anal. At. Spectrom.*, 2001, **16**, 806.

127   A. J. Walder and P. A. Freedman, *J. Anal. At. Spectrom.*, 1992, **7**, 571.

128   S. Ehrlich, G. Gavrieli, L.-B. Dor and L. Halicz, *J. Anal. At. Spectrom.*, 2001, **16**, 1389.

129   H. Downes, T. Kostoula, A. P. Jones, A. D. Beard, M. F. Thirlwall and J. L. Bodinier, *Contrib. Mineral. Petrol.*, 2002, **144**, 78.

130   P. D. Kempton, J. A. Pearce, T. L. Barry, J. G. Fitton, C. Langmuir and D. M. Christie, *Geochem. Geophys. Geosys.*, 2002, **3**, 1039.

131   K. W. W. Sims, S. J. Goldstein, J. Blichert-Toft, M. R. Perfit, P. Kelemen, D. J. Fornari, P. Michael, M. T. Murrell, S. R. Hart, D. J. DePaolo, G. Layne, L. Ball, M. Jull and J. Bender, *Geochim. Cosmochim. Acta*, 2002, **66**, 3481.

132   T. Waight, J. Baker and D. Peate, *Int. J. Mass Spectrom.*, 2002, **221**.

133   J. N. Christensen, A. N. Halliday, D. C. Lee and C. M. Hall, *Earth Planet. Sci. Lett.*, 1995, **136**, 79.

134   M. Bizzarro, A. Simonetti, R. K. Stevenson and S. Kurszlaukis, *Geochim. Cosmochim. Acta*, 2003, **67**, 289.

135   P. M. Outridge, S. R. Chenery, J. A. Babaluk and J. D. Reist, *Environ. Geol.*, 2002, **42**, 891.

136   K. David, J. L. Birck, P. Telouk and C. J. Allegre, *Chem. Geol.*, 1999, **157**, 1.

137   C. Münker, S. Weyer, E. Scherer and K. Mezger, *Geochem. Geophys. Geosys.*, 2001, **2**, art. no 2001GC000183.

138   S. Weyer, C. Münker, M. Rehkämper and K. Mezger, *Chem. Geol.*, 2002, **187**, 295.

139   S. Weyer, C. Münker and K. Mezger, *Earth Planet. Sci. Lett.*, 2003, **205**, 309.

140   T. Hirata and T. Yamaguchi, *J. Anal. At. Spectrom.*, 1999, **14**, 1455.

141   T. Hirata, *Chem. Geol.*, 2001, **176**, 323.

142   A. Giussani, P. Roth, E. Werner, P. Schramel, I. Wendler and F. Nusslin, *Isotopes Environ. Health Stud.*, 1997, **33**, 207.

143   D. C. Lee and A. N. Halliday, *Int. J. Mass Spectrom. Ion Processes*, 1995, **146**, 35.

144   J. Barling, G. L. Arnold and A. D. Anbar, *Earth Planet. Sci. Lett.*, 2001, **193**, 447.

145   A. D. Anbar, K. A. Knab and J. Barling, *Anal. Chem.*, 2001, **73**, 1425.

146   C. Siebert, T. F. Nagler and J. D. Kramers, *Geochem. Geophys. Geosys.*, 2001, **2**, art. no. 2000GC000124.

147   N. Dauphas, L. Reisberg and B. Marty, *Anal. Chem.*, 2001, **73**, 2613.

148   M. Rehkämper, A. N. Halliday, J. G. Fitton, D. C. Lee, M. Wieneke and N. T. Arndt, *Geochim. Cosmochim. Acta*, 1999, **63**, 3915.

149   J. H. Yang, S. Y. Jiang and G. Brugmann, *Acta Petrol. Sin.*, 2001, **17**, 325.

150   G. Köllensperger, S. Hann and G. Stingeder, *J. Anal. At. Spectrom.*, 2000, **15**, 1553.

151   S. Hann, G. Köllensperger, K. Kanitsar and G. Stingeder, *J. Anal. At. Spectrom.*, 2001, **16**, 1057.

152   H. Becker, C. Dalpe and R. J. Walker, *Analyst*, 2002, **127**, 775.

153   R. W. Carlson and E. H. Hauri, *Geochim. Cosmochim. Acta*, 2001, **65**, 1839.

154   J. P. Valles Mota, J. R. Encinar, M. R. F. de la Campa, J. I. G. Alonso and A. Sanz-Medel, *J. Anal. At. Spectrom.*, 1999, **14**, 1467.

155   C. J. Park, K. H. Cho, J. K. Suh and M. S. Han, *J. Anal. At. Spectrom.*, 2000, **15**, 567.

156   W. Yi, A. N. Halliday, D. C. Lee and M. Rehkämper, *Geostand. Newsl.*, 1998, **22**, 173.

157   P. Klingbeil, J. Vogl, W. Pritzkow, G. Riebe and M. J., *Anal. Chem.*, 2001, **73**, 1881.

158   W. Yi, A. N. Halliday, D. C. Lee and J. N. Christensen, *Geochim. Cosmochim. Acta*, 1995, **59**, 5081.

159   R. Clayton, P. Andersson, N. H. Gale, C. Gillis and M. J. Whitehouse, *J. Anal. At. Spectrom.*, 2002, **17**, 1248.

160   A. J. Walder, I. Platzner and P. A. Freedman, *J. Anal. At. Spectrom.*, 1993, **8**, 19.

161   B. Luais, P. Telouk and F. Albarède, *Geochim. Cosmochim. Acta*, 1997, **61**, 4847.

162   C. J. Ballentine, D. C. Lee and A. N. Halliday, *Chem. Geol.*, 1997, **139**, 111.

163   D. Vance and M. Thirlwall, *Chem. Geol.*, 2002, **185**, 227.

164   E. E. Scherer, K. L. Cameron and J. Blichert-Toft, *Geochim. Cosmochim. Acta*, 2000, **64**, 3413.

165   J. Blichert-Toft and R. Frei, *Geochim. Cosmochim. Acta*, 2001, **65**, 3177.

166   J. Blichert-Toft, M. Boyet, P. Telouk and F. Albarède, *Earth Planet. Sci. Lett.*, 2002, **204**, 167.

167   I. C. Kleinhanns, K. Kreissig, B. S. Kamber, T. Meisel, T. F. Nagler and J. D. Kramers, *Anal. Chem.*, 2002, **74**, 67.

168   J. Baker, T. Waight and D. Ulfbeck, *Geochim. Cosmochim. Acta*, 2002, **66**.

169   I. Segal, L. Halicz and I. T. Platzner, *Int. J. Mass Spectrom.*, 2002, **216**, 177.

170   A. N. Halliday, D. C. Lee, J. N. Christensen, M. Rehkämper, W. Yi, X. Z. Luo, C. M. Hall, C. J. Ballentine, T. Pettke and C. Stirling, *Geochim. Cosmochim. Acta*, 1998, **62**, 919.

171   A. J. Walder, D. Koller, N. M. Reed, R. C. Hutton and P. A. Freedman, *J. Anal. At. Spectrom.*, 1993, **8**, 1037.

172   J. Blichert-Toft and F. Albarède, *Earth Planet. Sci. Lett.*, 1997, **148**, 243.

173   Y. Amelin, D. C. Lee, A. N. Halliday and R. T. Pidgeon, *Nature*, 1999, **399**, 252.

174   N. Mattielli, D. Weis, J. Blichert-Toft and F. Albarède, *J. Petrol.*, 2002, **43**, 1327.

175   K. David, M. Frank, R. K. O'Nions, N. S. Belshaw and J. W. Arden, *Chem. Geol.*, 2001, **178**, 23.

176   M. Andres, J. Blichert-Toft and J. G. Schilling, *Geochem. Geophys. Geosys.*, 2002, **3**, 8477.

177   S. Duchene, J. Blichert-Toft, B. Luais, P. Telouk, J. M. Lardeaux and F. Albarède, *Nature*, 1997, **387**, 586.

178   J. Blichert-Toft, *Geostand. Newsl.*, 2001, **24**, 41.

179   S. S. Schmidberger, A. Simonetti, D. Francis and C. Gariepy, *Earth Planet. Sci. Lett.*, 2002, **197**, 245.

180   M. F. Thirlwall and A. J. Walder, *Chem. Geol.*, 1995, **122**, 241.

181   D. C. Lee and A. N. Halliday, *Nature*, 1995, **378**, 771.

182   D. C. Lee and A. N. Halliday, *Science*, 1996, **274**, 1876.

183   T. Hirata, *J. Anal. At. Spectrom.*, 2002, **17**, 204.

184   T. Hirata, T. Akagi, H. Shimuzu and A. Masuda, *Anal. Chem.*, 1989, **61**, 2263.

185   D. R. Hassler, B. Peucker-Ehrenbrink and G. E. Ravizza, *Chem. Geol.*, 2000, **166**, 1.

186   A. T. Townsend, *Fres. J. Anal. Chem.*, 2000, **367**, 614.

187   D. Malinovsky, I. Rodushkin, D. Baxter and B. Ohlander, *Anal. Chim. Acta*, 2002, **463**, 111.

188   S. F. Boulyga, I. Segal, I. T. Platzner, L. Halicz and J. S. Becker, *Int. J. Mass Spectrom.*, 2002, **218**, 245.

189   R. Schoenberg, T. F. Nagler and J. D. Kramers, *Int. J. Mass Spectrom.*, 2000, **197**, 85.

190   M. Norman, V. Bennett, M. McCulloch and L. Kinsley, *J. Anal. At. Spectrom.*, 2002, **17**, 1394.

191   M. Hattori and T. Hirata, *Analyst*, 2001, **126**, 846.

192   T. Hirata, M. Hattori and T. Tanaka, *Chem. Geol.*, 1998, **144**, 269.

193   O. Alard, W. L. Griffin, N. J. Pearson, J. P. Lorand and S. Y. O'Reilly, *Earth Planet. Sci. Lett.*, 2002, **203**, 651.

194   N. J. Pearson, O. Alard, W. L. Griffin, S. E. Jackson and S. Y. O'Reilly, *Geochim. Cosmochim. Acta*, 2002, **66**, 1037.

195   H. Hintelmann and N. Ogrinc, *ACS Symposium Series*, 2003, **835**, 321.

196   R. D. Evans, H. Hintelmann and P. J. Dillon, *J. Anal. At. Spectrom.*, 2001, **16**, 1064.

197   D. S. Lauretta, B. Klaue, J. D. Blum and P. R. Buseck, *Geochim. Cosmochim. Acta*, 2001, **65**, 2807.

198   M. Rehkämper and A. N. Halliday, *Geochim. Cosmochim. Acta*, 1999, **63**, 935.

199   M. Rehkämper, M. Frank, J. R. Hein, D. Porcelli, A. Halliday, J. Ingri and V. Liebetrau, *Earth Planet. Sci. Lett.*, 2002, **197**, 65.

200   M. A. Geyh and H. Schleicher, '*Absolute age determination: Physical and chemical dating methods and their application*', Springer-Verlag, Heidelberg, 1990.

201   R. Gwiazda, D. Woolard and D. Smith, *J. Anal. At. Spectrom.*, 1998, **13**, 1233.

202   T. A. Hinners, R. Hughes, P. M. Outridge, W. J. Davis, K. Simon and D. R. Woolard, *J. Anal. At. Spectrom.*, 1998, **13**, 963.

203   A. T. Townsend, Z. Yu, P. McGoldrick and J. A. Hutton, *J. Anal. At. Spectrom.*, 1998, **13**, 809.

204   T. Prohaska, M. Watkins, C. Latkoczy, W. W. Wenzel and G. Stingeder, *J. Anal. At. Spectrom.*, 2000, **15**, 365.

205   T. Doring, M. Schwikowski and H. W. Gaggeler, *Fres. J. Anal. Chem.*, 1997, **359**, 382.

206   A. T. Townsend and I. Snape, *J. Anal. At. Spectrom.*, 2002, **17**, 922.

207   G. De Wannemacker, F. Vanhaeke, L. Moens, A. Van Mele and H. Thoen, *J. Anal. At. Spectrom.*, 2000, **15**, 323.

208   D. Woolard, R. Franks and D. R. Smith, *J. Anal. At. Spectrom.*, 1998, **13**, 1015.

209   F. Poitrasson, S. H. Dundas, J. P. Toutain, M. Munoz and A. Rigo, *Earth Planet. Sci. Lett.*, 1999, **169**, 269.

210   A. J. Walder and N. Furuta, *Anal. Sci.*, 1993, **9**, 675.

211   T. Hirata, *Analyst*, 1996, **121**, 1407.

212   N. S. Belshaw, P. A. Freedman, R. K. O'Nions, M. Frank and Y. Guo, *Int. J. Mass Spectrom.*, 1998, **181**, 51.

213   M. Rehkämper and A. N. Halliday, *Int. J. Mass Spectrom.*, 1998, **181**, 123.

214   M. F. Thirlwall, *Chem. Geol.*, 2000, **163**, 299.

215   W. M. White, F. Albarède and P. Télouk, *Chem. Geol.*, 2000, **167**, 257.

216   I. Platzner, S. Ehrlich and L. Halicz, *Fres. J. Anal. Chem.*, 2001, **370**, 624.

217   K. D. Collerson, B. S. Kamber and R. Schoenberg, *Chem. Geol.*, 2002, **188**, 65.

218   J. Woodhead, *J. Anal. At. Spectrom.*, 2002, **17**, 1381.

219   J. R. Encinar, J. I. G. Alonso, A. Sanz-Medel, S. Main and P. J. Turner, *J. Anal. At. Spectrom.*, 2001, **16**, 315.

220   M. F. Thirlwall, *Chem. Geol.*, 2002, **184**, 255.

221   M. Rehkämper and K. Mezger, *J. Anal. At. Spectrom.*, 2000, **15**, 1451.

222   S. Ehrlich, Z. Karpas, L. Ben-Dor and L. Halicz, *J. Anal. At. Spectrom.*, 2001, **16**, 975.

223   L. Halicz and S. Ehrlich, *Geochim. Cosmochim. Acta*, 2002, **66**, A303.

224   A. J. R. Kent, J. A. Baker, T. E. Waight, I. A. Ukstins, J. Vry, S. Stos, I. J. Graham and I. C. Wright, *Geochim. Cosmochim. Acta*, 2002, **66**, A395.

225   B. J. A. Willigers, J. A. Baker, E. J. Krogstad and D. W. Peate, *Geochim. Cosmochim. Acta*, 2002, **66**, 1051.

226   E. M. Krupp, C. Pécheyran, S. Meffan-Main and O. F. X. Donard, *Fres. J. Anal. Chem.*, 2001, **370**, 573.

227   E. M. Krupp, C. Pécheyran, H. Pinaly, M. Motelica-Heino, D. Koller, S. M. M. Young, I. B. Brenner and O. F. X. Donard, *Spectrochim. Acta Part B*, 2001, **56**, 1233.

228   C. R. Widmer, U. Krahenbuhl, J. Kramers and L. Tobler, *Fres. J. Anal. Chem.*, 2000, **366**, 171.

229   P. Flament, M. L. Bertho, K. Deboudt, A. Veron and E. Puskaric, *Sci. Total Environ.*, 2002, **296**, 35.

230   M. Barbaste, L. Halicz, A. Galy, B. Medina, H. Emteborg, F. C. Adams and R. Lobinski, *Talanta*, 2001, **54**, 307.

231   D. Bridgwater, D. J. Scott, V. V. Balagansky, M. J. Timmerman, M. Marker, S. A. Bushmin, N. L. Alexeyev and J. S. Daly, *Terr. Nova*, 2001, **13**, 32.

232   N. M. White, R. R. Parrish, M. J. Bickle, Y. M. R. Najman, D. Burbank and A. Maithani, *J. Geol. Soc.*, 2001, **158**, 625.

233   G. Foster, H. D. Gibson, R. Parrish, M. Horstwood, J. Fraser and A. Tindle, *Chem. Geol.*, 2002, **191**, 183.

234   J. N. Christensen, A. N. Halliday, L. V. Godfrey, J. R. Hein and D. K. Rea, *Science*, 1997, **277**, 913.

235   W. Kerl, J. S. Becker, H. J. Dietze and W. Dannecker, *Fres. J. Anal. Chem.*, 1997, **359**, 407.

236   H. A. Furusawa, J. E. S. Sarkis, M. H. Kakazu and C. Rodrigues, *J. Radioanal. Nucl. Chem.*, 1999, **242**, 647.

237   S. F. Boulyga, C. Testa, D. Desideri and J. S. Becker, *J. Anal. At. Spectrom.*, 2001, **16**, 1283.

238   S. F. Boulyga and J. S. Becker, *Fres. J. Anal. Chem.*, 2001, **370**, 612.

239   S. F. Boulyga, J. L. Matusevich, V. P. Mironov, V. P. Kudrjashov, L. Halicz, I. Segal, J. A. McLean, A. Montaser and J. S. Becker, *J. Anal. At. Spectrom.*, 2002, **17**, 958.

240   S. F. Boulyga and J. S. Becker, *J. Anal. At. Spectrom.*, 2002, **17**, 1143.

241   J. S. Becker, M. Burow, S. F. Boulyga, C. Pickhardt, R. Hille and P. Ostapczuk, *At. Spectrosc.*, 2002, **23**, 177.

242   P. Krystek and R. Ritsema, *Anal. Bioanal. Chem.*, 2002, **374**, 226.

243   J. A. McLean, J. S. Becker, S. F. Boulyga, H.-J. Dietze and A. Montaser, *Int. J. Mass Spectrom.*, 2001, **208**, 193.

244   C. C. Shen, R. L. Edwards, H. Cheng, J. A. Dorale, R. B. Thomas, S. B. Moran, S. E. Weinstein and H. N. Edmonds, *Chem. Geol.*, 2002, **185**, 165.

245   M. S. Choi, R. Francois, K. Sims, M. P. Bacon, S. Brown-Leger, A. P. Fleer, L. Ball, D. Schneider and S. Pichat, *Mar. Chem.*, 2001, **76**, 99.

246   R. S. Pappas, B. G. Ting, J. M. Jarrett, D. C. Paschal, S. P. Caudill and D. T. Miller, *J. Anal. At. Spectrom.*, 2002, **17**, 131.

247   J. Hinrichs and B. Schnetger, *Analyst*, 1999, **124**, 927.

248   S. Nakai, S. Fukuda and S. Nakada, *Analyst*, 2001, **126**, 1707.

249   X. Z. Luo, M. Rehkämper, D. C. Lee and A. N. Halliday, *Int. J. Mass Spectrom.*, 1997, **171**, 105.

250   M. Labonne, C. Hillaire-Marcel, B. Ghaleb and J. L. Goy, *Quat. Sci. Rev.*, 2002, **21**, 1099.

251   L. F. Robinson, G. M. Henderson and N. C. Slowey, *Earth Planet. Sci. Lett.*, 2002, **196**, 175.

252   S. Fukuda and S. Nakai, *Geochem. J.*, 2002, **36**, 465.

253   A. J. Pietruszka, R. W. Carlson and E. H. Hauri, *Chem. Geol.*, 2002, **188**, 171.

254   N. Vigier, B. Bourdon, S. Turner and C. J. Allegre, *Earth Planet. Sci. Lett.*, 2001, **193**, 549.

255   L. Kinsley, G. Mortimer, T. M. Esat and M. McCulloch, *Geochim. Cosmochim. Acta*, 2002, **66**, A399.

256   L. F. Robinson and G. M. Henderson, *Geochim. Cosmochim. Acta*, 2002, **66**, A642.

257   T. Warneke, I. W. Croudace, P. E. Warwick and R. N. Taylor, *Earth Planet. Sci. Lett.*, 2002, **203**, 1047.

258   S. Turner, P. van Calsteren, N. Vigier and L. Thomas, *J. Anal. At. Spectrom.*, 2001, **16**, 612.

259   C. R. Quétel, J. Vogl, T. Prohaska, S. Nelms, P. D. P. Taylor and P. De Bièvre, *Fres. J. Anal. Chem.*, 2000, **368**, 148.

260   C. H. Stirling, D. C. Lee, J. N. Christensen and A. N. Halliday, *Geochim. Cosmochim. Acta*, 2000, **64**, 3737.

261   M. Yamamoto, A. Tsumura, Y. Katayama and T. Tsukatani, *Radiochim. Acta*, 1996, **72**, 209.

262   S. H. Lee, J. Gastaud, J. J. La Rosa, L. L. W. Kwong, P. P. Povinec, E. Wyse, L. K. Fifield, P. A. Hausladen, L. M. Di Tada and G. M. Santos, *J. Radioanal. Nucl. Chem.*, 2001, **248**, 757.

263   S. Stürup, H. Dahlgaard and S. C. Nielsen, *J. Anal. At. Spectrom.*, 1998, **13**, 1321.

264   I. Rodushkin, P. Lindahl, E. Holm and P. Roos, *Nucl. Instrum. Methods Phys. Res. Sect. A-Accel. Spectrom. Dect. Assoc. Equip.*, 1999, **423**, 472.

265   C. S. Kim and C. K. Kim, *Anal. Chem.*, 2002, **74**, 3824.

266   C.-S. Kim, C.-K. Kim, J.-I. Lee and K.-J. Lee, *J. Anal. At. Spectrom.*, 2000, **15**, 247.

267   Y. R. Jin, L. Z. Zhang, S. J. Han, F. R. Zhu, J. F. Bai, G. Q. Zhou, F. Ma and L. X. Zhang, *Acta Chim. Sin.*, 2000, **58**, 1291.

268   E. J. Wyse, S. H. Lee, J. La Rosa, P. Povinec and S. J. de Mora, *J. Anal. At. Spectrom.*, 2001, **16**, 1107.

269   R. N. Taylor, T. Warneke, A. J. Milton, I. W. Croudace, P. E. Warwick and R. W. Nesbitt, *J. Anal. At. Spectrom.*, 2001, **16**, 279.

270   J. S. Becker and H. J. Dietze, *J. Anal. At. Spectrom.*, 1999, **14**, 1493.

271   J. S. Becker, C. Pickhardt and H. J. Dietze, *Int. J. Mass Spectrom.*, 2000, **202**, 283.

272 C. K. Kim, C. S. Kim, B. H. Rho and J. I. Lee, *J. Radioanal. Nucl. Chem.*, 2002, **252**, 421.

273 W. Kerl, J. S. Becker, H. J. Dietze and W. Dannecker, *J. Anal. At. Spectrom.*, 1996, **11**, 723.

274 M. Yamamoto, H. Kofuji, A. Tsumura, S. Yamasaki, K. Yuita, M. Komamura, K. Komura and K. Ueno, *Radiochim. Acta*, 1994, **64**, 217.

275 M. Agarande, S. Benzoubir, P. Bouisset and D. Calmet, *Appl. Radiat. Isot.*, 2001, **55**, 161.

Chapter 3

Combined High Resolution/Multi-Collector ICP-MS for Measurement of Total Zn and Zn Isotope Ratios in Faecal Samples from a Human Nutrition Study

3.1 Introduction

Zn is an essential element in the human diet, having an important function in many metabolic pathways. It is involved in cellular growth and differentiation and is therefore of particular importance in early childhood and during pregnancy. Zn is required for the function of a wide range of enzymes, and is reported to have a structural role in biological membranes, cell receptors used for hormone recognition and the proteins involved in gene expression. Among other effects, Zn deficiency leads to impairment of normal immune function, leading to greater susceptibility to infection.[1] The metabolic behaviour of Zn is therefore of great interest.

There are five stable isotopes of Zn, ranging from 0.6 to 48.6 % natural abundance. The low abundance isotopes can be used to label dietary Zn to monitor the metabolism of Zn in the body. Volunteers are given solutions and foods enriched in a low abundance isotope, and the resultant isotope ratio change in the blood, urine or faeces is measured. In order to provide useful information on the metabolism of Zn in the body, the total Zn content and at least one isotope ratio involving the isotope label must be determined.

A number of measurement techniques have previously been employed for the determination of Zn isotope ratios. Thermal ionisation mass spectrometry (TIMS) provides the best precision for isotope ratio determinations, and has been used to measure Zn ratios in biological samples to a level of 0.1 – 1 % relative standard deviation (%RSD).[2] The major drawback to TIMS analysis is that the analyte must be chemically separated from the sample matrix prior to determination, a

process that is both complex and time consuming. Fast-atom bombardment mass spectrometry (FAB-MS) has also been used in the study of Zn absorption and metabolism,[3] however this technique also requires extensive sample preparation. When confronted with the numbers of samples produced during a large scale nutritional study, the low throughput resulting from extensive sample preparation procedures and lengthy analysis times presents serious logistical problems.

The inductively coupled plasma is an excellent ion source for inorganic mass spectrometry, allowing the determination of a wide range of elements in many different sample types. For the majority of elemental analyses, inductively coupled plasma mass spectrometry (ICP-MS) does not require extensive clean-up of samples, acid digestion and dilution is sufficient. Sample throughput can easily be in excess of 100 samples per week. ICP-MS using a quadrupole mass analyser has been applied to Zn determinations in biological samples. However, due to spectral interferences arising from combination of the argon plasma and the sample matrix, the sample processing time had to be lengthened to include chemical separation of Zn from the matrix in order to obtain accurate isotope ratio data. Typical precision using this technique was in the range 0.3 – 1.5 %RSD depending on the isotope ratio being considered.[4-7]

Stürup has described the use of double focussing ICP-MS instrumentation operated at increased resolution for the determination of Zn isotope ratios in human samples.[8] A resolution setting of 6000 was used to measure the Zn isotopes free from plasma-based spectral interferences. A mathematical correction was applied to compensate for the $^{64}Ni^+$ overlap on $^{64}Zn^+$. A precision of 0.7 – 0.8 %RSD was recorded for 10 replicate measurements of the $^{66}Zn^+/^{68}Zn^+$, $^{67}Zn^+/^{68}Zn^+$ and $^{70}Zn^+/^{68}Zn^+$ ratios in acid digests of freeze-dried faecal material.

Multi-collector ICP-MS has been used for the measurement of Zn isotope ratios in geological materials to a precision equivalent to that achievable by TIMS.[9] As multi-collector ICP-MS is usually limited to low resolution determinations, extensive preparation procedures had to be employed to separate Zn from the samples prior to analysis.

This chapter describes the development of a method for the simultaneous determination of Zn totals and isotope ratios in acid digested faecal samples using multi-collector ICP-MS, with the Faraday detector on the axial channel replaced with an electron multiplier detector *via* the instrument control software. This configuration, with the axial detector channel operated at increased resolution, can measure the ^{70}Zn$^+$ free from the ^{40}Ar^{14}N^{16}O$^+$ interference. The use of the higher sensitivity electron multiplier detector on the axial channel also allowed more accurate measurement of the low abundance ^{70}Zn$^+$ isotope, whilst the more abundant isotopes were simultaneously detected on the Faraday collector array.

The method was validated through the measurement of a certified reference material, NIST 1577b (bovine liver), and comparison with the certified Zn concentration and published natural isotopic abundance data. Additionally, isotope ratio results for the same set of faecal samples analysed by the new method, by TIMS and by multi-collector ICP-MS with a collision cell were compared.

3.2 Background

The method described in this chapter was developed for the measurement of Zn in faecal samples from a human nutritional study co-ordinated by the Institute of Food Research (IFR), Norwich. The study used ^{70}Zn as a stable isotope tracer to investigate the absorption of Zn by 90 volunteers on one of three different diet types (meat, poultry and fish, vegetarian). 1.5 mg of a spike enriched with ^{70}Zn was mixed into a meal given to the volunteers and faecal samples were collected one day prior to and for at least 10 days after administration of the stable isotope label.

A known amount of dysprosium was also given in the dose meal. The rare earth elements are not absorbed by the body, therefore comparison of the total amount of dysprosium in the faeces from each volunteer with the amount given in the test meal could be used to ensure that all useful samples had been collected.

The precision required for isotope ratio measurements in the faecal samples was calculated by scientists at IFR according to the following procedure. The modelling software package SAAMII (SAAM Institute Inc., Seattle, USA) was used to simulate a nutritional study to find the amount of element (Zn) from a given dose (*e.g.* 1.5 mg) expected to appear in a certain sample (faeces in this case) at a certain time (day 1 or 5 or 10 etc). This information was then converted into an isotope ratio, as measured by mass spectrometry, by assuming a certain level of natural abundance element present in the faeces (or blood or urine), based on reference tables.[10] Random error was added to the isotope ratios by setting an initial, realistic precision for each ratio. An algorithm, developed at IFR, was then applied to calculate the within-sample precision required to limit the error in the final calculated absorption to a certain value, in this case 15 %. For the investigation of Zn absorption using faecal monitoring, the required within-sample precision for a ratio involving the stable isotope label was 0.4 %RSD.

3.3 Reagents and Sample Preparation

Aristar grade nitric acid (Merck-BDH, Poole, Dorset, UK) diluted with 18.2 MΩ cm water (Millipore, Bedford, MA, USA) was used for sample preparation and sample and standard dilution. All elemental standards were dilutions of 1000 μg ml^{-1} stock solutions (Merck-BDH) and the reference material used was NIST 1577b bovine liver (National Institute of Standards and Technology, Gaithersburg, MD, USA).

0.5 g of the freeze-dried faecal samples was digested in 5 ml of concentrated nitric acid using a Multiwave microwave digestion system (Perkin-Elmer Ltd, Beaconsfield, Buckinghamshire, UK). The faecal samples were digested in duplicate, with each batch of samples containing three replicates of NIST 1577b and at least three procedural blanks. The resulting solutions were diluted to 10 ml with Millipore water. Prior to analysis, the digests were diluted a further 100 fold with Millipore water containing gallium at 15 ng ml^{-1} as an internal standard. A 100 ng ml^{-1} Zn standard solution was analysed after every sixth sample for use as a bracket calibration standard to correct the raw data for instrumental drift.

3.4 Method Development

A VG Axiom magnetic sector ICP-MS system (Thermo Elemental, Winsford, Cheshire, UK) at the Central Science Laboratory, equipped with a multiple Faraday collector array was used throughout the study. Typical instrument operating parameters are given in Table 3.1.

Table 3.1 Instrument operating conditions

Forward power	1250 W
Plasma gas	14 L min^{-1}
Auxiliary gas	0.85 L min^{-1}
Nebuliser	400 μL min^{-1} Meinhardt (pumped uptake)
Neb gas	0.75-0.85 L min^{-1}
Lenses and torch position	Optimised for maximum Zn signal

Instrument sensitivity for ^{67}Zn was around 10^6 counts s^{-1} for a 1 μg ml^{-1} Zn solution, typical blank and sample concentrations are given in Table 3.2. The background Zn level was more than 100 times lower than the concentration found in samples, and since the procedural blank was subtracted from sample data for each batch, the contribution of natural Zn contamination to isotope ratios in the samples was negligible. Blank acid and procedural blank concentrations were very similar, suggesting that the majority of the background Zn originated in the acid and water used and that relatively little contamination was introduced during the sample preparation procedure.

Table 3.2 Comparison of typical background and sample Zn concentrations

	Blank acid	Procedural blank	Digested + diluted faecal sample
Conc. Zn	1.5 ng ml^{-1}	2 ng ml^{-1}	250 ng ml^{-1}

A variety of interferences for the Zn isotopes have been reported,[8] the principal species are summarised in Table 3.3. The Zn isotopes were individually scanned

at a resolution setting of 10,000 in a 1 in 100 dilution of an acid digested faecal sample. The only significant interference in the samples investigated was found to be $^{40}Ar^{14}N^{16}O^+$ at m/z 70.

Table 3.3 Spectral interferences encountered in Zn analysis by ICP-MS

Isotope	Natural abundance[11]	Principal interferences
$^{64}Zn^+$	48.63 %	$^{64}Ni^+$, $^{40}Ar^{24}Mg^+$
$^{66}Zn^+$	27.90 %	$^{40}Ar^{26}Mg^+$, $^{132}Ba^{2+}$
$^{67}Zn^+$	4.10 %	$^{134}Ba^{2+}$
$^{68}Zn^+$	18.75 %	$^{40}Ar^{28}Si^+$, $^{40}Ar^{14}N_2^+$, $^{136}Ba^+$
$^{70}Zn^+$	0.62 %	$^{35}Cl_2^+$, $^{40}Ar^{14}N^{16}O^+$

The VG Axiom offers two different modes of single collector data acquisition. Normal mode, in which the magnetic sector is scanned to alter the mass of the ions detected, can be used to acquire data across the whole mass range, but is relatively slow scanning, limiting the achievable isotope ratio precision. The second mode of acquisition is electrostatic analyser (ESA) scanning. This mode is restricted to a total mass range of approximately 15 % of the central mass measured, but is much faster than magnetic sector scanning and should therefore provide more precise isotope ratio data.

This theory was investigated through measurement of a Zn standard solution using both scanning modes, example isotope ratio precisions are given in Table 3.4. The acquisition parameters were as similar as possible given the different software for the two scan types, the dwell times were 10 ms for ^{66}Zn and ^{68}Zn and 100 ms for ^{70}Zn. The isotope ratio precision recorded for the ESA mode was significantly better than that for normal (magnet scan) mode, confirming the above statement.

Table 3.4 Within sample isotope ratio precision (n = 5) using different single collector scan modes for a 10 ng ml^{-1} Zn standard solution

	^{66}Zn / ^{70}Zn RSD	^{68}Zn / ^{70}Zn RSD
Magnet scan	0.73 %	0.85 %
ESA scan	0.36 %	0.64 %

Having demonstrated good isotope ratio precision for Zn standard solutions, the single collector, ESA scanning mode of acquisition was tested using a batch of 36 acid digested faecal samples from the nutritional study. Test analyses of reference material and faecal digests were used to determine the acquisition parameters, which are summarised in Table 3.5. The amount of sample available for the determination was limited to 5 ml by the autosampler used, therefore the settings applied were a compromise between the achievable precision and the time required for a run (sample consumption).

Table 3.5 Acquisition parameters for ESA analysis of acid digested faecal samples

Points per peak	15	Resolution setting	3000
Peak widths	3	Dwell times	^{67}Zn – 80 ms
Sweeps	10		^{68}Zn – 45 ms
Runs per sample	3		^{70}Zn – 100 ms

Within-sample isotope ratio precision better than 0.2 %RSD was achieved for ^{67}Zn / ^{70}Zn and ^{68}Zn / ^{70}Zn in some samples, however most samples had precision in the range 0.6 – 1.2 %RSD, with some as bad as 2 %RSD. The unreliability of isotope ratio precision was unacceptable for the demands of the nutritional study.

In order to improve the isotope ratio precision, a modified multi-collector configuration was investigated. The axial Faraday of the multi-collector array was retracted using the instrument software, and a secondary electron multiplier used for detection on this channel. This configuration allowed the resolution of the axial channel to be increased, while simultaneously detecting up to 8 other isotopes at low resolution on the multi-collector array (Fig. 3.1).

$^{70}Zn^+$ was collected on the axial channel, allowing increased resolution to be used to separate $^{40}Ar^{14}N^{16}O^+$ from the analyte signal. Use of the electron multiplier on this channel also provided sensitive detection of the lowest abundance Zn isotope. The mass dispersion of the magnet used in the Axiom ICP-MS system is such that the full range of the multi-collector array is limited to 10% of the centre mass.

Thus the detection of $^{70}Zn^+$ using the axial channel made the collection of $^{64}Zn^+$ and $^{66}Zn^+$ impossible. Faraday detectors in the multi-collector array were used to collect $^{67}Zn^+$, $^{68}Zn^+$ and $^{69}Ga^+$ and $^{71}Ga^+$ as internal standard isotopes.
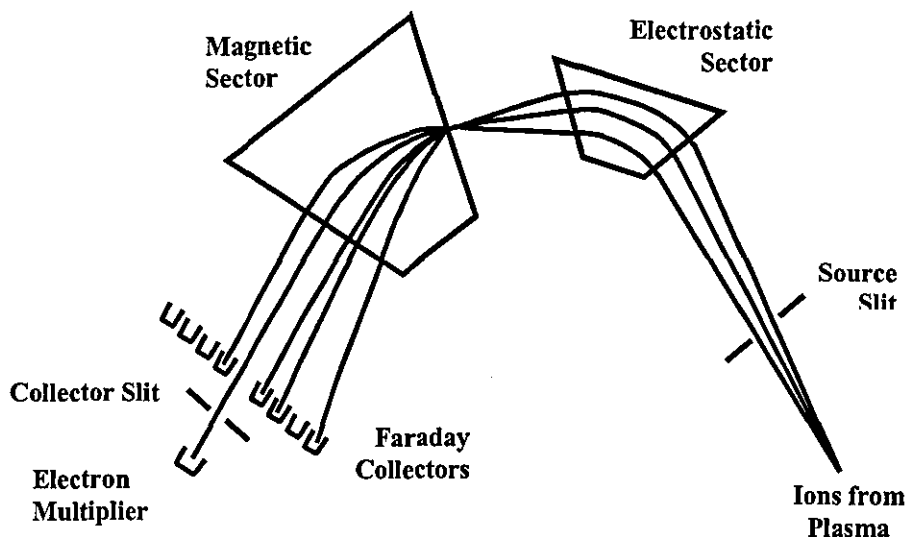
Fig. 3.1 Schematic of the combined multi-collector/high resolution detector configuration.

The narrow peak shape observed at increased resolution is not ideal for performing high-precision multi-collector measurements, as any mass calibration drift on the gaussian peak would cause the count rate recorded to change. A more stable signal was achieved by alteration of the slit settings. Firstly, the slits were set to the default values for a resolution of 3000, sufficient to separate the $ArNO^+$ interference on $^{70}Zn^+$. The width of the collector slit was then increased while continuously scanning the mass region m/z 69.9 to 70.1 to ensure full resolution of the interference. This had the effect of flattening the high resolution peak, thereby providing a more stable signal. The final collector slit setting was 50 units wider than the initial value, and resulted in a working resolution of 2350.

The combined high resolution/multi-collector configuration was tested through measurement of the same set of acid digested faecal samples used to evaluate the ESA method above. Acquisition parameters are given in Table 3.6. The within-sample isotope ratio precision for all 36 samples was between 0.14 and 0.38 %RSD for both ^{67}Zn / ^{70}Zn and ^{68}Zn / ^{70}Zn. This was within the precision level prescribed by the kinetic modelling procedure, therefore this method was applied

to the determination of Zn in samples from all 90 volunteers on the nutritional study.

Table 3.6 Parameters for high resolution/multi-collector acquisitions

Acquisition	2 sets	Dwell time	5 s
	25 points	Resolution setting	2350

3.5 Data Correction

Due to the large numbers of samples requiring analysis in this study, analytical runs of up to 18 hours were a very regular occurrence. Therefore, an accurate method for compensation of instrumental drift was required. Internal standardisation was the first method examined. A 15 ng ml^{-1} gallium spike was added to the samples via the diluent, ^{69}Ga and ^{71}Ga were measured simultaneously with the Zn isotopes using the multi-collector array. The results of this correction, as applied to replicate measurement of a Zn standard solution spiked with gallium, are presented in Fig. 3.2a. The solutions were analysed at regular intervals over a 14 hour period, samples from the nutritional study were measured between each replicate of the standard.

Ideally, the corrected relative response should be 1 for all replicate measurements, however the different detectors used for the determination of the different isotopes limited the effectiveness of the gallium internal standardisation. The relatively flat profile of the ^{67}Zn trace in Fig. 3.2a shows that reasonable correction was achieved for this isotope, which like the Ga isotopes, was measured using a Faraday detector on the multi-collector array. The drift observed for the ^{70}Zn signal, measured using the electron multiplier, was not accurately accounted for. Considering the difference in the mode of operation of the two types of detector, it is not surprising that the change over time of a signal collected using a Faraday collector did not match the changes in a signal recorded using the electron multiplier.
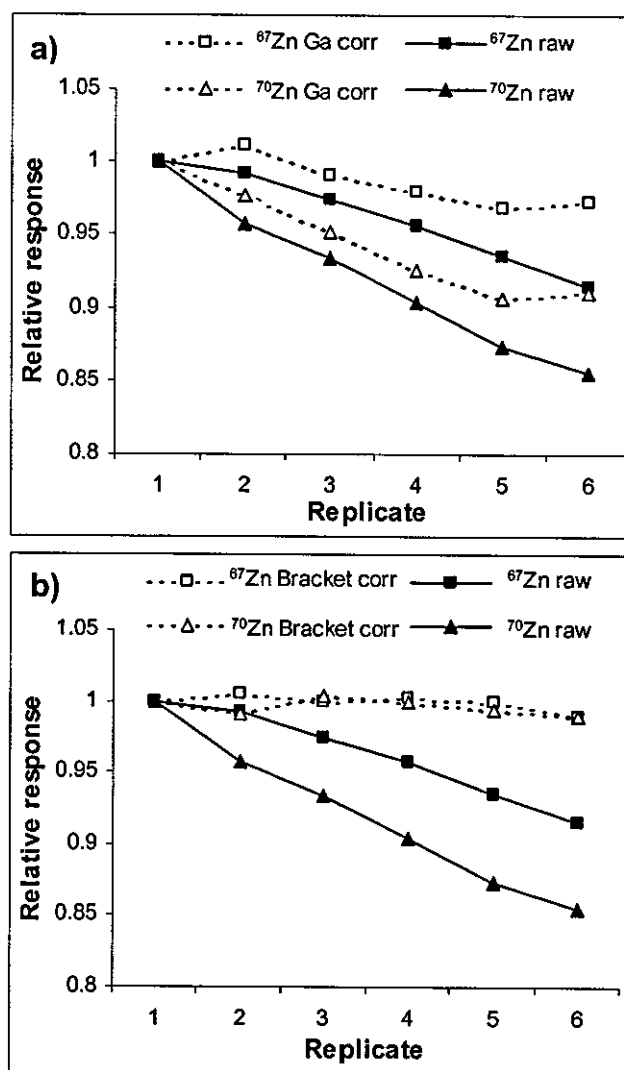
Fig. 3.2 Replicate measurement of a Zn standard solution over a 14 hour period. Nitric acid digests of faecal samples from the nutritional study were analysed between each measurement of the standard. Data was corrected using **a)** gallium internal standard and **b)** bracket standard solutions.

Due to the lack of effectiveness of internal standardisation, the response from bracket standard solutions, was investigated as a means of data correction. The procedure was implemented using equation 3.1.

$$I_{corr} = I_{meas} \times \frac{I_1^S}{\overline{I}_b^S}$$

3.1

Where I_{corr} and I_{meas} are the corrected and measured isotope intensities, I_1^S is the isotope intensity in the original standard solution and $\overline{I}_b^S$ is the mean of the isotope intensities measured in the bracket standard solutions.

Fig. 3.2b shows the results of this correction, applied to the same data as in Fig. 3.2a. After correction, there was little change in the intensity of the ^{67}Zn and ^{70}Zn signals over time, indicating that the drift observed for both isotopes was accurately compensated for by the bracket standardisation procedure. This protocol was therefore applied to data recorded for all samples from the nutritional study.

3.6 Method Validation

3.6.1 Total Zn content
Each batch of faecal samples digested contained at least three replicate digestions of the certified reference material NIST 1577b. Over a seven month period, a total of 190 separate digests of the reference material were analysed, randomly dispersed amongst samples from the nutritional study. The mean total Zn content of all 190 digests, calculated using external calibration, was 125 ± 14 µg g^{-1}, showing excellent agreement with the certified value of 127 ± 16 µg g^{-1}. External calibration was also used to determine the concentration of Zn in samples from the nutritional study, based on the response for the non-enriched ^{67}Zn isotope. This concentration of natural abundance Zn, together with the isotope ratio data, was then used by nutritionists to calculate the fraction of labelled Zn in the sample.

3.6.2 Isotope ratios
The bias on ^{67}Zn / ^{70}Zn and ^{68}Zn / ^{70}Zn was considerable, around 7 % per mass unit in favour of the heavier isotope, compared with a typical value of 2 % per mass unit for ^{67}Zn / ^{68}Zn. This difference was due to the mixed detector configuration employed. The electron multiplier used to measure ^{70}Zn was not cross-calibrated with the Faradays in the multi-collector array; the greater sensitivity of the electron multiplier compared to the Faraday collectors outweighed the reduction in sensitivity due to the increased resolution used on the axial channel. The difference between the collector channels was compensated for using control samples collected from each volunteer at the start of the nutritional study. As the sample was collected prior to administration of the isotope dose, it

was known to contain only natural abundance Zn. The factor required to convert the ^{67}Zn / ^{70}Zn ratio measured in this 't = 0' sample to the natural value was determined and applied to the remaining samples for each individual volunteer. For application to the large number of samples from the nutritional study, this procedure was automated in a Microsoft Excel® macro by staff at CSL.

The corrected isotope ratio results for replicate dilutions of the same digest of NIST 1577b are given in Table 3.7. The results showed good agreement with published natural abundance data,[11] with precision levels of 0.11, 0.10 and 0.07 %RSD for the ^{67}Zn / ^{70}Zn, ^{68}Zn / ^{70}Zn and ^{67}Zn / ^{68}Zn ratios respectively. The precision for the ratios measured in the three separate acid digests of the reference material included within each batch of samples was typically in the range 0.2-0.6 %RSD. Typical within-sample precision for acid digested faecal samples was 0.1-0.3 %RSD for all ratios considered, meeting the requirements of this human study.

Table 3.7 Corrected isotope ratio data for replicate analyses of NIST 1577b.
Natural ratios[11]: ^{67}Zn / ^{70}Zn = 6.613; ^{68}Zn / ^{70}Zn = 30.24; ^{67}Zn / ^{68}Zn = 0.2187

	^{67}Zn / ^{70}Zn	^{68}Zn / ^{70}Zn	^{67}Zn / ^{68}Zn
	6.602	30.18	0.2187
	6.616	30.23	0.2188
	6.613	30.23	0.2185
Mean	6.610	30.22	0.2187
%RSD	0.11 %	0.10 %	0.07 %

Typically, three digestion batches were analysed in a single overnight acquisition and most digestion batches contained samples from more than one volunteer. As each digestion was performed in duplicate, a single overnight acquisition contained up to 12 separate digests of 't = 0' faecal samples. Table 3.8 gives the uncorrected isotope ratio precision for the 't = 0' samples from 3 overnight acquisitions performed over a 2 month period. The data shows excellent within batch reproducibility, the precision of isotope ratios involving ^{70}Zn (detected

using the electron multiplier) was comparable to that for the ^{67}Zn / ^{68}Zn ratio (both isotopes detected using Faraday collectors).

The overall precision of uncorrected isotope ratio measurements from the 3 acquisitions was approximately 2 %RSD for ^{67}Zn / ^{70}Zn and ^{68}Zn / ^{70}Zn, and 0.4 %RSD for ^{67}Zn / ^{68}Zn. This difference was attributed to the long term change in performance of the electron multiplier as a function of the number of counts recorded, which is not matched by a similar change for Faraday collectors.

Table 3.8 Precision of isotope ratio measurements from 3 overnight analyses.

Date of analysis	No. t = 0 samples	Relative standard deviation		
		^{67}Zn / ^{70}Zn	^{68}Zn / ^{70}Zn	^{67}Zn / ^{68}Zn
1st Jun	10	0.75 %	0.30 %	0.61 %
2nd Jul	8	0.53 %	0.39 %	0.33 %
7th Aug	12	0.43 %	0.26 %	0.30 %
Overall precision		2.00 %	1.97 %	0.44 %

The correction based on the t = 0 samples was effective in accounting for this difference, illustrated by isotope ratio data for the reference materials from the above batches, given in Table 3.9. Prior to correction, ratios involving ^{70}Zn had a worse precision than ^{67}Zn / ^{68}Zn. After correction of the data for each reference material using t = 0 samples that were analysed in the same batch, the overall precision of the isotope ratios from the three analyses was similar, regardless of the detectors involved in measuring the isotopes.

Table 3.9 Sample-to-sample precision for replicate digests of NIST 1577b from batches analysed 1st Jun, 2nd Jul and 7th Aug (n = 24).

	^{67}Zn / ^{70}Zn	^{68}Zn / ^{70}Zn	^{67}Zn / ^{68}Zn
Prior to correction	2.06 %	1.82 %	0.78 %
After 't = 0' correction	0.89 %	0.50 %	0.75 %

3.6.3 Comparison with alternative techniques

It is vital that newly developed analytical methods are validated by comparison with known reliable techniques, such as TIMS. To test the current method, samples collected from one volunteer on the study were subjected to a clean-up procedure at IFR, following the method described by Eagles *et al.*[12] These fractions were then analysed using TIMS, an Axiom ICP-MS system in high resolution/multi-collector mode and a Micromass Isoprobe multi-collector ICP-MS instrument.

TIMS measurements were carried out by staff at IFR, using a Finnigan Thermaquad system (Finnigan MAT, GmbH, Bremen, Germany), following previously described methods.[12] Solutions from the sample preparation procedure were loaded onto single rhenium filaments, dried and analysed. A dwell time of 4 sec was used for these acquisitions, each ratio was the average of 50 replicates. The analytical protocol outlined above was used for the high resolution/multi-collector measurements, Zn fractions from the sample preparation were diluted by a factor of 25 prior to measurement. Determinations using a Micromass Isoprobe ICP-MS system were performed at Micromass Ltd., Manchester. This instrument is a multi-collector system, with a magnetic sector for the filtering of ions by mass, preceded by a collision cell. For Zn analyses, Ar was used in the collision cell at a flow rate of 1.8 ml min^{-1}. The principal purpose of the cell gas was to energy focus the ion beam, however interference reducing effects of reactive contaminants in the cell gas cannot be ruled out.[13] Zn fractions from the sample preparation procedure were diluted by a factor of 12.5 prior to analysis.

For all three sets of data, the 't = 0' correction described above was used to account for mass bias. Corrected ^{70}Zn / ^{67}Zn isotope ratios for the fractions from the clean-up procedure are illustrated in Fig. 3.3 for the three different instruments. As shown, there is reasonable agreement between the data sets.

To test for significant difference, paired, two-tailed T-tests were carried out. The t-statistic was calculated using equation 3.2.

$$t = \frac{\overline{d}\sqrt{n}}{s_d}$$

3.2

Where $\overline{d}$ and s_d are the mean and standard deviation of the differences between the ratios measured by the two techniques being compared; n is the number of samples.
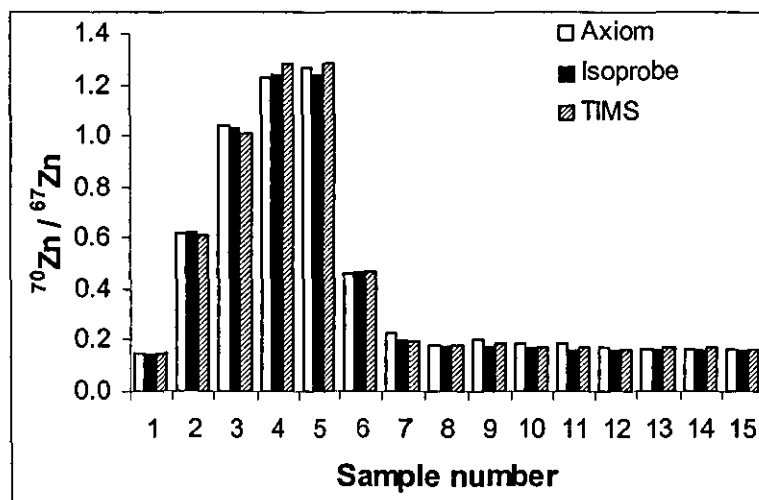
Fig. 3.3 ^{70}Zn / ^{67}Zn isotope ratios measured in the same samples by three different techniques.

A summary of the t-test results is presented in Table 3.10. From statistical tables, for a 95 % confidence interval and n = 15, the critical value of t is 2.14. All of the calculated absolute values of the t-statistic were lower than the critical value, therefore at a 95 % confidence level there was no significant difference between ^{70}Zn / ^{67}Zn ratios in the cleaned up samples measured by TIMS, by high resolution/multi-collector double focussing ICP-MS (Axiom) and by multi-collector single focussing ICP-MS with a collision cell (Isoprobe).

Table 3.10 T-test statistics for ^{70}Zn / ^{67}Zn ratios in the cleaned up faecal samples. Critical value of t = 2.14 (p = 0.05, n = 15).

	Axiom vs. Isoprobe	Axiom vs. TIMS	Isoprobe vs. TIMS
$\overline{d}$	0.005	0.001	-0.005
s_d	0.013	0.021	0.016
t - statistic	1.544	0.127	-1.136

The above data illustrates the accuracy of the high resolution/multi-collector method for determinations in clean solutions, however samples from the nutritional study were only acid digested and diluted prior to analysis. Confirmation of the applicability of the new technique for determinations in real samples was therefore required. Fig. 3.4 shows ^{70}Zn / ^{67}Zn isotope ratio results from the TIMS analysis of the fully cleaned up samples and Axiom ICP-MS data for the acid digested solutions of the same faecal samples.
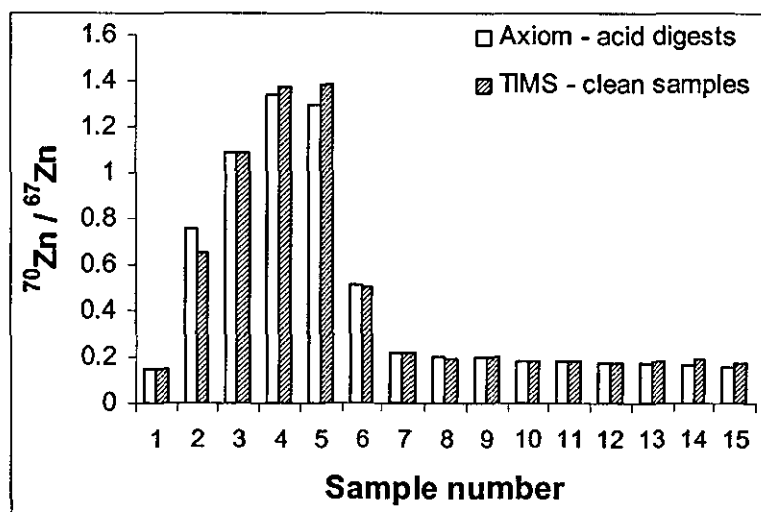
Fig. 3.4 ^{70}Zn / ^{67}Zn ratio results for a faecal sample set measured by ICP-MS after nitric acid digestion and by TIMS following a full sample clean-up.

To test for significant difference between the two data sets, a paired t-test was carried out. The mean of the differences was 0.005 and the standard deviation was 0.038. For n = 15, this gave t = 0.55, as before the critical value (95 % confidence interval) was 2.14. The calculated absolute t-statistic was less than the critical value, therefore the two sets of data were not significantly different. The high resolution/multi-collector ICP-MS method provided accurate isotope ratio data for faecal samples without the need for extensive sample preparation procedures.

3.7 Conclusion

When performing analysis for large numbers of samples, the time required for sample preparation and measurement are important considerations. The method described in this chapter was developed specifically for a nutritional study involving 90 human volunteers, each producing 10 to 15 faecal samples to be analysed in duplicate for total Zn and Zn isotope ratios. The precision required for the isotope ratio determinations was set by nutritionists using kinetic modelling techniques.

Increased resolution was required for the analysis of Zn by double focussing ICP-MS, the interference of $^{40}Ar^{14}N^{16}O^+$ on ^{70}Zn was the limiting factor requiring a resolution of approximately 3000 to be separated from the analyte signal. Single collector acquisition using ESA scanning was investigated, however the isotope ratio precision achieved in samples from the nutritional study was not consistently within the required level. To improve the precision, a novel combination of high resolution and multi-collector detection techniques was developed. ^{70}Zn was detected on the axial channel of the multi-collector array, allowing increased resolution for this isotope. Additionally, the use of an electron multiplier on this channel allowed accurate measurement of the low abundance ^{70}Zn, while simultaneously detecting the higher abundance isotopes using Faraday collectors in the multi-collector array. This configuration provided isotope ratio determinations that were reliably within the precision level set by the kinetic model.

The accuracy of the ICP-MS high-resolution/multi-collector method for the determination of Zn totals and isotope ratios in human faecal samples was illustrated using certified reference materials and by comparison with independent analytical techniques. External standardisation accurately corrected for the different drift characteristics of the electron multiplier and the Faraday collectors, and the 't = 0' sample for each volunteer was effective in correcting the mass bias. The large number of samples involved in the nutritional study meant that the quick, simple sample preparation and the increased speed of the ICP-MS analysis compared to TIMS were of great importance.

References

1   National Institutes of Health Clinical Center, Facts About Dietary Supplements, http://www.cc.nih.gov/ccc/supplements/zinc.html, Jan. 2002

2   P. Kastenmayer, in *Stable Isotopes in Human Nutrition, Inorganic Nutrient Metabolism*, ed. F. A. Mellon and B. Sandström, Academic Press, London, England, 1996.

3   J. A. Eagles and F. A. Mellon, in *Stable Isotopes in Human Nutrition, Inorganic Nutrient Metabolism*, ed. F. A. Mellon and B. Sandström, Academic Press, London, England, 1996.

4   C. J. Amarasiriwardena, A. Krushevska, H. Foner, M. D. Argentine and R. M. Barnes, *J. Anal. At. Spectrom.*, 1992, **7**, 915.

5   D. C. Grégoire and J. Lee, *J. Anal. At. Spectrom.*, 1994, **9**, 393.

6   C. Veillon, K. Y. Patterson and P. B. Moser-Veillon, *J. Anal. At. Spectrom.*, 1996, **11**, 727.

7   R. Roehl, J. Gomez and L. R. Woodhouse, *J. Anal. At. Spectrom.*, 1995, **10**, 15.

8   S. Stürup, *J. Anal. At. Spectrom.*, 2000, **15**, 315.

9   C. N. Maréchal, P. Télouk and F. Albarède, *Chem. Geol.*, 1999, **156**, 251.

10   *'Geigy Scientific Tables'*, 8th edition, ed. C. Lentner, CIBA-Geigy, Basel, Switzerland, 1981.

11   K. J. R. Rosman and P. D. P. Taylor, *J. Anal. At. Spectrom.*, 1999, **14**, 5N.

12   J. Eagles, S. J. Fairweather-Tait, D. E. Portwood, R. Self, A. Götz and K. G. Heumann, *Anal. Chem.*, 1989, **61**, 1023.

13   M. Dexter, P. Appelblad, C. Ingle, J. Batey, H. Reid and B. Sharp, *J. Anal. At. Spectrom.*, 2002, **17**, 183.

Chapter 4

Development of a High Resolution ICP-MS Method for the Measurement of Fe and Fe Isotope Ratios in Acid Digests of Faecal Samples from a Human Nutrition Study

4.1 Introduction

Fe is an essential nutrient, with a dietary requirement of approximately 10 and 15 mg day^{-1} for men and women respectively. Fe deficiency anaemia is the most common nutritional deficiency disorder, affecting some 2 billion people worldwide.[1]

There are four naturally occurring stable isotopes of iron, three of which have low natural abundance. These isotopes can be used to label dietary Fe to monitor the metabolism of Fe in the body. Volunteers are given solutions and foods enriched in one of the lower abundance isotopes, and the resultant isotope ratio change in the blood or faeces is measured.[2] The principal advantage of labelling with stable isotopes over the use of radioisotopes is that stable isotopes pose little or no risk to the volunteer, thereby facilitating ethical approval for use in vulnerable population groups such as infants, children and pregnant women.

In order to provide useful information on the metabolic behaviour of iron, the isotope ratio in the samples must be measured with a high level of both accuracy and precision. Thermal ionisation mass spectrometry (TIMS) is acknowledged as providing the best precision for isotope ratio determinations, and has been applied to the measurement of Fe ratios for many stable isotope studies.[3, 4] However, a second analysis technique (*e.g.* atomic absorption spectrometry) is often required to determine the total element concentration. Unfortunately, samples for TIMS analysis must be loaded in the form of the pure element, meaning that clinical samples must undergo a costly and time consuming preparation procedure prior to analysis.

Inductively coupled plasma mass spectrometry (ICP-MS) has a high sample throughput, and can determine isotope ratios and total element levels with a precision sufficient for many stable isotope studies.[5] Additionally, ICP-MS allows introduction of liquid samples at atmospheric pressure, without having to isolate the element prior to analysis. A summary of the use of ICP-MS for Fe isotope ratio measurements has recently been published by Vanhaecke et al.[6]

Analysis by ICP-MS using a quadrupole mass spectrometer can be hampered by the occurrence of spectral interferences (molecular or atomic species with the same nominal mass as the isotope of interest). The principal interferences that affect the analysis of Fe by ICP-MS are given in Table 4.1. Alternative sample introduction techniques, such as electrothermal vaporisation (ETV),[7] have been shown to reduce the level of oxide and hydroxide interferences sufficiently to allow the measurement of Fe by quadrupole ICP-MS. However, compared to solution nebulisation, ETV is relatively slow and, in general, cannot produce the same levels of isotope ratio precision, due to the transient signals produced and the variability of the vaporisation process.[8]

Table 4.1 Interferences encountered in Fe analysis by ICP-MS. Isotopic abundance data taken from reference 19.

Isotope	Abundance / atom %	Interfering species
$^{54}Fe^+$	5.85	$^{54}Cr^+$, $^{40}Ar^{14}N^+$
$^{56}Fe^+$	91.75	$^{40}Ar^{16}O^+$, $^{40}Ca^{16}O^+$
$^{57}Fe^+$	2.12	$^{40}Ar^{16}O^1H^+$, $^{40}Ca^{16}O^1H^+$
$^{58}Fe^+$	0.28	$^{58}Ni^+$, $^{40}Ar^{18}O^+$, $^{40}Ca^{18}O^+$, $^{42}Ca^{16}O^+$

'Cool' plasma techniques have also been applied to reduce the Ar based spectral interferences in Fe isotope ratio measurements.[9, 10] It is widely accepted however, that the lower rf power used under cool plasma conditions leads to increased non-spectral interferences (the influence of concomitant ions on the analyte signal), and increased levels of oxide interferences, such as CaO^+. This technique is therefore only generally applicable to the analysis of low salt content samples such as high purity acids and waters.[11]

Despite the problem of spectral interference, quadrupole-based ICP-MS systems have been used for the measurement of Fe isotope ratios for studies of Fe absorption in humans, with ^{54}Fe, ^{57}Fe and/or ^{58}Fe as the stable isotope label.[4] Ting and Janghorbani[12] employed isotope dilution techniques for the determination of Fe concentrations in human faecal matter, the level of Fe in the analysed samples (20 μg ml^{-1}) was such that the level of spectral interference was not significant. Whittaker et al.[13] have determined Fe absorption levels using ETV sample introduction to determine isotope ratios in blood serum, and latterly using instrumental optimisation to reduce polyatomic interferences,[14] allowing isotope ratios to be determined in aqueous solutions of whole blood at Fe concentrations of 10 – 20 μg ml^{-1}.

High resolution techniques using a double focussing ICP-MS system allow the determination of many isotopes free from their overlapping molecular ion interferences, without altering either the plasma conditions or the sample introduction strategy. Muñiz et al.[15] have used a nominal resolution of 3000 to separate the argon based molecular ion interferences from ^{56}Fe$^+$ and ^{57}Fe$^+$ for the determination of total Fe by isotope dilution techniques. High resolution ICP-MS has also been used for the determination of Fe isotope ratios in human serum.[6] Chromium levels in the samples were insignificant compared to the Fe concentration allowing precise determination of isotope ratios involving ^{54}Fe$^+$, however correction for the nickel overlap at mass-to-charge ratio (m/z) 58 significantly affected the precision of the ^{58}Fe$^+$ / ^{56}Fe$^+$ ratio.

The use of multi-collector ICP-MS for the determination of Fe isotope ratios has also been reported.[16, 17] Isotope ratio precision comparable to that achievable by TIMS was recorded through the use of sample preparation procedures to eliminate the sample matrix and desolvation to reduce the level of Ar based spectral interferences. As stated above, the lengthy preparation procedures required for the analysis of clinical samples presents a serious logistical challenge when large numbers of samples are to be analysed.

Aside from spectral interferences, the sample matrix also affects isotope ratios measured by ICP-MS. The presence of the matrix influences the extent of space charge effects, leading to changes in the mass bias.[18] Therefore ideally, internal standardisation should be used to correct for mass bias, as in this case the bias is measured in the sample solution itself. If it is not possible to apply internal standardisation, the matrix of the external standard used to determine the bias should be matched as closely as possible to that of the sample.

This chapter describes the development of a method for the analysis of Fe in faecal samples. A double focussing ICP-MS instrument was used, at a resolution setting of 4000, for the simultaneous determination of Fe concentrations and isotope ratios in acid digests of the faecal samples. In addition to the Fe isotopes, $^{53}Cr^+$ and $^{60}Ni^+$ were also monitored, and a mathematical correction was applied to account for the contribution of $^{54}Cr^+$ and $^{58}Ni^+$ to the signals at m/z 54 and 58. The method was validated by measurement of certified reference material NIST 1577b, and through comparison of isotope ratio data for high resolution ICP-MS, TIMS and multi-collector ICP-MS with a collision cell for both energy focussing of the ion beam and removal of plasma based interferences.

4.2 Method Development

4.2.1 Nutritional study

The method described in this chapter was developed for the measurement of Fe in faecal samples from the nutritional study described in Chapter 3. The study, organised by the Institute of Food Research (IFR), aimed to investigate Fe absorption by 90 human volunteers on meat, poultry/fish or vegetarian diets. A solution enriched in the stable isotope ^{58}Fe was mixed into a meal given to the volunteers and faecal samples were collected one day prior to and for at least ten days after administration of the dose. Calculation of the Fe absorption required determination of both an isotope ratio involving the stable isotope tracer and the total concentration of Fe in the faeces.

In order to determine the isotope ratio precision required, a kinetic modelling procedure comparable to that described in the previous chapter for Zn was performed by scientists at IFR. The required within-sample precision for a ratio involving the stable isotope label was 1 %RSD.

4.2.2 Sample preparation

Freeze-dried faecal samples from the nutritional study were microwave digested as described in the previous chapter. As stated, each digestion batch contained three replicates of certified reference material NIST 1577b (bovine liver) and at least three procedural blanks. After 100 fold dilution of the digested solutions with Millipore water, the analysed samples typically contained $100-300$ ng ml^{-1} Fe. A 100 ng ml^{-1} Fe standard solution was analysed after every sixth sample and used to correct the raw data for any instrumental drift.

4.2.3 Measurement strategy

All measurements were performed using a VG Axiom double focusing ICP-MS instrument (ThermoElemental, Winsford, Cheshire), in single collector mode. Typical operating conditions and experimental acquisition parameters are summarised in Table 4.2.

Table 4.2 Instrument operating conditions and experimental acquisition parameters

Forward power	1250 W
Cool gas	14 L min^{-1}
Auxiliary gas	0.8 L min^{-1}
Nebuliser gas	$0.75-0.80$ L min^{-1}
Resolution setting	4000
Scan mode	Electrostatic sector scanning
Dwell time	12 ms
Points per peak width	25
Scan window	2.5 peak widths
Sweeps	30
Masses monitored	*m/z* 53, 54, 57, 58 and 60
Total acquisition time	112.5 s

The spectral interferences arising from a 1 in 100 dilution of an acid digested faecal sample were investigated. It was found that a resolution setting of 4000 was sufficient to separate all the argon and calcium based interferences from the Fe isotopes. The theoretical resolution required to resolve $^{54}Cr^+$ from $^{54}Fe^+$ is 28,000; that required to separate $^{58}Ni^+$ from $^{58}Fe^+$ is 74,000. These resolutions are well beyond the capabilities of current commercial instrumentation. Therefore, chromium and nickel were monitored at m/z 53 and 60 respectively, and the contribution to the signals at m/z 54 and 58 calculated using published natural abundance data.[19]

At a resolution of 4000, the instrument gave a signal of 4×10^5 counts s^{-1} for ^{57}Fe in a 100 ng ml^{-1} Fe solution. The concentrations of Fe, chromium and nickel measured in reagent and procedural blanks are compared to the typical sample level in Table 4.3. The Fe concentration in the samples was more than 250 times the typical level in the procedural blanks, therefore following blank subtraction the contribution of contaminant Fe to the measured isotope ratios was not significant. The level of chromium in the reagents was around 10 % of that found in the samples, however the total concentration chromium was very low. The majority of the nickel in the measured solutions came from the faecal samples rather than the reagents or preparation procedure. The background level of nickel was 100 times lower than the concentration present in the samples.

Table 4.3 Comparison of typical background and sample Fe concentrations

	Blank acid	Procedural blank	Digested + diluted faecal sample
Conc. Fe	0.2 ng ml^{-1}	0.7 ng ml^{-1}	200 ng ml^{-1}
Conc. Cr	0.003 ng ml^{-1}	0.003 ng ml^{-1}	0.04 ng ml^{-1}
Conc. Ni	0.01 ng ml^{-1}	0.02 ng ml^{-1}	2 ng ml^{-1}

Problems were encountered with the linear dynamic range of the system. In the Axiom instrument used, signals above approximately 1.5×10^6 counts s^{-1} were automatically measured using a Faraday collector to prevent damage to the

electron multiplier. Although the two detectors could be accurately calibrated, the transition between them was not instantaneous and could not be relied upon to provide accurate data. This presented significant difficulties for measurement of samples from the nutritional study. Good measurement of the tracer isotope ^{58}Fe was essential, however this isotope has a natural abundance of only 0.28 %. To ensure a sufficient count rate for ^{58}Fe in samples with natural Fe abundance, the dilution factor used for the acid digested samples was limited to 100. At this dilution, the count rate for ^{56}Fe (95.7 % natural abundance) was consistently above the electron multiplier trip limit. ^{56}Fe was therefore excluded from the acquisitions.

4.2.4 Correction of isobaric interferences

In order to check the validity of the method used to correct for the chromium and nickel interferences, a 100 ng ml^{-1} Fe standard solution was spiked with the interfering elements at a range of concentrations and analysed using the method outlined above. The chromium and nickel concentrations added to the Fe standard reflected those expected in the faecal digests. The interference-corrected ^{58}Fe^{+} signal was calculated using equation 4.1.

$$^{58}\text{Fe}^{+} = {}^{58}\text{Total} - \left(\left({}^{58}\text{Ni}/{}^{60}\text{Ni} \right)_{Nat} \times {}^{60}\text{Ni}^{+}{}_{obs} \times k \right) \qquad 4.1$$

Where $\left({}^{58}\text{Ni}/{}^{60}\text{Ni} \right)_{Nat}$ is the natural nickel isotope ratio, $^{60}\text{Ni}^{+}{}_{obs}$ is the observed signal intensity for $^{60}\text{Ni}^{+}$ and k is a constant. $^{54}\text{Fe}^{+}$ was calculated using a comparable expression involving ^{54}Cr and ^{53}Cr in place of ^{58}Ni and ^{60}Ni.

The calculated $^{54}\text{Fe}^{+}$ and $^{58}\text{Fe}^{+}$ were ratioed to $^{57}\text{Fe}^{+}$, which is free from interference at a resolution of 4000. The relative values of the isotope ratios in the spiked solutions compared to those in a clean Fe standard were then calculated, and the log of the results taken to allow direct comparison of relative values above and below 1. Data for the nickel-doped solutions are presented in Fig. 4.1.
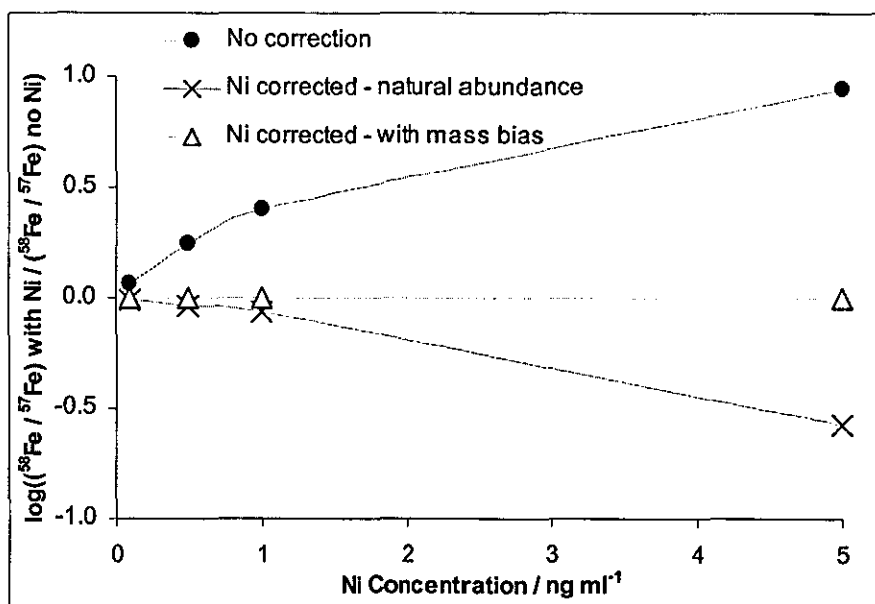
Fig. 4.1 $^{58}Fe^{+}$ / $^{57}Fe^{+}$ in 100 ng ml^{-1} Fe standards spiked with increasing concentrations of nickel, relative to that measured in a clean Fe solution.

For correction using natural isotopic abundance, the value of k in equation 4.1 was set to 1. For mass bias correction, k was evaluated by measurement of a clean nickel standard solution, using equation 4.2.

$$k = \frac{\left(^{58}Ni/^{60}Ni\right)_{obs}}{\left(^{58}Ni/^{60}Ni\right)_{Nat}}$$

4.2

Initial correction using the published natural abundance values[19] led to an over estimation of the contribution of nickel to the signal at m/z 58, and hence under-calculation of the signal due to $^{58}Fe^{+}$. The $^{58}Fe^{+}$ / $^{57}Fe^{+}$ ratio in the nickel-doped solutions was therefore lower than that measured in the clean Fe solution. This error was due to mass bias, the tendency of the instrument to transmit heavier ions more favourably than lighter ones, leading to a relatively increased signal at m/z 60 (assigned to $^{60}Ni^{+}$) and hence an overestimation of the $^{58}Ni^{+}$ signal. Accurate results were only obtained when the mass bias was corrected for, using external standardisation. The value of k was typically around 0.8, equivalent to a mass bias of 4 % per mass unit.

The results for the chromium-doped solutions are given in Fig. 4.2. The signal assigned to $^{54}Fe^+$ was overestimated when the natural chromium isotopic abundance values were used to calculate the correction, leading to $^{54}Fe^+ / ^{57}Fe^+$ ratios that were higher in the chromium-doped solutions than in the Fe standard. As for nickel above, a clean chromium standard was measured in order to determine the mass bias correction factor, k, which typically had a value of 1.05. When the mass bias was taken into account, there was good agreement between the ratios measured in the clean and spiked solutions.
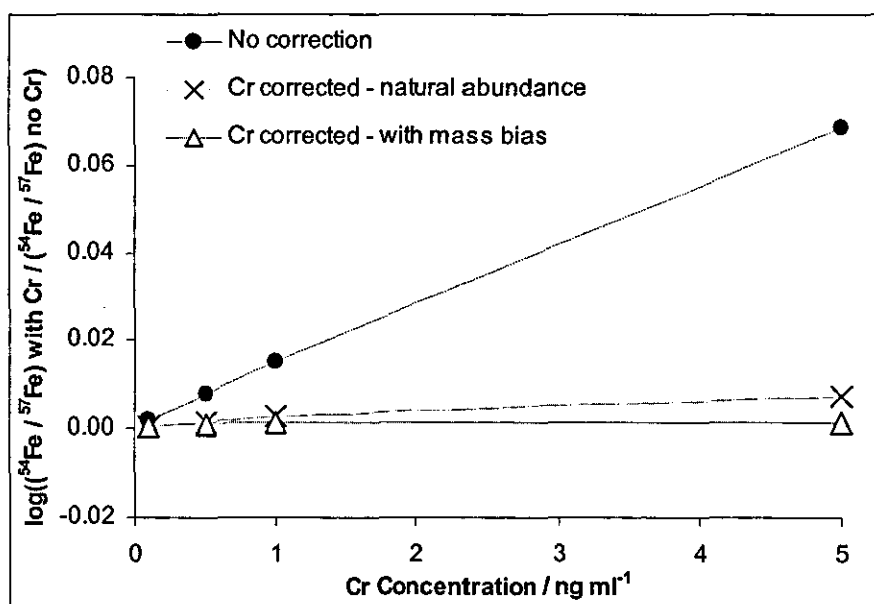
Fig. 4.2 $^{54}Fe^+ / ^{57}Fe^+$ in 100 ng ml^{-1} Fe standards spiked with increasing concentrations of chromium, relative to that measured in a clean Fe solution.

The influence of the mass bias at m/z 54 was much less significant than at m/z 58, largely due to the difference in the proportion of interference at the two masses. In the 100 ng ml^{-1} Fe solution doped with 5 ng ml^{-1} Cr, 14 % of the signal at m/z 54 was attributed to $^{54}Cr^+$, while for the same concentration of Ni spike, 89 % of the signal at m/z 58 was attributed to $^{58}Ni^+$. However, a correction for the mass bias was still required for the chromium interference at m/z 54, as the effect would become more pronounced if samples contained higher relative chromium concentrations.

4.3 Validation of Measurements

4.3.1 Total Fe content

As stated above, each batch of faecal samples digested also contained replicate digests of the certified reference material NIST 1577b. In total 190 separate digests of this reference material were analysed over a seven month period, randomly dispersed amongst samples from the nutritional study. The mean total Fe content of all 190 digests, calculated using external calibration was 182 ± 16 $\mu g\ g^{-1}$, showing excellent agreement with the certified value of $184 \pm 15\ \mu g\ g^{-1}$.

4.3.2 Fe isotope ratios

Isotope ratio data from individual control samples collected from each volunteer on the study were used to determine the mass bias factors required for the nickel and chromium corrections, which were then applied to the remaining samples for that specific volunteer. As the control sample was collected prior to administration of the stable isotope label (*i.e.* at t = 0), it was known to contain only Fe with natural isotopic abundance. This correction method has the advantage that the solutions used to determine the mass bias correction factor are closely matched to the samples to which the correction is applied, in terms of matrix components. It is noted that it was impossible to separate the effect of the mass bias between the two isotopes of the interfering element from that of the mass bias between the Fe isotopes, and that the correction procedure applied accounted for both bias effects together. Corrected isotope ratio data for the reference materials from three sample batches analysed in separate overnight runs are shown in Table 4.4, each result is the mean of three separate digests of NIST 1577b.

Table 4.4 Corrected isotope ratio data for NIST 1577b. Each value is the mean of three separate digests measured as part of a sample batch. Natural ratios: $^{54}Fe\ /\ ^{58}Fe = 20.73$, $^{57}Fe\ /\ ^{58}Fe = 7.514$.

	Batch 1		Batch 2		Batch 3	
	Mean	RSD	Mean	RSD	Mean	RSD
$^{54}Fe\ /\ ^{58}Fe$	20.63	1.0 %	20.67	0.96 %	20.65	1.2 %
$^{57}Fe\ /\ ^{58}Fe$	7.508	0.73 %	7.514	1.1 %	7.521	1.3 %

The mean value of ^{57}Fe / ^{58}Fe agreed well with published natural abundance data,[19] with a precision of approximately 1 %RSD for each set of three digests. The mean result for ^{54}Fe / ^{58}Fe was reliably within one standard deviation of the natural value, however the measured ratio was slightly, but consistently, lower than published data. This may suggest the presence of an unidentified interference that was still not being fully corrected for, or that biological fractionation effects had altered the Fe isotopic abundance in the bovine liver reference material. This effect did not affect the quality of the human study data, as the ^{57}Fe / ^{58}Fe was the ratio used in the faecal absorption calculations. Typical within sample precision for acid digested faecal samples was 0.2 – 0.7 %RSD for both isotope ratios, meeting the requirements set by the kinetic model.

4.3.3 Comparison with independent techniques

As for Zn determinations, the samples collected from one volunteer on the study were subjected to a clean-up procedure at IFR to separate Fe from the sample matrix. The method used has been previously published.[20] Fe isotope ratios were determined in these samples by TIMS, by high resolution single collector ICP-MS and by multi-collector ICP-MS with a collision cell for both energy focussing of the ion beam and removal of plasma based spectral interferences.

TIMS measurements were carried out at IFR using a Finnegan Thermaquad system (Finnegan MAT, GmbH, Bremen, Germany), following previously described methods.[20] Solutions from the sample preparation procedure were loaded onto single rhenium filaments, dried and analysed. A dwell time of 4 sec was used for these acquisitions, each ratio was the average of 50 replicates. High resolution single collector ICP-MS determinations were performed using the instrument and procedure described above. Fe fractions from the sample preparation were diluted by a factor of 500 before analysis.

The third instrument used was a Micromass Isoprobe ICP-MS system at Micromass Ltd., Manchester. This is a multi-collector system, with a magnetic sector for the filtering of ions by mass, preceded by a collision cell. Fe measurements were performed with Ar and H_2 supplied to the collision cell at

flow rates of 1.8 and 0.5 ml min^{-1} respectively. H_2 was added to reduce the Ar based interferences (see Table 4.1) to minimal levels. Fe sample fractions were diluted by a factor of 250 prior to measurement.

All three data sets were corrected for mass bias using the t = 0 samples. Corrections for chromium and nickel were not necessary as these elements were removed during the sample preparation. ^{58}Fe / ^{57}Fe isotope ratio data for the three techniques is presented in Fig. 4.3.
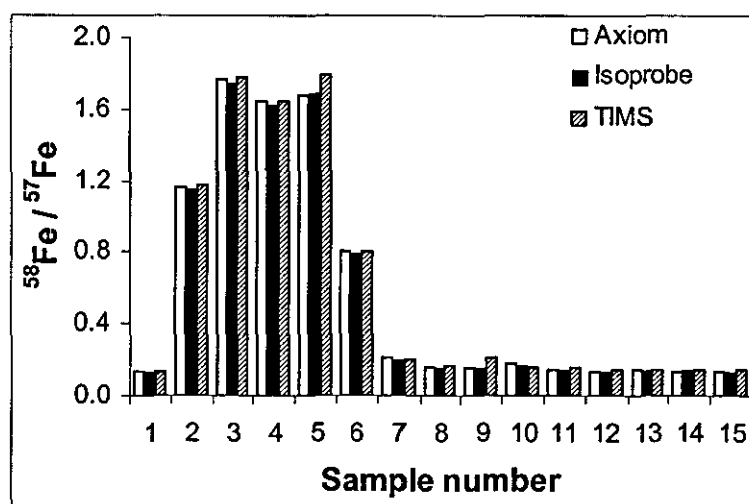
Fig. 4.3 ^{58}Fe / ^{57}Fe isotope ratios measured by three different techniques.

Similar to Zn data in the previous chapter, reasonable agreement between the three techniques was observed, although the isotope ratios were not exactly the same in all samples. A paired t-test was carried out to test for significant difference between the data sets, the t statistic was calculated using equation 3.2, reproduced below for reference.

$$t = \frac{\bar{d}\sqrt{n}}{s_d}$$

4.3

Where $\bar{d}$ and s_d are the mean and standard deviation of the differences between the ratios measured by the two techniques being compared; n is the number of samples.

The results of the t-test are given in Table 4.5. From statistical tables, the critical value of t for $n = 15$ and a 95 % confidence interval was 2.14. All of the absolute calculated values of t were less than the critical value, therefore the differences between isotope ratios measured by the three techniques were not statistically significant at the 95 % confidence level.

Table 4.5 T-test statistics for ^{58}Fe / ^{57}Fe ratios in the cleaned up faecal samples. Critical value of t = 2.14 (p = 0.05, n = 15).

	Axiom vs. Isoprobe	Axiom vs. TIMS	Isoprobe vs. TIMS
$\bar{d}$	0.005	-0.013	0.011
s_d	0.011	0.034	0.029
t - statistic	1.743	-1.489	1.473

The accuracy of the high resolution ICP-MS method for Fe isotope ratio determinations in acid digested faecal material was investigated by comparison of data for the same set of faecal samples analysed by TIMS following a full clean-up procedure and by ICP-MS following microwave acid digestion. Fig. 4.4 shows ^{58}Fe / ^{57}Fe isotope ratio results from the two analyses, each set of data was corrected according to the procedure described above.

To test for significant difference between the two data sets, a paired t-test was carried out. The mean of the differences was 0.019; the standard deviation was 0.044. Using equation 4.3, for $n = 15$, this gave $t = 1.70$; the critical value (95 % confidence interval) was 2.14. The calculated absolute t value was less than the critical value, therefore the two sets of data were not significantly different. The high resolution ICP-MS method and the correction procedure implemented for the nickel interference provided accurate isotope ratio data, without the requirement for extensive sample clean-up.
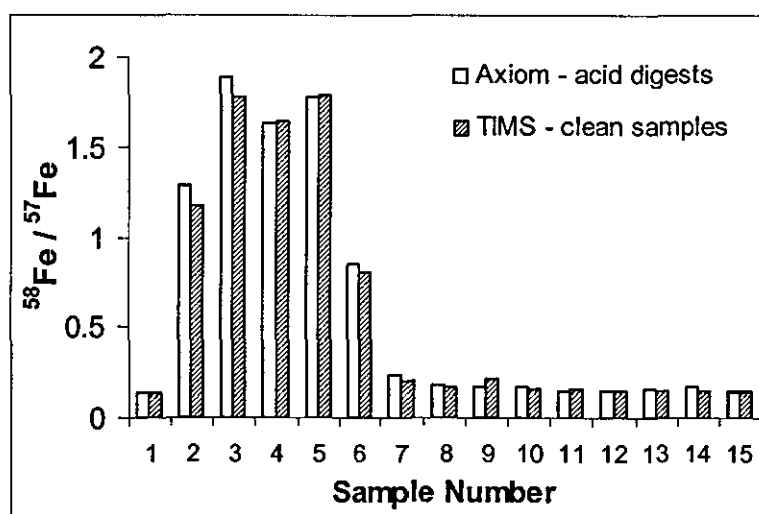
Fig. 4.4 Comparison of ^{58}Fe / ^{57}Fe ratio results for a faecal sample set measured by ICP-MS after nitric acid digestion and by TIMS following a full sample clean-up.

4.4 Conclusion

Fe isotopic analysis by ICP-MS is affected by a number of spectral interferences. Argon and calcium based interferences can be separated from the Fe isotopes using a resolution setting of 4000, however without the use of complex and time consuming sample preparation procedures, the isobaric overlaps of chromium and nickel are significant problems in the analysis of faecal samples. The resolutions required to separate these interferences from the Fe isotopes are well beyond the capabilities of current commercial instrumentation. In this work, other isotopes of the interfering elements were monitored to enable calculation of the contribution of each interference to the analyte signals. Accurate data for spiked Fe standard solutions was only achieved when the mass bias between the isotopes of the interfering elements was taken into account.

The accuracy of the high-resolution ICP-MS method for the determination of Fe and Fe isotope ratios in nitric acid digests of faecal samples from a nutritional study was illustrated by measurement of a certified reference material and by comparison of isotope ratio data with two independent techniques. Using t = 0 samples to determine correction factors for the chromium and nickel interferences, accurate and precise results were obtained without the requirement for further

sample clean-up. Although TIMS or multi-collector ICP-MS may have provided better isotope ratio precision, the results obtained from high resolution ICP-MS were of sufficient quality to meet the demands of the nutritional study. The large number of samples involved in the study meant that the quicker, simpler sample preparation and the increased speed of the method used were of great importance.

References

1   World Health Organisation, http:\\www.who.int, Nov. 2001

2   S. J. Fairweather-Tait, *J. Nutr.*, 2001, **131**, 1383S.

3   T. Walczyk, L. Davidsson, N. Zaveleta and R. F. Hurrell, *Fres. J. Anal. Chem.*, 1997, **359**, 445.

4   K. Y. Patterson and C. Veillon, *Exp. Biol. Med.*, 2001, **226**, 271.

5   R. Roehl, J. Gomez and L. R. Woodhouse, *J. Anal. At. Spectrom.*, 1995, **10**, 15.

6   F. Vanhaecke, L. Balcaen, G. De Wannemacker and L. Moens, *J. Anal. At. Spectrom.*, 2002, **17**, 933.

7   J. M. Carey, E. H. Evans, J. A. Caruso and W.-L. Shen, *Spectrochim. Acta Part B*, 1991, **46**, 1711.

8   H. E. Taylor, R. A. Huff and A. Montaser, 'Novel applications of ICP-MS' in *Inductively Coupled Plasma Mass Spectrometry*, ed. A. Montaser, Wiley-VCH, New York, 1998.

9   S. D. Tanner, M. Paul, S. A. Beres and E. R. Denoyer, *At. Spectrosc.*, 1995, 16.

10 L. S. Huang and K. C. Lin, *Spectrochim. Acta Part B*, 2001, **56**, 123.

11 D. J. Douglas and S. D. Tanner, 'Fundamental considerations in ICP-MS' in *Inductively Coupled Plasma Mass Specrometry*, ed. A. Montaser, Wiley-VCH, New York, 1998.

12 B. T. G. Ting and M. Janghorbani, *Anal. Chem.*, 1986, **58**, 1334.

13 P. G. Whittaker, T. Lind, J. G. Williams and A. L. Gray, *Analyst*, 1989, **114**, 675.

14 P. G. Whittaker, J. F. R. Barrett and J. G. Williams, *J. Anal. At. Spectrom.*, 1992, **7**, 109.

15 C. S. Muñiz, J. M. M. Gayon, J. I. G. Alonso and A. Sanz-Medel, *J. Anal. At. Spectrom.*, 1999, **14**, 1505.

16 N. S. Belshaw, X. K. Zhu, Y. Guo and R. K. O'Nions, *Int. J. Mass Spectrom.*, 2000, **197**, 191.

17 A. Stenberg, D. Malinovsky, I. Rodushkin, H. Andren, C. Ponter, B. Ohlander and D. C. Baxter, *J. Anal. At. Spectrom.*, 2003, **18**, 23.

18 S. D. Tanner, *Spectrochim. Acta Part B*, 1992, **47**, 809.

19   K. J. R. Rosman and P. D. P. Taylor, *J. Anal. At. Spectrom.*, 1999, **14**, 5N.

20   A. Götz and K. G. Heumann, *Int. J. Mass Spectrom. Ion Processes*, 1988, **83**, 319.

Chapter 5

Instrument Response Functions, Mass Bias and Matrix Effects in Isotope Ratio Measurements and Semi-Quantitative Analysis by Double Focussing ICP-MS

5.1 Introduction

The efficiency of ion transmission through an ICP-MS system varies depending on the mass of the ion, which leads to non-uniform sensitivity across the mass range and inaccurate isotope ratio measurements. This effect is known as mass bias.

It was put forward some time ago that the majority of mass bias observed in a quadrupole ICP-MS system was due to processes occurring in the interface region, including the space charge effect.[1] Mutual repulsion between the positively charged ions in the ion beam leads to ions being lost from the system. Lighter ions are repelled from the ion beam to a greater extent as they have lower translational energy, which leaves the ion beam enriched in heavier ions. Increased accelerating voltages do reduce the space charge (and so the mass bias),[2] however quadrupole mass analysers require low ion kinetic energies and a narrow energy distribution for effective mass resolution. This means that after a greater accelerating potential on extraction, the ions must be slowed before entering the quadrupole. In this deceleration, it is expected that space charge effects will occur, and mass dependent effects will be seen.[3]

Double focussing ICP-MS instruments typically utilise accelerating potentials of the order of 8 kV, much higher than those used in quadrupole systems,[4] and it was expected that the increased accelerating potentials would result in reduced space charge effects.[5, 6] Several groups have found that the mass bias is similar for double focussing and quadrupole instrumentation,[7, 8] suggesting that the majority of the bias may originate in the field free regions between the sampler and the

skimmer and/or immediately behind the skimmer where there is no penetration from the extraction field. It has also been put forward that mass bias may originate in the plasma itself.[9]

The non-analyte species present in the ion beam are also said to contribute to the total mass bias.[10] Among other effects, high concentrations of matrix elements result in an increased ion beam density, leading to greater space charge effects that exacerbate the loss of lighter ions from the ion beam.

A mathematical correction must be applied to take the mass bias into account. This requires the measurement of a known isotope ratio to calculate the bias, which is then applied to the analyte ratio. The reference ratio is either determined in reference solutions, analysed periodically through the sample run (external standardisation or standard bracketing), or in the sample solutions themselves (internal standardisation). The advantage of external correction is that the mass bias can be measured at the same masses and approximate abundances as the analyte isotopes, however the magnitude of the mass bias may change in the time lapse between measurement of the standard and the sample. Internal standardisation allows near continuous monitoring of the mass bias and can also be used to correct for matrix effects. This method may be inaccurate, however, as the isotopes used to calculate the bias have masses, ionisation characteristics and isotopic abundances that are different to the analyte isotopes. The calculated mass bias is applied to correct the analyte ratio using standard mathematical expressions, the most common being:[6, 11]

Linear model $\qquad R^{true} = R^{obs} \Big/ (1 + \Delta m B)$ $\qquad$ 5.1

Power model $\qquad R^{true} = \dfrac{R^{obs}}{(1 + B)^{\Delta m}}$ $\qquad$ 5.2

Exponential model $\qquad R^{true} = R^{obs} \Big/ \exp(\Delta m B)$ $\qquad$ 5.3

Where B is the bias per mass unit and Δm is the mass difference between the isotopes that make up the ratio R. These, and other mass bias correction expressions are discussed in detail in section 5.3. It is important to note that B is defined and determined locally for a specific isotope pair. Subsequent incorporation of B into one or other of the models requires the assumption that B is constant over the mass range of interest. This assumption is incorrect. In this chapter, the bias is shown to vary over just a few mass units, and taken to the extreme case, this assumption would predict equal bias for the ratios ^{6}Li / ^{7}Li and ^{207}Pb / ^{208}Pb, which does not accord with common experience.[8] Defining B locally raises a further potential difficulty; it may incorporate a contribution from unsuspected spectral interferences that could vary from sample to sample, and thus make it unrepresentative of the bias at adjacent masses.

Nevertheless, these models have been shown to approximate data acquired by ICP-MS. Taylor et al.,[6] using a multi-collector double focussing system, found the power and exponential laws to be most effective for the correction of mass bias in U measurements, as did Rehkämper and Mezger[12] for Pb. Park et al.[13] found the three correction equations to be almost equally effective when calculating a Sn isobaric interference for Cd ratios measured by single collector double focussing ICP-MS. Using quadrupole ICP-MS, Begley and Sharp[11] found the linear and power law functions to be equivalent for Pb isotope measurements using Tl as an internal standard, and the linear model to be at least as valid as the two alternatives for the correction of Pt isotope ratios.

A different approach has been favoured for the correction of mass bias in thermal ionisation mass spectrometry (TIMS). The equation employed is:[14, 15]

$$R^{true} = R^{obs} \bigg/ \left(\frac{m_2}{m_1} \right)^f \qquad\qquad 5.4$$

where m_1 and m_2 are the masses of the isotopes that make up the ratio R and f is the 'mass bias factor'. Note that f is still defined and measured locally, but this equation should be a much better approximation to the true situation as it indicates that the correction depends on the absolute masses of the isotopes that make up the ratio. This equation was first described by Russell et al.[13] and is referred to as the Russell correction expression throughout this chapter.

This expression is often adapted to apply internal standardisation in a single mathematical step. Considering the example of Tl as an internal standard for the correction of Pb isotope ratios, rearrangement of equation 5.4 for $R = {}^{205}\text{Tl} / {}^{203}\text{Tl}$ gives:

$$f = \ln\left(\frac{\left({}^{205}\text{Tl}\big/{}^{203}\text{Tl}\right)^{obs}}{\left({}^{205}\text{Tl}\big/{}^{203}\text{Tl}\right)^{true}}\right)\bigg/ \ln\left(\frac{205}{203}\right) \qquad 5.5$$

Equation 5.5 can then be substituted into equation 5.4 for $R = {}^{206}\text{Pb} / {}^{204}\text{Pb}$, which following rearrangement gives:

$$\left({}^{206}\text{Pb}\big/{}^{204}\text{Pb}\right)^{corr} = \frac{\left({}^{206}\text{Pb}\big/{}^{204}\text{Pb}\right)^{obs}}{\left(\dfrac{\left({}^{205}\text{Tl}\big/{}^{203}\text{Tl}\right)^{obs}}{\left({}^{205}\text{Tl}\big/{}^{203}\text{Tl}\right)^{true}}\right)^{\left(\frac{\ln(206/204)}{\ln(205/203)}\right)}} \qquad 5.6$$

These correction expressions have been shown to be applicable to multi-collector ICP-MS for several isotope systems.[9, 16, 17] In these cases it was found that the mass bias factors for the analyte and internal standard were not equal, but that the ratio of the two was constant during an analytical session, and could be used to successfully correct for the mass bias.

Maréchal et al.[9] showed that the power model (equation 5.2) and the Russell expression (equation 5.4) can be regarded as particular cases of a 'generalised power law':

$$R^{true} = \frac{R^{obs}}{g\left(m_2{}^n - m_1{}^n\right)} \qquad\qquad 5.7$$

where g is a function of a mass independent coefficient and n is an arbitrary number. It was shown that $n = 1$ for the power model and zero for the Russell expression.[9]

This chapter studies the mass bias characteristics of a double focussing ICP-MS system operated in both single and multi-collector modes. Areas of particular interest include the variation of the bias with mass, mass difference and time. Cd and Sn were measured for these investigations, giving coverage of the mass spectrum from m/z 108 to 124. The effect of increasing concentrations of matrix elements (bismuth and calcium) on measured isotope ratios is also examined.

In the second part of the chapter, the link between the mass bias and the response function of an ICP-MS instrument is defined. It is shown that the instrument response function can be used to determine a mass bias correction model specific to an individual instrument, providing more accurate isotope ratio determinations. Additionally, a method of performing semi-quantitative analysis is described that uses the mass bias for a series of measured isotope ratios to define the instrument response function. This approach is demonstrated for the calculation of 20 elemental concentrations in a multi-element solution based on knowledge of the concentration of a single internal standard.

Note: To avoid ambiguity, the term isotope ratio error (E^{obs}) is used in place of mass bias throughout this chapter, and is defined as:

$$E^{obs} = \frac{\left(R^{obs} - R^{true}\right)}{R^{true}} \qquad\qquad 5.8$$

5.2 Investigation of E^{obs} in Double Focussing ICP-MS

5.2.1 Data acquisition

The experiments were performed on Thermo Elemental VG Axiom double focussing ICP-MS instruments at the NERC Isotope Geosciences Laboratory (NIGL), Keyworth, Nottingham and at the Central Science Laboratory (CSL), Sand Hutton, York. Both instruments were used in solution mode, without sample desolvation. All standard solutions were prepared by dilution of 1000 μg ml^{-1} single element stocks (Claritas PPT, Spex Certiprep Inc., Metuchen, NJ) using double Teflon distilled 2 % nitric acid.

Data were acquired in both single and multi-collector modes; acquisition parameters for each mode and typical instrument operating conditions are given in Table 5.1. The instrument was allowed to warm up for at least one hour prior to recording any data. Measurements using the multi-collector were acquired statically; the collector positions and solution concentrations used are shown in Table 5.2. Prior to data acquisition, baselines 0.5 mass units either side of the axial mass were measured. These values were subtracted from the data by the instrument software prior to any calculations.

Table 5.1 Instrument operating conditions and experimental acquisition parameters

Instrument Parameters		
Forward power	1250 W	
Plasma gas	14 L min^{-1}	
Auxiliary gas	0.85 L min^{-1}	
Nebuliser	100 μL min^{-1} Meinhardt (pumped uptake) Gas flow optimised for maximum signal at ^{115}In	
Resolution setting	400	
Lens settings	Optimised for maximum signal at ^{115}In	
Experimental Parameters		
	Single collector	**Multi-collector**
Detector	Electron multiplier	Nine Faraday collectors
Dwell time	10 ms	5 s
Data acquisition	3 peak widths	2 sets
	20 points per peak	25 points per set
	10 sweeps	

Table 5.2 Solutions measured for the multi-collector acquisitions and the masses monitored therein. Ax = axial Faraday collector. L1 to L4 and H1 to H4 refer to the low and high mass Faraday collectors respectively.

	L4	L3	L2	L1	Ax	H1	H2	H3	H4
200 ng ml^{-1} Cd	---	^{108}Cd	---	^{110}Cd	^{111}Cd	^{112}Cd	^{113}Cd	^{114}Cd	^{116}Cd
200 ng ml^{-1} Sn	^{116}Sn	^{117}Sn	^{118}Sn	^{119}Sn	^{120}Sn	---	^{122}Sn	---	^{124}Sn

Typical instrument sensitivity recorded for the 200 ng ml^{-1} elemental standards was 5×10^7 counts s^{-1} for ^{112}Cd (24.1 % abundance) and 8×10^7 counts s^{-1} for ^{118}Sn (24.2 % abundance).

For single collector determinations, electrostatic sector scanning was used with a secondary electron multiplier for ion detection. 2.5 ng ml^{-1} Cd or Sn was used as the sample; the masses monitored corresponded to those available using the multi-collector array. For a particular mode of data acquisition each set of analyses was performed on a single day and the order in which the solutions were analysed was randomised to minimise the effect of drift on the data.

5.2.2 Correlation of signals

The first data analysis method examined was linear regression of the ion signals. For each separate experiment incorporating data for an individual element, the ion signal recorded at each m/z value was plotted against every other ion signal over the course of an acquisition. The data recorded in multi-collector mode showed significantly higher correlation than the single collector, typical R^2 values for one mass unit difference between the isotopes were 0.999 and 0.4 respectively. High correlation was expected for the multi-collector data because the isotopes that are being compared were detected simultaneously. As the different isotopes leave the plasma at the same time, the level of noise associated with them is the same, leading to high correlation between the ion signals over the course of an acquisition.

The single collector is limited to sequential detection of ions. Each isotope measured using this system will have left the plasma at a slightly different time and will have a different level of noise associated with it due to the instability of

the plasma source. This leads to a low correlation between the ion signals over time. It is worth noting that as the mass difference between the isotopes increased, the correlation of the signals decreased. At a difference of 8 mass units, the R^2 values were 0.94 and 0.25 for multi-collector and single collector modes respectively.

5.2.3 Variation of E^{obs} with time

The error in the observed Cd and Sn isotope ratios was calculated using equation 5.8. Published natural isotopic abundance data[18] was used to calculate R^{true} values. Typical values for E^{obs} per unit mass were 1.2 – 1.4 % for the multi-collector and 1.0 – 2.4 % for the single collector determinations. These values compare reasonably with literature values for elements of a similar mass, Heumann et al.[8] found the mass bias to be 1.7 % per mass unit on measurements of the ^{79}Br / ^{81}Br ratio by single collector double focussing ICP-MS and Walder et al.[19] found the bias using a multi-collector system to be approximately 1.2 % per mass unit at m/z 144.

The variation of E^{obs} for multi-collector isotope ratio data over a 50 min. period was examined. The changes in ^{114}Cd / ^{112}Cd and ^{119}Sn / ^{118}Sn were typical of the data recorded, E^{obs} for these ratios is plotted against time in Fig. 5.1. Note that because time was the independent variable, an arbitrary reference point has been chosen rather than the ensemble average. The instrument was stable to within two times the standard error of the population over a 20 to 30 min. timescale, after which significant deviation from the original E^{obs} value was seen. Therefore in all acquisitions, only data acquired within a 20 min. period was considered to be comparable.

E^{obs} for data acquired in single collector mode varied over a wider range than in multi-collector mode, typically ±10 % compared to ±1 %. Due to the difference in measurement precision of the two detection systems however, the drift observed in single collector mode was also within two times the standard error of the population over a 20 min. acquisition period.
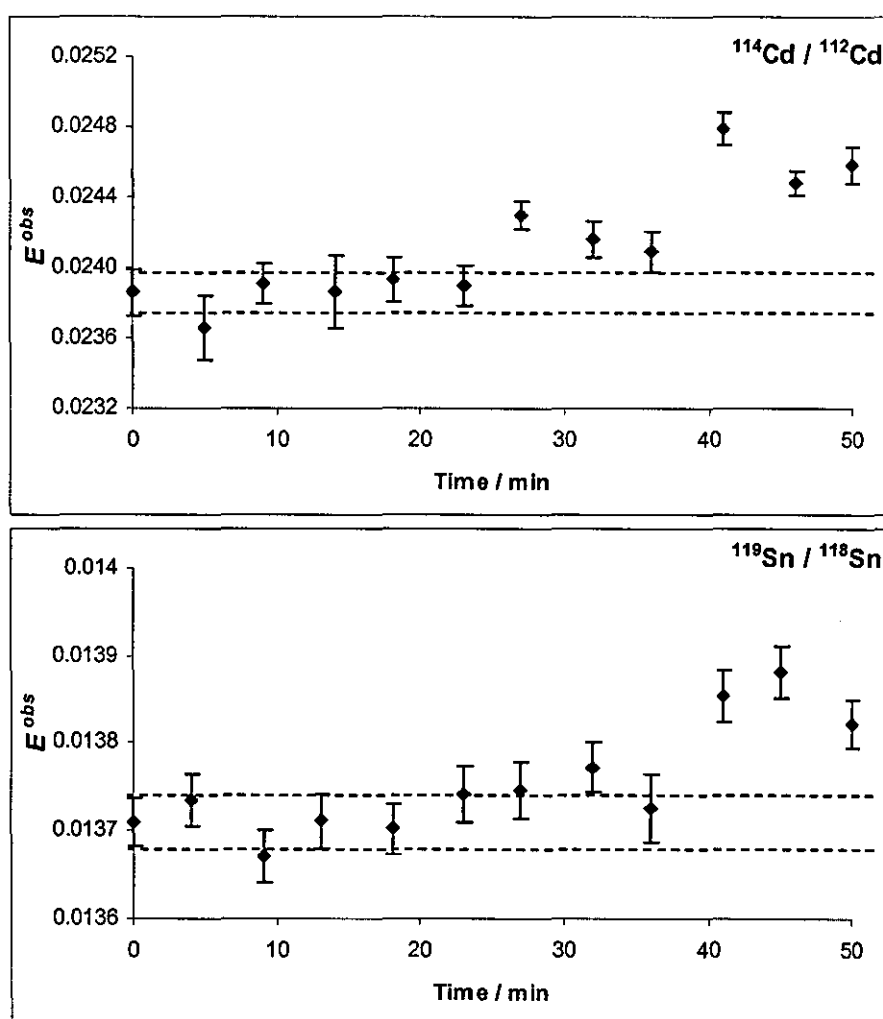
Fig. 5.1 Variation of E^{obs} for Cd and Sn in multi-collector mode, over a 50 min. period. Error bars represent 2 times the standard error (SE) of the individual points, dotted lines mark $\pm 2 \times \sqrt{\sum \left(SE^2 \right)/n}$ from the initial measurement.

5.2.4 Variation of E^{obs} with absolute mass

Isotope ratios with a mass difference between the isotopes (Δm) of one were used to investigate the change in E^{obs} with the average mass of the isotopes that make up a ratio; Cd and Sn have 8 such ratios between them. The time between starting the Cd and Sn measurements was kept to a minimum (approximately 10 min.) to ensure that results for the two elements could be treated as a single data set. The data is presented in Fig. 5.2 for single and multi-collector modes of acquisition; each point is the mean of 50 integrations, error bars represent 1 standard deviation. The single collector data (Fig. 5.2a) showed no significant variation from the ensemble mean (dotted line) as the mean mass of the isotopes changed,

112
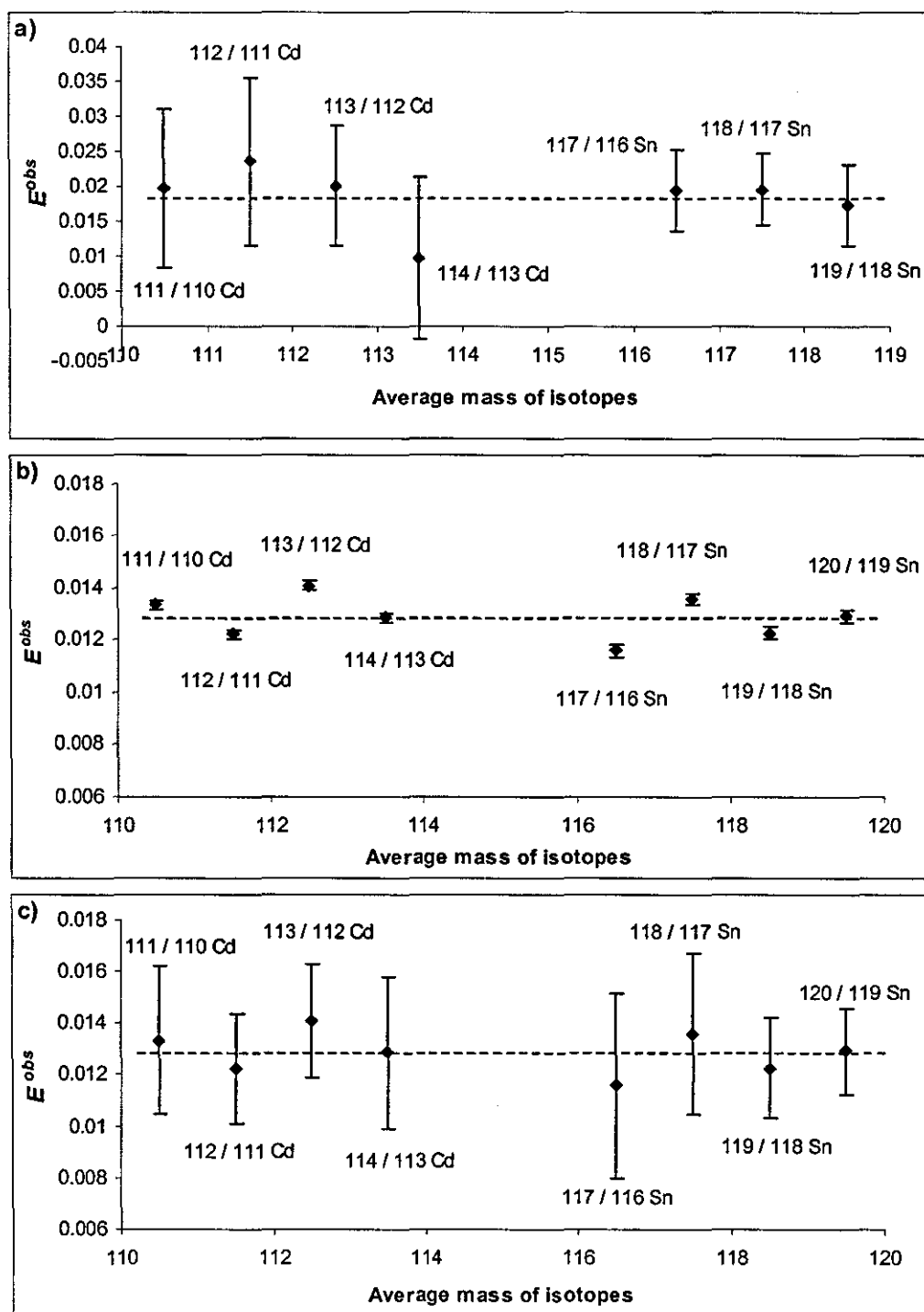
Fig. 5.2 E^{obs} *vs.* average mass of isotopes for ratios with a mass difference of 1 for **a)** single collector, **b)** and **c)** multi-collector data. Dotted lines mark the mean E^{obs} value and error bars represent one standard deviation, in **a)** and **b)** for the measurement only, in **c)** for the combined measurement and natural isotopic abundance uncertainty.[18]

owing to the magnitude of the error in the data. During single collector Sn acquisitions, the maximum count rate recorded for ^{120}Sn was above the electron multiplier trip level, the signal was automatically measured using a Faraday cup in order to protect the electron multiplier from the high intensity. The ^{120}Sn / ^{119}Sn

isotope ratio was therefore excluded from the single collector data set as it was not directly comparable to the remaining Sn ratios.

The greater precision achieved using the multi-collector array allowed significant changes in E^{obs} with average mass to be seen (Fig. 5.2b). The published natural isotopic abundances used to calculate E^{obs} have uncertainties associated with them;[18] a plot of E^{obs} vs. average isotope mass for the multi-collector data including these uncertainties is given in Fig. 5.2c. The absolute uncertainties given by Rosman and Taylor[18] were propagated into the standard deviation of the analysis using accepted error calculation expressions.[20] As shown in Fig. 5.2c, the variation of E^{obs} including the natural isotopic abundance uncertainties was within one standard deviation of the mean value for both Cd and Sn isotope ratios. It was found, however, that the pattern of results around the mean value was reproduced in subsequent determinations. Fig. 5.3 shows E^{obs} relative to the mean value for the initial Cd measurements, and replicate data recorded 2 months later.
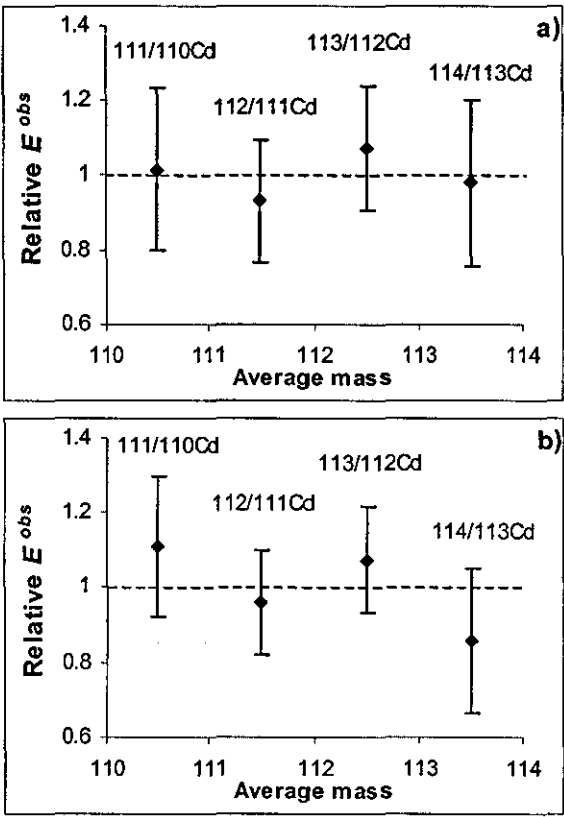
Fig. 5.3 E^{obs} relative to the mean E^{obs} value vs. average mass for Cd isotope ratios a) original data, b) + 2 months. Error bars represent the combined standard deviation, as in Fig 5.2c.

The mean value of E^{obs} for the repeat measurements was 0.015, compared to 0.013 in the original determinations. Variation in the absolute value of E^{obs} was expected, however the reproducibility of the pattern of the individual E^{obs} values about the mean was not.

There are three possible explanations for deviation from the mean E^{obs} and the reproducibility of the pattern of deviation. Firstly, imperfection in the gain calibration of the Faraday amplifiers could have led to uneven response across the multi-collector array. The reproduction of the same pattern of variation on different occasions and following recalibration of the amplifiers, along with the magnitude of the deviation, is strong evidence against this explanation.

Secondly, there may have been spectral interferences affecting the analyses. The solution used in the measurements was investigated at resolution settings up to 10,000, but no resolvable spectral interferences were found. As the resolution of the system is increased however, the sensitivity decreases meaning that even if they were present, low levels of resolvable spectral interferences such as Ar_2NO^+, $Ar_2O_2^+$, KrO_2^+ and $KrNO^+$ would not be seen. A number of oxide interferences fall in the mass range under investigation, and would not be separated using maximum resolution. None of the possible elements (Ru, Mo, Zr, Rb) were found at detectable levels in the analyte solutions, even at low resolution, therefore the oxides were almost certainly not present. Despite these observations, spectral interference, possibly in the form of a combination of species, may have been the cause of the observed pattern of deviation about the mean value of E^{obs}. As ICP-MS systems become more sensitive, and more precise measurements are performed using multi-collector detection techniques, it is inevitable that low level spectral interferences previously hidden by poor measurement precision will become problematic.

A third explanation for the observed patterns is that the natural isotope abundance values used to calculate E^{obs} did not match the true isotopic abundance in the analysed solutions. By decreasing the 'true' ^{112}Cd abundance value from 24.13 to 24.12 %, and increasing ^{111}Cd and ^{113}Cd by 0.005 % to maintain a total of 100 %, all analyses in Fig 5.3a display the same E^{obs}. Similarly for Sn, small changes to

the values used as the true isotopic abundance removed the variation completely. These changes are well within the uncertainty ranges of the natural isotopic abundances specified by Rosman and Taylor,[18] suggesting a slight variation to the reference isotope ratios may be recommended. The reproducibility of the pattern of deviation indicates that this explanation is the most plausible.

5.2.5 Variation in E^{obs} with mass difference (Δm)

The change in E^{obs} with Δm was investigated by examining sets of ratios with a single isotope as denominator. Results for ^{X}Sn / ^{117}Sn for single and multi-collector determinations are presented in Fig. 5.4 by way of example.
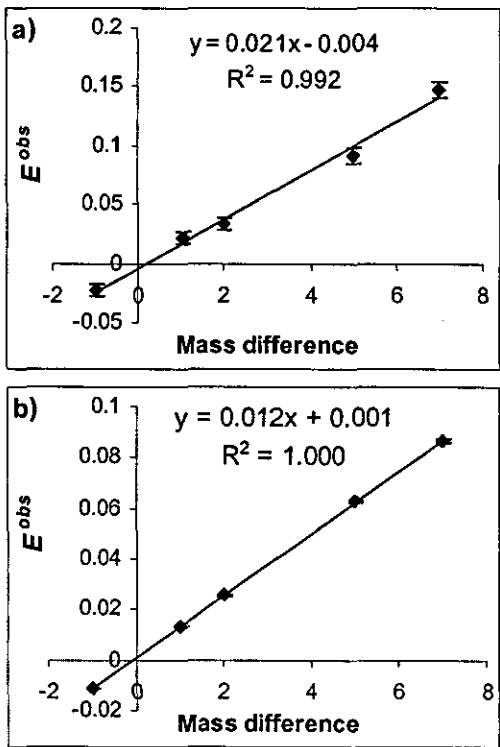
Fig. 5.4 E^{obs} vs. mass difference for ^{X}Sn / ^{117}Sn, where X = all other Sn isotopes, for a) single collector (SC) and b) multi-collector (MC) modes. Error bars represent the measurement standard deviation.

The straight line trend was reproduced when other Sn isotopes were used as the reference point, and in similar examination of Cd isotope ratios. Although this immediately suggested the linear correction model to be most appropriate to this system, when the ^{X}Sn / ^{117}Sn multi-collector isotope ratio data was used to evaluate B for the power and exponential models using equations 5.2 and 5.3, and

116

then multiplied by Δm to convert bias per mass unit into E^{obs}, the plots of E^{obs} vs. Δm were also linear, with an R-squared value of 0.9995. This outcome is due to the relatively small mass range examined; over only eight mass units the power and exponential functions are approximately linear.

The multi-collector data always displayed a very strong linear relationship between E^{obs} and Δm. Upon further investigation, it was found that as the mass of the reference isotope decreased, the gradient of the regression line increased such that the gradient for ^{X}Sn / ^{124}Sn was 0.0114 and that for ^{X}Cd / ^{110}Cd was 0.0134, where X represents the other isotopes of Sn or Cd. The change in gradient across the mass range examined is illustrated in Fig. 5.5. The trend observed clearly demonstrated that E^{obs} did change with the mass analysed, and therefore that the power, linear and exponential mass bias correction expressions that are dependent solely on the mass difference between the isotopes are fundamentally incorrect.
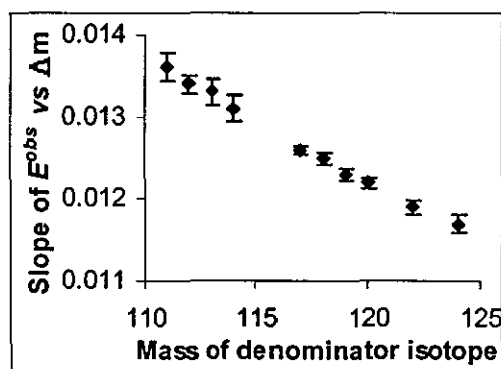
Fig. 5.5 Change in the gradient of the regression line of the plots of E^{obs} vs. mass difference with mass of the denominator isotope for multi-collector Cd and Sn data. Error bars are one standard deviation of the gradient of each regression line calculated using standard statistical techniques.[20]

As shown in Fig. 5.4a, the single collector data was not as closely linear as the multi-collector data, however a correlation coefficient of 0.99 is still suggestive of a strong linear relationship, and E^{obs} for all ratios considered was within one standard deviation of the line of best fit drawn through the data. The gradient of the plot for single collector data was significantly higher than that for the equivalent multi-collector data, a result that was repeated in subsequent acquisitions. The change in the gradient of the line of best fit with mass of the reference isotope was also generally greater for the single collector

117

determinations. On changing the reference isotope from ^{116}Sn to ^{124}Sn, the gradient of the single collector plots decreased by approximately 20 %, compared to a 10 % decrease for multi-collector data. This discrepancy is most likely due to the difference in the modes of acquisition and the use of electrostatic sector scanning for the single collector experiments. This scan mode introduces extra bias to the system because the changes in the electrostatic sector voltage with mass also affect the sensitivity.[4]

5.2.6 Effect of matrix elements on isotope ratio measurements in multi-collector mode

The effect of high concentrations of i) heavy and ii) light, easily ionisable matrix elements was studied by separately spiking 200 ng ml^{-1} Cd and Mg standard solutions with bismuth and calcium in concentrations of 1, 10, 50 and 100 μg ml^{-1}. The data were collected in static multi-collector mode. Collector positions as in Table 5.2 were used for Cd acquisitions. Data for ^{25}Mg was collected in the axial position, ^{24}Mg and ^{26}Mg were detected by the L4 and H4 collectors respectively (note that the dispersion of the instrument is fixed, the mass range that can be covered by the multi-collector array is 10 % of the mass of the axial isotope). Typical instrument sensitivity for a 200 ng ml^{-1} Mg solution was 10^6 counts s^{-1} for ^{25}Mg (10.0 % abundance). At the same concentration of Cd, a signal of 4×10^7 counts s^{-1} was recorded for ^{113}Cd (12.2 %). The samples for each element were analysed in random order and a solution containing only Cd or Mg was measured before and after each spiked sample. 2 % nitric acid was aspirated for at least 10 min. between analysis of the doped and 'clean' solutions. The use of Cd and Mg as analytes and calcium and bismuth as matrix elements enabled the influence of both analyte and matrix element mass to be investigated.

Firstly, the effect of the matrix on absolute ion intensities was considered. 1 and 10 μg ml^{-1} of both calcium and bismuth had no significant effect on the magnitude of the signals recorded for the Cd isotopes. Higher concentrations of matrix element led to a reduction in sensitivity, the ion signals for Cd in the presence of 100 μg ml^{-1} of calcium and bismuth were respectively 80 and 65 % of the signal with no matrix present. High concentrations of matrix elements reduce the ionisation efficiency of the ICP, therefore lowering the sensitivity for analytes

with higher ionisation potentials (Cd IP = 9.0 eV). Additionally, the high concentration of non-analyte ions extracted from the plasma raises the ion beam density leading to increased space charge effects in the interface region, and therefore a greater loss of analyte ions from the beam. The greater sensitivity loss observed in the solutions doped with bismuth compared to those doped with calcium confirmed previous statements that heavier matrix elements have a greater effect than light. [1, 2, 10]

The intensities recorded for all Mg isotopes in the solutions doped with calcium were approximately 4 times those recorded in the Mg only solutions. The spectral interference of $^{48}Ca^{2+}$ on ^{24}Mg explains some of the increase for this isotope, however as all isotopes were affected it is clear that Mg contamination in the calcium standard solution was a significant problem. The sensitivities in the samples doped with bismuth were approximately equal to the responses in the clean Mg solutions. Contamination is again a possible explanation, however given that the ionisation potential of Mg is lower than that of Cd by 1.4 eV, the intensities of the Mg ion signals are less likely to be affected by matrix induced reductions in plasma ionisation efficiency.

On closer examination, it was found that in the presence of matrix, higher mass analyte isotopes were reduced in intensity relative to lower mass isotopes, and that the effect was enhanced as the concentration of matrix increased. The effect of these changes on isotope ratios is illustrated for the ^{X}Cd / ^{111}Cd ratios in Figs. 5.6 and 5.7 for calcium and bismuth matrices respectively. ^{111}Cd was chosen as the reference isotope as it was collected on the axial channel of the multi-collector array.

For 1 and 10 μg ml^{-1} calcium matrices, little significant difference between the ratios in the spiked and clean solutions was observed. As the concentration of the calcium was increased, a clear pattern emerged. Ratios involving isotopes collected using Faraday cups at the extreme low mass side of the multi-collector array increased in the presence of the calcium matrix, reflecting an increase in the intensity recorded by those collectors relative to that recorded by the axial

collector. Conversely, the ratios involving isotopes collected to the extreme high mass side of the array decreased with the matrix present as a result of a relative reduction in the intensity recorded by collectors to the high mass side of the array. The observed effect was progressive, collectors further from the axial position showed a greater change than those closer in.
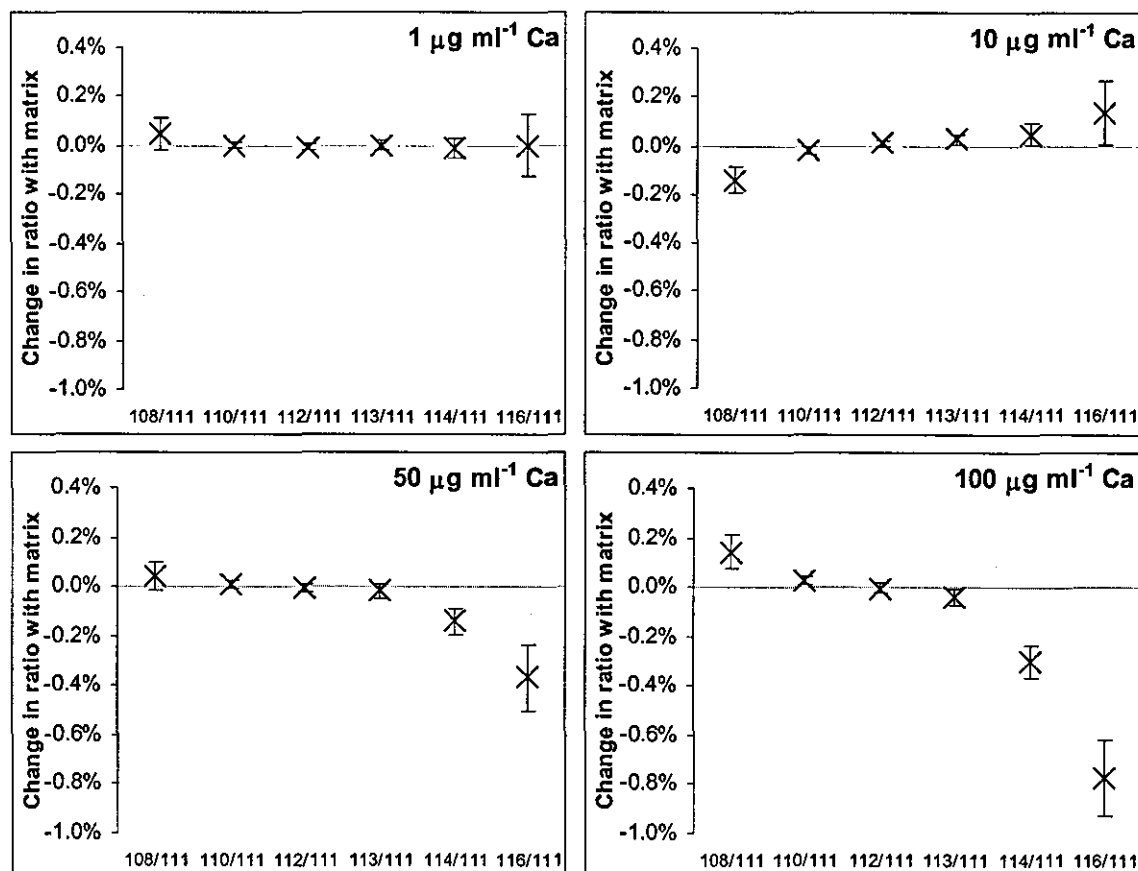
Fig. 5.6 Cd isotope ratios measured in the presence of increasing concentrations of calcium matrix, relative to ratios measured in Cd only solutions. Error bars are one standard deviation.

The intensity changes observed led to a reduction in all values of E^{obs}. Although an important result, the underlying cause of the change in E^{obs} was the different responses of the ion signals to the high matrix concentrations, dependent on the position on the multi-collector array in which the isotopes were collected. This dependence on collector position was confirmed by examination of ratios with a constant mass difference of 2 between the isotopes. With 100 µg ml⁻¹ calcium present, the ratios that displayed significant difference to those in the 'Cd only' solutions were ^{108}Cd / ^{110}Cd (collector L3 / collector L1), ^{112}Cd / ^{114}Cd (H1 / H3) and ^{114}Cd / ^{116}Cd (H3 / H4). The other ratios, involving only isotopes in the L1 to

120

H2 range showed no significant difference from their values in the unspiked samples.

The results for the 10 μg ml⁻¹ calcium solution were not in line with the other solutions. Although an observable matrix effect is not unreasonable at this concentration, the trend seen was opposite to that for higher calcium levels and it is therefore felt that these results do not represent the true situation for Cd with a 10 μg ml⁻¹ calcium matrix.
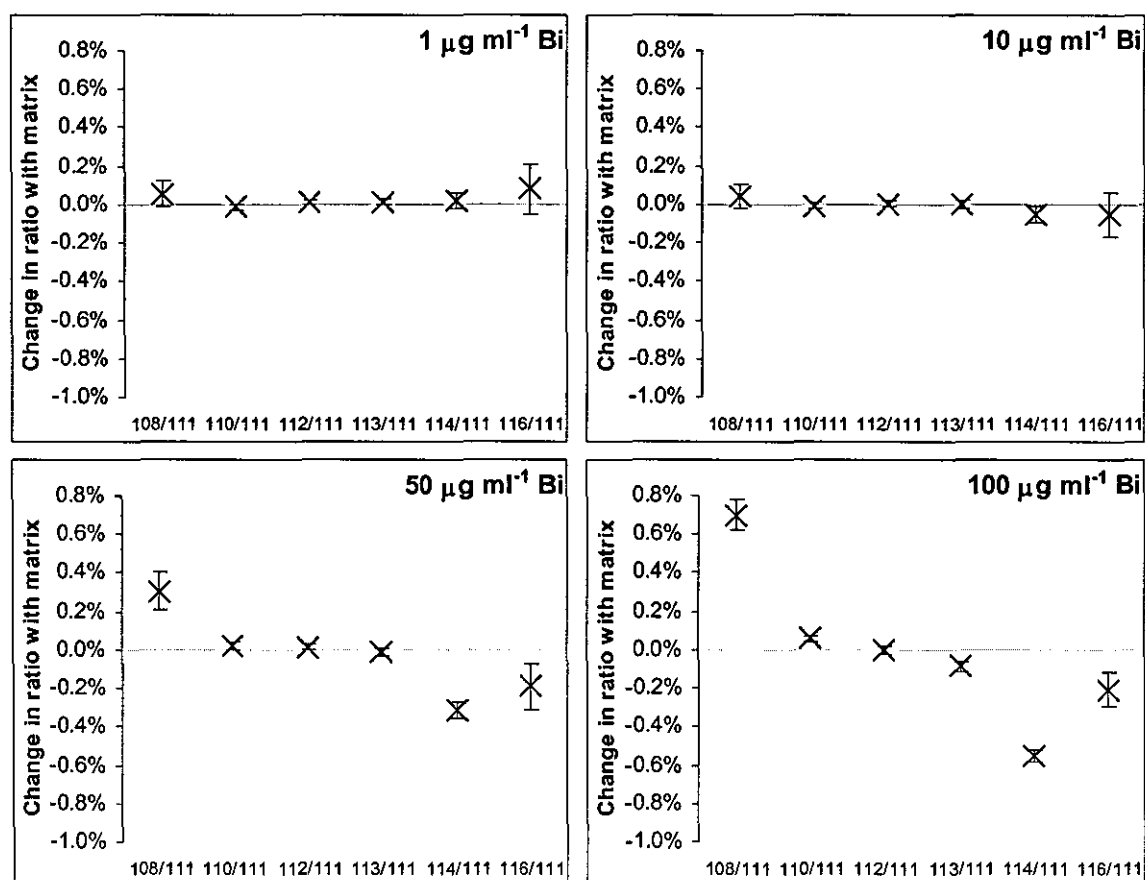
Fig. 5.7 Cd isotope ratios measured in the presence of increasing concentrations of bismuth matrix, relative to ratios measured in Cd only solutions. Error bars are one standard deviation.

The results for Cd isotope ratio measurements with a bismuth matrix (Fig. 5.7) were broadly similar to those with calcium. The ^{X}Cd / ^{111}Cd ratios in solutions with 1 and 10 μg ml⁻¹ bismuth were not significantly different to those in surrounding 'Cd only' solutions. With 50 and 100 μg ml⁻¹ bismuth, significant differences were observed and the effect was more pronounced further from the

axial position. As shown in Fig. 5.7, ^{116}Cd / ^{111}Cd did not fit the observed trend. Tin contamination in the bismuth standard solution was most likely responsible for this anomaly. ^{116}Sn (natural abundance 14.5 %) would increase the ^{116}Cd signal, leading to an apparently reduced matrix effect for this isotope.

The ^{48}Ca^{2+} interference at m/z 24 meant that only one ratio, ^{26}Mg / ^{25}Mg, could be examined in the Mg solutions doped with calcium. Poor isotope ratio precision for Mg solutions with both calcium and bismuth matrices also limited the usefulness of the data. Typical within sample precision was 0.2 – 0.5 % relative standard deviation (%RSD) compared to 0.01 to 0.03 %RSD for the Cd determinations.

The only samples to show significant changes in the isotope ratios were the Mg + 50 μg ml^{-1} calcium/bismuth solutions. In these samples, the effect of the matrix was found to be dependent on the position in which the isotopes were collected on the multi-collector array, similar to the previous observations for Cd. The intensity of ^{26}Mg, detected using H4, was significantly decreased relative to both other isotopes, the intensity of ^{24}Mg (collector L4) was increased relative to ^{26}Mg, but not significantly increased relative to ^{25}Mg.

The changes observed were opposite to those expected, it was thought that the increased space charge due to the presence of the matrix would lead to increased losses of the lighter isotopes. Nonetheless, heavy-light element effects as previously reported[1, 2, 10] were still seen. Mg was more seriously affected than Cd by the same concentration of matrix, e.g. with 50 μg ml^{-1} Ca, ^{26}Mg / ^{25}Mg was reduced by 1.1 % while ^{116}Cd / ^{111}Cd was reduced by only 0.37 % (both ratios represent collector H4 ratioed to the axial collector). Additionally changes caused by the presence of bismuth were greater than those due to calcium, as summarised in Table 5.3 for Cd isotope ratios.

Table 5.3 Change in Cd isotope ratios in the presence of calcium and bismuth

	^{114}Cd / ^{111}Cd	^{108}Cd / ^{111}Cd
+100 μg ml^{-1} Ca	-0.30 %	+0.14 %
+100 μg ml^{-1} Bi	-0.55 %	+0.70 %

One possible explanation for the collector dependent effects seen in this study is that non-analyte ions were detected by the Faraday collectors, possibly following collision with the walls of the flight tube, with the geometry of the double focussing system leading to maximum effect at the low mass end of the multi-collector array, and a gradual decline across to the higher collectors. A general increase in signal response across the array would not necessarily occur as the 'bouncing ion' effect would be small compared to the loss of analyte ions suggested by the data. Investigation of the baselines measured 0.5 mass units either side of the analyte masses revealed that their magnitude was no different in the matrix doped and clean solutions. This ruled out any non-analyte ion effect as any 'bouncing' ions would result in an increased baseline level in the solutions doped with high levels of a matrix element.

All of the data discussed above was acquired using an Axiom ICP-MS instrument at the NERC Isotope Geosciences Laboratory (NIGL). Measurements using the instrument at the Central Science Laboratory (CSL) showed a much lower degree of matrix effect. In the presence of 100 μg ml^{-1} of matrix element, Cd signal intensities were approximately 93 % of the signal measured in bracketing Cd only solutions, compared to 65 % in the original acquisitions. This was reflected in the isotope ratios, the maximum change in analyte ratio with the matrix was approximately half the magnitude of the changes observed in the original data. The set-up of the two instruments was not identical, therefore it is unsurprising that different levels of matrix effects were observed. The nebulisers used were not the same and gas flows, torch position and ion lens tuning parameters were optimised for maximum signal on a daily basis. Therefore it was extremely unlikely that the secondary discharge in the two systems was equal.

The collector dependent matrix effects reported above were not apparent in the acquisitions at CSL. It may be that the dependence on collector position only becomes apparent when significant matrix-induced enhancement or reduction of the ion signal occurs. An alternative explanation may be the different multi-collector hardware of the two instruments. At the time of the acquisitions, the Axiom at NIGL was fitted with multi-ion counters in addition to the nine Faraday

collectors. It is possible that the presence of the extra detectors caused the collector dependent effects that were observed on this instrument, and not seen on the CSL system that was equipped with the standard single ion counter and multi-Faraday array.

The influence of high levels of matrix elements on isotope ratios measured by multi-collector ICP-MS is evidently a complicated issue; the behaviour of individual instruments should be carefully evaluated prior to the analysis of such samples. Any collector dependent effects will strongly influence internal standardisation procedures. If such effects are observed, it is advisable to avoid use of the extreme Faraday collectors whenever possible.

5.3 Isotope Ratio Error Correction Expressions

5.3.1 Standard correction models

The mathematical models used to apply the measured isotope ratio error to correct an analyte isotope ratio are arbitrary and are based on linear, power or exponential functions.[6, 11]

It has previously been shown that for the case where the bias per mass unit, B_{xy} is locally defined for isotopes at masses x and y, the compound error is given by:[21]

$$R^{true} = \frac{R^{obs}}{(1 + B_{(i+1),i})(1 + B_{(i+2),(i+1)})\ldots(1 + B_{(j),(j-1)})} \qquad 5.9$$

where R^{true} and R^{obs} are the true and observed ratios of the isotopes i and j. Equation 5.9 was derived from the original equation[21] simply by dividing both sides by the isotopic signal for isotope j.

For three adjacent isotopes at masses N, N+1 and N+2, and making the assumption that B is in fact constant, the compound error in the isotope ratio (N+2) / N becomes:

$$R^{true} = \frac{R^{obs}}{(1+B_{N+1,N})(1+B_{N+2,N+1})} = \frac{R^{obs}}{(1+B)(1+B)} = \frac{R^{obs}}{(1+B)^2} \qquad 5.10$$

or in general terms,

$$R^{true} = \frac{R^{obs}}{(1+B)^{\Delta m}} \qquad 5.11$$

Where Δm is the mass difference between the isotopes that make up the ratio R. The above expression is identical to the power law correction. Thus the power law is arrived at as a direct algebraic consequence of assuming the bias to be a constant. The series expansion of equation 5.11 is:

$$R^{true} = \frac{R^{obs}}{1+\Delta mB + \dfrac{\Delta m(\Delta m-1)B^2}{2!} + \cdots} \qquad 5.12$$

The linear model is given by:

$$R^{true} = R^{obs} \Big/ (1+\Delta mB) \qquad 5.13$$

The exponential model is expressed as:

$$R^{true} = R^{obs} \Big/ \exp(\Delta mB) \qquad 5.14$$

which can be expanded to give:

$$R^{true} = \frac{R^{obs}}{1+\Delta mB + \dfrac{(\Delta mB)^2}{2!} + \cdots} \qquad 5.15$$

125

Noting the series expansions, the linear and exponential models may be regarded as approximations to the power law model that may compensate for the error in the basic assumption that B is constant. For example if Δm is 2 and terms higher than second order in B are ignored, the linear correction factor is reduced by B^2 whereas the exponential correction factor is raised by B^2, relative to that predicted by the power law.

For reference, the Russell correction expression frequently used for the correction of TIMS data is given by:[14]

$$R^{true} = R^{obs} / \left(\frac{m_2}{m_1} \right)^f \tag{5.16}$$

where m_1 and m_2 are the masses of the isotopes that make up the ratio R and f is the 'mass bias factor'.

The different standard correction models were applied to multi-collector Cd isotope ratios, the optimal value of B or f was found using the Solver function in Microsoft Excel® to minimise the sum of the squares of the differences between corrected ratios and the reference values calculated from natural isotopic abundance data.[18] The percentage error in the corrected results was then calculated, data for $^{110}Cd / {}^{111}Cd$ and $^{114}Cd / {}^{111}Cd$ are given in Table 5.4. No single correction expression provided the best correction for all ratios examined.

Table 5.4 Error in Cd isotope ratios after correction using different methods

	$^{110}Cd / {}^{111}Cd$	$^{114}Cd / {}^{111}Cd$
No correction	-1.32 %	4.00 %
Linear	0.002 %	0.025 %
Power	-0.027 %	0.008 %
Exponential	-0.027%	0.008 %
Russell	-0.007 %	0.011 %
Variations		
Equation 5.18	-0.182 %	0.027 %
Equation 5.21	0.125 %	0.088 %
Equation 5.23	0.002 %	0.025 %
Equation 5.24	0.002 %	0.026 %

5.3.2 Variations on the standard models

As stated above, the power model is theoretically correct if the bias per mass unit is constant. Since it is known that this is not the true situation, various expressions were investigated that incorporate an extra variation into the power law. These included:

$$R^{true} = \frac{R^{obs}}{(1 + Bk^{\Delta m - 1})^{\Delta m}} \qquad 5.17$$

$$R^{true} = \frac{R^{obs}}{(1 + B(1 + (\Delta m - 1)k))^{\Delta m}} \qquad 5.18$$

where B is the bias calculated for a ratio with $\Delta m = 1$ and k is a constant. These correction expressions were applied to $^{X}Cd / ^{111}Cd$ isotope ratio data using the measured error in $^{112}Cd / ^{111}Cd$ to calculate B and Solver to evaluate k, as described above. The results for equation 5.18 were typical, and are compared to application of the standard models in Table 5.4. When tested, these expressions provided no better correction than the standard models and in some cases the correction was significantly worse.

It was seen in the section 5.2 that the isotope ratio error had a linear relationship with the mass difference between the isotopes in a ratio, therefore

$$E^{obs} = \Delta mk + k' \qquad 5.19$$

Where k and k' are constants.

If $\Delta m = x$, it follows that

$$k = \frac{E^{obs}_{\Delta m = x} - k'}{x} \qquad 5.20$$

Substitution into equation 5.19 for $\Delta m = y$ gives

$$E^{obs}_{\Delta m = y} = \frac{y E^{obs}_{\Delta m = x} - k'(x - y)}{x}$$

5.21

Therefore in theory, the isotope ratio error for any ratio can be calculated from that of a second ratio. This expression was applied to the correction of $^{X}Cd / ^{111}Cd$ isotope ratio data using the measured error in $^{112}Cd / ^{111}Cd$ to calculate the error for all other isotope ratios and Solver to find k'. The result was again no better than that provided by the standard models (Table 5.4).

As observed in section 5.2, the gradient of the E^{obs} vs. Δm plots was not constant, and small deviations from linearity occurred point by point. Therefore, the case of E^{obs} varying with Δm according to an infinitely variable function was considered.

i.e. $E^{obs} = k\Delta m + k'\Delta m^2 + k''\Delta m^3 + k'''\Delta m^4 + \cdots$

5.22

Expressions that expand to give this type of statement were investigated for the correction of E^{obs}, including:

$$R^{true} = \frac{R^{obs}}{(1 + \tan(\Delta mk))}$$

5.23

$$R^{true} = \frac{R^{obs}}{(1 + \arctan(\Delta mk))}$$

5.24

Similar to previous attempts, after optimisation of k these equations provided corrections that were comparable to, but no better than the standard models (see Table 5.4).

Where all variations on the standard power model fail is that they are dependent on Δm and not the absolute mass of the isotopes. As demonstrated in section 5.2 and in the literature,[8] the isotope ratio error changes with mass such that ratios with the same Δm do not have the same value of E^{obs}. Clearly a different approach to determining the appropriate isotope ratio error correction model is required. Iterative investigation of mathematical functions until one is found that provides perfect fit to the data is a time consuming process that is hindered by potential unreliability in the data such as spectral interference and inaccurate calibration of detectors.

5.3.3 The relationship between instrument response and isotope ratio error

In the majority of literature examples, a trial and error method has been employed to determine which of the standard expressions should be used to correct isotope ratio data. The expression giving the right answer for samples of known isotopic abundance has then been applied to the remaining samples. Rather than starting from acquired data, this work considers the error in isotope ratio measurements as being a direct consequence of the way in which the instrument response changes with mass.

The instrument response is defined in terms of the sensitivity, S, and is dependent on the mass examined, m, such that

$$S = f(m) \qquad\qquad 5.25$$

Where f is a continuous function with no singularities.

The intensity observed at $m = m_1$ is given by

$$I_{m_1}^{obs} = S_{m_1} \times A_{m_1} \times C \times \eta \qquad\qquad 5.26$$

Where A_{m_1} is the abundance of the isotope at $m = m_1$, C is the elemental concentration, and η the fractional ionisation of the element. $I_{m_2}^{obs}$ is similarly

defined, and if the two isotopes at $m = m_1$ and $m = m_2$ are of the same element, the observed isotope ratio can be calculated:

$$R^{obs} = \frac{I_{m_2}^{obs}}{I_{m_1}^{obs}} = \frac{S_{m_2} \times A_{m_2} \times C \times \eta}{S_{m_1} \times A_{m_1} \times C \times \eta}$$

$$R^{obs} = \frac{S_{m_2}}{S_{m_1}} \times R^{true} \qquad\qquad 5.27$$

The fractional error in the measured ratio, E^{obs}, is given by:

$$E^{obs} = \frac{R^{obs} - R^{true}}{R^{true}} \qquad\qquad 5.28$$

Substituting equation 5.27:

$$E^{obs} = \frac{S_{m_2}}{S_{m_1}} - 1 \qquad\qquad 5.29$$

The function S could take any form, however there are certain conditions that should be fulfilled. At $m = 0$, the instrument response should be equal to a constant, ϕ, that is non-zero but arbitrary, and that cancels when isotope ratios are calculated. It is not logical that an isotope ratio could be dependent on the instrument response at zero mass. The function should also include one or more other constants that help to define the change in response with mass. If all these constants are set to zero, S should equal ϕ for all values of m.

It is possible to define plausible instrument response functions that can be shown to lead to the common mass bias correction expressions.

(i) Instrument response: $S = \phi(1+k)^m$, a power law model where k is an arbitrary constant. Substituting into the above equations for the ratio of two isotopes at masses m_1 and m_2,

$$R^{obs} = \left(1+k\right)^{m_2-m_1} \times R^{true}$$ 5.30

$$E^{obs} = \left(1+k\right)^{m_2-m_1} - 1$$ 5.31

If k is defined as the bias per unit mass, equation 5.30 is equivalent to the standard power law mass bias correction model given in equation 5.11, with k being numerically equal to B.

(ii) Instrument response: $S = \phi\, e^{km}$

Then,

$$R^{obs} = e^{k(m_2-m_1)} \times R^{true}$$ 5.32

$$E^{obs} = e^{k(m_2-m_1)} - 1$$ 5.33

As before, if k is defined as the bias per unit mass, equation 5.32 is equivalent to the standard exponential correction model given in equation 5.14.

Expanding either of the expressions for R^{obs} given above, and assuming k to be small (terms in k^n with n > 1 are ignored) yields

$$R^{obs} = \left(1+k\left(m_2 - m_1\right)\right) \times R^{true}$$ 5.34

and therefore,

$$E^{obs} = k\left(m_2 - m_1\right)$$ 5.35

Defining k as the bias per unit mass, equation 5.34 is the same as the linear correction model (equation 5.13). This again shows that the linear model is an approximation of the other models.

As mentioned above, these expressions for E^{obs} are all dependent on the mass difference between the isotopes and not the absolute masses, and as such are completely detached from the real situation.

(iii) Instrument response: $S = \phi(m)^k$ (Note this function does not equal ϕ when $m = 0$)

Then,

$$R^{obs} = \left(\frac{m_2}{m_1}\right)^k \times R^{true}$$

5.36

$$E^{obs} = \left(\frac{m_2}{m_1}\right)^k - 1$$

5.37

Equation 5.36 is equivalent to the correction expression given by Russell *et al.*[14] (equation 5.16). The expression for E^{obs} does depend on the absolute masses of the isotopes involved in the ratio, and as such this instrument response function is more likely to be representative of the true instrument behaviour than the other models considered thus far.

The constant k can be determined using optimisation software such as the Solver function in Microsoft Excel® to find the value of k that minimises the sum of the squared differences between E^{obs} calculated from instrumental data and that predicted by the response model. Using E^{obs} rather than S for the optimisation eliminates the requirement to evaluate ϕ as well as k.

Internal standardisation can also be used to determine constants in the instrument response function. The equations given above for R^{obs} can be rearranged to allow

determination of k from measurement of a known isotope ratio. As with the above method, this approach requires that the true form of the instrument response function is known.

5.3.4 Determination of the true instrument response function

A multi-element standard solution was measured in order to determine the response function of the instrument used in this study. The acquisition used magnetic sector scanning and a single Faraday collector with a dwell time of 2 sec. The solution contained 19 elements ranging in mass from m/z 6 (Li) to 193 (Ir). Molar concentration, isotopic abundance and fractional ionisation were taken into account, and the instrument response was plotted against mass. Masses affected by spectral interference or contamination could easily be eliminated as they were not part of the smooth trend defined by the remaining isotopes. The fractional ionisation of elements was calculated using equation 5.38, known as the Saha equation.[22]

$$\frac{N_{ix}N_e}{N_{ax}} = \frac{(2\pi m_e kT)^{3/2}}{h^3} \times \frac{2Z_{ix}e^{-E_x/kT}}{Z_{ax}} \qquad 5.38$$

where $\quad N_{ix}$ $\quad$ concentration of ions of species x

$\qquad\qquad N_{ax}$ $\quad$ concentration of atoms of species x

$\qquad\qquad N_e$ $\quad$ concentration of free electrons (assumed to be 10^{21} m^{-3})

$\qquad\qquad m_e$ $\quad$ electron mass = 9.109×10^{-31} kg

$\qquad\qquad k$ $\quad$ Boltzmann constant = 1.381×10^{-23} J K^{-1}

$\qquad\qquad h$ $\quad$ Planck constant = 6.626×10^{-34} J s

$\qquad\qquad Z_{ix}$ $\quad$ partition function of ions of species x

$\qquad\qquad Z_{ax}$ $\quad$ partition function of atoms of species x

$\qquad\qquad E_x$ $\quad$ ionisation energy of species x

$\qquad\qquad T$ $\quad$ ionisation temperature (assumed to be 7500 K)

The theoretical instrument response function for each of the models was calculated across the same mass range, Solver optimisation was used to determine the values of the constants in the response functions, as described above. The

value of ϕ was ascertained using Solver to minimise the sum of the square differences between the experimental instrument response, and that predicted by the models at each mass. The optimised forms of the power and exponential models are compared to the true instrument response in Figs. 5.8a and b respectively. As illustrated, both models provided poor fit to the experimental data, the functions are simply the wrong shape.
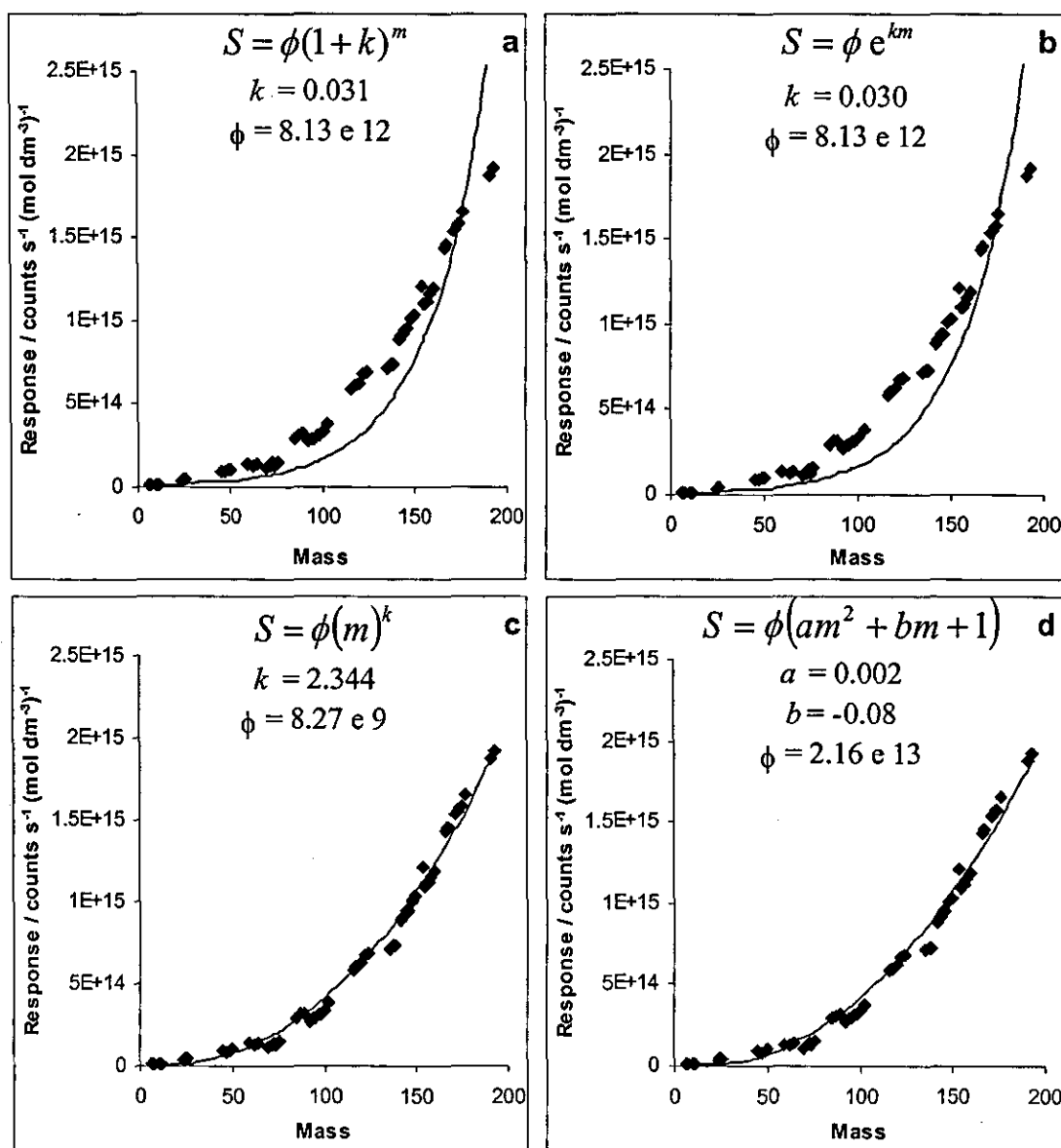
Fig. 5.8 Comparison of experimental ($\blacklozenge$) and theoretical ($-$) instrument response functions.

Regression analysis was performed using the experimental response as the y-variable and the response predicted by the models as the x-variable, and the standard deviation of the y residuals, $s_{y/x}$ was calculated using equation 5.39.

$$S_{y/x} = \sqrt{\frac{\sum_i (y_i - \hat{y}_i)^2}{(n-2)}}$$ 5.39

The $\hat{y}_i$ values are the points on the calculated regression line corresponding to the individual x-values (masses), n is the number of points (61). Smaller values of $s_{y/x}$ demonstrate better fit to the data. For both the power and exponential models, $s_{y/x}$ was 2×10^{14}. The magnitude of this value was due to the fact that the elemental concentrations were converted into molar form before calculation of the instrument response at the individual masses (the units for the response were counts s^{-1} (mol $dm^{-3})^{-1}$). For the Russell $et\ al.$ response function, the fit to the experimental data after optimisation of the constants was very good, as shown in Fig. 5.8c. The standard deviation of the y residuals, $s_{y/x}$ was 6×10^{13}, showing significantly better fit than the power and exponential models.

Other forms of response function were also considered, some examples are given in Table 5.5. Solver optimisation was used to find values of k and ϕ, as described previously. Some of the functions investigated were very different to the experimental data over parts of the mass range and none of them fitted the data as well as the Russell model.

Table 5.5 Alternative instrument response functions

	k	ϕ	$s_{y/x}$
$S = \phi(1 + km)$	-0.075	-7×10^{13}	2×10^{14}
$S = \phi(\ln(km)$	0.064	3×10^{14}	4×10^{14}
$S = \phi(1 + \ln(1+km))$	0.051	2×10^{14}	3×10^{14}

The shape of the experimental response function in Fig. 5.8 clearly approximates a polynomial model. Thus the theoretical response function

$$S = \phi(am^2 + bm + 1)$$ was considered. After optimisation, good fit to the experimental data was observed for this model (Fig 5.8d), $s_{y/x}$ was 6×10^{13}. The

polynomial response function was as good a match to the data as $S = \phi(m)^k$ (Russell law).

For the polynomial instrument response function,

$$R^{obs} = \frac{am_2^2 + bm_2 + 1}{am_1^2 + bm_1 + 1} \times R^{true} \qquad 5.40$$

$$E^{obs} = \frac{a\left(m_2^2 - m_1^2\right) + b\left(m_2 - m_1\right)}{am_1^2 + bm_1 + 1} \qquad 5.41$$

Note that E^{obs} is dependent on the absolute masses of the isotopes. When the optimisation method was used to determine the constants, it was found that Solver could not find optima for a and b from certain starting values. Initial values of -1 for both parameters generally provided successful optimisation. Internal standardisation can also be applied to find the values a and b, although measurement of two known isotope ratios is required.

The different instrument response models were applied to the correction of multi-collector Cd isotope ratio data; Fig. 5.9 summarises the results. Initial measurement of a Cd standard solution was used to find the optimum parameters for each instrument response function, using Solver in Microsoft Excel® as described above. The parameters were then used to correct isotope ratios measured in a separate 200 ng ml^{-1} standard solution. The ratios that were corrected were not the same as those used in the optimisation.

As shown in Fig. 5.9, although ratios with low mass difference were corrected to within one standard deviation of the natural ratios by all models, the power and exponential instrument response functions gave poor correction when the mass difference between the isotopes increased. The polynomial and 'Russell' response functions consistently provided better correction of isotope ratio data; ratios corrected using the polynomial model were closest to the published natural values.
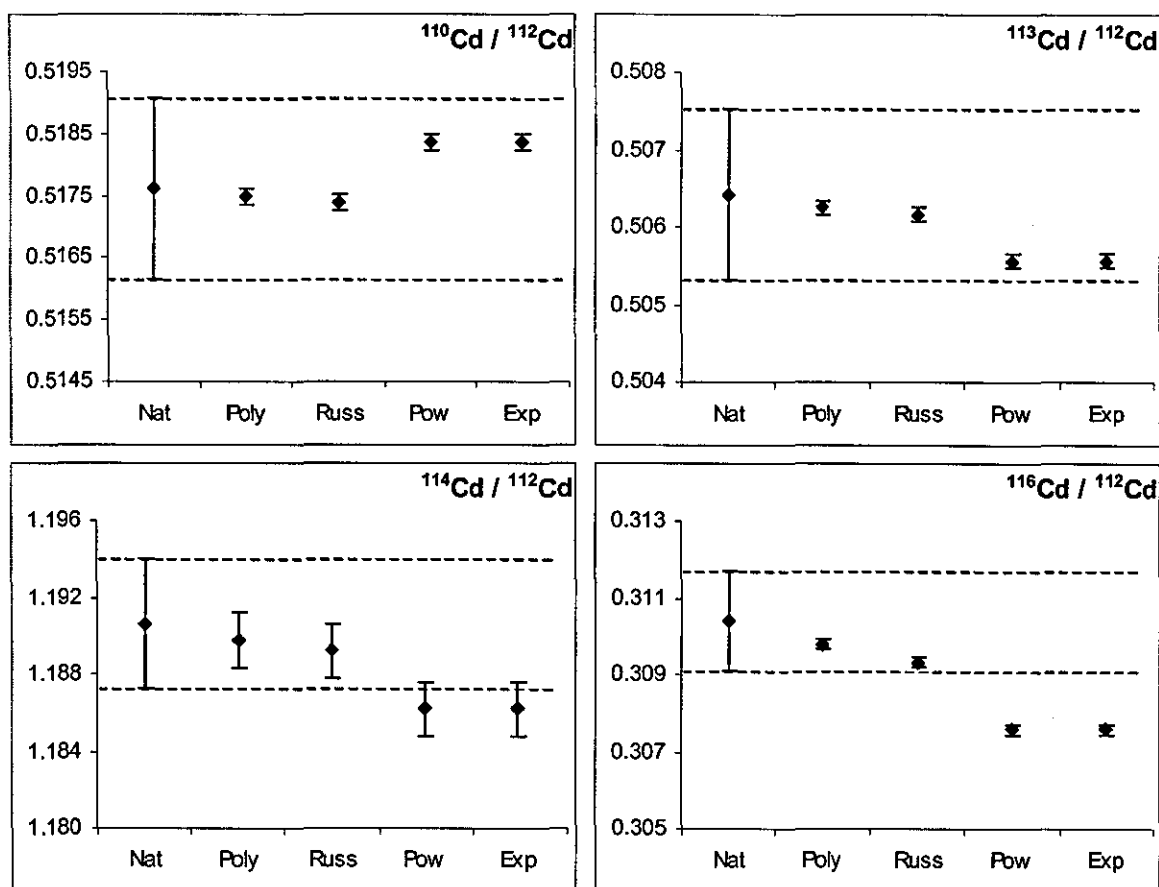
Fig. 5.9 Corrected Cd isotope ratio data from a 200 ng ml^{-1} standard solution. Nat = natural ratio, Poly = polynomial, Russ = Russell, Pow = power, Exp = exponential correction models. Dotted lines = ± 1 sd of the natural ratio, error bars are 1 sd. Natural isotope ratios and errors calculated from published data.[18]

The conclusion of this study is that for all ICP-MS systems, the true instrument response function should be investigated by measurement of a multi-element standard solution, and the function that provides best fit to the data should be used to derive the isotope ratio correction model.

5.3.5 Effect of matrix on correction models

The effect of the presence of a matrix element on the isotope ratio correction provided by the models was also investigated. Parameters in the instrument response functions were optimised separately for each sample as above, and used to correct other Cd ratios measured in the same solution. The 'residual bias' of Cd isotope ratios corrected using each model was calculated for clean standards and solutions spiked with increasing levels of matrix elements. The results for a Cd + 100 μg ml^{-1} calcium solution, relative to those for a clean Cd standard are presented in Fig. 5.10.

137
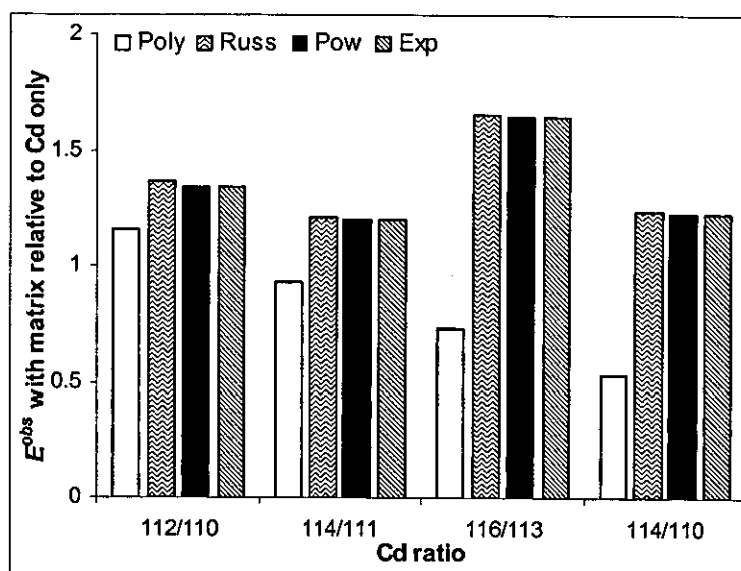
Fig. 5.10 Residual E^{obs} for a series of Cd isotope ratios, calculated after correction using the different models for a 200 ng ml^{-1} Cd + 100 μg ml^{-1} calcium solution, relative to that in a clean 200 ng ml^{-1} Cd standard.

The Russell, power and exponential models resulted in a higher residual bias when the matrix was present, compared to the clean standard solutions, for all isotope ratios investigated. After correction using the polynomial model, most, but not all, of the ratios had a residual bias that was lower in the matrix doped samples than in the 'Cd only' solutions. This slightly unexpected result derives from the fact that the matrix-induced changes in the absolute intensities occurred in a manner that reduced the magnitude of E^{obs}, as described above. Although not universal, this result suggests that the two parameter polynomial model is more adaptive to matrix-induced changes in E^{obs} than the other functions investigated.

5.4 Semi-Quantitative Analysis Using E^{obs}

ICP-MS is an ideal technique for semi-quantitative analysis, allowing rapid determination of the concentration of a large number of elements in a wide range of sample types, with a reasonable degree of accuracy (30 to 50 %).[23] In general, prior measurement of a standard or reference material is performed to determine relative sensitivity factors for the analyte elements, which are then used to calculate sample concentrations. This procedure is equivalent to a one point calibration for each element; any elements that are to be quantified in the sample

must also be present in the reference solution. Spectral overlaps and matrix effects may be problematic if the standard and sample are not well matched in terms of matrix components.

Alternatively the instrument response function can be determined by using the intensities of selected isotopes across the mass range. Unknowns are determined by interpolation from this function. This is the most commonly used method of semi-quantitative analysis, and has the advantage of requiring only a few standard isotopes to model the entire mass range, however extrapolation of the function may lead to inaccurate determinations.

Another method of determining the response function suggests itself from the above discussion of the relationship between E^{obs} and the instrument response. Firstly, a number of isotope ratios that are free from spectral interference were measured across the mass range. This was performed as part of the semi-quantitative analysis; the elements involved could be analytes as long as their natural isotopic ratio was known and constant. The values of E^{obs} were then calculated using equation 5.28, and the sum of the squared differences between these measured values of E^{obs}, and those calculated from equation 5.29, was minimised by altering the value of the constant(s) in the instrument response function, using optimisation software as described.

These parameters were then used to calculate the concentration of the analyte elements, *via* the following procedure. The numerical value of the instrument response for the internal standard was calculated from the data, using rearrangement of equation 5.26. The concentration of all other elements was then evaluated using the instrument response function to calculate the relative response at each analyte mass, and factors for the degree of ionisation and isotopic abundance.

The principal advantages of this method are that any matrix induced variations are taken into account as the samples themselves are used to determine the instrument response, and that quantification requires knowledge of only one elemental concentration, that of the internal standard. The instrument response function is

determined using only a series of isotope ratios. Spectral interference remains a potential problem, as for any other method of quantitation.

To test this method of semi-quantitative analysis, a multi-element standard solution containing 100 ng ml^{-1} of Li, B, Mg, Sc, Ti, Co, Cu, Ge, Rb, Y, Mo, Rh, Sn, Ba, Nd, Gd, Er, Yb, W, Ir, Pt, Pb, Bi and U was analysed. Acquisitions were performed in single collector mode at a resolution setting of 400, using magnetic sector scanning (magnet settle time = 100 ms), a Faraday collector and a dwell time of 2 secs. The scan parameters were 2 peak widths per isotope and 10 points per peak width. All non-overlapping isotopes were measured, giving a total of 79 isotopes in all. A total of 14 isotope ratios were used for optimisation of the constants in the instrument response function. These were $^{26/24}$Mg, $^{49/47}$Ti, $^{65/63}$Cu, $^{72/70}$Ge, $^{87/85}$Rb, $^{94/92}$Mo, $^{100/98}$Mo, $^{122/120}$Sn, $^{137/135}$Ba, $^{148/146}$Nd, $^{160/158}$Gd, $^{176/174}$Yb, $^{186/184}$W and $^{193/191}$Ir. The concentration of 23 analyte elements was calculated using the optimised response function and Rh as an internal standard, and the percentage error in the calculated concentration of each element was evaluated. Table 5.6 gives the results of this calculation and the percentage errors obtained when 6 internal standards were used to determine the instrument response function. For both approaches, a polynomial instrument response of the form $S = \phi\left(am^2 + bm + 1\right)$ was assumed.

Table 5.6 Percentage difference between calculated and true concentrations for semi-quantitative analysis using isotope ratios and internal standards to define the instrument response function. Std = element used as an internal standard.

	Isotope ratios method	Internal standards method		Isotope ratios method	Internal standards method
Li	16 %	Std	Sn	15 %	-1 %
B	4 %	-285 %	Ba	1 %	Std
Mg	350 %	666 %	Nd	11 %	12 %
Sc	101 %	78 %	Gd	11 %	22 %
Ti	72 %	54 %	Er	26 %	47 %
Co	43 %	Std	Yb	25 %	51 %
Cu	13 %	3 %	W	-23 %	-4 %
Ge	-11 %	-15 %	Ir	21 %	57 %
Rb	22 %	20 %	Pt	-16 %	10 %
Y	19 %	16 %	Pb	1 %	35 %
Mo	-5 %	-5 %	Bi	-15 %	Std
Rh	Std	Std	U	-7 %	Std

Using isotope ratios to define the instrument response function, 17 of the 23 calculated element concentrations were within ± 25 % of their true value, including Li, B, Pb and U. By the internal standards method, the calculated concentrations of 11 out of the remaining 18 analyte elements were within ± 25 % of the true values. The majority of the elements outside this range were the same for the internal standards method as for the E^{obs} approach, suggesting that contamination (Mg) and/or spectral interferences (argon or nitric acid based for Sc and Ti; oxide interferences for Er and Yb) may have been responsible. A greater number of elements could be quantified using the isotope ratio approach, as this method required only one internal standard, compared to six for the alternative procedure.

5.5 Conclusion

The isotope ratio error in a double focussing ICP-MS system has been investigated. The error in measured Cd and Sn isotope ratios was found to be stable over 20 to 30 min. in both single and multi-collector modes. After this time, significant variations were observed. Once the uncertainty in natural isotopic abundance was included in the calculation, there was found to be no significant variation in the isotope ratio error with mass. The reproducibility of the pattern of the data about the mean value suggested either the presence of unexpected spectral interferences, or that the reference values used for calculation of the true isotope ratios did not match the actual isotopic abundances in the solutions. Using a single isotope as the denominator for a series of isotope ratios, isotope ratio error was found to have a linear relationship with mass difference between the isotopes. The gradient of these plots decreased as the mass of the reference isotope increased, demonstrating variation in the isotope ratio error with mass. The presence of a matrix element was found to significantly affect Cd isotope ratios measured in multi-collector mode. Using one instrument, these effects were more severe at the extremes of the multi-collector array. Careful investigation of individual instrument behaviour should be undertaken prior to measurement of samples containing high levels of matrix elements.

A new approach to the modelling and correction of instrumentally derived bias in isotope ratio measurements is proposed. The first step is to characterise the instrument response function over as wide a range of masses as possible. A smooth continuous function is used (in contrast to the locally defined mass bias) because no other choice is logical, and it follows that data points that fall off this curve must be due to spectral interference, poor calibration of individual detectors, or the true isotopic abundances in the sample not being equal to the published values. The instrument response function is then used to define the expression that should be used to correct isotope ratio data, from equation 5.27. The constants in the response function are determined at the time of analysis using rearrangement of this equation, and measurement of an internal or external standard. The corrected analyte isotope ratio can then be evaluated by substitution of the constants and the masses of the isotopes into the correction expression. The use of internal standardisation to determine the constants is preferred as the presence of the sample matrix is expected to influence the values.

Ultimately the response function applied will depend on the individual instrument used to perform the analysis, and may even vary between different systems that are the same make and model. Continuing improvements in performance and increasing numbers of collectors will allow (and indeed require) more refined functions to accurately model the data. The use of this approach for quadrupole ICP-MS systems may be hindered by the achievable isotope ratio precision. It is conceivable that the difference in quality of fit of alternative correction models to the experimental data may be insignificant. Conversely, time of flight instruments can acquire data for the entire mass range by measuring isotopes that all left the plasma at the same time. It should therefore be possible to define the instrument response function of these systems with great precision, allowing a detailed mass bias model to be constructed.

Error in isotope ratio measurements can be used to define the instrument response function for the purpose of semi-quantitative analysis. This approach gave results of similar quality to standard calibration methods, but only required a single internal standard. This allowed a greater number of analyte elements to be quantified.

References

1   G. R. Gillson, D. J. Douglas, J. E. Fulford, K. W. Halligan and S. D. Tanner, *Anal. Chem.*, 1988, **60**, 1472.

2   T. W. Burgoyne, G. M. Hieftje and R. A. Hites, *Anal. Chem.*, 1997, **69**, 485.

3   S. D. Tanner, *Spectrochim. Acta Part B*, 1992, **47**, 809.

4   P. J. Turner, D. J. Mills, E. Schröder, G. Lapitajs, G. Jung, L. A. Iacone, D. A. Haydar and A. Montaser, 'Instrumentation for Low- and High-Resolution ICP-MS' in *Inductively Coupled Plasma Mass Spectrometry*, ed. A. Montaser, Wiley-VCH, New York, 1998.

5   I. Feldmann, W. Tittes, N. Jakubowski, D. Stuewer and U. Giessmann, *J. Anal. At. Spectrom.*, 1994, **9**, 1007.

6   P. D. P. Taylor, P. De Bièvre, A. J. Walder and A. Entwistle, *J. Anal. At. Spectrom.*, 1995, **10**, 395.

7   N. Jakubowski, L. Moens and F. Vanhaecke, *Spectrochim. Acta Part B*, 1998, **53**, 1739.

8   K. G. Heumann, S. M. Gallus, G. Rädlinger and J. Vogl, *J. Anal. At. Spectrom.*, 1998, **13**, 1001.

9   C. N. Maréchal, P. Télouk and F. Albarède, *Chem. Geol.*, 1999, **156**, 251.

10   E. H. Evans and J. J. Giglio, *J. Anal. At. Spectrom.*, 1993, **8**, 1.

11   I. S. Begley and B. L. Sharp, *J. Anal. At. Spectrom.*, 1997, **12**, 395.

12   M. Rehkämper and K. Mezger, *J. Anal. At. Spectrom.*, 2000, **15**, 1451.

13   C. J. Park, K. H. Cho, J. K. Suh and M. S. Han, *J. Anal. At. Spectrom.*, 2000, **15**, 567.

14   W. A. Russell, D. A. Papantastassiou and T. A. Tombrello, *Geochim. Cosmochim. Acta*, 1978, **42**, 1075.

15   S. R. Hart and A. Zindler, *Int. J. Mass Spectrom. Ion Processes*, 1989, **89**, 287.

16   W. M. White, F. Albarède and P. Télouk, *Chem. Geol.*, 2000, **167**, 257.

17   A. D. Anbar, K. A. Knab and J. Barling, *Anal. Chem.*, 2001, **73**, 1425.

18   K. J. R. Rosman and P. D. P. Taylor, *J. Anal. At. Spectrom.*, 1999, **14**, 5N.

19   A. J. Walder, I. Platzner and P. A. Freedman, *J. Anal. At. Spectrom.*, 1993, **8**, 19.

20   J. N. Miller and J. C. Miller, '*Statistics and Chemometrics for Analytical Chemistry*', Pearson Education Ltd., 2000.

21   B. L. Sharp, A. S. Bashammakh, C. M. Thong, J. Skilling and M. Baxter, *J. Anal. At. Spectrom.*, 2002, **17**, 459.

22   L. de Galan, R. Smith and J. D. Winefordner, *Spectrochim. Acta Part B*, 1968, **23**, 521.

23   H. E. Taylor, R. A. Huff and A. Montaser, 'Novel applications of ICP-MS' in *Inductively Coupled Plasma Mass Spectrometry*, ed. A. Montaser, Wiley-VCH, New York, 1998.

Chapter 6

The Authentication of Premium Rice Using Trace Element Concentrations and Isotope Ratios

6.1 Introduction

The market for premium foods has increased dramatically over recent years; consumers are ever more aware of produce originating from around the world. There are many food products that are of superior quality (taste, texture, fragrance etc.) because of the locale in which they are cultivated. Environmental conditions, such as local climate and soil characteristics, combine to yield crops that exhibit specific traits. Clearly higher quality produce demands higher market prices, therefore unscrupulous traders may attempt to increase profits by deliberately mislabelling foods, or by increasing the volume of a good quality batch through adulteration with sub-standard produce.

In recent years, there has been increasing legislation to protect the rights of honest producers.[1,2] To enforce these laws, a measure of the authenticity of samples must be made, most often in the form of proving the presence/absence of adulterants, or verifying geographical or cultivar origin by comparison with known and reliable samples. The latter method often includes the use of multivariate statistical techniques such as principal components analysis, canonical variance analysis and partial least squares regression to investigate sample data.[3]

A number of techniques have been used for food authentication. DNA analysis has been applied to prove the species origin of several meat,[4-8] fish,[9-15] and plant products,[16,17] a matter of concern for reasons of lifestyle, religion and health (*e.g.* allergy control). IR spectroscopy has been widely applied for the detection of adulterants and the assignment of geographical or cultivar origin.[18] Products analysed by this method include fruit juice,[19] olive oil,[20-24] fish and meat,[25-27] beverages,[28] maple syrup,[29] starch,[30,31] and honey. [32,33] Gas and liquid

chromatographic techniques have also been used for the determination of the profile of organic components in several foodstuffs. The fat,[34-37] protein,[38, 39] carbohydrate[40, 41] or other natural compound profiles[42-45] have been used to provide species and geographical differentiation. In several cases, enantiomeric composition has been utilised.[39, 42, 45, 46] These methods of discrimination rely on of samples of different species and/or different geographical origin having different chemical compositions. This is not always the case, samples from the same location have been found to contain different components and conversely samples from different regions may display identical chemical composition.[47]

Other techniques applied for food authentication include capillary electrophoresis and isotachophoresis,[48-50] sensor arrays[51-53] and the examination of physical characteristics.[54, 55] This latter approach has been shown to be subject to human inconsistencies in the case of wine tasting.[56]

Stable isotope techniques enable differentiation of chemically identical substances through their isotopic fingerprint, and have been used in authenticity studies for many food products.[57] The isotopic composition of light elements in plant material varies depending on location. Although the local geology, climate and anthropogenic factors such as pollution, pesticides and fertilisers have an effect,[47] the dominant factor is the influence of latitude on the fractionation of the elements in groundwater.[58] Fractionation occurs during physical processes such as evaporation. Lighter isotopes evaporate very slightly faster than their heavier counterparts, therefore in warmer regions where the amount of evaporation is higher, the isotopes are fractionated to a greater degree. The discrimination between isotopes in such physical processes is only significant for light elements, with a high relative mass difference between the isotopes. Thus hydrogen ratios, measured by site-specific natural isotope fractionation nuclear magnetic resonance (SNIF-NMR), and carbon, nitrogen, oxygen and sulfur isotope ratios measured by isotope ratio mass spectrometry (IRMS) have been applied to the authentication of foods. Fats and oils,[42, 59-63] flavours,[64-66] wines,[67-69] fruit juice[70-72] and several other products[47, 73-76] have been classified using stable isotope analysis.

The elemental composition of vegetation reflects (to a certain extent) that of the soil in which it has grown,[77] which in turn depends on the topography, geology and soil characteristics. Therefore no two countries have identical soil maps, and the concentration of elements in produce can be used to assign the geographical origin of a product. As in other methods of authentication, a database of samples of known origin must be available against which unknown samples can be compared. The most useful elements for the assignment of origin are those that are not homeostatically controlled. Elements such as K, Ca and Zn are actively absorbed by organisms and will therefore be present in samples at similar levels, regardless of the environmental conditions experienced. Elements that have no role in normal physiological processes, such as the rare earth elements (REEs) and the heavy metals, are passively absorbed. The concentration of these elements in an organism is strongly dependent on the environmental levels to which the organism has been exposed.

Several studies have used multi-element concentration profiles in the determination of food authenticity, either alone or in combination with chromatographic or stable isotope ratio data.[68, 78-81] Elemental concentrations were determined by atomic absorption spectrometry (AAS),[82-85] inductively coupled plasma atomic emission spectrometry (ICP-AES)[86-92] or inductively coupled plasma mass spectrometry (ICP-MS).[89, 91-95]

Several trace elements have variable natural isotopic abundance due to the decay of radioactive isotopes. These include Li, B, Cu, Sr, Nd, Hf, Pb and U.[96] The composition and age of the local rocks dictates the abundance of the radioactive precursors and their daughter species.[97] This fact has been widely exploited for environmental applications,[98-103] archaeology[104-108] and geochronology and geochemistry.[109-116] Elements are taken up into plants in the same isotopic proportions as they occur in the soil and in precipitation.[97, 117] Therefore isotope ratios in plant-derived food products depend on the geology of the region in which the source crop was grown, and are different in produce of different geographical origin. There have, however, been relatively few reports of the use of heavier stable isotope ratio measurements for the authentication of foodstuffs. For many years thermal ionisation mass spectrometry (TIMS) was the only technique

capable of performing isotope ratio measurements with sufficient precision to allow geographical assignment of food products based on trace element isotopic composition. Samples for TIMS analysis must be loaded in the form of the pure element, meaning that extensive sample preparation is required if this technique is to be applied. Nonetheless, TIMS has been used for Sr isotopic measurements for the regional assignment of wines[117] and butter.[47] In the latter case Sr, C, N, O and S isotopic profiles were subjected to discriminant analysis, allowing assignment of the regional origin of unknown samples by comparison with samples of certified origin.

Inductively coupled plasma mass spectrometry (ICP-MS) is now a well established technique for isotopic trace element determinations.[118] ICP-MS allows rapid analysis of a large range of sample types, requires minimal sample preparation and due to the ionising power of the ICP, can be applied to a wider range of elements than TIMS. The precision of isotope ratio analyses by ICP-MS has only recently matched that achievable by TIMS, through the application of double focussing mass analysers coupled to multi-collector detection arrays. The increasing availability of multi-collector ICP-MS is likely to lead to wider application of heavier stable isotope ratio measurements to the authentication of food products.

There have recently been two reports of the use of Sr isotope ratios measured by ICP-MS for the regional assignment of wines. Using quadrupole ICP-MS, an isotope ratio precision of 0.3 % relative standard deviation (%RSD) was achieved;[119] by multi-collector double focussing instrumentation, the ^{87}Sr / ^{86}Sr ratio was determined to a precision of 0.003 %RSD.[120] Although the Pb isotopic profiles of port wines have also been measured by ICP-MS, and found to a certain extent to depend on the age of the wine,[121] few other studies of trace element isotope ratios for food authentication have been carried out.

Rice is susceptible to mislabelling due to the higher price commanded by the Basmati class of rice – certain varieties grown only in the Haryana, Punjab and Uttar Pradesh regions of India and Pakistan. The fragrance and flavour of Basmati rice apparently cannot be reproduced by growing the seed in other regions. With

the increasing market for premium rice comes the increased possibility that unscrupulous producers may mislabel rice grown in other regions to increase profits. Previously, a study undertaken by a group at the Central Science Laboratory used trace element concentrations in combination with stable isotope ratio measurements of oxygen and carbon to discriminate between rice samples grown in different parts of the world.[77] Nine variables were identified by canonical discriminant analysis as being best for the differentiation between rice originating from Europe, USA and India/Pakistan. In the current study, authentic American, European and Asian rice samples were investigated using double focussing ICP-MS. Multi-collector mode was used for isotope ratio determinations of B, Cu, Sr and Pb; single collector mode, with variable resolution, was used to measure the concentration of 67 elements. Simple and multivariate data analysis techniques were used to assess the potential of isotope ratios and elemental concentrations for the geographical assignment of rice samples of unknown origin.

6.2 Sample Preparation and Measurement

The samples used in this study were selected from a batch previously analysed for ^{18}O and ^{13}C abundances by isotope ratio mass spectrometry and for multi-element concentrations by quadrupole ICP-MS. The samples were originally obtained from reliable sources such as the International Rice Research Institute in the Philippines. 19 samples were selected from the batch, representing 6 from USA (Arkansas, Louisiana, Mississippi and Texas), 7 from Europe (Italy, Spain and French Carmargue), and 6 from India/Pakistan. Of the samples from Asia, 4 were known to be traditional Basmati varieties, which can only be grown in the foothills of the Himalayas, since their flowering cycle is dependent on the amount of sunlight they receive.[122] The remaining Asian samples were Pusa Basmati and Kasturi. Although these varieties can legally be sold as Basmati,[123] they have been bred for a high yield and their photoperiod insensitivity that allows them to be grown outside the traditional Basmati cultivating regions. These varieties therefore do not have the same quality of aroma and texture as the traditional

Basmati varieties. A further 4 rice samples were chosen as unknowns to test the efficacy of the method for assignment of geographical origin.

Approximately 0.5 g of each rice sample was digested in 5 ml of concentrated Aristar grade nitric acid (Merck-BDH, Poole, Dorset, UK) using a Multiwave microwave digestion system (Perkin-Elmer Ltd, Beaconsfield, Buckinghamshire, UK) and the program summarised in Table 6.1.

Table 6.1 Microwave digestion program

Step	Power / W	Time / min
1	0 – 500	2
2	500	5
3	500 – 1000	2
4	1000	20
5	0	15

The digestion batch contained a total of 4 procedural blanks and one blank spiked with a 69 element standard solution. Reference materials NIST 1547 (peach leaves), NIST 1566a (oyster tissue) and NIST 1577b (bovine liver) were randomly distributed amongst the rice samples. The digested samples were diluted to a volume of 10 ml with 18.2 MΩ cm water (Millipore, Bedford, MA, USA). These solutions were then diluted 5 fold with 1 % nitric acid prior to analysis using a Thermo Elemental Axiom double focussing ICP-MS system. Typical operating parameters are given in Table 6.2.

Table 6.2 Typical operating parameters of the Axiom ICP-MS system

Forward power	1250 W
Cool gas	14 L min^{-1}
Auxiliary gas	0.8 L min^{-1}
Nebuliser gas	0.75 – 0.80 L min^{-1}
Ion lens settings and torch position	Optimised for maximum ^{115}In signal

The analyses were divided into two categories. Firstly, B, Cu, Sr and Pb isotope ratio measurements were carried out in separate multi-collector acquisitions, Table 6.3 gives the parameters for these determinations. Subsequently a multi-element

determination was performed on the samples in single collector mode, using the acquisition parameters and resolution settings outlined in Table 6.4.

Table 6.3 Acquisition parameters for isotope ratio determinations

Instrument mode			Multi-collector		Points acquired		25		
Scan mode			Static		Dwell time		5 s		
Collector	L4	L3	L2	L1	Ax	H1	H2	H3	H4
B	$^{10}B^+$	--	--	--	--	--	--	--	$^{11}B^+$
Cu	--	--	$^{63}Cu^+$	--	--	--	$^{65}Cu^+$	--	--
Sr	--	$^{84}Sr^+$	$^{85}Rb^+$	$^{86}Sr^+$	$^{87}Rb^+$ & $^{87}Sr^+$	$^{88}Sr^+$	--	--	--
Pb	--	--	--	--	--	$^{204}Pb^+$	$^{206}Pb^+$	$^{207}Pb^+$	$^{208}Pb^+$

Table 6.4 Acquisition parameters for multi-element determinations

Instrument mode	Single collector
Scan mode	Electrostatic sector scanning
Dwell time	10 ms
Points per peak width	10
Scan window	3 peak widths
Sweeps	10
Runs per sample	3

Resolution	Isotopes
400	$^{6}Li^+$, $^{7}Li^+$, $^{9}Be^+$, $^{10}B^+$, $^{11}B^+$, $^{23}Na^+$, $^{69}Ga^+$, $^{71}Ga^+$, $^{72}Ge^+$, $^{73}Ge^+$, $^{74}Ge^+$, $^{75}As^+$, $^{77}Se^+$, $^{78}Se^+$, $^{82}Se^+$, $^{85}Rb^+$, $^{86}Sr^+$, $^{87}Rb^+$, $^{88}Sr^+$, $^{89}Y^+$, $^{90}Zr^+$, $^{91}Zr^+$, $^{93}Nb^+$, $^{95}Mo^+$, $^{97}Mo^+$, $^{99}Ru^+$, $^{101}Ru^+$, $^{103}Rh^+$, $^{105}Pd^+$, $^{107}Ag^+$, $^{108}Pd^+$, $^{109}Ag^+$, $^{111}Cd^+$, $^{114}Cd^+$, $^{117}Sn^+$, $^{118}Sn^+$, $^{119}Sn^+$, $^{120}Sn^+$, $^{121}Sb^+$, $^{123}Sb^+$, $^{125}Te^+$, $^{126}Te^+$, $^{128}Te^+$, $^{133}Cs^+$, $^{135}Ba^+$, $^{137}Ba^+$, $^{138}Ba^+$, $^{139}La^+$, $^{140}Ce^+$, $^{141}Pr^+$, $^{142}Ce^+$, $^{143}Nd^+$, $^{145}Nd^+$, $^{146}Nd^+$, $^{147}Sm^+$, $^{149}Sm^+$, $^{151}Eu^+$, $^{152}Sm^+$, $^{153}Eu^+$, $^{155}Gd^+$, $^{156}Gd^+$, $^{157}Gd^+$, $^{158}Gd^+$, $^{159}Tb^+$, $^{160}Gd^+$, $^{161}Dy^+$, $^{162}Dy^+$, $^{163}Dy^+$, $^{164}Dy^+$, $^{165}Ho^+$, $^{166}Er^+$, $^{167}Er^+$, $^{169}Tm^+$, $^{171}Yb^+$, $^{172}Yb^+$, $^{173}Yb^+$, $^{175}Lu^+$, $^{176}Lu^+$, $^{177}Hf^+$, $^{178}Hf^+$, $^{179}Hf^+$, $^{181}Ta^+$, $^{182}W^+$, $^{183}W^+$, $^{184}W^+$, $^{185}Re^+$, $^{187}Re^+$, $^{188}Os^+$, $^{189}Os^+$, $^{190}Os^+$, $^{191}Ir^+$, $^{193}Ir^+$, $^{194}Pt^+$, $^{195}Pt^+$, $^{197}Au^+$, $^{200}Hg^+$, $^{201}Hg^+$, $^{202}Hg^+$, $^{203}Tl^+$, $^{205}Tl^+$, $^{206}Pb^+$, $^{207}Pb^+$, $^{208}Pb^+$, $^{209}Bi^+$, $^{232}Th^+$, $^{238}U^+$
2000	$^{24}Mg^+$, $^{25}Mg^+$, $^{26}Mg^+$, $^{27}Al^+$, $^{28}Si^+$, $^{29}Si^+$, $^{30}Si^+$
4000	$^{42}Ca^+$, $^{43}Ca^+$, $^{44}Ca^+$, $^{45}Sc^+$, $^{46}Ti^+$, $^{47}Ti^+$, $^{49}Ti^+$, $^{50}Ti^+$, $^{51}V^+$, $^{52}Cr^+$, $^{53}Cr^+$, $^{55}Mn^+$, $^{56}Fe^+$, $^{57}Fe^+$, $^{58}Ni^+$, $^{59}Co^+$, $^{60}Ni^+$, $^{62}Ni^+$, $^{63}Cu^+$, $^{64}Zn^+$, $^{65}Cu^+$, $^{66}Zn^+$, $^{67}Zn^+$, $^{68}Zn^+$
6000	$^{31}P^+$, $^{32}S^+$, $^{34}S^+$
11000	$^{39}K^+$

6.3 Data Processing

For the multi-collector acquisitions, a standard solution containing the analyte was measured after every eighth rice sample (approximately every 25 min). The results from these bracket standards were used to correct the data for any time dependent instrumental drift using equation 6.1.

$$I_{corr} = I_{meas} \times \frac{I_1^S}{\overline{I}_b^S}$$

6.1

Where I_{corr} and I_{meas} are the corrected and measured isotope intensities in the sample, I_1^S is the isotope intensity in the first standard solution and $\overline{I}_b^S$ is the mean of the isotope intensities measured in the bracketing standard solutions.

Following the bracket correction, the mean of the procedural blanks was subtracted from the sample data and for B, Cu and Pb multi-collector determinations, isotope ratios were then calculated. Data for Sr required an extra stage of calculation due to the overlap of ^{87}Rb on ^{87}Sr. The ion signal at ^{85}Rb was used to calculate the observed ^{87}Rb intensity, $\left(^{87}\text{Rb}\right)^{obs}$. The mass bias for this calculation was initially corrected using the ^{88}Sr / ^{86}Sr ratio measured in the rice samples. This ratio has a constant natural value[96] of 8.3753. Equation 6.2, an adaptation of the expression given by Russell et al.[124] widely used for the correction of multi-collector isotope ratio data,[125-127] was used to apply the correction.

$$\left(^{87}\text{Rb}\right)^{obs} = \left(^{85}\text{Rb}\right)^{obs} \times \left(\frac{^{87}\text{Rb}}{^{85}\text{Rb}}\right)^{true} \times \left(\frac{\left(^{88}\text{Sr}/\,^{86}\text{Sr}\right)^{obs}}{\left(^{88}\text{Sr}/\,^{86}\text{Sr}\right)^{true}}\right)^{\left(\frac{\ln(87/85)}{\ln(88/86)}\right)}$$

6.2

Some of the samples had a calculated value of $\left(^{87}\text{Rb}\right)^{obs}$ that was larger than the total ion signal recorded at m/z 87, suggesting that spectral interference was affecting either ^{85}Rb, leading directly to overestimation of ^{87}Rb, and/or ^{88}Sr

resulting in overestimation of the mass bias. Examination of $\left(^{88}Sr/^{86}Sr\right)^{obs}$ in the rice samples showed its value to be very variable in different samples, a range of 8.6 to 9.2 was recorded corresponding to a variation of 1.6 to 5.2 % in the calculated bias per mass unit. The variation was not smooth with time, suggesting varying levels of spectral interference at m/z 88 in different samples. Potential interfering species include argon based species (e.g. $^{40}Ar^{48}Ti^+$, $^{40}Ar^{48}Ca^+$), oxides ($^{72}Ge^{16}O^+$) and doubly charged ions (Yb^{2+}, Lu^{2+}, Hf^{2+}). Internal standardisation was therefore not an option for compensation of the bias in the calculation of the ^{87}Rb interference.

The bracket standard solutions measured after every eighth sample were examined for their potential as external standards. The $\left(^{88}Sr/^{86}Sr\right)^{obs}$ in these solutions was in the range 8.942 to 8.945, corresponding to a bias per mass unit of 3.38 to 3.40 %. Although it is possible that there was the same level of spectral interference in all of the standard solutions, this data shows the external standardisation approach to be much more reliable than the internal standardisation method for use in the correction of the bias in the calculation of the ^{87}Rb intensity. Equation 6.2 was used to apply the external standardisation, the term $\left(^{88}Sr/^{86}Sr\right)^{obs}$ was replaced by the mean of the $^{88}Sr / ^{86}Sr$ ratio measured in the bracket standard solutions.

The analyte isotope ratios were not corrected for mass bias. In this study, differences between ratios in different samples were of interest, not the absolute values. The bracket correction procedure described above corrected each isotope individually for instrumental drift, which included any drift in the mass bias of the system. The ratios measured in all samples were therefore directly comparable to one another.

For single collector acquisitions, a 69 element standard solution was analysed after every eighth sample. Data for each element was corrected for the response of bracket standards using equation 6.1, blank subtracted and the concentration in the samples was calculated based on the response of the standard solution (one-point calibration). Results for the spiked blank sample and reference materials were used as a measure of the recovery and accuracy of the method respectively. Data

for an element was only accepted if it was within the in-house specification of ±40 % of the either the spiked concentration or the certified limits.

6.4 Calibration Samples

6.4.1 Isotope ratio data

Table 6.5 gives ^{10}B / ^{11}B, ^{63}Cu / ^{65}Cu, ^{87}Sr / ^{86}Sr and ^{207}Pb / ^{206}Pb isotope ratios for the 19 calibration rice samples measured by multi-collector ICP-MS.

Table 6.5 Multi-collector isotope ratio data after bracket standard and blank correction. Figures in brackets are one standard deviation (sd) and refer to the final figures of each ratio.

Sample	Rice variety	^{10}B / ^{11}B	^{63}Cu / ^{65}Cu	^{87}Sr / ^{86}Sr	^{207}Pb / ^{206}Pb
Arkansas 1	Kaybonnet	0.2221 (3)	2.072 (2)	0.63 (2)	0.79 (1)
Arkansas 2	Cypress	0.2211 (3)	2.068 (3)	0.69 (2)	0.79 (1)
Louisiana	Cypress	0.2208 (3)	2.071 (2)	0.59 (4)	0.85 (1)
Mississippi	L202	0.2223 (3)	2.074 (1)	0.65 (6)	0.84 (1)
Texas 1	TORO2	0.2217 (4)	2.069 (1)	0.68 (3)	0.83 (1)
Texas 2	L202	0.2201 (5)	2.076 (2)	0.63 (5)	0.84 (2)
Italy 1	Thaibonnet	0.2148 (22)	2.067 (3)	0.73 (1)	0.86 (3)
Italy 2	Thaibonnet	0.2179 (34)	2.071 (2)	0.66 (3)	0.89 (1)
Italy 3	Thaibonnet Riseria C	0.2149 (39)	2.075 (1)	0.82 (6)	0.94 (4)
Spain 1	Thaibonnet	0.2139 (21)	2.070 (2)	0.69 (1)	0.88 (5)
Spain 2	Thaibonnet	0.2179 (23)	2.067 (2)	0.65 (3)	0.86 (2)
France 1	Thaibonnet	0.2093 (45)	2.075 (2)	0.27 (13)	0.87 (1)
France 2	US variety A301	0.2079 (41)	2.077 (1)	0.69 (2)	0.87 (2)
India 1	Basmati	0.2111 (21)	2.073 (1)	0.70 (1)	0.88 (5)
India 2	Basmati	0.2150 (30)	2.074 (1)	0.69 (4)	0.80 (1)
India 3	Pusa Basmati	0.2121 (29)	2.072 (2)	0.73 (2)	0.85 (2)
India 4	Kasturi	0.2145 (17)	2.080 (1)	0.71 (2)	0.87 (2)
Pakistan 1	Basmati	0.2217 (32)	2.071 (2)	0.65 (4)	0.87 (2)
Pakistan 2	Basmati	0.2130 (42)	2.077 (2)	0.59 (6)	0.90 (1)

The Sr and Pb ratios recorded in most samples were lower than expected for natural samples of terrestrial origin, correcting for the mass bias would not have accounted for the deviation. Additionally, the standard deviations of these ratios were larger than expected by at least an order of magnitude. For Sr, the incorrect ratios could have been due to spectral interference of ^{86}Kr falsely increasing the

^{86}Sr signal, leading to a reduced ^{87}Sr / ^{86}Sr ratio. Additionally, the correction for the rubidium overlap was almost certainly responsible for the more extreme ratios (*e.g.* France 1), as discussed below. The deviation observed for Pb is unlikely to be due to spectral overlap as there are very few interfering species that affect the major Pb isotopes. The inaccuracies and poor precision observed for both Sr and Pb were most likely due to the relatively low signals recorded for these elements. Instrument sensitivity for all elements measured in multi-collector mode is summarised in Table 6.6.

Table 6.6 Range of signals (counts s^{-1}) recorded in rice samples for elements measured in multi-collector mode

	^{10}B	^{65}Cu	^{86}Sr	^{207}Pb
Max. signal	8×10^5	3×10^6	3×10^5	3×10^5
Min. signal	5×10^4	8×10^5	3×10^4	2×10^4

The high baseline count rate of Faraday collectors means that signals lower than around 10^5 counts s^{-1} may be severely affected by noise. This leads to poor isotope ratio precision and as the noise of different Faraday collectors is uncorrelated, determinations can be seriously inaccurate. In addition to Sr and Pb data, the low signal recorded for B in some samples may have resulted in the wide range of ^{10}B / ^{11}B isotope ratios observed. The variation in this ratio approached the full range seen in terrestrial samples. The usefulness of the isotope ratio data is therefore limited. A more extensive sample preparation procedure involving concentration of the analyte elements is required before the use of trace element isotope ratios for the authentication of rice can be properly assessed.

Despite the above comments, the isotope ratio data did display some correlation with the geographical origin of rice samples. The ^{10}B / ^{11}B ratio in all of the USA samples was higher than in both the European and Indian/Pakistani samples, with the exception of one of the samples from Pakistan. Additionally, both of the French samples analysed had a lower boron ratio than the remaining European and Asian samples, and formed a regional group of their own. The mean, maximum and minimum of the ^{10}B / ^{11}B ratios in the remaining European samples, the USA

samples and the Asian samples excluding the Pakistani sample mentioned above, are plotted in Fig. 6.1.

Fig. 6.1 Mean (dashed line), maximum and minimum ^{10}B / ^{11}B ratio in samples from each region. Error bars are ± 2 sd from the mean.

The lowest ^{10}B / ^{11}B ratio measured in the USA samples was higher than the mean of the European by more than 2 times the sd of the European samples, and more than 3 times the sd higher than the mean of the Indian/Pakistani samples. Therefore samples from the USA had a significantly higher ^{10}B / ^{11}B ratio than the vast majority of the remaining samples analysed. From this limited data set, the following comments can be made. A ^{10}B / ^{11}B ratio of less than approximately 0.210 in a rice sample suggests the country of origin to be France, a ratio greater than 0.220 strongly suggests the USA as the country of origin. Samples with a ratio between these two values could be either Indian/Pakistani or European other than France.

Although the Cu isotope ratio did vary from sample to sample, this variation was not related to the geographical origin. As illustrated in Fig. 6.2, there was no significant difference in the ^{63}Cu / ^{65}Cu isotope ratio measured in rice samples from different regions. There was a general trend for samples from USA to have a lower ratio than samples from Europe, which in turn had a generally lower ratio than samples from Asia, however the variation was not sufficient to allow regional assignment.

Fig. 6.2 Mean (dashed line), maximum and minimum ^{63}Cu / ^{65}Cu ratio in samples from each region. Error bars are ± 2 sd from the mean.

The ^{87}Sr / ^{86}Sr ratios presented in Table 6.5 have been corrected for overlap from ^{87}Rb using the procedure described above. There was no clear differences between the ^{87}Sr / ^{86}Sr ratio in samples originating in different parts of the world, however the level of Rb in the rice samples varied widely. This was illustrated by the Rb to Sr concentration ratios in the samples, given in Table 6.7.

Table 6.7 Rb / Sr concentration ratios for calibration rice samples

Sample	Rb / Sr	Sample	Rb / Sr
Arkansas 1	16	Spain 1	11
		Spain 2	1.3
Arkansas 2	10	France 1	115
Louisiana	22	France 2	0.6
Mississippi	28	India 1	6.4
Texas 1	19	India 2	4.2
Texas 2	27	India 3	7.4
Italy 1	0.5	India 4	9.0
Italy 2	6.3	Pakistan 1	33
Italy 3	5.3	Pakistan 2	42

The ratio was less than 10 for most European and Indian samples, between 10 and 30 in samples from USA and over 30 for rice from Pakistan. The Rb / Sr ratio was more than 100 in sample 'France 1', which contained over 9 $\mu g \ g^{-1}$ Rb. This

sample had a calculated ^{87}Sr / ^{86}Sr of 0.27, and was so different from the any other sample that it was excluded from further analyses of the Sr isotope ratio data. Although the ^{87}Sr / ^{86}Sr ratios in the remaining samples did not to depend on the Rb concentration, the extent of the correction required made the reliability of the results uncertain. Separation of Rb and Sr and confirmation of the accuracy of the measurements using an isotopic reference material is required before the applicability of Sr ratio data to the problem of rice authenticity can be properly assessed.

The mean of the ^{207}Pb / ^{206}Pb ratio in the European samples was 0.923 ± 0.056 (2 sd), in the Asian samples the mean was 0.903 ± 0.066 and in samples from the USA the mean was 0.859 ± 0.056. The data is illustrated in Fig. 6.3. Similar to the Cu data, the range of Pb isotope ratios in samples from a single region was too great to allow discrimination by geographical origin. The following comments can be made. The ^{207}Pb / ^{206}Pb ratio in rice samples from the USA was lower than samples from the other two regions; samples grown in the state of Arkansas had a particularly low ratio. One Asian sample (India 2) also had a low ^{207}Pb / ^{206}Pb ratio and one European sample (Italy 3) had a particularly high ratio.
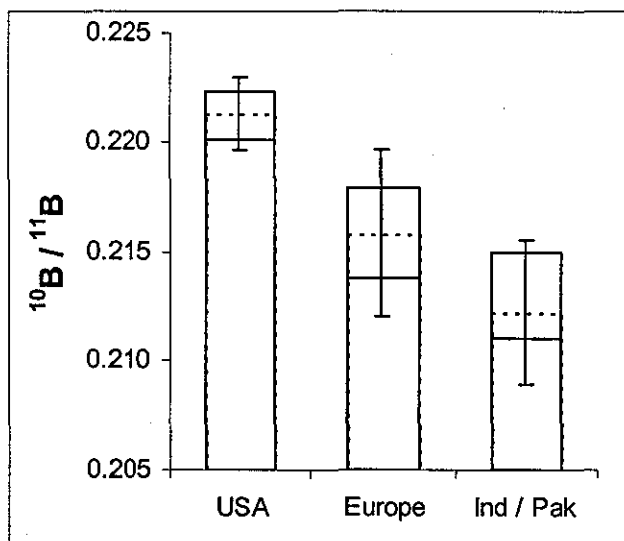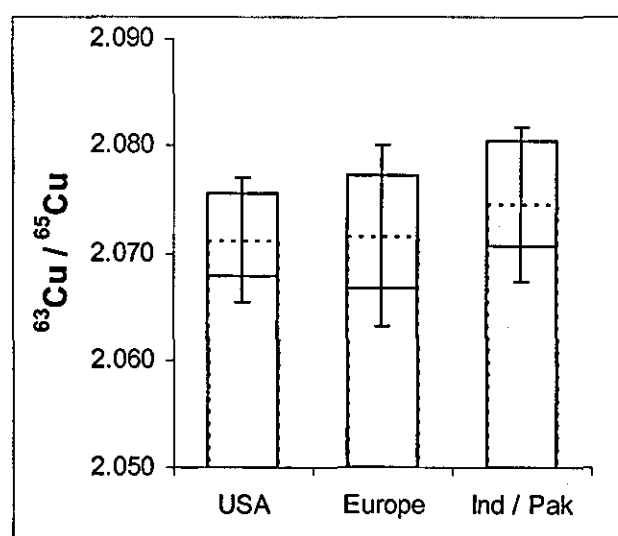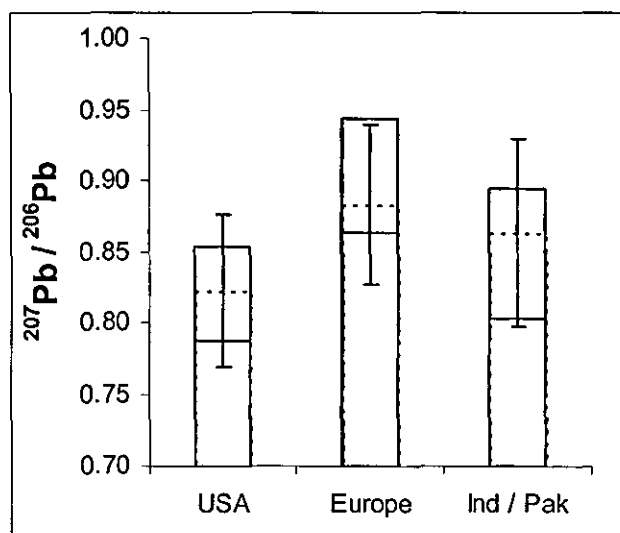

Fig. 6.3 Mean (dashed line), maximum and minimum ^{207}Pb / ^{206}Pb ratio in samples from each region. Error bars are ± 2 sd from the mean.

6.4.2 Principal components analysis of isotope ratios

The combined isotope ratio data was evaluated using principal components analysis (PCA). As the numerical values of the ratios were very different, each of the ratios was scaled by dividing by the standard deviation of the ratio measured in all the samples. Additionally, all data was mean centred prior to PCA analysis. France 1 and Italy 3 were shown to be outliers in preliminary analyses, these samples were excluded from the final PCA runs. Three PCs were found to account for more than 91 % of the variance in the data. Examination of the loadings (the extent to which each variable contributes to each PC) showed that PC 1 was strongly influenced by all of the ratios; Cu, Sr and Pb ratios contributed significantly to PC 2; PC 3 was principally dependent on the Cu and Pb ratios.

A plot of PC 3 against PC1 (Fig. 6.4) gave best separation of the calibration samples by geographical origin. As shown in Fig. 6.4, this analysis allowed discrimination between US samples and the Asian and European samples. The majority of the European samples had a PC 3 score significantly lower than the Asian samples, France 2 being the exception. As mentioned above, the low ^{10}B / ^{11}B ratio measured in the French rice made these samples unique.
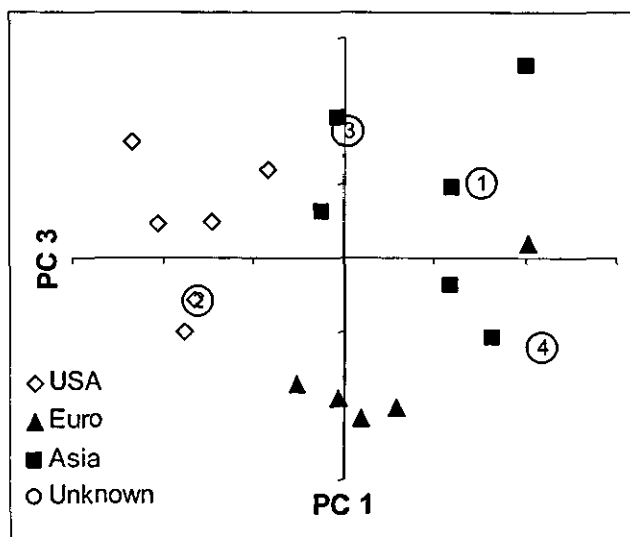
Fig. 6.4 Scores plot for PCA of isotope ratio data. Explained variance: 53 % PC 1; 13 % PC 3. Circled numbers represent the unknown samples (see below).

Table 6.8 Elemental concentration data (ng ml^{-1}) for calibration rice samples. Figures in brackets are 1 sd and refer to the final figures quoted. * Concentration below detection limit.

	Li	Be	B	Na	Mg	Al	P	S	K	Ca	Sc	Ti	V	Cr
Scale factor	1	10^{-2}	1	10	10^4	10	10^5	10^4	10^5	10^3	0.1	1	1	1
Arkansas 1	3.39 (5)	8 (2)	5867 (30)	118 (4)	23.4 (2)	75.5 (7)	13 (1)	108.8 (6)	8 (2)	304 (1)	25 (7)	10.0 (1)	1.59 (3)	11.7 (7)
Arkansas 2	2.26 (3)	11 (1)	6206 (36)	112 (2)	24.4 (3)	165 (1)	15.2 (5)	118.0 (7)	4.8 (1)	285 (3)	10 (2)	11 (1)	1.93 (4)	10.1 (6)
Louisiana	1.49 (6)	*	4932 (21)	195 (6)	26.4 (2)	50.2 (3)	14.5 (8)	98.5 (9)	5.4 (1)	42 (1)	10 (1)	3.7 (3)	0.6 (3)	20.9 (5)
Mississippi	27.0 (4)	6 (5)	4782 (22)	214 (2)	21.0 (2)	219 (1)	12.6 (1)	114.8 (3)	5.7 (9)	85.4 (7)	5 (1)	10.0 (1)	4.31 (5)	26 (2)
Texas 1	3.77 (2)	9 (5)	4160 (19)	163 (1)	17.4 (2)	395 (2)	11.4 (4)	106.7 (2)	6.1 (1)	247 (6)	7 (3)	27 (1)	3.9 (3)	65 (2)
Texas 2	4.79 (7)	7 (4)	4372 (32)	166 (4)	16.6 (2)	102 (1)	11.2 (7)	98 (2)	4.7 (1)	174 (2)	5 (1)	4.2 (4)	1.5 (3)	30.0 (8)
Italy 1	0.83 (5)	*	584 (1)	147 (3)	120 (4)	99 (2)	98 (8)	92 (1)	53.9 (9)	98.1 (3)	3 (2)	114 (1)	2.3 (2)	*
Italy 2	0.62 (4)	*	376 (1)	82 (1)	33.0 (1)	137.4 (7)	18 (4)	93.8 (4)	24.1 (1)	41.8 (6)	*	16 (1)	0.8 (2)	*
Italy 3	0.38 (2)	*	350 (1)	75 (1)	23.0 (2)	47.7 (5)	14.1 (6)	104 (1)	6.0 (1)	42 (1)	*	7.2 (2)	0.3 (1)	*
Spain 1	2.26 (4)	*	683 (5)	198 (3)	137 (2)	85 (2)	116 (7)	122 (1)	63 (2)	90.1 (5)	0.5 (7)	66 (3)	1.4 (1)	*
Spain 2	14.4 (2)	3 (4)	549 (2)	346 (20)	24.1 (4)	88 (1)	13.3 (2)	121 (1)	10 (2)	35.5 (6)	5 (2)	3.3 (4)	1.3 (1)	7.7 (8)
France 1	4.96 (5)	*	367 (1)	84 (2)	39.9 (4)	59.1 (8)	18 (2)	98 (1)	31 (2)	49 (1)	1 (1)	7.3 (6)	1.1 (1)	4.2 (3)
France 2	7.7 (1)	*	331 (1)	108 (3)	36.8 (3)	79 (1)	17 (3)	111.7 (8)	23 (2)	54.1 (8)	*	6.6 (3)	0.80 (2)	*
India 1	11.42 (6)	5 (4)	784 (2)	128 (12)	78 (5)	134 (1)	31 (5)	144 (3)	31.2 (2)	55.6 (2)	*	42 (1)	2.7 (1)	56 (2)
India 2	26.8 (2)	2 (1)	555 (2)	75 (4)	50 (3)	107 (2)	19 (3)	133 (2)	18 (2)	50.8 (6)	*	6.2 (3)	2.19 (8)	70 (2)
India 3	5.10 (4)	*	580 (2)	135 (3)	91 (4)	25.6 (4)	62 (3)	107.2 (5)	36 (1)	58 (1)	*	13 (1)	1.6 (6)	7.0 (7)
India 4	8.4 (1)	6 (4)	1098 (4)	209 (2)	97.7 (6)	86.4 (4)	73 (3)	166 (4)	43.9 (4)	59 (1)	*	10 (3)	2.35 (1)	7.9 (9)
Pakistan 1	14.7 (2)	1 (6)	590 (2)	144 (3)	92 (1)	68 (1)	35 (8)	128 (2)	31 (1)	74.5 (3)	4 (2)	4.7 (9)	2.0 (2)	14 (2)
Pakistan 2	12.2 (1)	1 (1)	518 (2)	162 (2)	91 (2)	147 (2)	39 (8)	123.7 (9)	34 (1)	84 (2)	5 (2)	14 (1)	2.4 (3)	22.9 (5)

6.4.3 Multi-element concentration data

Results for two elements (Si and Mo) were outside ± 40 % of the certified reference material concentrations and the known spike concentrations and were therefore excluded from the data set. The concentrations of the remaining 67 elements determined in the 19 rice samples are presented in Table 6.8.

Table 6.8 (cont) Elemental concentration data (ng ml^{-1}) for calibration rice samples. Figures in brackets are 1 sd and refer to the final figures quoted.
* Concentration below detection limit.

	Mn	Fe	Ni	Co	Cu	Zn	Ga	Ge	As	Se	Rb	Sr	Y	Zr	Nb	Ru	Rh
Scale factor	10^2	10^2	1	1	10	10^2	1	1	1	1	10	1	1	1	0.1	10^{-2}	10^{-2}
Arkansas 1	141.5 (8)	24.1 (6)	4 (2)	12.8 (2)	125.4 (8)	175.7 (3)	5.4 (1)	2.4 (2)	399 (8)	437 (6)	280 (3)	175 (1)	15.8 (3)	1.85 (6)	5.1 (1)	4.2 (9)	3.0 (6)
Arkansas 2	152 (1)	21.8 (7)	9.6 (3)	7.8 (1)	115 (2)	158.6 (6)	5.37 (3)	2.9 (3)	479 (2)	345 (12)	154 (6)	159.0 (8)	14.9 (2)	1.78 (3)	7.7 (2)	1 (2)	4.0 (4)
Louisiana	178.8 (1)	20.2 (3)	36 (2)	6.8 (3)	186 (2)	129.8 (3)	5.43 (7)	1.33 (4)	193 (3)	228 (5)	138 (4)	63.1 (6)	0.108 (8)	1.16 (4)	1.3 (2)	1 (1)	1.2 (5)
Mississippi	85.7 (4)	37.1 (7)	71 (2)	1.9 (4)	290 (2)	133 (2)	5.05 (7)	1.53 (1)	98 (1)	113 (2)	146 (1)	52.3 (4)	0.98 (3)	3.08 (3)	3.8 (1)	2.3 (8)	0.2 (5)
Texas 1	69.8 (8)	41.5 (5)	82 (2)	5.4 (2)	185 (2)	161 (3)	4.85 (4)	1.39 (7)	631 (1)	153 (4)	234 (2)	121 (1)	0.94 (2)	5.5 (2)	12.2 (1)	1.3 (7)	*
Texas 2	80.0 (4)	27.3 (4)	63 (3)	7.2 (3)	184 (2)	143 (1)	3.54 (4)	0.7 (1)	701 (12)	132 (2)	222 (7)	82 (2)	0.8 (3)	2.1 (2)	2.34 (9)	1 (1)	*
Italy 1	201 (1)	90 (3)	86 (3)	3.00 (1)	93.2 (4)	253 (3)	12.4 (2)	3.7 (3)	133 (1)	35 (2)	10.3 (1)	192 (3)	0.367 (6)	4.53 (2)	40.1 (2)	1.1 (6)	0.7 (6)
Italy 2	175 (2)	22.9 (6)	71.4 (8)	1.10 (7)	206 (1)	132 (1)	6.59 (8)	2.5 (2)	79 (1)	70 (4)	43.5 (6)	68.9 (3)	0.18 (4)	0.9 (3)	6.9 (3)	3 (1)	0.8 (8)
Italy 3	112.2 (4)	15.9 (4)	218 (4)	2.5 (2)	276 (4)	148.1 (8)	5.0 (2)	3.5 (2)	57.3 (7)	52.2 (9)	18.4 (2)	34.6 (5)	0.10 (1)	0.81 (6)	3.3 (3)	1.5 (6)	*
Spain 1	678 (10)	97 (2)	73 (3)	25.5 (5)	185 (2)	201 (2)	14.7 (2)	5.3 (2)	479 (4)	431 (12)	362 (4)	331 (4)	0.42 (1)	3.2 (1)	24.6 (1)	1 (1)	1 (1)
Spain 2	64.7 (4)	21.4 (4)	30 (2)	4.0 (1)	127 (2)	91 (1)	4.73 (6)	0.6 (2)	54 (1)	34 (2)	9.30 (5)	71.1 (6)	0.49 (3)	0.89 (3)	1.7 (3)	*	*
France 1	175.8 (9)	53.5 (7)	132 (3)	10.19 (7)	247 (1)	126 (3)	6.5 (1)	1.4 (2)	36.3 (5)	23 (4)	922 (15)	79.8 (7)	0.29 (3)	1.8 (3)	2.0 (3)	3 (2)	0.3 (3)
France 2	133.2 (9)	40.0 (8)	37.3 (4)	3.6 (2)	267 (2)	163 (2)	6.3 (1)	2.80 (8)	174 (3)	56 (3)	6.88 (5)	108.0 (8)	0.18 (3)	1.3 (2)	3.4 (1)	1 (1)	3 (1)
India 1	96.8 (5)	63.3 (8)	220 (3)	7.0 (3)	260.4 (4)	168 (2)	7.82 (8)	1.8 (1)	31.1 (6)	178 (5)	132 (16)	204 (2)	2.32 (4)	2.7 (2)	22.2 (6)	1.9 (7)	1.4 (7)
India 2	80.7 (6)	59 (1)	245 (4)	5.86 (8)	263 (2)	153 (2)	7.0 (1)	1.5 (1)	44.7 (8)	171 (3)	46.2 (2)	109 (1)	0.40 (2)	0.44 (6)	2.2 (6)	2.9 (8)	*
India 3	95.6 (8)	53.7 (8)	35 (4)	16 (1)	157 (1)	137 (2)	8.1 (2)	2.0 (2)	105 (2)	29 (3)	125 (27)	169 (1)	0.12 (1)	0.9 (1)	3.8 (1)	2 (1)	2 (1)
India 4	110 (1)	74.9 (5)	64 (2)	86 (1)	330 (2)	269 (1)	9.10 (4)	2.13 (8)	106.4 (4)	36 (3)	134 (6)	149 (2)	0.24 (2)	1.8 (3)	2.85 (3)	2.9 (6)	5.1 (6)
Pakistan 1	150 (1)	59 (1)	35 (3)	5.6 (1)	159.5 (9)	181.1 (5)	8.2 (1)	2.1 (2)	148 (2)	24 (4)	298 (4)	89.5 (7)	0.25 (2)	1.2 (2)	2.5 (2)	3 (2)	*
Pakistan 2	157 (1)	64 (2)	46.4 (9)	6.6 (2)	224 (3)	208.5 (8)	8.25 (6)	2.16 (6)	101 (1)	49 (3)	388 (9)	91.8 (7)	1.08 (3)	1.5 (1)	5.4 (1)	3 (1)	2 (1)

Table 6.8 (cont) Elemental concentration data (ng ml^{-1}) for calibration rice samples. Figures in brackets are 1 sd and refer to the final figures quoted.
* Concentration below detection limit.

	Pd	Ag	Cd	Sn	Sb	Te	Cs	Ba	La	Ce	Pr	Nd	Sm	Eu	Gd	Tb	Dy	Ho
Scale factor	10^{-2}	1	1	1	10^{-2}	0.1	0.1	1	0.1	0.1	0.1	0.1	0.1	10^{-2}	10^{-2}	10^{-2}	10^{-2}	10^{-2}
Arkansas 1	52 (2)	10.9 (3)	6.64 (8)	2.2 (3)	21 (3)	7.6 (8)	10.9 (4)	125 (2)	111.9 (7)	66.6 (9)	24.3 (2)	100.5 (1)	20.0 (7)	36 (1)	221.9 (7)	33.9 (5)	200 (2)	38 (1)
Arkansas 2	49 (1)	11.3 (1)	6.8 (1)	4.2 (1)	19 (2)	8 (2)	5.9 (4)	109 (1)	94.4 (5)	39.0 (4)	19.9 (1)	84 (1)	16.6 (1)	31.6 (6)	197 (5)	30.8 (1)	181.2 (5)	34.74 (7)
Louisiana	6.9 (3)	4.14 (1)	9.0 (2)	2.3 (1)	17 (2)	13 (1)	5.7 (4)	94 (1)	1.5 (1)	2.9 (3)	0.57 (7)	1.41 (6)	0.34 (3)	3.9 (7)	1.8 (5)	0.55 (3)	2.2 (7)	0.5 (2)
Mississippi	8 (2)	6.0 (1)	29.7 (4)	7.9 (1)	27.7 (8)	3 (2)	6.3 (2)	43.6 (2)	13.2 (2)	26.7 (4)	3.67 (4)	13.3 (2)	2.7 (2)	5.22 (7)	26 (2)	3.8 (3)	20.2 (2)	3.6 (3)
Texas 1	13 (1)	17.9 (3)	6.3 (2)	165 (1)	56 (1)	10 (2)	12.1 (3)	96 (2)	10.8 (2)	20.5 (3)	2.78 (8)	9.7 (4)	2.12 (6)	6.0 (9)	21 (2)	2.8 (3)	18 (1)	2.97 (6)
Texas 2	9 (2)	9.9 (1)	9.8 (2)	140 (2)	98 (3)	8 (1)	10.8 (3)	63 (5)	12 (4)	17 (4)	3.0 (6)	9 (2)	1.54 (9)	4.3 (1)	16 (1)	2.0 (2)	9 (2)	2.22 (8)
Italy 1	14 (2)	2.0 (1)	13.2 (2)	0.7 (1)	66 (2)	14.2 (7)	2.12 (6)	75 (1)	3.82 (3)	8.15 (2)	1.12 (3)	3.7 (2)	0.75 (3)	3.8 (2)	8 (1)	1.2 (1)	6 (2)	1.3 (2)
Italy 2	5 (2)	2.9 (2)	31.9 (4)	1.54 (6)	21 (2)	1.6 (4)	4.0 (2)	53.3 (6)	1.48 (5)	1.2 (1)	0.38 (6)	0.5 (2)	0.19 (6)	2.7 (4)	3.0 (6)	0.4 (1)	3 (1)	0.45 (5)
Italy 3	3 (1)	2.1 (3)	280 (1)	1.28 (7)	31 (2)	*	2.8 (2)	41.3 (7)	1.80 (7)	2.01 (5)	0.32 (4)	0.8 (1)	0.17 (2)	2.4 (3)	1.3 (5)	0.3 (2)	3 (1)	0.4 (2)
Spain 1	25 (2)	4.1 (2)	12.2 (4)	0.49 (3)	40 (2)	11 (2)	14.8 (3)	197 (2)	4.4 (2)	8.9 (3)	1.3 (1)	4.1 (1)	0.89 (6)	6.7 (1)	9.5 (6)	1.36 (5)	6.8 (4)	1.7 (2)
Spain 2	4.0 (9)	5.0 (2)	2.32 (8)	4.07 (9)	21 (2)	26 (2)	2.6 (7)	15.6 (2)	6.0 (1)	7.7 (2)	1.38 (9)	4.3 (2)	0.8 (1)	2.6 (4)	8.49 (7)	1.13 (9)	6 (1)	1.6 (1)
France 1	8 (3)	1.3 (1)	6.2 (2)	9.2 (1)	93 (5)	1 (2)	45.3 (3)	159 (3)	3.0 (1)	6.0 (3)	0.93 (4)	2.7 (1)	0.53 (1)	5.7 (4)	5 (2)	0.9 (2)	6.0 (8)	1.1 (3)
France 2	10 (3)	1.8 (1)	8.2 (2)	10.5 (3)	28 (3)	3 (3)	2.9 (3)	58 (1)	1.2 (4)	2.8 (1)	0.51 (6)	1.2 (5)	0.27 (6)	2.5 (4)	2 (1)	0.5 (1)	3.2 (8)	0.7 (2)
India 1	20 (2)	2.9 (2)	19.4 (2)	1.2 (2)	40 (2)	0.9 (8)	9.2 (3)	61 (2)	5.3 (1)	11.6 (4)	1.64 (6)	5.8 (5)	1.6 (1)	4.8 (2)	20.9 (5)	4.8 (1)	33.3 (9)	7.8 (9)
India 2	9 (2)	1.2 (2)	24.5 (2)	1.0 (1)	9.9 (5)	2.1 (4)	9.8 (3)	68.0 (7)	4.7 (4)	10.0 (1)	1.37 (6)	4.53 (6)	1.10 (7)	3.7 (3)	9 (2)	1.62 (9)	8 (2)	1.5 (2)
India 3	13.9 (9)	13.7 (2)	29.3 (4)	8.5 (1)	51 (3)	5 (1)	4.3 (5)	176 (3)	1.76 (3)	3.7 (3)	0.6 (1)	1.5 (1)	0.26 (6)	5.7 (5)	2.9 (8)	0.5 (1)	4 (2)	0.36 (6)
India 4	17 (7)	37.2 (3)	45.9 (7)	13.3 (1)	59 (3)	14 (3)	5.3 (5)	64.0 (4)	3.78 (4)	15.6 (2)	1.02 (4)	3.1 (2)	0.6 (1)	4.0 (4)	6.4 (2)	1.1 (1)	6 (1)	0.8 (3)
Pakistan 1	17 (6)	4.0 (3)	37.8 (2)	5.6 (1)	37 (2)	13 (1)	26.8 (2)	41.1 (5)	5.2 (1)	8.7 (2)	1.12 (2)	3.4 (3)	0.7 (1)	2.8 (1)	6.50 (4)	1.0 (1)	4.8 (4)	0.9 (2)
Pakistan 2	11.4 (7)	1.1 (2)	48.6 (5)	38.6 (7)	163 (3)	4.1 (6)	28.0 (6)	105 (1)	3.35 (6)	7.5 (2)	0.99 (8)	3.47 (4)	0.8 (1)	5 (1)	11 (1)	2.4 (3)	16 (3)	3.9 (3)

Table 6.8 (cont) Elemental concentration data (ng ml^{-1}) for calibration rice samples. Figures in brackets are 1 sd and refer to the final figures quoted.
* Concentration below detection limit.

	Er	Tm	Yb	Lu	Hf	Ta	W	Re	Os	Ir	Pt	Au	Hg	Tl	Pb	Bi	Th	U
Scale factor	10^{-2}	10^{-2}	10^{-2}	10^{-2}	10^{-2}	10^{-2}	10^{-2}	10^{-3}	10^{-3}	10^{-3}	10^{-3}	10^{-2}	1	10^{-2}	1	10^{-2}	10^{-2}	10^{-2}
Arkansas 1	98 (4)	12.8 (3)	68 (2)	9.0 (1)	5.2 (8)	3.52 (9)	*	2.1 (8)	16 (18)	2 (2)	7 (1)	9 (3)	16.6 (5)	7.2 (2)	10.4 (1)	11.1 (3)	58.9 (8)	21.3 (4)
Arkansas 2	93 (5)	11.4 (3)	64 (1)	8.31 (9)	5 (1)	23.6 (3)	*	1.5 (9)	9 (8)	1 (2)	3 (5)	22.5 (7)	12.6 (5)	5 (1)	15.19 (7)	8.7 (2)	33 (1)	19 (1)
Louisiana	1.7 (5)	0.3 (1)	0.9 (2)	0.27 (8)	2.0 (4)	1.8 (2)	*	*	*	1 (1)	5 (6)	8 (2)	3.4 (2)	2.2 (5)	26.3 (1)	8.3 (2)	4.8 (2)	1.68 (3)
Mississippi	11 (1)	1.5 (2)	7.3 (4)	1.21 (6)	6.9 (7)	2.78 (6)	*	2 (2)	1 (3)	2 (1)	6 (4)	5 (2)	1.3 (1)	4.9 (4)	24.9 (4)	13.3 (3)	38 (1)	9.1 (8)
Texas 1	10 (1)	1.4 (3)	10 (1)	1.5 (4)	12.9 (5)	8.7 (4)	*	0.4 (8)	4 (3)	*	6 (3)	163 (8)	2.59 (4)	6.4 (2)	37.0 (2)	30.0 (9)	37.6 (6)	38.8 (9)
Texas 2	6.0 (7)	0.9 (2)	4 (1)	0.48 (7)	3 (1)	3.2 (3)	*	0.8 (9)	4 (4)	1 (2)	2 (3)	8 (1)	3.2 (2)	2.4 (5)	21.7 (2)	41 (2)	64 (28)	21.0 (6)
Italy 1	4.2 (4)	0.7 (1)	3.8 (8)	0.5 (2)	11.9 (7)	9.3 (7)	*	0.9 (4)	3 (7)	4 (3)	4 (5)	5 (2)	2.6 (1)	5.8 (7)	10.6 (3)	7.5 (1)	15.5 (8)	4.6 (2)
Italy 2	2.3 (2)	0.6 (2)	3 (1)	0.6 (1)	2.7 (3)	11.0 (5)	*	*	*	*	1 (5)	8 (2)	4.6 (2)	4.2 (7)	5.5 (1)	22 (1)	5.1 (2)	2.8 (2)
Italy 3	1.6 (8)	0.1 (2)	0.5 (1)	0.2 (1)	1.1 (2)	2.0 (1)	*	0.5 (2)	3 (5)	1 (2)	5 (3)	8 (3)	4.0 (4)	2.0 (2)	10.8 (2)	39.9 (4)	2.8 (3)	1.7 (2)
Spain 1	4.4 (5)	0.6 (1)	4 (2)	0.71 (6)	7.4 (4)	4.6 (3)	*	1 (1)	3 (5)	4 (2)	3 (6)	1.9 (5)	7.0 (3)	7 (1)	2.5 (1)	21.4 (7)	14.6 (2)	4.6 (4)
Spain 2	4.6 (6)	0.6 (2)	2.6 (2)	0.49 (3)	2.0 (7)	2.2 (3)	*	2 (1)	24 (15)	3 (2)	7 (7)	6 (2)	2.7 (3)	10 (2)	14.6 (2)	11.7 (4)	10.3 (5)	2.7 (2)
France 1	3.9 (7)	0.5 (2)	2.2 (3)	0.55 (4)	2.6 (2)	3.0 (1)	*	*	6 (6)	3 (2)	*	4 (2)	1.8 (1)	6 (1)	55.0 (4)	5.0 (7)	10.6 (4)	4 (1)
France 2	4.0 (9)	0.2 (1)	2.2 (1)	0.4 (8)	3.3 (8)	8.8 (5)	54 (2)	0.4 (8)	*	2 (1)	8 (3)	1.0 (8)	2.4 (2)	4.4 (8)	26.3 (5)	5.2 (6)	5.0 (3)	3.1 (2)
India 1	26.3 (7)	3.5 (3)	23 (2)	3.5 (8)	6.6 (4)	12.2 (6)	31 (4)	5 (2)	5 (4)	*	2 (5)	2.2 (8)	1.1 (1)	4.8 (2)	1.1 (3)	9.3 (6)	29 (2)	14.3 (2)
India 2	4.9 (5)	0.68 (7)	3.2 (5)	0.48 (4)	1 (1)	3.4 (3)	34 (3)	4 (1)	*	1.0 (4)	2 (7)	*	1.40 (3)	4.9 (5)	0.90 (3)	5.0 (6)	23.7 (6)	7 (1)
India 3	2.3 (2)	0.49 (5)	1.0 (6)	0.4 (1)	2.0 (4)	5.7 (4)	193 (7)	0.8 (7)	6 (5)	3 (2)	9 (2)	19 (1)	7.0 (1)	2.8 (1)	13.9 (1)	6.4 (6)	31 (14)	4.0 (6)
India 4	4 (1)	0.7 (2)	2.6 (7)	0.6 (1)	4.1 (6)	8.6 (4)	49 (1)	0.3 (4)	2 (3)	5 (2)	7 (4)	60 (7)	15.4 (2)	2.0 (3)	19.0 (3)	11.5 (4)	23 (2)	8.2 (4)
Pakistan 1	2.6 (1)	1.0 (5)	1.9 (4)	0.6 (1)	2.7 (4)	4.9 (2)	255 (7)	0.2 (5)	85 (76)	*	10 (4)	12 (1)	4.7 (2)	3.2 (5)	20.6 (2)	15.0 (5)	18 (1)	3.5 (3)
Pakistan 2	13.2 (6)	2.1 (2)	13.2 (6)	1.8 (2)	4.4 (8)	5.3 (3)	149 (6)	0.2 (3)	15 (10)	4 (2)	2 (2)	22 (6)	4.94 (4)	3.3 (1)	127 (1)	41.0 (5)	17.2 (2)	9.1 (2)

With the exception of Spain 2, none of the samples cultivated in Europe had a Li concentration higher than 8 ng g^{-1}. Samples originating in Italy were found to have particularly low concentrations of Li, less than half that found in any other European sample. Samples from USA contained Li at concentrations less than 5 ng g^{-1}, although the rice from Mississippi contained nearly 30 ng g^{-1}, providing a parameter for assignment of the state of origin of a sample known to be American. The traditional Basmati rice varieties grown in Asia all contained Li at 11 ng g^{-1} or higher. The two modern rice strains, India 3 and India 4, had Li concentrations of 5 and 8 ng g^{-1}, values more akin to an American or European sample than the traditional Basmati rice. A relatively high Li content in a sample known to be Indian/Pakistani in origin is therefore an indication that the sample is likely to be a traditional Basmati variety.

The B concentration in samples from the USA was much higher than in samples grown elsewhere. The difference was much more significant than the variation in the B isotope ratios reported above. Rice from the state of Arkansas contained a particularly high concentration of B.

The Asian samples had generally higher Cd levels than samples from other regions, with a minimum of 19 ng g^{-1}. The Cd concentrations in two of the three Italian samples and the rice from Mississippi were similar to the Asian samples, and significantly higher than other samples from the same regions.

The concentration of the 14 lanthanides (La, Ce, Pr, Nd, Sm, Eu, Gd, Tb, Dy, Ho, Er, Tm, Yb and Lu) measured in the Arkansas samples was approximately an order of magnitude higher than in any other USA samples and, for the majority of these elements, an order of magnitude higher than the concentrations found in any of the European or Asian samples as well. By contrast, the sample grown in Louisiana contained these rare earth elements at concentrations around ten times lower than rice from Mississippi or Texas. Additionally, the Texan samples could be distinguished from other rice. Sn was present at around 150 ng g^{-1} in rice grown in Texas compared to less than 10 ng g^{-1} in all the other American samples, and a maximum of 39 ng g^{-1} in samples from other regions.

All of the samples from India/Pakistan contained significantly higher W concentrations than the European and American samples. The lowest concentration recorded in an Asian sample was 0.3 ng g^{-1}, every sample from the other regions had W concentrations below the detection limit.

From the above observations, the decision tree shown in Fig. 6.5 was constructed for the assignment of a rice sample to its country of origin.
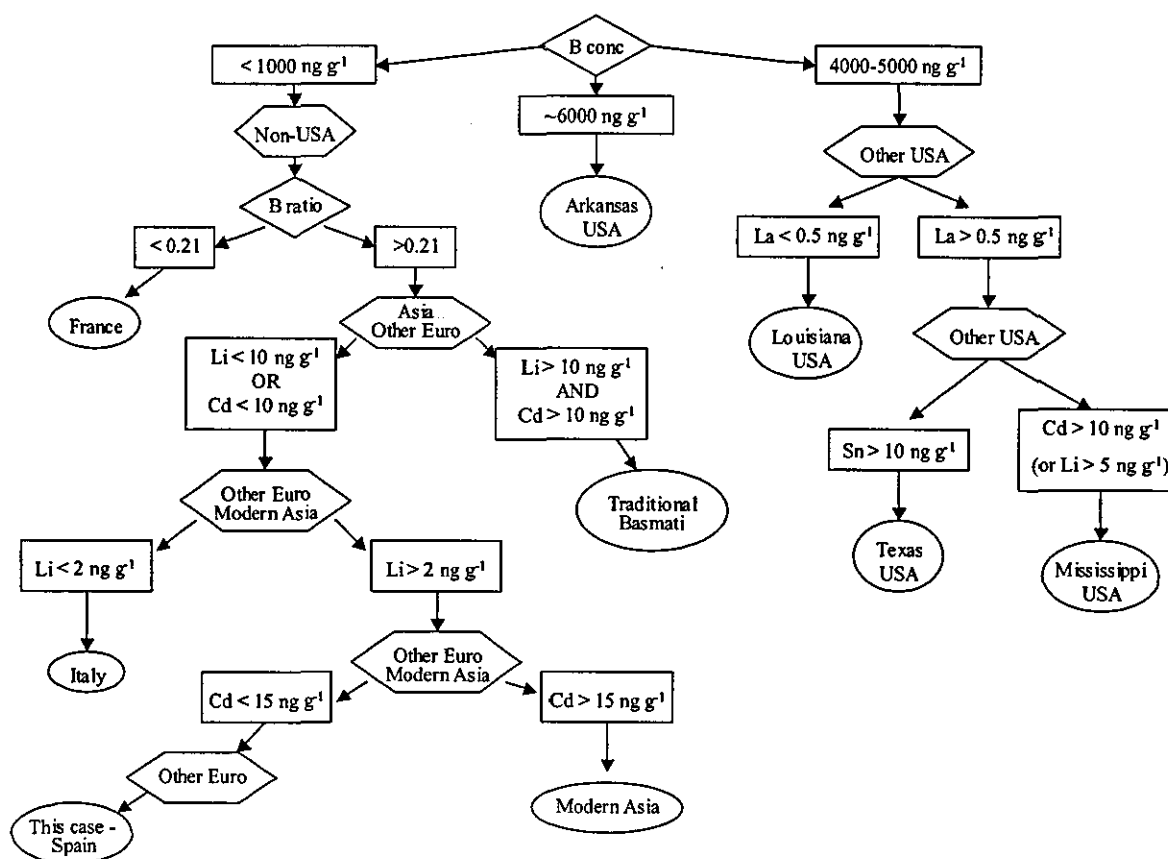

Fig. 6.5 Decision tree for the assignment of rice samples to country of origin.

6.4.4 Principal components analysis of multi-element data

PCA was performed using 8 variables: Li, B, Cd, Sn, La, Nd, Ho and W. As all the lanthanides had similar variations with geographical origin, La, Nd and Ho were selected as representative of this group. The standard deviation of each variable was used to scale the data, which was also mean centred. In preliminary analyses, the wide range of Cd concentrations in the samples resulted in this variable being excluded as an outlier. It was also found that improved separation

of the calibration samples according to geographical origin was achieved by the inclusion of ^{10}B / ^{11}B ratio as a variable. In the final analysis, 5 PCs accounted for over 97 % of the variance in the data, with PCs 1, 2 and 3 totalling 83 % of the calibration variance.

The absolute values of the loadings for the first three PCs were calculated and scaled to the variable with the highest loading. The results are illustrated in Fig. 6.6. The lanthanides and B provided the most significant contributions to PC 1, Sn was the highest factor in PC 2 and Li and W were the biggest contributors to PC 3. All variables except Sn made significant contributions to at least two of the first three PCs.
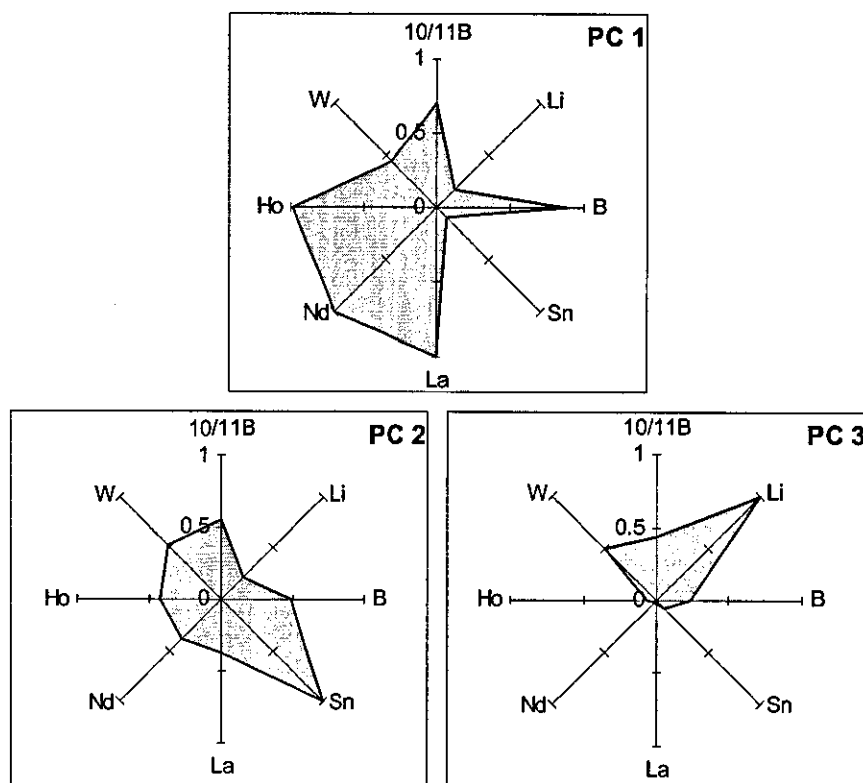
Fig 6.6 Absolute relative loadings for the first three principal components from PCA analysis of multi-element data.

The scores for PCs 1, 2 and 3 are listed in Table 6.9 and plotted in Fig. 6.7. The plot of PC 2 *vs*. PC 1 separated the samples from the USA from the remaining samples. European samples (excluding Spain 2) had a significantly lower score for PC 3 than the Asian samples. Additionally, the two French samples had a lower PC 1 score than the remaining European samples.

166

Table 6.9 Scores for PCA of selected variables

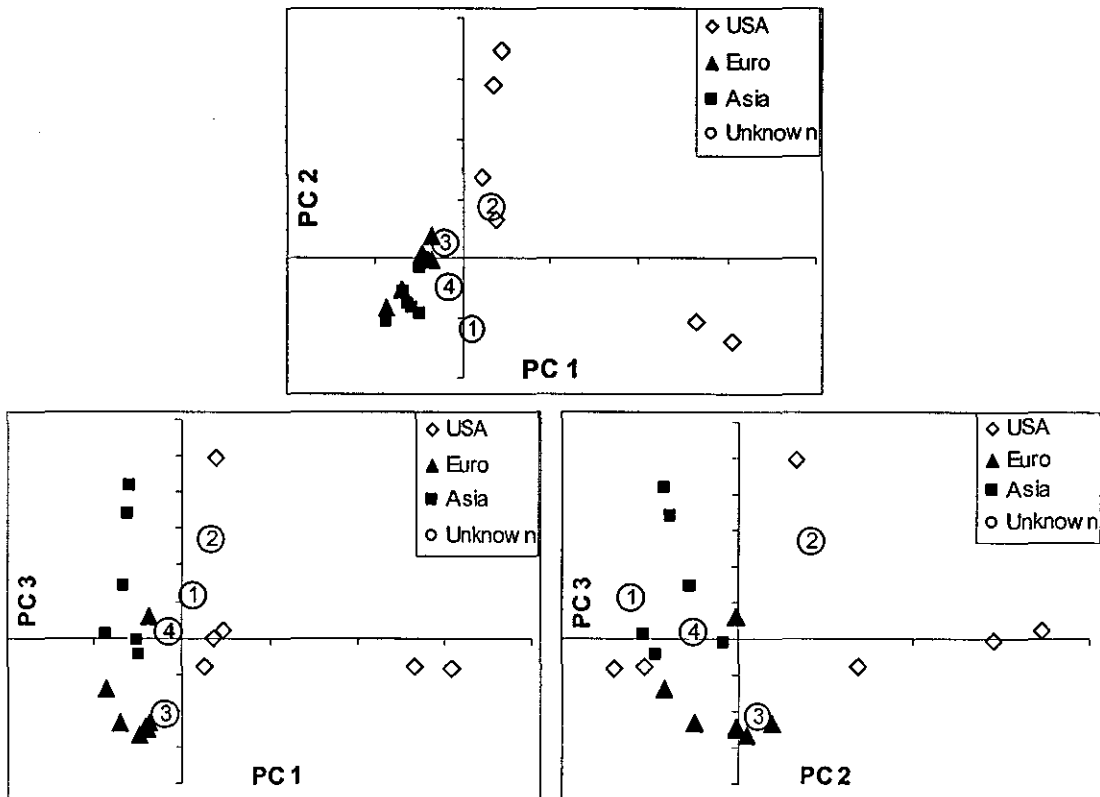|	PC 1	PC 2	PC 3
Arkansas 1	6.1	-1.4	-0.4
Arkansas 2	5.3	-1.1	-0.4
Louisiana	0.5	1.4	-0.4
Mississippi	0.8	0.7	2.5
Texas 1	0.9	3.5	0.1
Texas 2	0.7	2.9	0.0
Italy 1	-0.8	0.0	-1.2
Italy 2	-0.7	0.4	-1.2
Italy 3	-1.0	0.1	-1.3
Spain 1	-0.8	0.0	-1.2
Spain 2	-0.7	0.0	0.3
France 1	-1.4	-0.5	-1.2
France 2	-1.8	-0.8	-0.7
India 1	-1.0	-0.9	-0.2
India 2	-1.2	-0.8	1.7
India 3	-1.7	-1.1	0.0
India 4	-1.0	-0.2	0.0
Pakistan 1	-1.2	-0.8	2.1
Pakistan 2	-1.3	-0.6	0.7

Fig. 6.7 Scores plots for PCA of selected variables. Explained variance: 49 % PC 1; 19 % PC 2; 15 % PC 3. Circled numbers represent the unknown samples (see below).

167

The PCA analysis also provided good separation of rice samples from different states of the USA. The scores for these samples are plotted without the remaining data in Fig. 6.8. As shown, all three comparisons gave some separation of samples from the different states, although the plot of PC 3 *vs.* PC 2 provided the best discrimination. Samples from Arkansas were strongly negative in PC 2 and weakly negative in PC 3; the Louisiana sample scored slightly positive in PC 2 and slightly negative in PC 3; the sample from Mississippi was weakly positive in PC 2 but strongly positive in PC 3; Texas samples scored highly in PC 2 and near zero in PC 3.
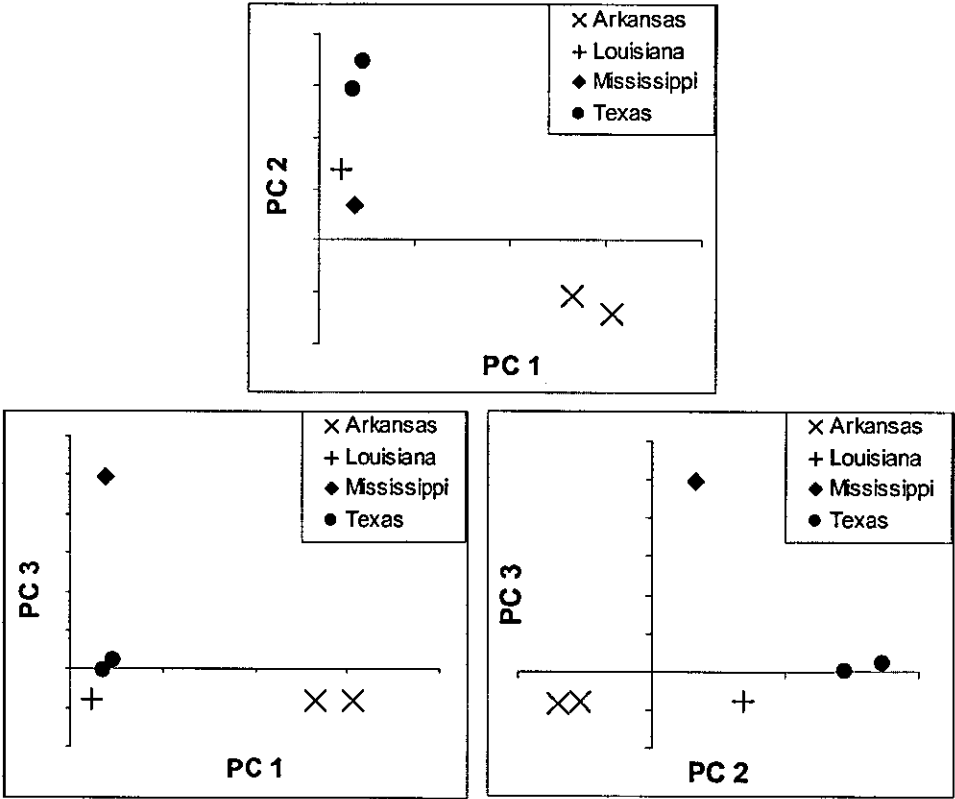
Fig. 6.8 PC scores from Fig. 6.6 for the USA rice samples only

6.5 Unknown Samples

Isotope ratio data for the 4 unknown rice samples is presented in Table 6.10. With a ^{10}B / ^{11}B ratio of 0.221, unknown 2 was almost certainly from the USA. Additionally, none of the unknown samples had a ^{10}B / ^{11}B ratio lower than 0.21, and were therefore probably not grown in France. The unknowns were included in PCA analysis of all isotope ratio data; the scores for PCs 1 and 3 are plotted in

Fig. 6.4. Examination of the PC scores for the unknown samples confirmed the assignment of unknown 2, and suggested that the other unknowns were all Asian samples.

Table 6.10 Isotope ratios for samples of unknown origin. Figures in brackets are 1 sd and refer to the final figures of each ratio.

	$^{10}B / {}^{11}B$	$^{63}Cu / {}^{65}Cu$	$^{87}Sr / {}^{86}Sr$	$^{207}Pb / {}^{206}Pb$
Unknown 1	0.2159 (31)	2.075 (1)	0.72 (2)	0.89 (2)
Unknown 2	0.2213 (4)	2.071 (1)	0.62 (3)	0.85 (2)
Unknown 3	0.2180 (24)	2.076 (1)	0.72 (1)	0.83 (1)
Unknown 4	0.2159 (29)	2.075 (1)	0.70 (3)	0.95 (3)

Key multi-element concentration data for the unknown samples is presented in Table 6.11. The unknown samples were included in PCA of the selected variables described above; the resulting PC scores are illustrated in Fig. 6.7. The plot of PC 2 *vs.* PC 1 shows unknown 2 to be from the USA. Furthermore the scores for this sample for all PCs were closest to the calibration sample from Mississippi, suggesting unknown 2 was cultivated in this state. The PC 3 scores suggest unknown 3 to be European. Although no positive conclusions as to country of origin can be drawn, the PC 1 score for this rice is significantly higher than the French calibration samples. The plot of PC 3 *vs.* PC 2 shows both unknowns 1 and 4 to be Asian, however further assignment is not possible.

Table 6.11 Key concentration data (ng g^{-1}) for samples of unknown origin. Figures in brackets are 1 sd and refer to the final figures. * Below detection limit.

	Unknown 1	Unknown 2	Unknown 3	Unknown 4
Li	14.5 (3)	17.22 (4)	1.16 (4)	12.4 (1)
B	559 (2)	4585 (19)	694 (3)	490 (1)
Cd	11.4 (2)	38.0 (7)	30.3 (5)	24.9 (7)
Sn	1.9 (1)	9.8 (2)	0.7 (2)	3.46 (1)
La	3.5 (1)	1.13 (2)	0.76 (3)	2.06 (5)
Nd	3.15 (6)	0.96 (4)	0.71 (2)	1.63 (7)
Ho	0.082 (3)	0.035 (3)	0.0184 (4)	0.037 (5)
W	0.58 (3)	*	*	*

Using the decision tree in Fig. 6.5, the actual multi-element data could be used to provide more detailed assignments. Unknown 1 had a B concentration of 559 ng g^{-1}, a B ratio of 0.216, a Li concentration of 15 ng g^{-1} and a Cd concentration of 11 ng g^{-1}. This led to the conclusion that unknown 1 was a traditional Basmati rice variety from India or Pakistan. The W concentration in unknown 1 was 0.6 ng g^{-1} (*i.e.* above the detection limit), confirming the regional assignment. Unknown 2 had a B concentration of 4585 ng g^{-1}, a La concentration of 1.1 ng g^{-1} and a Cd concentration of 38 ng g^{-1}. This led to Mississippi, USA as the origin of unknown 2. The Li concentration of 17 ng g^{-1} in this sample could also have been used in the final step.

Unknown 3 had a B concentration of 694 ng g^{-1}, a B ratio of 0.218, a Cd concentration of 30 ng g^{-1} and a Li concentration of 1.2 ng g^{-1}. Unknown 3 was therefore most likely grown in Italy. Finally, unknown 4 had a B concentration of 490 ng g^{-1}, a B ratio of 0.216, a Cd concentration of 25 ng g^{-1} and a Li concentration of 12 ng g^{-1}. From Fig 6.5, this lead to unknown 4 being assigned as traditional Basmati rice from India/Pakistan. Note that the W concentration in this sample was lower than the detection limit, therefore European origin cannot be entirely ruled out. If this were the case, the Li concentration of 12 ng g^{-1} in unknown 4 would lead to Spain being assigned as the country of origin.

6.6 Conclusion

^{10}B / ^{11}B was the most successful of the isotope ratios investigated for the authentication of premium rice, allowing discrimination between USA, France and other countries of origin. The variations of both Cu and Pb isotope ratios in rice grown in different regions were too small to be useful for origin assignment. The ^{87}Sr / ^{86}Sr isotope ratio may prove to be effective; this study was hindered by the low Sr and high Rb levels in the samples.

PCA of 7 elemental concentrations and the ^{10}B / ^{11}B ratio could be used to discriminate between USA, European and Asian samples. More detailed regional assignment was made by inspection of Li, B, Cd, Sn, and La data. By following a

specific order of examination, the American state or European country of origin could be assigned, and traditional and modern Basmati rice grown in India/ Pakistan could be differentiated. Further investigations are required using a wider range of samples, both in terms of country of origin and rice variety, before the general applicability of these findings can be confirmed.

References

1   European Union,
     http://europa.eu.int/comm/agriculture/external/wto/officdoc/geogr_en.htm,
     November, 2002

2   B. Ilbery, M. Kneafsey and M. Bamford, *Outlook on Agriculture*, 2000,
     29, 31.

3   N. E. Tzouros and I. S. Arvanitoyannis, *CRC Crit. Rev. Food Sci. Nutr.*,
     2001, **41**, 287.

4   R. Meyer, F. Chardonnens, P. Hubner and J. Luthy, *Z. Lebensm.-Unters.-
     Forsch.*, 1996, **203**, 339.

5   M. Burgener and P. Hubner, *Z. Lebensm.-Unters.-Forsch. A*, 1998, **207**,
     261.

6   A. K. Lockley and R. G. Bardsley, *Trends Food Sci.Technol.*, 2000, **11**,
     67.

7   J. H. Calvo, P. Zaragoza and R. Osta, *Poult. Sci.*, 2001, **80**, 522.

8   A. Abdulmawjood and M. Bulte, *J. Food Sci.*, 2002, **67**, 1688.

9   H. Rehbein, G. Kress and T. Schmidt, *J. Sci. Food Agric.*, 1997, **74**, 35.

10   V. J. Russell, G. L. Hold, S. E. Pryde, H. Rehbein, J. Quinteiro, M. Ray-
     Mendez, C. G. Sotelo, R. I. Perez-Martin, A. T. Santos and C. Rosa, *J.
     Agric. Food Chem.*, 2000, **48**, 2184.

11   J. Quinteiro, R. Vidal, V. Izquierdo, C. G. Sotelo, M. J. Chapela, R. I.
     Perez-Martin, H. Rehbein, G. L. Hold, V. J. Russell, S. E. Pryde, P. Rosa,
     A. T. Santos and M. Ray-Mendez, *J. Agric. Food Chem.*, 2001, **49**, 5108.

12   G. L. Hold, V. J. Russell, S. E. Pryde, H. Rehbein, J. Quinteiro, R. Vidal,
     M. Ray-Mendez, C. G. Sotelo, R. I. Perez-Martin, A. T. Santos and C.
     Rosa, *J. Agric. Food Chem.*, 2001, **49**, 1175.

13   G. L. Hold, V. J. Russell, S. E. Pryde, H. Rehbein, J. Quinteiro, M. Ray-
     Mendez, C. G. Sotelo, R. I. Perez-Martin, A. T. Santos and C. Rosa, *Eur.
     Food Res. Technol.*, 2001, **212**, 385.

14   E. Klossa-Kilia, V. Papasotiropoulos, G. Kilias and S. Alahiotis, *Food
     Control*, 2002, **13**, 169.

15   M. J. Chapela, C. G. Sotelo, P. Calo-Mata, R. I. Perez-Martin, H. Rehbein, G. L. Hold, J. Quinteiro, M. Ray-Mendez, C. Rosa and A. T. Santos, *J. Food Sci.*, 2002, **67**, 1672.

16   B. Popping, *J. Biotechnol.*, 2002, **98**, 107.

17   R. Siret, O. Gigaud, J. P. Rosec and P. This, *J. Agric. Food Chem.*, 2002, **50**, 3822.

18   G. Downey, *TrAC Trends Anal. Chem. (Pers. Ed.)*, 1998, **17**, 418.

19   S. Sivakesava, J. M. K. Irudayaraj and R. L. Korach, *Appl. Eng. Agric.*, 2001, **17**, 815.

20   Y. W. Lai, E. K. Kemsley and R. H. Wilson, *Food Chem.*, 1995, **53**, 95.

21   G. P. Blanch, M. D. Caja, M. L. R. del Castillo and M. Herraiz, *J. Agric. Food Chem.*, 1998, **46**, 3153.

22   A. N. Davies, P. McIntyre and E. Morgan, *Appl. Spectrosc.*, 2000, **54**, 1864.

23   L. Kupper, H. M. Heise, P. Lampen, A. N. Davies and P. MaIntyre, *Appl. Spectrosc.*, 2001, **55**, 563.

24   V. Baeten, P. Dardenne and R. Aparicio, *J. Agric. Food Chem.*, 2001, **49**, 5098.

25   H. B. Ding and R. J. Xu, *J. Agric. Food Chem.*, 2000, **48**, 2193.

26   T. Yang and J. Irudayaraj, *Lebensm.-Wiss. Technol.*, 2001, **34**, 402.

27   I. Murray, L. S. Aucott and I. H. Pike, *J. Near Infrared Spectrosc.*, 2001, **9**, 297.

28   G. Downey, R. Briandet, R. H. Wilson and E. K. Kemsley, *J. Agric. Food Chem.*, 1997, **45**, 4357.

29   M. M. Paradkar, S. Sakhamuri and J. Irudayaraj, *J. Food Sci.*, 2002, **67**, 2009.

30   L. Dolmotova, V. Tchistiakov, C. Ruckebusch, N. Dupuy, J. P. Huvenne and P. Legrand, *J. Chem. Inf. Comput. Sci.*, 1999, **39**, 1027.

31   N. Dupuy, C. Wojciechowski, C. D. Ta, J. P. Huvenne and P. Legrand, *J. Mol. Struct.*, 1997, **410**, 551.

32   J. Irudayaraj and S. Sivakesava, *Trans. ASAE*, 2001, **44**, 643.

33   S. Sivakesava and J. Irudayaraj, *Int. J. Food Sci. Technol.*, 2002, **37**, 351.

34   J. Parcerisa, M. Rafecas, A. I. Casellote, R. Codony, A. Farran, J. Garcia, A. Lopez, A. Romero and J. Boatella, *Food Chem.*, 1994, **50**, 245.

35   M. S. Valdenebro, M. Leon-Camacho, F. Pablos, A. G. Gonzalez and M. J. Martin, *Analyst*, 1999, **124**, 999.

36   J. Parcerisa, I. Casals, J. Boatella, R. Codony and M. Rafecas, *J. Chromatogr., A*, 2000, **881**, 149.

37   M. J. Martin, F. Pablos, A. G. Gonzalez, M. S. Valdenebro and M. Leon-Camacho, *Talanta*, 2001, **54**, 291.

38   S. Biswas, P. Biswas and G. O. Phillps, *Food Hydrocolloids*, 1995, **9**, 151.

39   T. Erbe and H. Bruckner, *J. Chromatogr., A*, 2000, **881**, 81.

40   J. Prodolliet and C. Hischenhuber, *Z. Lebensm.-Unters.-Forsch. A*, 1998, **207**, 1.

41   B. S. Radovic, R. White, I. Parker, M. J. Dennis, M. Sharman, H. Geiss and E. Anklam, *Deutsche Lebensmittel-Rundschau*, 2001, **97**, 380.

42   C. Bicchi, A. D'Amato and P. Rubiolo, *J. Chromatogr., A*, 1999, **843**, 99.

43   P. P. Mouly, E. M. Gaydou and J. Corsetti, *J. Chromatogr., A*, 1999, **844**, 149.

44   P. P. Mouly, E. M. Gaydou and J. Corsetti, *J. Agric. Food Chem.*, 1999, **47**, 968.

45   M. L. R. del Castillo, M. Herraiz and G. P. Blanch, *J. Agric. Food Chem.*, 2000, **48**, 1186.

46   M. Kreck, A. Scharrrer, S. Bilke and A. Masandl, *Eur. Food Res. Technol.*, 2001, **213**, 389.

47   A. Rossmann, G. Haberhauer, S. Holzl, P. Horn, F. Pichlmayer and S. Voerkelius, *Eur. Food Res. Technol.*, 2000, **211**, 32.

48   L. Saavedra, A. Garcia and C. Barbas, *J. Chromatogr., A*, 2000, **881**, 395.

49   I. Recio, M. Ramos and R. Lopez-Fandino, *Electrophoresis*, 2001, **22**, 1489.

50   J. Jezek and M. Suhaj, *J. Chromatogr., A*, 2001, **916**, 185.

51   E. Schaller, J. O. Bosset and F. Escher, *Lebensm.-Wiss. Technol.*, 1998, **31**, 305.

52   C. Steine, F. Beaucousin, C. Siv and G. Peiffer, *J. Agric. Food Chem.*, 2001, **49**, 3151.

53   D. L. Garcia-Gonzalez and R. Aparicio, *J. Agric. Food Chem.*, 2002, **50**, 1809.

54   S. M. Martin, A. D. Marquina and M. T. O. Villanueva, *Milchwissenschaft*, 2001, **56**, 22.

55   C. Inocencio, F. Alcaraz, F. Calderon, C. Obo and D. Rivera, *Eur. Food Res. Technol.*, 2002, **214**, 335.

56   A. Vaamonde, P. Sanchez and F. Vilarino, *J. Food Qual.*, 2000, **23**, 363.

57   A. Rossmann, *Food Rev. Int.*, 2001, **17**, 347.

58   H. Craig, *Science*, 1961, **133**, 1702.

59   O. Breas, C. Guillou, F. Reniero, E. Sada and F. Angerosa, *Rapid Commun. Mass Spectrom.*, 1998, **12**, 188.

60   S. E. Woodbury, R. P. Evershed and J. B. Rossell, *J. Chromatogr., A*, 1998, **805**, 249.

61   G. Fronza, C. Fuganti, P. Grasselli, S. Serra, F. Reniero and C. Guillou, *Rapid Commun. Mass Spectrom.*, 2001, **15**, 763.

62   S. D. Kelly and C. Rhodes, *Grasas y Acietes*, 2002, **53**, 34.

63   W. Meier-Augenstein, *Anal. Chim. Acta*, 2002, **465**.

64   U. Hener and A. Mosandl, *Deutsche Lebensmittel-Rundschau*, 1993, **89**, 307.

65   H. Casabianca, J. B. Graff, P. Jame, C. Perrucchietti and M. Chastrette, *J. High Resolut. Chromatogr.*, 1995, **18**, 279.

66   A. Mosandl, R. Braunsdorf, G. Bruche, A. Dietrich, U. Hener, V. Karl, T. Kopke, P. Kreis, D. Lehmann and B. Maas, 'New methods to assess authenticity of natural flavors and essential oils' in Fruit Flavors, *ACS Symposium Series*, 1995, **596**, 94.

67   O. Breas, F. Reniero and G. Serrini, *Rapid Commun. Mass Spectrom.*, 1994, **8**, 967.

68   G. J. Martin, M. Mazure, C. Jouitteau, Y. L. Martin, L. Aguile and P. Allain, *Am. J. Enol. Viticulture*, 1999, **50**, 409.

69   A. Hermann, *Z. Lebensm.-Unters.-Forsch. A*, 1999, **208**, 194.

70   H. L. Schmidt, M. ButzenLechner, A. Rossmann, S. Schwarz, H. Kexel and K. Kempe, *Z. Lebensm.-Unters.-Forsch.*, 1993, **196**, 105.

71   G. G. Martin, V. Hanote, M. Lees and Y. L. Martin, *J. AOAC Int.*, 1996, **79**, 62.

72   P. S. Belton, I. Delgadillo, A. M. Gil, P. Roma, F. Casuscelli, I. J. Colquhoun, M. J. Dennis and M. Spraul, *Magn. Reson. Chem.*, 1997, **35**, s52.

73   A. Rossmann, M. Butzenlechner and H. L. Schmidt, *Plant Physiol.*, 1991, **96**, 609.

74   G. G. Martin, Y. L. Martin, N. Naulet and H. J. D. McManus, *J. Agric. Food Chem.*, 1996, **44**, 3206.

75   B. E. Kornexl, T. Werner, A. Rossmann and H. L. Schmidt, *Z. Lebensm.-Unters.-Forsch. A*, 1997, **205**, 19.

76   B. Weckerle, E. Richling, S. Heinrich and P. Schreier, *Anal. Bioanal. Chem.*, 2002, **374**, 886.

77   S. Kelly, M. Baxter, S. Chapman, C. Rhodes, J. Dennis and P. Brereton, *Eur. Food Res. Technol.*, 2002, **214**, 72.

78   M. P. Day, B. L. Zhang and G. J. Martin, *Am. J. Enol Viticulture*, 1994, **45**, 79.

79   M. J. Latorre, R. Pena, S. Garcia and C. Herrero, *Analyst*, 2000, **125**, 307.

80   M. J. Martin, F. Pablos and A. G. Gonzalez, *Anal. Chim. Acta*, 1996, **320**, 191.

81   S. Rebolo, R. M. Pena, M. J. Latorre, S. Garcia, A. M. Botana and C. Herrero, *Anal. Chim. Acta*, 2000, **417**, 211.

82   U. Gottelt, G. Henrion and H. Henrion, *Fres. J. Anal. Chem.*, 1997, **358**, 781.

83   O. Cankur, N. K. Aras, I. Olmez, W. Zhang, W. E. Goodwin and A. Chatt, *Biol. Trace Elem. Res.*, 1999, **71-2**, 109.

84   M. E. Conti, F. Cubadda and M. Carcea, *Food Addit. Contam.*, 2000, **17**, 45.

85   P. M. Padin, R. M. Pena, S. Garcia, R. Iglesias, S. Barro and C. Herrero, *Analyst*, 2001, **126**, 97.

86   K. A. Anderson, B. A. Magnuson, M. L. Tschirgi and B. Smith, *J. Agric. Food Chem.*, 1999, **47**, 1568.

87   P. L. Fernandez-Caceres, M. J. Martin, F. Pablos and A. G. Gonzalez, *J. Agric. Food Chem.*, 2001, **49**, 4775.

88   V. Gundersen, D. McCall and I. E. Bechmann, *J. Agric. Food Chem.*, 2001, **49**, 3808.

89   A. Marcos, A. Fisher, G. Rea and S. J. Hill, *J. Anal. At. Spectrom.*, 1998, **13**, 521.

90   M. J. Martin, F. Pablos and A. G. Gonzalez, *Food Chem.*, 1999, **66**, 365.

91   A. Moreda-Pineiro, A. Marcos, A. Fisher and S. J. Hill, *J. Environ. Monitor.*, 2001, **3**, 352.

92   A. Yasui and K. Shindoh, *Bunseki Kagaku*, 2000, **49**, 405.

93   M. J. Baxter, H. M. Crews, M. J. Dennis, I. Goodall and D. Anderson, *Food Chem.*, 1997, **60**, 443.

94   H. P. Dettmar, G. S. Barbour, K. T. Blackwell, T. P. Vogl, D. L. Alkon, F. S. Fry, J. E. Totah and T. L. Chambers, *Comput. Chem.*, 1996, **20**, 261.

95   V. Gundersen, I. E. Bechmann, A. Behrens and S. Stürup, *J. Agric. Food Chem.*, 2000, **48**, 6094.

96   K. J. R. Rosman and P. D. P. Taylor, *J. Anal. At. Spectrom.*, 1999, **14**, 5N.

97   P. Horn, S. Hölzl, W. Todt and D. Matthies, *Isotopes Environ. Health Stud.*, 1998, **34**, 31.

98   L. Halicz, J. W. H. Lam, M. J. Peters and P. J. Tisdale, *Spectrochim. Acta Part B*, 1994, **47**, 637.

99   S. Stürup, H. Dahlgaard and S. C. Nielsen, *J. Anal. At. Spectrom.*, 1998, **13**, 1321.

100   J. S. Becker and H. J. Dietze, *Fres. J. Anal. Chem.*, 1999, **364**, 482.

101   M. Kunert, K. Friese, V. Weckert and B. Markert, *Environ. Sci. Technol.*, 1999, **33**, 3502.

102   J. G. Farmer, L. J. Eades, M. C. Graham and J. R. Bacon, *J. Environ. Monit.*, 2000, **2**, 49.

103   C.-S. Kim, C.-K. Kim, J.-I. Lee and K.-J. Lee, *J. Anal. At. Spectrom.*, 2000, **15**.

104   G. Åberg, G. Fosse and H. Stray, *Sci. Total Environ.*, 1998, **224**, 109.

105   C. Latkoczy, T. Prohaska, G. Stingeder and M. Teschler-Nicola, *J. Anal. At. Spectrom.*, 1998, **13**, 561.

106   G. De Wannemacker, F. Vanhaeke, L. Moens, A. Van Mele and H. Thoen, *J. Anal. At. Spectrom.*, 2000, **15**, 323.

107   C. Latkoczy, T. Prohaska, M. Watkins, M. Teschler-Nicola and G. Stingeder, *J. Anal. At. Spectrom.*, 2001, **16**, 806.

108   T. Prohaska, C. Latkoczy, G. Schultheis, M. Teschler-Nicola and G. Stingeder, *J. Anal. At. Spectrom.*, 2002, **17**, 887.

109   M. A. Geyh and H. Schleicher, 'Absolute age determination: Physical and chemical dating methods and their application', Springer-Verlag, Heidelberg, 1990.

110   D. C. Grégoire, B. M. Acheson and R. P. Taylor, *J. Anal. At. Spectrom.*, 1996, **11**, 765.

111   A. T. Townsend, Z. Yu, P. McGoldrick and J. A. Hutton, *J. Anal. At. Spectrom.*, 1998, **13**, 809.

112   N. H. Gale, A. P. Woodhead, Z. A. Stos-Gale, A. J. Walder and I. Bowen, *Int. J. Mass Spectrom. Ion Processes*, 1999, **184**, 1.

113   F. Vanhaeke, G. De Wannemacker, L. Moens and J. Hertogen, *J. Anal. At. Spectrom.*, 1999, **14**, 1691.

114   X. K. Zhu, R. K. O'Nions and Y. Guo, *Chem. Geol.*, 2000, **163**, 139.

115   S. Turner, P. van Calsteren, N. Vigier and L. Thomas, *J. Anal. At. Spectrom.*, 2001, **16**, 612.

116   F. Vanhaecke, G. De Wannemacker, L. Moens and P. Van den Haute, *Fres. J. Anal. Chem.*, 2001, **371**, 915.

117   P. Horn, P. Schaaf, B. Holbach, S. Hölzl and H. Eschnauer, *Z. Lebensm.-Unters.-Forsch.*, 1993, **196**, 407.

118   H. E. Taylor, R. A. Huff and A. Montaser, 'Novel applications of ICP-MS' in Inductively Coupled Plasma Mass Spectrometry, ed. A. Montaser, Wiley-VCH, New York, 1998.

119   C. M. Almeida and M. T. S. D. Vasconcelos, *J. Anal. At. Spectrom.*, 2001, **16**, 607.

120   M. Barbaste, K. Robinson, S. Guilfoyle, B. Medina and R. Lobinski, *J. Anal. At. Spectrom.*, 2002, **17**, 135.

121   C. M. Almeida and M. T. S. D. Vasconcelos, *J. Anal. At. Spectrom.*, 1999, **14**, 1815.

122   A. B. Sharma, http://www.financialexpress.com/fe20011025/an1.html#, November, 2002

123   Food Standards Agency, http://www.foodstandards.gov.uk/multimedia/pdfs/basmati.pdf, November 2002

124   W. A. Russell, D. A. Papantastassiou and T. A. Tombrello, *Geochim. Cosmochim. Acta*, 1978, **42**, 1075.

125   C. N. Maréchal, P. Télouk and F. Albarède, *Chem. Geol.*, 1999, **156**, 251.

126   W. M. White, F. Albarède and P. Télouk, *Chem. Geol.*, 2000, **167**, 257.

127   A. D. Anbar, K. A. Knab and J. Barling, *Anal. Chem.*, 2001, **73**, 1425.

Chapter 7

Conclusions

7.1 Development of Methods for Zn and Fe Analysis in Samples from a Nutritional Study

For everyday analysis of large sample numbers, fitness for purpose of an analytical method is more important than the absolute achievable isotope ratio precision. In this work, methods were needed for Zn and Fe analysis of faecal samples from a human nutrition study employing stable isotope labels. The required precision for Zn and Fe isotope ratio measurements in acid digested faecal samples was set by nutritionists using kinetic modelling techniques.

For Zn analysis, the required precision was 0.4 %RSD. Increased resolution was required to separate the $^{40}Ar^{14}N^{16}O^+$ interference from $^{70}Zn^+$, however the standard single collector method did not consistently provide a sufficient level of isotope ratio precision. Therefore, a novel combined high resolution/multi-collector detection strategy was employed, with $^{70}Zn^+$ detected at increased resolution on the axial channel using an electron multiplier, and $^{67}Zn^+$ and $^{68}Zn^+$ detected at low resolution on the multi-collector Faraday array. The response from bracket standard solutions was used to correct for the different drift observed for the two kinds of detector.

For Fe analysis, the specified precision was 1 %RSD, which could be achieved using standard single collector methods. A resolution of 4000 was used to separate the Ar based interferences, however the isobaric overlap of $^{54}Cr^+$ and $^{58}Ni^+$ had to be corrected mathematically through monitoring isotopes of the interfering elements at m/z 53 and 60 for Cr and Ni respectively. Accurate results were only obtained when the mass bias between isotopes of the interfering elements was taken into account.

For both the above analyses, the mass bias in the isotope ratio determinations was corrected using the initial sample collected from each volunteer on the study. This sample, known to contain the elements in natural isotopic abundance, was used to calculate a correction factor for the remaining samples for each volunteer.

Samples from one volunteer were cleaned up for Zn and Fe analysis by TIMS. The resulting fractions were analysed using the double focussing ICP-MS methods developed, TIMS and single focussing ICP-MS with a collision cell for interference removal and energy focussing of the ion beam. No significant differences were found between the results from each technique. Additionally, there were no statistically significant differences between Zn and Fe isotope ratios measured in acid digested faecal samples using the methods developed, and in cleaned up faecal samples analysed by TIMS.

The sample throughput of the ICP-MS methods was limited by the preparation procedure. A typical batch of 24 freeze-dried faecal samples could be digested in duplicate (with reference materials and procedural blanks), diluted and ready to analyse in two days. A single overnight instrumental acquisition generally consisted of three digestion batches. Therefore in a two week (10 day) working period, it would be possible for a single analyst to carry out digestion, dilution and analysis of 120 samples in duplicate. This compares very favourably with the time required for the equivalent processes for analysis by TIMS.

The methods developed for Fe and Zn analysis were used at CSL over a seven month period for the measurement of samples from the 'CuFeZ' nutritional study. From the results, nutritionists at the Institute of Food Research calculated the fractional absorption of each element for study volunteers on 3 different diet types (meat, poultry and vegetarian). Initial results from the study have shown no significant differences between the fractions of Fe and Zn absorbed by volunteers on the different diet types.

Although the analytical methods developed provided sufficient isotope ratio precision to meet the demands of the nutritional study, measurements using sample desolvation techniques may have provided more precise determinations.

This approach significantly reduces the level of interferences that are problematic in both Zn and Fe analyses, allowing conventional multi-collector detection at low resolution. Desolvation increases the efficiency of sample transport to the plasma, however it is worth noting that the resulting signals may not be as stable as those achievable by direct nebulisation. Additionally, the sample matrix remaining after acid digestion of some samples, including faecal matter, may be problematic in the routine application of a desolvating membrane.

New instrumentation allowing simultaneous detection of several isotopes at increased resolution will enhance the precision achievable for isotope ratios of Zn, Fe and other elements affected by resolvable spectral interferences. The isotope ratio precision achievable using these systems will be strongly dependent on the stability of the high resolution peak shape. Additionally, the relatively poor sensitivity of Faraday collectors may limit the instrument performance. If electron multipliers are used, the stability of the cross-calibration of the detectors will be extremely important.

7.2 Mass Bias in ICP-MS

7.2.1 Mass bias characteristics of a double focussing ICP-MS system

Isotope ratio determinations by ICP-MS are inherently inaccurate due to the mass dependent transmission of the mass spectrometer. The variation of the mass bias in a multi-collector ICP-MS system with time, mass and mass difference was investigated using Cd and Sn isotope ratios. Continuous data acquisition for each element showed that the mass bias was only stable over relatively short acquisition periods. Once the error in the published natural abundance data was included in the calculation, the variation of the mass bias with increasing average mass of the isotopes in a ratio was within the standard deviation of the data. The reproducibility of the position of the points about the mean value suggested that low levels of spectral interference were influencing the analysis, or that the natural isotopic abundance values used in the calculation of the bias did not match the actual isotopic abundance in the solutions analysed. The relationship between mass bias and the mass difference between isotopes that made up a ratio was

found to be linear. The change in the gradient of the line with different isotopes as the reference point revealed the mass bias to be decreasing as the mass increased.

Investigation into the effect of high concentrations of matrix elements on the mass bias suggested that the position of collection of the isotopes on the multi-collector array might influence the extent to which an isotope ratio is affected by the matrix. This area would benefit from further experimentation using ICP-MS instruments with different multi-collector configurations.

Spectral interference is a significant problem in low resolution ICP-MS analysis. As the precision of isotope ratio measurements improves, low levels of interferences that were previously insignificant are likely to become problematic. In future, spectral modelling techniques may be more widely applied in order to assess the contribution of each interfering species to the signal at a given mass. This approach requires knowledge of all possible interferences arising from a particular sample matrix, information that can only be gained by using ultra-pure reagents to formulate synthetic sample matrices without the analyte element.

Further investigation using well characterised isotope systems and certified isotopic reference materials may allow the changes in mass bias over small mass ranges to be examined in greater detail. The uncertainty in the 'true' isotopic abundance must be as low as possible to allow significant alterations in the bias to be seen.

7.2.2 Correction of mass bias

Mass bias must be mathematically corrected in order to achieve accurate isotope ratio determinations. This requires measurement of a known isotope ratio, and application of the error in the determination to compensate for the bias in the analyte ratio. The commonly used linear, power and exponential mass bias correction models define the variation of the bias with changing mass difference between the isotopes that make up a ratio, and not with changing mass. As illustrated by the plots of mass bias against mass difference for Cd and Sn isotope ratios, the mass bias does vary with absolute mass. These three expressions are therefore approximations to the true situation.

Correction expressions that predict variable mass bias with mass have been used, however the selection of a mass bias correction model often has the appearance of being arbitrary, the decision being based on which of the available models provides the correct answers for a particular acquisition. Using the description in Chapter 5 of the relationship between mass bias and the change in instrument response with mass, the mass bias model particular to an individual instrument can be determined, by investigation of the true instrument response function. Once the form of the response function has been determined, the parameters that define the mass dependent variation are evaluated through measurement of a known isotope ratio.

The above process can also be reversed and applied to semi-quantitative analysis. This analytical method usually employs a series of internal standards to determine the instrument response function, which is then interpolated to analyte elements. Measurement of the bias of selected isotope ratios across the mass range can be used as an alternative method of determining the instrument response function, enabling calculation of the concentration of 20 or more elements on the basis of a single internal standard. A greater number of analyte elements can be determined using this second method since isotope ratios, and not concentrations, are used to define the instrument response.

By investigating the mass bias model that should be used for an individual instrument, more accurate and reproducible mass bias correction should be possible. This could also lead to wider application of internal standardisation as the variation of mass bias with mass is accurately defined. The approach has yet to be applied to quadrupole ICP-MS, the poorer isotope ratio precision achievable using these systems may mean that the difference between competing mass bias models is not significant.

The full potential of the method may only be apparent in the future if increased numbers of collectors are used for simultaneous detection of isotopes over a wide mass range, allowing precise modelling of the instrument response function. Time-of-flight mass analysers may therefore be the ideal field for application of

this approach. The detection across the mass spectrum of ions that all left the plasma at the same time will allow exact determination of the instrument response function, and therefore exact definition of the form of the mass bias correction model.

7.3 Authentication of Foods Using Trace Element Concentrations and Isotope Ratio Data

Assessment of product origin has become all the more important over recent years with the increasing amount of legislation in this area. Several techniques have been used for assignment of the varietal or geographic origin of foods, including stable isotope ratio analysis of H, N, O and S. Although multi-element concentration data has been applied in several studies, the use of trace element isotope ratio data has thus far been limited. Rice is susceptible to adulteration and mislabelling due the higher price commanded for premium Basmati varieties, which can only be grown in certain regions of northern India and Pakistan due to the photoperiod sensitivity of their flowering cycle. New rice varieties have been developed that can be cultivated elsewhere in the world, yet retain some of the aroma, texture and flavour characteristics of traditional Basmati. Trace element isotope ratio and concentration data measured by double focussing ICP-MS were investigated for the geographical assignment of rice samples from USA, Europe and traditional and modern Basmati varieties from India/Pakistan.

Although some trends were observed, Cu and Pb isotope ratios did not vary sufficiently in samples from the different regions to allow assignment of origin. Sr isotope ratio measurements were affected by the presence of high and variable levels of Rb in the samples. Pre-treatment procedures to remove (or at least reduce) the Rb are required before proper assessment of the applicability of Sr isotope ratios to the problem of rice authenticity can be made. The $^{10}B / ^{11}B$ ratio did allow some geographical assignments. Samples from USA had significantly higher $^{10}B / ^{11}B$ ratios, and the French samples had significantly lower ratios than rice from the remaining countries.

The ^{10}B / ^{11}B ratio and the concentration of Li, B, Cd, Sn, W and the lanthanides was combined to allow the country of origin of a sample to be determined. Principal components analysis enabled general regional assignment, however through examination of the actual data, a procedure was devised for the assignment of samples to a particular country. Discrimination between traditional and modern Basmati varieties grown in India/Pakistan and assignment of the state of origin of American samples was also possible. Following this procedure, the origin of four unknown samples was assigned. Measurement of a greater number of rice varieties from a wider range of countries is required to fully evaluate the strategy developed.

Rice is one of many products susceptible to adulteration and/or mislabelling. The use of trace element concentration and isotope ratio data for the authentication of various food products is likely to increase with the wider availability of high resolution and multi-collector ICP-MS instrumentation. High resolution techniques allow a larger number of elements to be quantified compared to quadrupole based systems, and the improved isotope ratio precision afforded by multi-collector technology permits smaller variations in isotope ratios to be measured, often without the lengthy sample preparation required for analysis by TIMS.